Legume and cereal defence metabolites as lead compounds for novel antimicrobials

Production, analysis, and structural modification

Wouter Johannes Catharina de Bruijn

School of Chemical and Biomedical Engineering,
Nanyang Technological University, Singapore
AND
Graduate School of Advanced studies in Food Technology,
Agrobiotechnology, Nutrition and Health Science,
Wageningen University, The Netherlands

2021

Legume and cereal defence metabolites as lead compounds for novel antimicrobials

Production, analysis, and structural modification

Wouter Johannes Catharina de Bruijn

School of Chemical and Biomedical Engineering,
Nanyang Technological University, Singapore
AND
Graduate School of Advanced studies in Food Technology,
Agrobiotechnology, Nutrition and Health Science,
Wageningen University, The Netherlands

A thesis submitted to the Nanyang Technological University
and Wageningen University in partial fulfilment of the requirement
for the degree of Doctor of Philosophy

2021

Statement of Originality

I hereby certify that the work embodied in this thesis is the result of original research, is free of plagiarised materials, and has not been submitted for a higher degree to any other University or Institution.

22-02-2021

. . . . . .

Date

. . . . . .

Wouter J.C. de Bruijn

Supervisor Declaration Statement

I have reviewed the content and presentation style of this thesis and declare it is free of plagiarism and of sufficient grammatical clarity to be examined. To the best of my knowledge, the research and writing are those of the candidate except as acknowledged in the Author Attribution Statement. I confirm that the investigations were conducted in accord with the ethics policies and integrity standards of Nanyang Technological University and that the research data are presented honestly and without prejudice.

22-02-2021

. . . . . .

Date

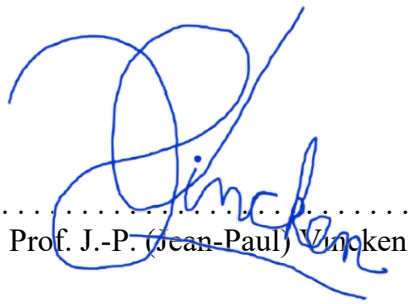

. . . . . .

Prof. J.-P. (Jean-Paul) Vinoken

Authorship Attribution Statement

This thesis contains material from 5 papers published in the following peer-reviewed journals in which I am listed as an author.

Chapter 2 is published as W.J.C. de Bruijn, C. Araya-Cloutier, J. Bijlsma, A. de Swart, M.G. Sanders, P. de Waard, H. Gruppen, J.-P. Vincken. Antibacterial prenylated stilbenoids from peanut (*Arachis hypogaea*). *Phytochemistry Letters* **28**, 13-18 (2018). DOI: 10.1016/j.phytol.2018.09.004

The contributions of the co-authors are as follows

- I conceived the experiments together with C. Araya-Cloutier, H. Gruppen, and J.-P. Vincken.
- I conducted the experiments together with C. Araya-Cloutier, J. Bijlsma, A. de Swart, and M.G. Sanders.
- Together with P. de Waard and J. Bijlsma, I performed NMR analysis of the samples at the MAGNEtic resonance research FacilitY (MAGNEFY) at Wageningen University.
- I wrote the first version of the manuscript, and revised it according to the feedback of all authors.

Chapter 3 is published as W.J.C. de Bruijn, J.-P. Vincken, K. Duran, and H. Gruppen. Mass spectrometric characterization of benzoxazinoid glycosides from *Rhizopus*-elicited wheat (*Triticum aestivum*) seedlings. *Journal of Agricultural and Food Chemistry* **64**, 6267-6276 (2016). DOI: 10.1021/acs.jafc.6b02889

The contributions of the co-authors are as follows

- All authors conceived the experiments
- I conducted the experiments and analysed the data together with K. Duran.
- I wrote the first version of the manuscript, and revised it according to the feedback of all authors.

Chapter 4 is published as W.J.C. de Bruijn, H. Gruppen, and J.-P. Vincken. Structure and biosynthesis of benzoxazinoids: Plant defence metabolites with potential as antimicrobial scaffolds. *Phytochemistry* **155**, 233-243 (2018). DOI: 10.1016/j.phytochem.2018.07.005

The contributions of the co-authors are as follows

- I conducted the literature review and wrote the first version of the manuscript.
- The manuscript was revised by H. Gruppen and J.-P. Vincken.

Chapter 5 is published as W.J.C. de Bruijn, J.A. Hageman, C. Araya-Cloutier, H. Gruppen, and J.-P. Vincken. QSAR of 1,4-benzoxazin-3-one antimicrobials and their drug design perspectives. *Bioorganic & Medicinal Chemistry* **26**, 6105-6114 (2018). DOI: 10.1016/j.bmc.2018.11.016

The contributions of the co-authors are as follows

- I conducted the literature review and curated the dataset.
- I performed the SAR study and prepared the input for the QSAR study.
- Together with J.A. Hageman and C. Araya-Cloutier, I designed the approach for the statistical analysis and QSAR study.
- J.A. Hageman performed the statistical analysis and QSAR study.
- Together with J.A. Hageman, I interpreted the outcomes of the QSAR study.
- I wrote the first version of the manuscript, and revised it according to the feedback of all authors.

Chapter 6 is published as W.J.C. de Bruijn, S. van Dinteren, H. Gruppen, and J.-P. Vincken. Mass spectrometric characterisation of avenanthramides and enhancing their production by germination of oat (*Avena sativa*). *Food Chemistry* **277**, 682-690 (2019). DOI: 10.1016/j.foodchem.2018.11.013

The contributions of the co-authors are as follows

- All authors conceived the experiments.
- I conducted the experiments and analysed the data together with S. van Dinteren.
- I wrote the first version of the manuscript, and revised it according to the feedback of all authors.

22-02-2021

. . . . . .
Date

. . . . . .
Wouter J.C. de Bruijn

Acknowledgements

In the past four years I have had the chance to develop as a researcher, which has finally resulted in this thesis. I would like to thank all of the people who have supported me and everyone who has contributed to the pleasant working environment at the Laboratory of Food Chemistry (FCH).

Allereerst wil ik Harry en Jean-Paul bedanken omdat jullie mij de kans boden om aan dit project te beginnen onder jullie begeleiding. Harry, jouw oog voor detail en kritische blik hebben geholpen om mijn teksten scherp te slijpen en jij leerde mij dat mijn eigen redenering voor een ander niet per se logisch zijn. Jean-Paul, jij gaf mij eigenlijk al heel snel alle vertrouwen. Je hielp mij om keuzes te maken en stimuleerde me om mijn kansen te grijpen binnen het onderzoek. Jouw positieve instelling, enthousiasme over nieuwe of veelbelovende resultaten, en je persoonlijke betrokkenheid heb ik erg gewaardeerd. Ik denk niet dat ik een veel betere (co-)promotor had kunnen hebben. Ook wil ik je bedanken omdat jij je binnen je nieuwe rol als professor van onze groep hebt ingezet voor het vervolg van mijn loopbaan bij FCH. Ik ben blij dat we onze mooie samenwerking de komende jaren kunnen voortzetten!

Prof. Chen, William, I would like to thank you for the collaboration and for introducing me to the world of metabolic engineering and molecular biology as means to produce natural compounds. Also, thank you for the invitation to come to Singapore and for your feedback on my thesis. Kuan Rei, thank you for sharing your research and for showing me how you do things in the lab at NTU.

A big thanks to all of the students that have contributed to my research. Katharina, Bowen, Annemieke, Sarah, and Erwin, who worked on secondary metabolites from various cereals. Anne, Isaac, Judith, and Lalu, who worked on production and modification of stilbenoids. And last but not least, Sylvia and Irene who worked on developing chemical elicitation procedures. I'm also happy to see that four of you, Sylvia, Judith, Katharina, and Sarah, have decided to join FCH to pursue a PhD of your own. It's nice to work with you again!

Jolanda, je bent werkelijk onmisbaar bij FCH, je hebt me met onnoembaar veel (kleine) dingen geholpen over de afgelopen jaren. Daarnaast sta je ook altijd open voor een praatje terwijl ik ondertussen de snoeppot bijvul of juist leegplunder.

Mark, jouw expertise op het vlak van LC-MS analyses en preparatieve chromatografie is van grote waarde geweest voor mijn onderzoek en ik heb veel van jou geleerd over deze technieken. Daarnaast wil ik ook alle andere technicians bedanken voor het operationeel houden van alle apparatuur en computers, het bestellen van chemicaliën, en al jullie andere essentiële bijdrages aan onze groep.

Ook wil ik nog een aantal mensen buiten FCH bedanken voor hun bijdrages aan mijn onderzoek. Maurice, bedankt voor de discussies over prenylering en reactiemechanismes en voor het beschikbaar stellen van een werkplek in jullie laboratorium. Jos, jouw statistische expertise heeft geleid tot een mooi gezamenlijk artikel, bedankt voor alle discussies en analyses. Pieter, jouw hulp met de NMR analyses en je expertise in interpretatie van de data zijn essentieel voor mijn werk.

Besides working on my research, I have thoroughly enjoyed the past four years at FCH. I appreciate the opportunities in our department to relax, recharge, and get to know your colleagues. The discussions and laughs during coffee breaks, lunch, PhD Trips, LFOTMs, activities, and so on have all contributed to that. Thanks to everyone at FCH for making these moments possible. Bianca, ik ben blij dat we, ondanks het feit dat ik "jouw" project wegkaapte, afgelopen jaren soms onze "PhD struggles" met elkaar hebben kunnen delen. Gijs, bedankt voor jouw goede (en slechte) woordgrappen en dat je altijd open staat om over onze onderzoeksprojecten en allerlei andere dingen te discussiëren. Annewieke en Geralt, jullie hebben niet in directe zin bijgedragen aan mijn onderzoek maar in de periode dat we samen bij FCH hebben gewerkt hebben jullie wel (bijna) elke dag gezorgd voor leuke of grappige momenten van ontspanning. Suzanne, Bianca, Yuxi, and Renske, thank you for the nice times we had in organising the PhD trip to Japan. I would also like to thank everyone who was part of the phytogroup in the past few years for the phytomeetings, discussion, and sharing of knowledge and practical experience.

Special thanks to my paranymphs, Carla and Roelant, for their support during the defence. Besides this, I would like to thank Carla for our discussions and fruitful collaborations. Your move to the same office, and later on also to the same neighbourhood, has brought us closer together (not only literally) and I'm glad for that. Roelant, naast onze gedeelde passie voor (analytische) chemie hebben we de afgelopen jaren ook ontdekt dat we het op veel andere vlakken goed met elkaar kunnen vinden. Bedankt voor de vele leuke en grappige gesprekken en interessante discussies op werk maar ook daarbuiten, dat laatste vaak onder het genot van een speciaal biertje.

Pap en mam, bedankt voor jullie onvoorwaardelijke steun en ik profiteer er elke dag van dat jullie mij altijd hebben gestimuleerd om nieuwsgierig te zijn. Jeroen, het samen bier drinken, gamen, en bingewatchen van TV series in het weekend is altijd een mooie manier om weer op te laden voor een week hard werk. Marjolein, jij was er in de afgelopen jaren altijd voor mij, ook wanneer ik zelf niet wist dat ik je nodig had. Ik waardeer je inlevingsvermogen en flexibiliteit enorm, bedankt voor al jouw steun.

Wouter

Table of contents

Summary

Plants produce secondary metabolites as a way to defend themselves against biological and environmental threats. These metabolites can be valuable for the food and pharmaceutical industries, as natural food preservatives and leads for new antibiotics, respectively. In many plants, germination increases the variety and quantity of secondary metabolites which can be further modulated by applying stress to the developing seedling.
Germination with simultaneous fungal elicitation of peanut has unveiled a set of promising antimicrobial compounds: prenylated stilbenoids. The first aim of this thesis was to establish the antimicrobial activity of prenylated stilbenoids.
Poaceae (grasses) is the most cultivated crop plant family worldwide. Various species of grasses can produce different types of defence metabolites. In this family, the effect of germination with simultaneous fungal elicitation has not yet been studied. Therefore, the second aim was to apply the germination and elicitation protocol to grasses to potentially unveil new classes of antimicrobial compounds.
Thirdly, we aimed to explore the possibility of one-pot synthetic prenylation as a means to diversify the structure and efficient production of prenylated (iso)flavonoids and stilbenoids.

In **Chapter 1**, the current state of knowledge on the antimicrobial activity of prenylated (iso)flavonoids and stilbenoids was summarized. Methods to produce plant secondary metabolites with defence functionalities were described. Additionally, the possibilities to achieve structural diversification of these metabolites were explored (i.e. chemical synthesis, metabolically engineered yeast). Besides this, the family Poaceae, which contains several important crops like wheat and oat, was explored with regards to its defence metabolites. Within this plant family several classes of metabolites may be found which could potentially present lead compounds for novel antimicrobials. In wheat, benzoxazinoids, comprising the classes of benzoxazinones and benzoxazolinones, are a set of metabolites with allelopathic and defence functionality. Avenanthramides from oat might possess similar functionalities. These compounds are amides with a phenylalkenoic acid (PA) and an anthranilic acid (AA) subunit. Based on this chapter we hypothesized that prenylated stilbenoids, benzoxazinoids, and avenanthramides would be defence metabolites with antimicrobial activity.

In **Chapter 2**, six monomeric prenylated stilbenoids, including the new compound arachidin-6, were isolated from extracts of fungus-elicited peanuts (*Arachis hypogaea*) using preparative liquid chromatography. Their structures were confirmed by MS^n, HRMS, and NMR spectroscopy and their antibacterial activity was evaluated against methicillin-resistant *Staphylococcus aureus* (MRSA). Similarly to other phenolic compounds, prenylated derivatives of stilbenoids were more active than their non-prenylated precursors piceatannol, resveratrol, and pinosylvin. Chiricanine A, a chain-prenylated pinosylvin derivative, was the most

potent compound tested, with a minimum inhibitory concentration (MIC) of 12.5 µg mL^{-1}. Arachidin-6, a ring-prenylated piceatannol derivative, had moderate potency (MIC 50-75 µg mL^{-1}). A pool of dimeric prenylated stilbenoids, including arahypin-6, had an MIC of 25 µg mL^{-1}. In conclusion, monomeric and dimeric prenylated stilbenoids represent a group of potential natural antibacterials which show promising activity against MRSA. The chemical stability of these compounds, however, is not yet fully understood and might therefore hinder their application.

In **Chapter 3**, the mass spectrometric behaviour of benzoxazinoids from the classes benzoxazin-3-one (with subclasses lactams, hydroxamic acids, and methyl derivatives) and benzoxazolinones was studied. Wheat seeds were germinated with simultaneous elicitation by *Rhizopus*. The seedling extract was screened for the presence of benzoxazinoid (glycosides) using RP-UHPLC-PDA-MS^n. Benzoxazin-3-ones from the different subclasses showed distinctly different ionization and fragmentation behaviour. These features were incorporated into a newly proposed decision guideline to aid the classification of benzoxazinoids. Glycosides of the methyl derivative 2-hydroxy-4-methoxy-1,4-benzoxazin-3-one were tentatively identified for the first time in wheat. We conclude that wheat seedlings germinated with simultaneous fungal elicitation contain a diverse array of benzoxazinoids, mainly constituted by benzoxazin-3-one glycosides.

In **Chapter 4**, the structural diversity of benzoxazinoids, their biosynthesis, role in allelopathy, and antimicrobial potential was reviewed. The effectivity of benzoxazinones in these functionalities is largely imposed by the subclasses (determined by *N* substituent). An overview of all currently known natural benzoxazinoids revealed that 32 unique compounds (excluding *C*2 glycosides) were reported to date. MIC values were only reported for a small number of these compounds. In this literature review, we concluded that monomeric natural benzoxazinoids seem to lack potency as antimicrobial agents. The 1,4-benzoxazin-3-one backbone, however, has been shown to be a potential scaffold for designing new antimicrobial compounds. This has been demonstrated by a number of studies that report potent activity of synthetic derivatives of 1,4-benzoxazin-3-one, which possess MIC values down to 6.25 µg mL^{-1} against pathogenic fungi (e.g. *C. albicans*) and 16 µg mL^{-1} against bacteria (e.g. *S. aureus* and *E. coli*).

In **Chapter 5**, quantitative structure-activity relationships (QSAR) of 1,4-benzoxazin-3-ones as antimicrobials were established. Data published in literature were curated into an extensive dataset of 111 compounds. Multiple linear regression performed by a genetic algorithm was used to identify important molecular descriptors. QSAR models revealed differences in requirements for activity against fungi, gram-positive and gram-negative bacteria. Based on the models generated, *in silico* designed lead compounds with a 1,4-benzoxazin-3-one scaffold were predicted to be up to 5 times more active than any of the compounds

in the dataset. The 1,4-benzoxazin-3-one scaffold was concluded to possess potential for the design of new antimicrobial compounds with potent antibacterial activity, a multi-target mode of action, and possibly reduced susceptibility to gram negatives' efflux pumps.

In **Chapter 6**, the mass spectrometric characterization of avenanthramides was studied and applied to assess the avenanthramide content of germinated oat. Oat seeds were germinated, extracted, and the avenanthramides analysed by a combination of UHPLC with ion trap and high resolution ESI-MS. Typical fragmentation pathways with corresponding diagnostic fragments belonging to the phenylalkenoic acid (PA) and an anthranilic acid (AA) subunits were identified and summarised in a decision guideline. Based on these findings 28 unique avenanthramides were annotated in the oat seed(ling) extracts, including the new avenanthramide 6f (with a 4/5-methoxy AA subunit). Avenanthramide content increased by 25 times from seed to seedling. Avenanthramides 2p, 2c, and 2f, which are commonly described as the major avenanthramides, represented less than 20% of the total content in the seedlings. Future quantitative analyses should, therefore, include a wider range of avenanthramides to avoid underestimation of the total avenanthramide content.

In **Chapter 7**, the results of the foregoing chapters were integrated and discussed alongside some unpublished results. The potential of fungal elicitation, an established method for diversification and enhancement of secondary metabolites in legumes, was also assessed in grasses (Poaceae). The amount and diversity of defence metabolites did not change significantly upon elicitation of grass seedlings. The antimicrobial potential of monomeric metabolites from wheat, oat, rye, and barley was found to be much lower than that of prenylated stilbenoids and (iso)flavonoids. However, there are indications that their antimicrobial potential might be boosted by dimerisation.
Additionally, an optimised one-pot synthetic method was used for prenylation of resveratrol, genistein, and naringenin. A combination of mono-, di-, *C*-, and *O*-prenylated derivatives were produced. The anti-*Saccharomyces cerevisiae* activity of these compounds was low. These findings indicated that a production method of prenylated compounds in metabolically engineered *S. cerevisiae* might be a viable option.
In conclusion, secondary metabolites and their derivatives might be used in the food and pharmaceutical industries as inspiration for antimicrobial compounds. Further structural optimization (e.g. dimerisation, prenylation) is necessary, especially for pharmaceutical applications.

CHAPTER 1

General introduction

Plants produce secondary metabolites as a way to defend themselves against biological and environmental threats. These metabolites can be valuable for the food and pharma industries, as natural food preservatives and leads for new antimicrobial (i.e. antibacterial and antifungal) compounds, respectively.
In many plants, germination increases the variety and quantity of secondary metabolites which can be further modulated by applying stress to the developing seedling. Stressed legume seedlings have been shown to produce phenolic compounds decorated with prenyl groups. Peanut, for example, produces prenylated stilbenoids which might be promising in terms of antimicrobial activity. To further investigate prenylated stilbenoids, these compounds will have to be obtained at high purity. This can be achieved by pilot-scale germination of peanuts with simultaneous elicitation. Alternatively, a one-pot synthetic method could be employed to obtain the desired compounds and to increase their structural diversity.
Poaceae (grasses) is the most cultivated crop plant family worldwide. Various species of grasses can each produce different types of defence metabolites. In this family, the effect of germination with simultaneous fungal elicitation has not yet been studied. In this chapter, the potential of defence metabolites from various grasses as antimicrobials will be discussed as well as methods for their production *in vivo*.

1.1. Plant defence metabolites

Plants produce secondary metabolites or phytochemicals that are not directly involved in growth, reproduction, and development of the plant. Secondary metabolites are typically small molecules, like phenolic compounds, terpenes, or alkaloids, with a variety of functions ranging from visual pollinator attractant (i.e. colourant) to olfactory pollinator attractant (i.e. aroma) to defence toxin.[8] In this way, these phytochemicals are essential for the survival of the plant. Since plants cannot move to avoid biological and non-biological environmental threats, they had to develop intricate chemical mechanisms to defend themselves. Biological threats include insects, nematodes, fungi, bacteria, or animals.[9] Other environmental threats include oxidative stress, heavy metals, drought, temperature changes, or UV radiation.[10] Secondary metabolites enable plants to respond to these threats and thereby also play an integral role in the disease resistance of many species, including those of agricultural importance.[11]

1.1.1. Importance in food and pharma

Secondary metabolites produced by plants can be valuable compounds for applications in the food, biochemical, and pharmaceutical industries. In the food industry for example, plant secondary metabolites are being applied as flavours (e.g. vanillin),[12] colourants (e.g. β-carotene, anthocyanins),[13,14] and preservatives (e.g. flavonoids).[15] Natural preservatives for food are in high demand because of increasing consumer interest in minimally processed and "natural" food, without any non-natural additives. To preserve minimally processed food, natural preservatives will need to be added to control, amongst other factors, bacterial growth.[16,17] A demand for new antimicrobial compounds, which includes antibacterials as well as antifungals, also comes from healthcare. One of the emerging pharmaceutical challenges is the increasing resistance of microorganisms to existing antibiotics. Between the 1930s (discovery of penicillin) and the 1980s, numerous classes of antibiotics were discovered and developed by medicinal chemists. The past 30 years, however, are being referred to as the "discovery void", because no new classes antibiotics have been approved for clinical use during this time.[18,19] Annually, infections with antibiotic-resistant pathogens are already responsible for tens-of-thousands of deaths and billions of dollars of health care costs in the USA alone.[19] Resistance to antibiotics can result in failure to treat infectious disease, possibly with lethal outcome. Generating potential leads for the design of new antibiotics is therefore essential and natural products, such as plant secondary metabolites, can be a valuable source in this respect.[20,21]

1.1.2. Elicitation of secondary metabolism

In plants, some secondary metabolites are produced constitutively (sometimes referred to as phytoanticipins), whereas others are produced *de novo* on demand, as a response to stress (sometimes referred to as phytoalexins).[22] The terms

phytoalexin and phytoanticipin are, however, not used consistently throughout literature and the fact that in some cases the same compound can fit both definitions[11] makes the use of them undesirable. Thus, in this thesis the term secondary metabolites or defence metabolites is preferred.

Stressed plants generally produce a different array of secondary metabolites from their non-stressed peers. For example, applying fungal stress to soybean cotyledons[23] or to soybean seedlings during their germination modulates the isoflavonoid profile of these seedlings.[24] Peanut, also a member of the legume family, produces stilbenoids rather than isoflavonoids and responds similarly to fungal stresses.[25] Peanut stilbenoids and their antimicrobial potential have been studied far less extensively than (iso)flavonoids from other legume species.

Besides legumes, there are four other important agricultural crop families, namely Brassicaceae (e.g. mustard, broccoli), Solanaceae (e.g. potato, tomato), Cucurbitaceae (e.g. cucumber, pumpkin) and Poaceae (e.g. maize, wheat). The latter, Poaceae, is the family of grasses which is by far the largest of these families in terms of global agricultural production (over the period of 2000-2016).[26] Grasses have not yet been subjected to simultaneous germination and fungal stress application. Therefore, elucidating the potential of such combined treatment for these crops to produce functional phytochemicals will be of great interest.

Given the above, this thesis will focus on peanut, the (prenylated) stilbenoid producer of the legume family. Besides, we will attempt to extend the protocol of germination with simultaneous fungal elicitation to plants of the Poaceae family.

1.2. Biosynthesis of defence metabolites

Plants from different families produce different types of secondary defence metabolites. Many of these defence metabolites possess an aromatic ring. Their origins, therefore, are from a common precursor, namely chorismic acid (more commonly referred to as chorismate), which is the final product of the shikimate pathway (**Figure 1.1**).[2] Chorismic acid can be converted to the three aromatic amino acids phenylalanine, tryptophan, and tyrosine.[27] Tyrosine is the precursor for several phenolic compounds, such as hordenine in barley, which will not be further discussed in this thesis.[5]

Phenylalanine serves as the starting point for the phenylpropanoid pathway which is responsible for the synthesis of phenolic compounds, such as hydroxycinnamic acids, flavonoids, and stilbenoids.[3] Phenylalanine is converted to cinnamic acid by phenylalanine ammonia lyase (PAL) and can consecutively be hydroxylated and activated by coenzyme A, yielding *p*-coumaroyl CoA.[3] This compound can then be converted to a wide variety of phenolic compounds by various pathways, depending on the plant species. Flavonoids and stilbenoids are formed by condensation of *p*-coumaroyl CoA with three molecules of malonyl-CoA.[7]

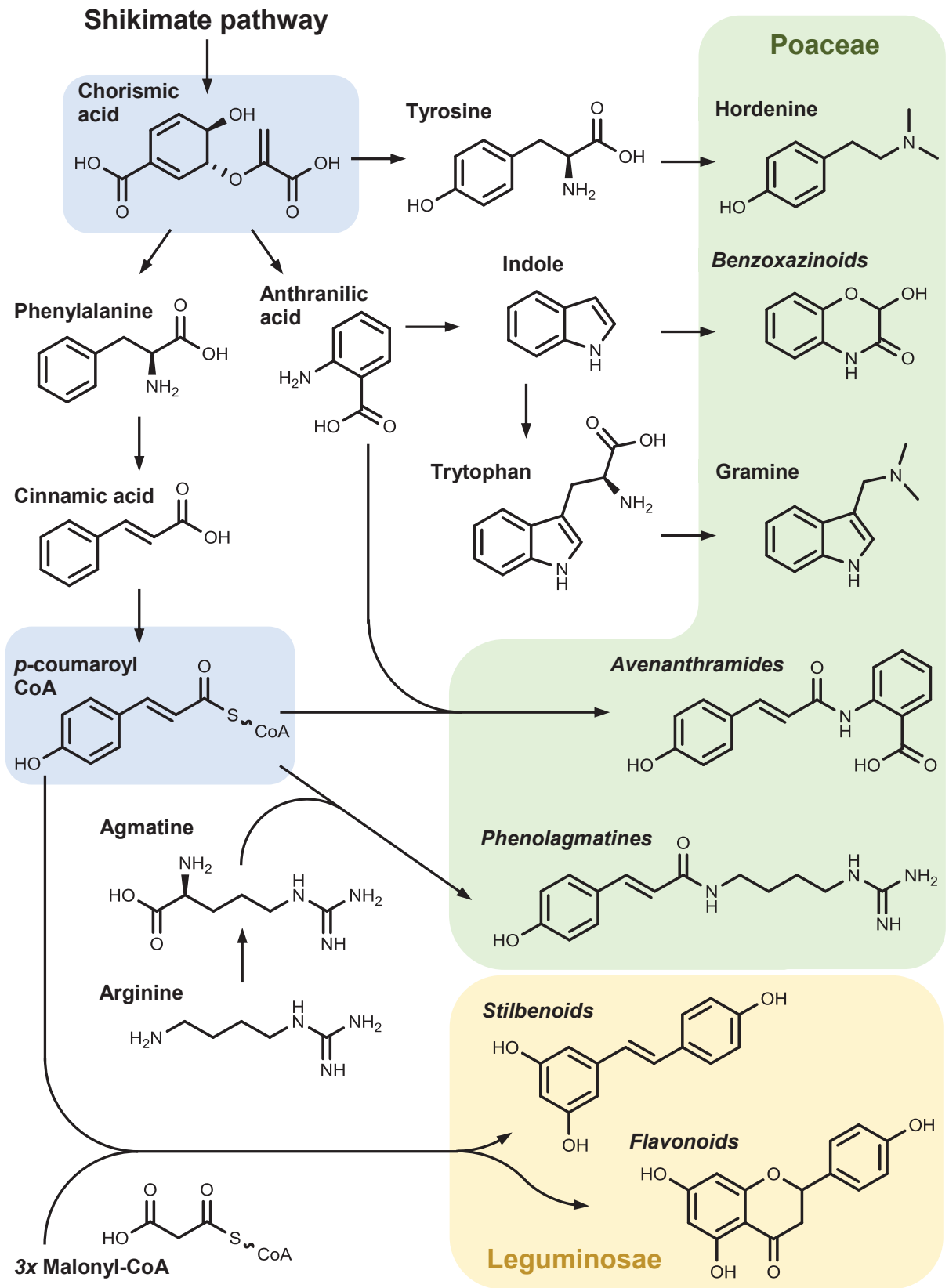

Figure 1.1. Biosynthesis of the main plant secondary metabolites described in this thesis, based on literature.[1-7] Arrows might indicate multiple reactions. Names in italic indicate class names, the structure shown is an example from its respective class. The blue boxes indicate the key intermediates chorismic acid and *p*-coumaroyl CoA.

Tryptophan is the precursor of alkaloid defence metabolites, such as gramine in barley.[6] Anthranilic acid is an intermediary product from the tryptophan biosynthesis, formed directly from chorismate by anthranilate synthase.[2] Indole is formed from indole-3-glycerol phosphate (IGP) which is an intermediate in the tryptophan biosynthesis, downstream of anthranilic acid. Indole is the precursor of many different alkaloids, including the group of compounds called benzoxazinoids.[2] The biosynthesis of benzoxazinoids is described more elaborately in **Chapter 5**. Agmatine does not originate from chorismate, rather it is produced by decarboxylation of the amino acid arginine.[4] The amines anthranilic acid and agmatine can be coupled to hydroxycinnamic acids to give phenolamides, frequently referred to as hydroxycinnamic acid amides (HCAAs).[4]

1.3. Germination and elicitation to modulate secondary metabolism

Plant seeds often contain secondary metabolites at low amounts and with limited structural diversity. The amount and structural diversity of these metabolites undergo an increase during the first 10 days of seed germination into a sprout or seedling (i.e. micro-malting).[28-32] The amount, type, and structure of secondary metabolites produced by the growing seedling is further changed when the plant is exposed to stress (**Figure 1.2**).[33-36]

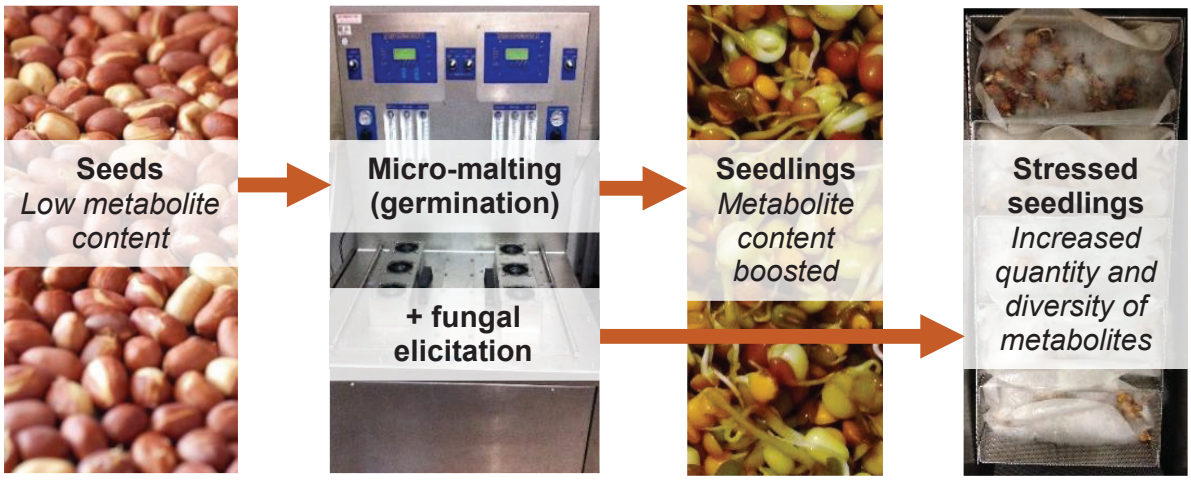

Figure 1.2. The effects of germination in a micro-malting system with or without simultaneous fungal elicitation on metabolite content of legume seeds.

Stress signals start upon perception of a biotic or abiotic stress by activation of receptors on the plant cell. These signals are then further transduced via several signalling cascades, eventually leading to the production of signalling molecules and plant hormones such as jasmonates and ethylene. These molecules affect gene expression and can thereby induce the biosynthesis of secondary metabolites.[37] Thus, by applying a stressor or elicitor, the amount, type, and structure of compounds produced can be modulated, potentially leading to the production of

molecules with interesting biofunctionality.[38,39] There are various types of elicitors that have been used to this end, which can be split into two major groups: biotic and abiotic elicitors. In most cases, these elicitors replicate threats that a plant might encounter in nature. Abiotic elicitors are physical or chemical stressors, for example wounding, UV light, heavy metals, or chemicals.[10] Biotic elicitors are stressors of biological origin, for example live microorganisms, microbial cell wall fragments, or plant hormones.[39,40] Signalling pathways seem to share resemblance across different plant species and for many elicitors it has been shown that they act effectively on different plants.[37] Elicitation of legumes has been investigated extensively and fungal elicitation of a germinating legume seed, for example with the food-grade fungus *Rhizopus oryzae*, can enhance the production and diversification of compounds produced in soybean and other species of legumes (**Figure 1.2**).[24,33,41] A similar approach of micro-malting grasses with simultaneous fungal elicitation has, however, not been investigated as such. Based on the commonality of signalling pathways, it is expected that this protocol will effectively induce the production of defence metabolites in grasses.

1.4. Phenolic compounds from legumes

Plants from the family Leguminosae include, amongst others, liquorice (*Glycyrrhiza* spp.), soybean (*Glycine max*), lupin (*Lupinus* spp.) and a large variety of other legumes.[42] A major group of secondary metabolites produced by plants of this family are (iso)flavonoids, such as naringenin and genistein.[43,44] These compounds have been investigated extensively for their biofunctionality, for example estrogenic activity[43,45,46] and anticancer activity[46], but they have also been shown to possess antimicrobial activity.[47,48]

1.4.1. Prenylation of phenolic compounds

A common modification of these phytochemicals is the addition of a prenyl (3-methyl-2-butene) moiety, referred to as prenylation. Prenyl groups can also occur in other configurations, such as a pyran-ring (**Figure 1.3**).[49,50]

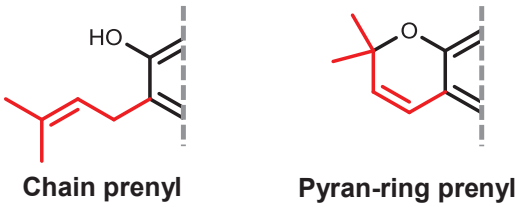

Figure 1.3. Two different types of prenyl-groups attached to an aromatic system.

Prenylation can alter the biofunctionality of these molecules, generally resulting in an enhancement of the antimicrobial activity (see **Section 1.4.3.**).[50] In legumes, prenylation is performed by prenyltransferases which have been identified and

characterized in some species, e.g. *Glycyrrhiza uralensis*,[51] *Glycine max*,[52] and *Sophora flavescens*.[53]

1.4.2. Prenylated stilbenoids from peanut

Peanut (*Arachis hypogaea*) produces mainly stilbenoids rather than (iso)flavonoids.[54] One of the most well-known stilbenoids is resveratrol, a phenolic compound found in wine which has been implicated to possess a variety of health promoting effects.[55] In peanut, stilbenoids can also be prenylated, by stilbenoid-specific prenyltransferases.[56] Prenylated stilbenoids have not been studied nearly as extensively as prenylated (iso)flavonoids. Studies on stilbenoid enriched fractions of peanut extract showed that prenylated stilbenoids are potentially interesting antibacterials, as evidenced by their activity against methicillin-resistant *Staphylococcus aureus*, *Listeria monocytogenes*, and *Escherichia coli*.[50,57] Thus, in **Chapter 2**, we have investigated the antimicrobial activity of purified prenylated stilbenoids from peanut.

As with other legumes, elicitation with fungi, like *R. oryzae*, can modulate the secondary metabolite profile, in this case resulting in production of prenylated derivatives of stilbenoids.[25,58,59] The major groups of prenylated peanut stilbenoids are arachidins and arahypins, which possess a pinosylvin, resveratrol, or piceatannol backbone with a chain or ring prenyl moiety (**Figure 1.4**).

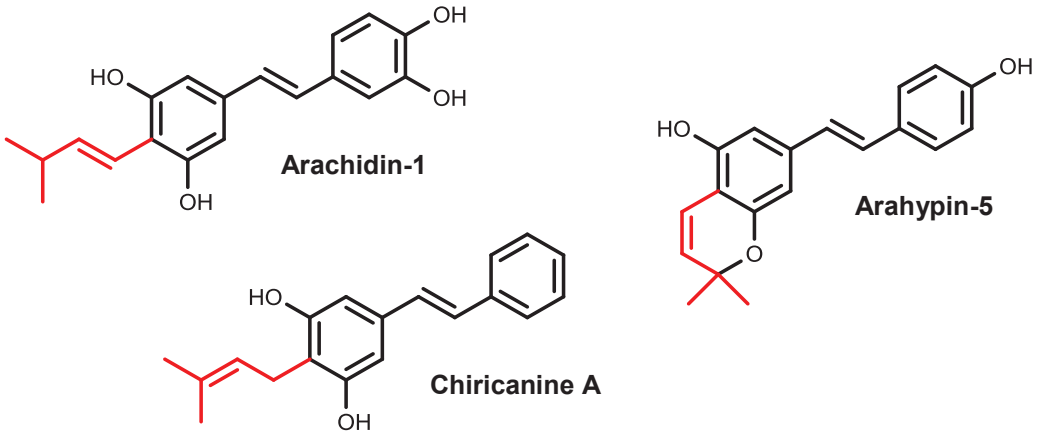

Figure 1.4. Structural diversity of peanut stilbenoids illustrated by: arachidin-1, piceatannol backbone with a 3-methyl-1-butene chain; arahypin-5, resveratrol backbone with a pyran-ring prenyl; chiricanine A, pinosylvin backbone with a 3-methyl-2-butene chain.

1.4.3. Antimicrobial activity of prenylated compounds from legumes

Two extensively studied and relevant microorganisms are the Gram positive methicillin-resistant *Staphylococcus aureus* (MRSA) and the Gram negative *Escherichia coli*. MRSA includes strains of *S. aureus* with resistance against a variety of antibiotics, like oxacillin. *S. aureus* is one of the microorganisms with the highest prevalence of antibiotic-resistance (40-60% resistance amongst

isolates), especially in healthcare settings where it is responsible for a wide variety of infections.[60] Whereas MRSA is of limited relevance in the food industry, *E. coli* is relevant in healthcare, with emerging resistance to e.g. fluoroquinolones, carbapenems, and cephalosporins,[60] as well as in the food industry, as evidenced by the large outbreak in Europe in 2011. In the outbreak, originating in Germany, foodborne *E. coli* caused hemolytic–uremic syndrome in 845 of a total of 3816 cases. In total 54 deaths were associated with this incident.[61] Stilbenoids (**Figure 1.4**) and (iso)flavonoids, for example naringenin and genistein (**Figure 1.5**), have been investigated for their *in vitro* antibacterial activity against these pathogenic bacteria, as shown in **Table 1.1**.

1.4.4. Structural features and antimicrobial activity

Minimum inhibitory concentration (MIC) is a quantitative measure of antimicrobial activity that is universally used and which can be determined by broth dilution methods.[62,63] Besides MIC, two other measures are used to describe antimicrobial activity, namely minimum bactericidal concentration (MBC) and time to detection (TTD) of bacterial growth.[50,57,64] The specialised efflux pumps in the cell envelope of *E. coli* and other gram-negative bacteria are capable of removing a wide variety of compounds from the cell[65], which reduces the observed efficacy of antimicrobials in assays against gram-negative bacteria.[66] Therefore, the antibacterial activity against *E. coli* is often evaluated in the presence of an efflux pump inhibitor (EPI). To this end phenylalanine-arginine β-naphthylamide (PaβN) is commonly used.[57,65-67]

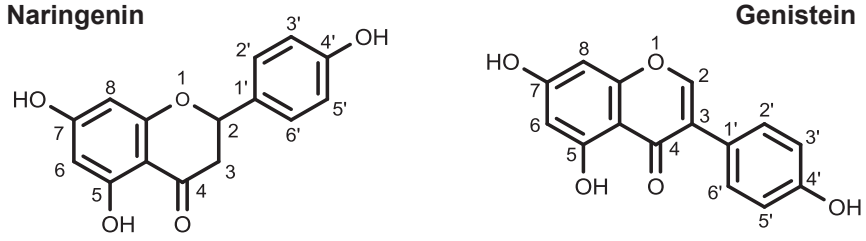

Figure 1.5. Structures of the flavanone naringenin and the isoflavone genistein.

Several general observations on the antimicrobial activity of (prenylated) stilbenoids and (iso)flavonoids can be made based on MICs reported in literature (**Table 1.1**). Firstly, prenylation enhances the antimicrobial activity of (iso)flavonoids, as evidenced by naringenin, genistein (**Figure 1.5**), and their prenylated derivatives. In addition, two prenyl chains generally seem to confer more activity than one against gram-positive bacteria, but not against gram negatives. Secondly, chain prenylation generally seems to be better than pyran-ring prenylation. This is illustrated by alpinumisoflavone, which is the pyran ring equivalent of wighteone. In another study a comparison of these two compounds resulted in the same conclusion (no MICs reported).[68] Additionally, pools rich in

ring prenylated isoflavonoids were found to be among the least active tested in two other studies.[50,57] Thirdly, the position of prenylation also plays a role in the activity as illustrated by the various mono-prenylated (iso)flavonoid derivatives[66] (see also **Table 1.1**) and results obtained with pools of prenylated isoflavonoids and stilbenoids.[50] Lastly, (prenylated) stilbenoids and (iso)flavonoids are not very active against the Gram negative *E. coli* without the addition of an EPI.

Table 1.1. Overview of the antimicrobial activity of selected stilbenoids and (iso)flavonoids against MRSA and *E. coli*. A range of activity indicates that different MIC values were found in different studies or against different strains.

Compound	Prenyl-type	Antimicrobial activity, MIC (μg mL^{-1})			Ref.
		MRSA	*E. coli*	*E. coli* + EPI	
Stilbenoids					
Resveratrol	n.a.	285	400	-	[69,70]
3,5-*O*-methylresveratrol [a]	n.a.	20-31.25	-	-	[70-72]
Flavonoids					
Naringenin	n.a.	73.5-400	125- >128	-	[73-75]
6-prenylnaringenin	Chain	50	>50	25	[66,76]
8-prenylnaringenin	Chain	25	-	-	[76]
6,8-diprenyleriodictyol	2x chain	1-4	-	-	[77]
Isoflavonoids					
Genistein	n.a.	>128	>128	-	[73]
3'-prenylgenistein [b]	Chain	32	>128	25	[66,73]
6-prenylgenistein [c]	Chain	6.25-12.5	-	15	[66,78]
8-prenylgenistein [d]	Chain	>25	-	>50	[66,78]
6-pyranprenylgenistein [e]	Pyran	32- >128	-	-	[79]
6,8-diprenylgenistein [f]	2x chain	8	>128	>50	[66,73]
8,3'-diprenylgenistein [g]	2x chain	1.56-3.13	-	-	[78]
Licoricidin	2x chain	6.25-16	>128	-	[73,80]

MRSA, methicillin-resistant *Staphylococcus aureus*; MIC, minimum inhibitory concentration; EPI, efflux pump inhibitor (PAβN). [a] Pterostilbene [b] Isowighteone, [c] Wighteone, [d] Lupiwighteone, [e] Alpinumisoflavone, [f] 8-Prenylwighteone, [g] Isolupalbigenin.

So far, quantitative structure-activity relationships (QSAR) of (prenylated) (iso)flavonoids have indicated that hydrophobicity plays an important role in antibacterial activity.[66,81] Against gram-positive bacteria increasing hydrophobicity enhances activity, whereas exceedingly hydrophobic compounds (e.g. diprenylated isoflavonoids) were less active against gram negative bacteria.[66] Suggested modes of action of (prenylated) (iso)flavonoids include

inhibition of DNA synthesis and disruption of the plasma membrane.[47,57,81] Further QSAR studies might also shed more light on the antibacterial mode of action of these prenylated compounds. For prenylated stilbenoids, no MIC values have been reported and not much is known regarding the effect of prenylation on specific positions or the difference between chain, pyran, and multiple prenyl groups.

1.5. Efficient production and diversification of prenylated compounds

In order to establish the antimicrobial activity of plant metabolites and to perform QSAR studies, there are two main requirements. Firstly, the metabolites of interest need to be isolated and their structure needs to be fully characterised. Secondly, a sufficiently wide variety of compounds is required to establish structure-activity relationships. In the case of prenylation, the position, type (e.g. chain, pyran), and number of attachments are three major factors which could affect the antimicrobial activity, as discussed in **Section 1.4.4**. In addition, the phenolic backbone will also influence the antimicrobial activity, as illustrated by the differences between resveratrol, naringenin, and genistein (**Table 1.1**).

1.5.1. Isolation and characterisation of metabolites produced *in planta*

As discussed in **Sections 1.3** and **1.4**, germination with simultaneous elicitation has already been established as a method for *in planta* production of defence metabolites. The enzymes involved in the biosynthesis of these metabolites are in most cases highly specific, i.e. they only accept a small range of donor and acceptor substrates to produce a small range of products.[82-84] Common donor substrates include *C*5 pyrophosphates from the non-mevalonate pathway, for example dimethylallyl pyrophosphate (DMAPP).[82,85] In addition to their substrate specificity, these prenyltransferases usually also prenylate at a specific position on the acceptor substrate.[51,56,82,84] For example, in peanut only *C*-prenylated stilbenoids are produced, most commonly with the prenyl attached on the *C*4 position (**Figure 1.4**), and *O*-prenylation does not occur.[56,59] The disadvantage of the specificity of plant prenyltransferases is that each plant species can only provide limited structural diversity for QSAR studies, depending on its array of prenyltransferases. Nevertheless, *in planta* production can be used to reveal novel natural compounds with antimicrobial activity (**Figure 1.6**).

The first step in the isolation and characterisation of metabolites from any type of plant tissue is usually extraction. Tissues with high fat content, such as soybean (19 %) or peanuts (45 %),[86] are usually defatted (e.g. with hexane) prior to extraction.[24,25] Typically, phytochemicals are extracted with organic solvents such as ethanol, methanol, ethyl acetate, or a combination of solvents.[54,87,88] Extracts of defatted plant tissues can be directly analysed by liquid chromatography (LC)

coupled to a variety of detectors, such as ultraviolet-visible light spectroscopy (UV-Vis) and mass spectrometry (MS)[89] or subjected to further sample clean-up, if necessary.[43] Pure compounds are preferable for nuclear magnetic resonance (NMR) spectroscopic structure determination and essential to accurately determine compound potency in antimicrobial activity assays. To this end, complex mixtures obtained upon extraction of plant tissues need to be separated (**Figure 1.6**). Purification can be achieved by subsequent fractionation and chromatographic purification steps, such as solid-phase extraction or flash chromatography followed by preparative HPLC.[20,43] The content of these phytochemicals in plant tissues varies depending on the specific metabolite, plant species, and plant tissue, and can range of from ng to mg per g dry weight (DW).[24,54,90]

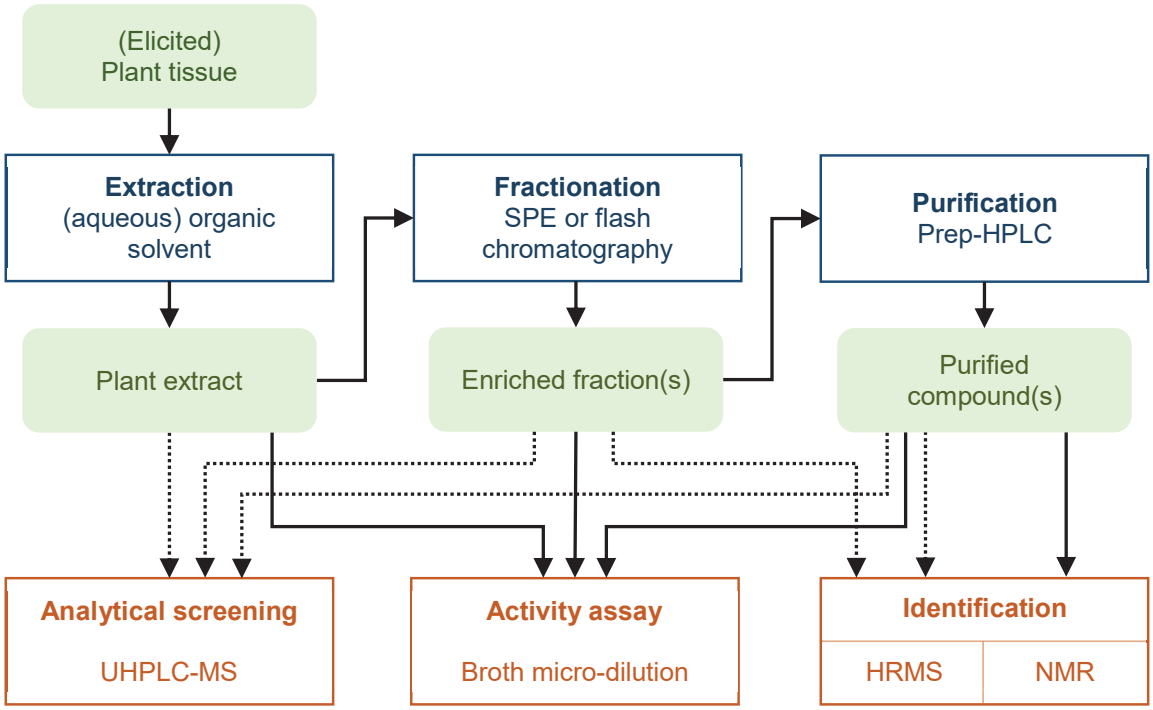

Figure 1.6. Simplified workflow for the screening, purification, and identification of plant secondary metabolites with antimicrobial activity. Dotted lines indicate analyses that only require small amounts (<1 µg per compound) of material. SPE, solid-phase extraction.

For example, in elicited peanut seedlings estimated quantities of prenylated stilbenoids range from below 0.01 to 1.99 mg per g DW.[25] Due to these relatively low contents in plant tissues, purifying sufficient quantities of these compounds is laborious, time-consuming, and expensive.

There are several alternative strategies to obtain pure prenylated compounds. One of the methods that were considered, but which was not explored further in this thesis, were bacterial prenyltransferases. These enzymes can be produced in *E. coli* and can perform *C*-, *O*-, and/or even *N*-prenylation.[91-94] Conversion rates of (iso)flavonoids or stilbenoids by these enzymes were, however, found to be rather low.[91]

1.5.2. Production by metabolically engineered yeast

Another possible production method is metabolic engineering of yeasts by incorporation of an exogenous prenyltransferase. The principle of such an approach has been demonstrated by (iso)flavonoid supplementation of a yeast expressing a plant prenyltransferase but conversion was not very efficient.[95]

A great advantage of this method is that the (iso)flavonoid can be produced constitutively by the yeast from simple precursors,[96] eliminating the need for supplementation with costly (iso)flavonoids and thereby making this method suitable for upscaling. By using plant prenyltransferases high conversion rate into prenylated (iso)flavonoids should be possible once the metabolic pathways have been further optimised. Recovery of the prenylated products from the yeast culture should be less laborious than extraction and isolation of plant material mainly due to higher concentration of the desired compounds and less structurally similar by-products.

This approach, like *in planta* production, is limited by the specificity of the plant prenyltransferases (i.e. mainly mono-*C*-prenylation). Therefore, metabolically engineered yeast cannot provide a wider structural diversity than plants. The latter can be an advantage if specific products are desired, but to produce compounds for QSAR studies, a larger structural diversity is preferred. Additionally, this production method might become a victim of its own success: The antimicrobial prenylated products could inhibit yeast growth. The antifungal activity of prenylated compounds against yeast needs to be further investigated to assess the viability of this production method.

1.5.3. Prenylation by chemical synthesis

Another option is to employ organic synthetic methods in order to produce the desired compounds *in vitro*. Total syntheses of prenylated flavonoids (e.g. 8-prenylnaringenin and 8-prenylapigenin),[97] isoflavonoids (e.g. glyceollin I),[98] and stilbenoids (e.g. arahypin-5 and chiricanine A)[99] have been described in literature. In our case, however, rather than developing a highly selective synthesis, the method should be capable of yielding different types of products in a limited number of steps. Preferably, it should be possible to obtain *C*-, *O*-, and diprenylated (iso)flavonoids or stilbenoids using one reaction. The reaction mixture can then be separated by preparative chromatography (analogous to starting with "Enriched fraction(s)" in **Figure 1.6**), yielding pure compounds with a wide variety of structural elements. A method like this has been described for baicalein and 3,7-dihydroxyflavone. In short, these two flavonoids were prenylated by incubation with prenyl bromide in acetone which yielded *C*-, *O*-, and diprenylated derivatives (**Figure 1.7**).[100]

In the original protocol the base used was K_2CO_3.[100] Typically, potassium counter ions favour *O*-alkylation, whereas lithium counter ions favour *C*-alkylation.[101]

Thus, the use of different counter ions for the carbonate could be a means to control and direct prenylation toward *C*- or *O*-prenylation. *C*-prenylation requires a carbanion intermediate, which is energetically less favourable than the phenoxide intermediate required for *O*-prenylation. Therefore, *C*-prenylation might be more difficult to achieve without the use of very strong bases like hydrides or *n*-butyllithium in combination with protection of the hydroxyl groups.[99,102]
As stated previously, *O*-prenylation is of interest because such compounds are not very abundant in nature and would be a valuable addition to the available set of molecules. Additionally, an *O*-butyl derivative of naringenin reportedly possesses very potent antibacterial activity (MIC 1.9 μg mL^{-1} against MRSA).[75]
Furthermore, varying the reaction time and stoichiometry might be means by which the reaction could be directed towards production of either predominantly mono- or di-prenylated products. The overview in **Table 1.1** illustrates the potency of di-chain prenylated phenolic compounds with MICs down to 1 μg mL^{-1}.

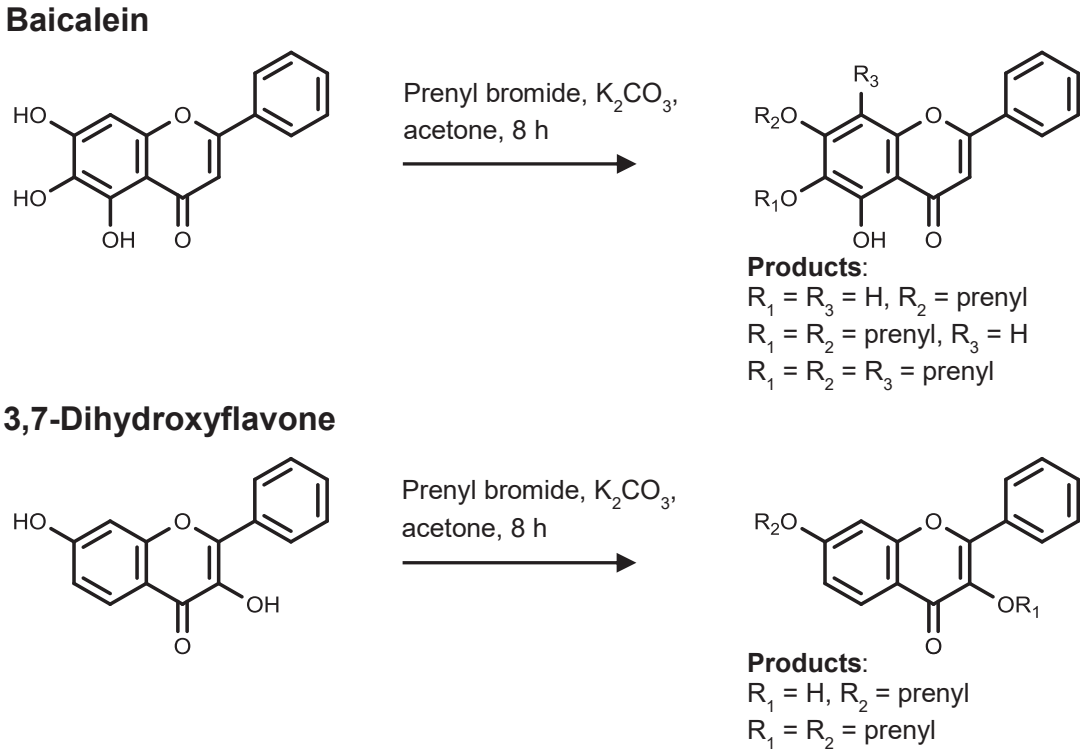

Figure 1.7. Synthesis of prenylated derivatives of baicalein and 3,7-dihydroxyflavone, based on Neves and co-workers (2011).[100]

In principle, this protocol can be applied to prenylate other phenolic compounds, resulting in prenylated compounds with various backbones such as resveratrol, naringenin, and genistein. In this way, the structural variation can be increased, providing a larger set of molecules for antimicrobial activity assays and QSAR studies. Compared to targeted synthetic routes, the approach described in this section has the advantages of its simplicity and the ability to prenylate in one step

whilst yielding multiple products. The main disadvantage of such an approach is that it requires the non-prenylated precursor which either needs to be synthesized before or purchased, which might be expensive depending on the desired product.

1.5.4. Prenylation *in planta* versus yeast metabolic engineering and one-pot synthetic prenylation

The main advantages of metabolically engineered yeast and organic synthesis over *in planta* methods are more efficient upscaling and reduced necessity for elaborate isolation procedures. In **Table 1.2**, the three approaches discussed in this section are summarised in terms of their suitability towards the different requirements to produce prenylated phenolic compounds for QSAR studies and for the elucidation of their mode of action.

Table 1.2. Suitability of three different production methods of prenylated phenolic compounds for QSAR studies and elucidation of their mode of action. Suitability of each method for each requirement is indicated, from most to least suitable: green +, orange +–, red –.

	Prenylation *in planta*	**Yeast metabolic engineering**	**One-pot synthetic prenylation**
C-prenylation	+	+	+–
O-prenylation	–	–	+
Di-prenylation	+–	+–	+
Backbone variations	+	+–	+
Isolation procedure	–	+–	+–
Efficient upscaling	–	+	+
Suitable for food application	+	+–	–

From this overview, it can be concluded that organic synthesis seems attractive to efficiently obtain a wide variety of prenylated phenolic structures. One of its major disadvantages is that *C*-prenylation, which is common *in planta*, will likely be challenging, as discussed previously. Additionally, artificial additives are increasingly less suitable for food applications, especially considering current "clean label" trends.[103] *In planta* production of prenylated compounds, which has been well established, will be the starting point of our research. Yeast metabolic

engineering might offer an alternative to *in planta* production that can be more easily upscaled and might be used for food applications, once it has been established that the prenylated compounds are not harmful to their production organism (i.e. yeast). We aim to set up a synthetic prenylation method to add structural diversity and produce larger quantities of prenylated compounds to be used for structure-antimicrobial activity relationship studies.

1.6. Defence metabolites in Poaceae

The plant family Poaceae contains several important staple crops, such as maize (*Zea mays*), wheat (*Triticum aestivum*), rye (*Secale cereale*), barley (*Hordeum vulgare*), rice (*Oryza sativa*) and oat (*Avena sativa*).[104,105] Of these species, maize (33%), rice (28%), and wheat (27%) account for 88% of the worldwide cereal production. In Europe, wheat is by far the most relevant species, accounting for 48% of European cereal production in the period of 2000-2016.[26]

In this thesis, the production and diversification of metabolites in wheat, rye, barley, spelt, and oat was investigated. Even though all these crop plants belong to the same plant family, they produce a variety of different secondary metabolites. Many of these metabolites have been associated with plant defence and plant-pathogen interactions.[106]

Like legumes, grasses can also produce flavonoids.[106] Kaempferol and naringenin, for example, have been suggested to be related to disease resistance in barley.[107] In wheat, various flavonoids have also been detected,[108] however, so far there are no reports of prenylation in Poaceae. Terpenoids are a diverse group of secondary metabolites, which are widely studied in Poaceae for their role as defence compounds.[106] Several classes of diterpenoids can be found in rice and maize, for example kauralexins and oryzalexins.[109-111] The production of these metabolites in maize can be induced by insect and fungal attack.[112] Wheat also possesses a gene cluster related to kauralexin production,[113,114] which might indicate that these compounds are possibly inducible in wheat and other grass species. Besides this several species of this plant family produce benzoxazinoids, a group of defence alkaloids unique to Poaceae and some dicots (**Section 1.6.1** and **Chapter 5**).

1.6.1. Benzoxazinoids

Wheat, maize, and rye are benzoxazinoid producers. Benzoxazinoids are characterized by an aromatic ring fused to a heterocycle, either a 1,4-oxazin-3-one or a 1,3-oxazol-2-one. These different heterocycles define two classes of benzoxazinoids, the benzoxazinones and the benzoxazolinones (**Figure 1.8**).[115] The classes are further divided into subclasses based on the *N* substituent (R_1), which in nature is most commonly –H (lactam), –OH (hydroxamic acid), or $–OCH_3$ (methyl derivative). Their functions include defence against (micro)biological threats and disease,[88] as well as allelopathy.[116] They have also been suggested

to possess potential benefits as dietary constituents, such as immunoregulatory and antimicrobial effects.[117]

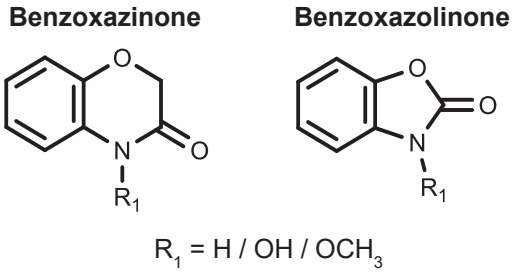

Figure 1.8. Structure of the benzoxazinoid classes benzoxazinones (1,4-benzoxazin-3-one) and benzoxazolinones (1,3-benzoxazol-2-one). The subclass is determined by R_1.

The antimicrobial effect of natural benzoxazinoids is limited as evidenced by 2,4-dihydroxy-7-methoxy-1,4-benzoxazin-3-one (DIMBOA). This compound is the most antimicrobial natural benzoxazinoid, although it has relatively poor activity (lowest reported MIC 250 µg mL^{-1} against *S. aureus*)[118] compared to (prenylated) stilbenoids and (iso)flavonoids (**Table 1.1**). Potentially, fungal elicitation of germinating wheat seeds could result in diversification of the benzoxazinoid structures produced, leading to more potent antimicrobials.
Besides this, organic synthesis has also been used to generate synthetic benzoxazinoids with a wide variety of substituents. Such non-natural derivatives of benzoxazinoids, mostly based on the 1,4-benzoxazin-3-one scaffold, have been described, which possess more potent antimicrobial activity. For example, 4-cyclohexyl-7-fluoro-1,4-benzoxazin-3-one was shown to possess good activity (MIC 16 µg mL^{-1}) against *S. aureus*.[119] This illustrates that 1,4-benzoxazin-3-one can serve as a lead compound for the design of novel antimicrobials. **Chapter 5** provides a more elaborate look at benzoxazinoids, in the form of a review of their structure, biosynthesis, functionality, and reactivity. In **Chapters 5** and **6** the synthetic modification of the natural benzoxazinoid backbones is also discussed in more detail. These chapters illustrate that besides prenylation, which is a natural modification, organic synthesis can be used to perform many different modifications to modulate the antimicrobial activity of nature-inspired scaffolds.

1.6.2. Phenolamides

Oat and barley, also members of the Poaceae family, do not produce benzoxazinoids.[106] Instead these species produce phenolamides, which are often collectively referred to as hydroxycinnamic acid amides (HCAAs) even though this term does not cover all structures within this class. Metabolites from this diverse group are known to be involved in plants' protection, mainly against biotic stresses.[120]

1.6.2.1. Avenanthramides

In the case of oat the main phenolamides are avenanthramides, amides of hydroxycinnamic acid derivatives and anthranilic acid (**Figure 1.9**).[121]

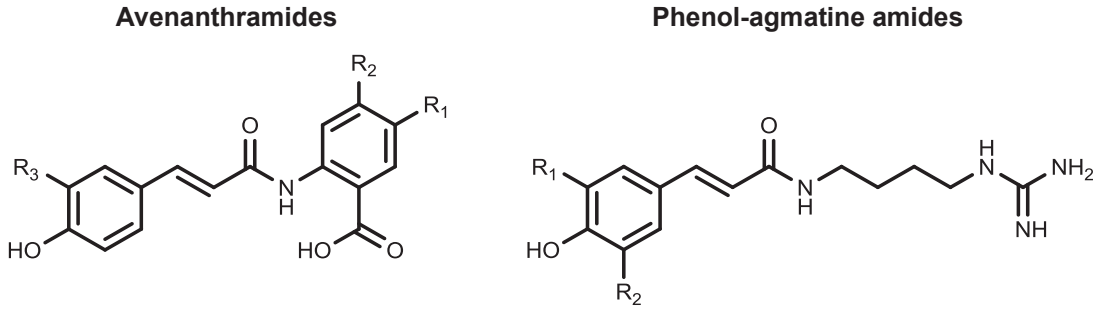

Figure 1.9. Structure of the phenolamides from oat, avenanthramides, and barley, phenol-agmatine amides. R-groups are H, OH, or OCH_3 in natural derivatives of these compounds.

Avenanthramides have been reported to be important contributors to disease-resistance in oat, specifically against the crown rot fungus *Puccinia corronata*.[99] Besides, avenanthramides have been shown to be bioavailable in humans and they exhibit health beneficial effects such as anti-oxidant and anti-inflammatory activity.[122] Potentially, these metabolites could be a source of natural, non-toxic antimicrobials.

1.6.2.2. Phenol-agmatine amides

Barley and several other grasses (e.g. winter wheat), produce phenol-agmatine amides, amides of hydroxycinnamic acids and agmatine **Figure 1.9**).[123,124] These metabolites have been suggested to be associated with stress responses and disease resistance.[125,126] The expression of agmatine coumaroyl-transferase has also been shown to be inducible by fungal infection.[127] It has also been shown phenol-agmatine amides, such as feruloylagmatine compounds are potential antifungals with activity against the phytopathogenic fungus *Microdochium nivale*.[124] Phenol-agmatine amides can be subject to enzymatic oxidative dimerization, yielding hordatines[126] which have been suggested to be even more potent antifungals.[128] No MICs, however, have been determined for phenol-agmatine amides or hordatines.

Additionally, barley produces the alkaloids hordenine and gramine (**Figure 1.1**).[6] Gramine is toxic to a wide variety of organisms, including mammals, plants, and bacteria,[129] whereas hordenine might play a role in allelopathy as suggested by its phytotoxicity.[130]

1.7. Aim and outline of thesis

Application of germination with simultaneous elicitation by *Rhizopus* to peanut has unveiled a set of defence metabolites: prenylated stilbenoids. Previous studies on mixtures of these metabolites from peanuts indicated that they could be promising as antimicrobials.[50,57] The first aim of this thesis will be to establish the antibacterial activity of prenylated stilbenoids. Secondly, we aim to apply the germination and elicitation protocol to grasses to potentially unveil new classes of antimicrobial compounds. Which classes of compounds will be produced is still to be established. Thirdly, we aim to explore the possibility of one-pot synthetic prenylation as a means to efficiently produce and diversify the structure of prenylated (iso)flavonoids and stilbenoids.

In **Chapter 2**, large-scale germination and elicitation of peanuts was performed, followed by the extraction and purification of prenylated stilbenoids by flash chromatography and preparative HPLC-MS. The prenylated stilbenoids were characterized by a combination of mass spectrometry and nuclear magnetic resonance spectroscopy. Their antibacterial activity was studied *in vitro* against methicillin-resistant *Staphylococcus aureus* (MRSA). In **Chapter 3**, germination with *Rhizopus*-elicitation was applied to wheat. The extracts of elicited wheat seedlings contained benzoxazinoids, which were mainly present as glycosides. The mass spectrometric behaviour of the benzoxazinoid glycosides was studied and applied to characterize the benzoxazinoid profile of the elicited wheat seedlings. In **Chapter 4**, the structure and biosynthesis of benzoxazinoid was reviewed. Additionally, the *in planta* functionality of these compounds was briefly investigated, along with the *in vitro* antimicrobial activity of natural benzoxazinoids. In **Chapter 5**, antimicrobial activities of natural and synthetic 1,4-benzoxazin-3-ones were evaluated by a QSAR approach. Molecular modelling was performed, yielding several models that can be used for drug design and discovery. In **Chapter 6**, germination was used to boost the avenanthramide content of oat. The mass spectrometry of avenanthramides was studied systematically with three available standards and the findings were applied to identify avenanthramides in oat seedlings. The effect of germination on the avenanthramide profile of oat seeds was studied by quantification of individual compounds. In **Chapter 7**, the results described in each of these chapters are put into perspective in an integrated discussion, in which future opportunities are shortly explored. Additionally, preliminary results of the one-pot synthetic prenylation approach are discussed along with the anti-yeast activity of the prenylated products.

1.8. References

[1] Bagni, N. and Tassoni, A. (2001) Biosynthesis, oxidation and conjugation of aliphatic polyamines in higher plants. *Amino Acids*, 20*(3)*: p. 301-317.

[2] Maeda, H. and Dudareva, N. (2012) The shikimate pathway and aromatic amino acid biosynthesis in plants. *Annual Review of Plant Biology*, 63: p. 73-105.

[3] Vogt, T. (2010) Phenylpropanoid biosynthesis. *Molecular Plant*, 3*(1)*: p. 2-20.

[4] Bassard, J.E., Ullmann, P., Bernier, F., and Werck-Reichhart, D. (2010) Phenolamides: Bridging polyamines to the phenolic metabolism. *Phytochemistry*, 71*(16)*: p. 1808-1824.

[5] Meyer, E. (1982) Separation of two distinct S-adenosylmethionine dependent N-methyltransferases involved in hordenine biosynthesis in *Hordeum vulgare*. *Plant Cell Reports*, 1*(6)*: p. 236-239.

[6] Larsson, K.A.E., Zetterlund, I., Delp, G., and Jonsson, L.M.V. (2006) N-methyltransferase involved in gramine biosynthesis in barley: Cloning and characterization. *Phytochemistry*, 67*(18)*: p. 2002-2008.

[7] Dewick, P.M. (1995) The biosynthesis of shikimate metabolites. *Natural Product Reports*, 12*(2)*: p. 101-133.

[8] Pichersky, E. and Gang, D.R. (2000) Genetics and biochemistry of secondary metabolites in plants: An evolutionary perspective. *Trends in Plant Science*, 5*(10)*: p. 439-445.

[9] Dangl, J.L. and Jones, J.D.G. (2001) Plant pathogens and integrated defence responses to infection. *Nature*, 411*(6839)*: p. 826-833.

[10] Akula, R. and Ravishankar, G.A. (2011) Influence of abiotic stress signals on secondary metabolites in plants. *Plant Signaling & Behavior*, 6*(11)*: p. 1720-1731.

[11] Dixon, R.A. (2001) Natural products and plant disease resistance. *Nature*, 411*(6839)*: p. 843-847.

[12] Schwab, W., Davidovich-Rikanati, R., and Lewinsohn, E. (2008) Biosynthesis of plant-derived flavor compounds. *Plant Journal*, 54*(4)*: p. 712-732.

[13] Timberlake, C.F. and Henry, B.S. (1986) Plant pigments as natural food colors. *Endeavour*, 10*(1)*: p. 31-36.

[14] Bridle, P. and Timberlake, C.F. (1997) Anthocyanins as natural food colours - selected aspects. *Food Chemistry*, 58*(1-2)*: p. 103-109.

[15] Negi, P.S. (2012) Plant extracts for the control of bacterial growth: Efficacy, stability and safety issues for food application. *International Journal of Food Microbiology*, 156*(1)*: p. 7-17.

[16] Carocho, M., Barreiro, M.F., Morales, P., and Ferreira, I.C.F.R. (2014) Adding molecules to food, pros and cons: A review on synthetic and natural food additives. *Comprehensive Reviews in Food Science and Food Safety*, 13*(4)*: p. 377-399.

[17] Cleveland, J., Montville, T.J., Nes, I.F., and Chikindas, M.L. (2001) Bacteriocins: Safe, natural antimicrobials for food preservation. *International Journal of Food Microbiology*, 71*(1)*: p. 1-20.

[18] World Health Organization (2014) Antimicrobial resistance: Global report on surveillance.

[19] Ventola, C.L. (2015) The antibiotic resistance crisis, part 1: Causes and threats. *Pharmacy and Therapeutics*, 40*(4)*: p. 277-283.

[20] Harvey, A.L., Edrada-Ebel, R., and Quinn, R.J. (2015) The re-emergence of natural products for drug discovery in the genomics era. *Nature Reviews Drug Discovery*, 14*(2)*: p. 111-129.

[21] Dias, D.A., Urban, S., and Roessner, U. (2012) A historical overview of natural products in drug discovery. *Metabolites*, 2*(2)*: p. 303-336.

[22] VanEtten, H.D., Mansfield, J.W., Bailey, J.A., and Farmer, E.E. (1994) Two classes of plant antibiotics: Phytoalexins versus "phytoanticipins". *Plant Cell*, 6*(9)*: p. 1191-1192.
[23] Boué, S.M., Carter, C.H., Ehrlich, K.C., and Cleveland, T.E. (2000) Induction of the soybean phytoalexins coumestrol and glyceollin by *Aspergillus*. *Journal of Agricultural and Food Chemistry*, 48*(6)*: p. 2167-2172.
[24] Simons, R., Vincken, J.-P., Roidos, N., Bovee, T.F.H., van Iersel, M., Verbruggen, M.A., and Gruppen, H. (2011) Increasing soy isoflavonoid content and diversity by simultaneous malting and challenging by a fungus to modulate estrogenicity. *Journal of Agricultural and Food Chemistry*, 59*(12)*: p. 6748-6758.
[25] Aisyah, S., Gruppen, H., Slager, M., Helmink, B., and Vincken, J.-P. (2015) Modification of prenylated stilbenoids in peanut (*Arachis hypogaea*) seedlings by the same fungi that elicited them: The fungus strikes back. *Journal of Agricultural and Food Chemistry*, 63*(42)*: p. 9260-9268.
[26] FAOSTAT (2018) Faostat > production > crops. http://www.fao.org/faostat/en/#data/QC accessed 8 May 2018.
[27] Ramakrishna, A., Giridhar, P., and Ravishankar, G.A. (2011) Phytoserotonin: A review. *Plant Signal Behav*, 6*(6)*: p. 800-809.
[28] Wu, Z.Y., Song, L.X., Feng, S.B., Liu, Y.C., He, G.Y., Yioe, Y., Liu, S.Q., and Huang, D.J. (2012) Germination dramatically increases isoflavonoid content and diversity in chickpea (*cicer arietinum* L.) seeds. *Journal of Agricultural and Food Chemistry*, 60*(35)*: p. 8606-8615.
[29] Randhir, R. and Shetty, K. (2005) Developmental stimulation of total phenolics and related antioxidant activity in light- and dark-germinated corn by natural elicitors. *Process Biochemistry*, 40*(5)*: p. 1721-1732.
[30] Dueñas, M., Hernández, T., Estrella, I., and Fernández, D. (2009) Germination as a process to increase the polyphenol content and antioxidant activity of lupin seeds (*Lupinus angustifolius* L.). *Food Chemistry*, 117*(4)*: p. 599-607.
[31] Cevallos-Casals, B.A. and Cisneros-Zevallos, L. (2010) Impact of germination on phenolic content and antioxidant activity of 13 edible seed species. *Food Chemistry*, 119*(4)*: p. 1485-1490.
[32] Skoglund, M., Peterson, D.M., Andersson, R., Nilsson, J., and Dimberg, L.H. (2008) Avenanthramide content and related enzyme activities in oats as affected by steeping and germination. *Journal of Cereal Science*, 48*(2)*: p. 294-303.
[33] Aisyah, S., Vincken, J.-P., Andini, S., Mardiah, Z., and Gruppen, H. (2016) Compositional changes in (iso)flavonoids and estrogenic activity of three edible Lupinus species by germination and *Rhizopus*-elicitation. *Phytochemistry*, 122: p. 65-75.
[34] Aisyah, S., Gruppen, H., Madzora, B., and Vincken, J.-P. (2013) Modulation of isoflavonoid composition of *Rhizopus oryzae* elicited soybean (*Glycine max*) seedlings by light and wounding. *Journal of Agricultural and Food Chemistry*, 61*(36)*: p. 8657-8667.
[35] Gawlik-Dziki, U., Dziki, D., Nowak, R., Świeca, M., Olech, M., and Pietrzak, W. (2016) Influence of sprouting and elicitation on phenolic acids profile and antioxidant activity of wheat seedlings. *Journal of Cereal Science*, 70: p. 221-228.
[36] Świeca, M. and Baraniak, B. (2014) Nutritional and antioxidant potential of lentil sprouts affected by elicitation with temperature stress. *Journal of Agricultural and Food Chemistry*, 62*(14)*: p. 3306-3313.
[37] Zhao, J., Davis, L.C., and Verpoorte, R. (2005) Elicitor signal transduction leading to production of plant secondary metabolites. *Biotechnology Advances*, 23*(4)*: p. 283-333.
[38] Poulev, A., O'Neal, J.M., Logendra, S., Pouleva, R.B., Timeva, V., Garvey, A.S., Gleba, D., Jenkins, I.S., Halpern, B.T., Kneer, R., Cragg, G.M., and Raskin, I.

(2003) Elicitation, a new window into plant chemodiversity and phytochemical drug discovery. *Journal of Medicinal Chemistry*, 46*(12)*: p. 2542-2547.

[39] Baenas, N., García-Viguera, C., and Moreno, D.A. (2014) Elicitation: A tool for enriching the bioactive composition of foods. *Molecules*, 19*(9)*: p. 13541-13563.

[40] Namdeo, A., Plant cell elicitation for production of secondary metabolites: A review. Vol. 1. 2007. 69-79.

[41] Aisyah, S., Gruppen, H., Andini, S., Bettonvil, M., Severing, E., and Vincken, J.-P. (2016) Variation in accumulation of isoflavonoids in Phaseoleae seedlings elicited by *Rhizopus*. *Food Chemistry*, 196: p. 694-701.

[42] The Plant List (2013) The Plant List > Angiosperms > Leguminosae. Version 1.1, http://www.theplantlist.org/1.1/browse/A/Leguminosae/ accessed 18 April 2018.

[43] van de Schans, M.G.M., Vincken, J.-P., de Waard, P., Hamers, A.R.M., Bovee, T.F.H., and Gruppen, H. (2016) Glyceollins and dehydroglyceollins isolated from soybean act as SERMs and ER subtype-selective phytoestrogens. *Journal of Steroid Biochemistry and Molecular Biology*, 156: p. 53-63.

[44] Veitch, N.C. and Grayer, R.J. (2008) Flavonoids and their glycosides, including anthocyanins. *Natural Product Reports*, 25*(3)*: p. 555-611.

[45] Simons, R., Gruppen, H., Bovee, T.F.H., Verbruggen, M.A., and Vincken, J.-P. (2012) Prenylated isoflavonoids from plants as selective estrogen receptor modulators (phytoserms). *Food & Function*, 3*(8)*: p. 810-827.

[46] Dixon, R.A. and Ferreira, D. (2002) Genistein. *Phytochemistry*, 60*(3)*: p. 205-211.

[47] Cushnie, T.P.T. and Lamb, A.J. (2011) Recent advances in understanding the antibacterial properties of flavonoids. *International Journal of Antimicrobial Agents*, 38*(2)*: p. 99-107.

[48] Cushnie, T.P.T. and Lamb, A.J. (2005) Antimicrobial activity of flavonoids. *International Journal of Antimicrobial Agents*, 26*(5)*: p. 343-356.

[49] Botta, B., Menendez, P., Zappia, G., de Lima, R.A., Torge, R., and Delle Monache, G. (2009) Prenylated isoflavonoids: Botanical distribution, structures, biological activities and biotechnological studies. An update (1995-2006). *Current Medicinal Chemistry*, 16*(26)*: p. 3414-3468.

[50] Araya-Cloutier, C., den Besten, H.M.W., Aisyah, S., Gruppen, H., and Vincken, J.-P. (2017) The position of prenylation of isoflavonoids and stilbenoids from legumes (Fabaceae) modulates the antimicrobial activity against Gram positive pathogens. *Food Chemistry*, 226: p. 193-201.

[51] Li, J.H., Chen, R.D., Wang, R.S., Liu, X., Xie, D., Zou, J.H., and Dai, J.G. (2014) GuA6DT, a regiospecific prenyltransferase from *Glycyrrhiza uralensis*, catalyzes the 6-prenylation of flavones. *Chembiochem*, 15*(11)*: p. 1672-1680.

[52] Akashi, T., Sasaki, K., Aoki, T., Ayabe, S., and Yazaki, K. (2009) Molecular cloning and characterization of a cDNA for pterocarpan 4-dimethylallyltransferase catalyzing the key prenylation step in the biosynthesis of glyceollin, a soybean phytoalexin. *Plant Physiology*, 149*(2)*: p. 683-693.

[53] Sasaki, K., Tsurumaru, Y., Yamamoto, H., and Yazaki, K. (2011) Molecular characterization of a membrane-bound prenyltransferase specific for isoflavone from *Sophora flavescens*. *Journal of Biological Chemistry*, 286*(27)*: p. 24125-24134.

[54] Sobolev, V.S., Horn, B.W., Potter, T.L., Deyrup, S.T., and Gloer, J.B. (2006) Production of stilbenoids and phenolic acids by the peanut plant at early stages of growth. *Journal of Agricultural and Food Chemistry*, 54*(10)*: p. 3505-3511.

[55] Smoliga, J.M., Baur, J.A., and Hausenblas, H.A. (2011) Resveratrol and health - a comprehensive review of human clinical trials. *Molecular Nutrition & Food Research*, 55*(8)*: p. 1129-1141.

[56] Yang, T., Fang, L., Rimando, A.M., Sobolev, V., Mockaitis, K., and Medina-Bolivar, F. (2016) A stilbenoid-specific prenyltransferase utilizes dimethylallyl

pyrophosphate from the plastidic terpenoid pathway. *Plant physiology*, 171*(4)*: p. 2483-2498.

[57] Araya-Cloutier, C., Vincken, J.-P., van Ederen, R., den Besten, H.M.W., and Gruppen, H. (2018) Rapid membrane permeabilization of *Listeria monocytogenes* and *Escherichia coli* induced by antibacterial prenylated phenolic compounds from legumes. *Food Chemistry*, 240: p. 147-155.

[58] Sobolev, V.S. (2013) Production of phytoalexins in peanut (*Arachis hypogaea*) seed elicited by selected microorganisms. *Journal of Agricultural and Food Chemistry*, 61*(8)*: p. 1850-1858.

[59] Sobolev, V.S., Krausert, N.M., and Gloer, J.B. (2016) New monomeric stilbenoids from peanut (*Arachis hypogaea*) seeds challenged by an *Aspergillus flavus* strain. *Journal of Agricultural and Food Chemistry*, 64*(3)*: p. 579-584.

[60] Sievert, D.M., Ricks, P., Edwards, J.R., Schneider, A., Patel, J., Srinivasan, A., Kallen, A., Limbago, B., Fridkin, S., Team, N., and Facilities, P.N. (2013) Antimicrobial-resistant pathogens associated with healthcare-associated infections: Summary of data reported to the National Healthcare Safety Network at the Centers for Disease Control and Prevention, 2009-2010. *Infection Control & Hospital Epidemiology*, 34*(1)*: p. 1-14.

[61] Frank, C., Werber, D., Cramer, J.P., Askar, M., Faber, M., an der Heiden, M., Bernard, H., Fruth, A., Prager, R., Spode, A., Wadl, M., Zoufaly, A., Jordan, S., Kemper, M.J., Follin, P., Muller, L., King, L.A., Rosner, B., Buchholz, U., Stark, K., Krause, G., and Team, H.I. (2011) Epidemic profile of shiga-toxin-producing *Escherichia coli* O104:H4 outbreak in germany. *The New England Journal of Medicine*, 365*(19)*: p. 1771-1780.

[62] Andrews, J.M. (2001) Determination of minimum inhibitory concentrations. *Journal of Antimicrobial Chemotherapy*, 48: p. 5-16.

[63] Jorgensen, J.H. and Ferraro, M.J. (2009) Antimicrobial susceptibility testing: A review of general principles and contemporary practices. *Clinical Infectious Diseases*, 49*(11)*: p. 1749-1755.

[64] Aryani, D.C., den Besten, H.M.W., Hazeleger, W.C., and Zwietering, M.H. (2015) Quantifying strain variability in modeling growth of *Listeria monocytogenes*. *International Journal of Food Microbiology*, 208: p. 19-29.

[65] Pagès, J.M., Masi, M., and Barbe, J. (2005) Inhibitors of efflux pumps in gram-negative bacteria. *Trends in Molecular Medicine*, 11*(8)*: p. 382-389.

[66] Araya-Cloutier, C., Vincken, J.-P., van de Schans, M.G.M., Hageman, J., Schaftenaar, G., den Besten, H.M.W., and Gruppen, H. (2018) QSAR-based molecular signatures of prenylated (iso)flavonoids underlying antimicrobial potency against and membrane-disruption in Gram positive and Gram negative bacteria. *Scientific Reports*, 8*(1)*: p. 9267.

[67] Mora-Pale, M., Bhan, N., Masuko, S., James, P., Wood, J., McCallum, S., Linhardt, R.J., Dordick, J.S., and Koffas, M.A. (2015) Antimicrobial mechanism of resveratrol-trans-dihydrodimer produced from peroxidase-catalyzed oxidation of resveratrol. *Biotechnology and Bioengineering*, 112*(12)*: p. 2417-2428.

[68] Akter, K., Barnes, E.C., Loa-Kum-Cheung, W.L., Yin, P., Kichu, M., Brophy, J.J., Barrow, R.A., Imchen, I., Vemulpad, S.R., and Jamie, J.F. (2016) Antimicrobial and antioxidant activity and chemical characterisation of *Erythrina stricta* Roxb. (Fabaceae). *Journal of Ethnopharmacology*, 185: p. 171-181.

[69] Bostanghadiri, N., Pormohammad, A., Chirani, A.S., Pouriran, R., Erfanimanesh, S., and Hashemi, A. (2017) Comprehensive review on the antimicrobial potency of the plant polyphenol resveratrol. *Biomedicine & Pharmacotherapy*, 95: p. 1588-1595.

[70] Yang, S.C., Tseng, C.H., Wang, P.W., Lu, P.L., Weng, Y.H., Yen, F.L., and Fang, J.Y. (2017) Pterostilbene, a methoxylated resveratrol derivative, efficiently eradicates planktonic, biofilm, and intracellular MRSA by topical application. *Frontiers in Microbiology*, 8: p. Article 1103.

[71] Ishak, S.F., Ghazali, A.R., Zin, N.M., and Basri, D.F. (2016) Pterostilbene enhanced anti-methicillin resistant *Staphylococcus aureus* (MRSA) activity of oxacillin. *American Journal of Infectious Diseases*, 12*(1)*: p. 1-10.

[72] Lee, W.X., Basri, D.F., and Ghazali, A.R. (2017) Bactericidal effect of pterostilbene alone and in combination with gentamicin against human pathogenic bacteria. *Molecules*, 22*(3)*.

[73] Hatano, T., Shintani, Y., Aga, Y., Shiota, S., Tsuchiya, T., and Yoshida, T. (2000) Phenolic constituents of licorice. VIII. Structures of glicophenone and glicoisoflavanone, and effects of licorice phenolics on methicillin-resistant *Staphylococcus aureus*. *Chemical & Pharmaceutical Bulletin*, 48*(9)*: p. 1286-1292.

[74] Parkar, S.G., Stevenson, D.E., and Skinner, M.A. (2008) The potential influence of fruit polyphenols on colonic microflora and human gut health. *International Journal of Food Microbiology*, 124*(3)*: p. 295-298.

[75] Lee, K.A., Moon, S.H., Lee, J.Y., Kim, K.T., Park, Y.S., and Paik, H.D. (2013) Antibacterial activity of a novel flavonoid, 7-O-butyl naringenin, against methicillin-resistant *Staphylococcus aureus* (MRSA). *Food Science and Biotechnology*, 22*(6)*: p. 1725-1728.

[76] Araya-Cloutier, C., 2018. Anti-MRSA assay results 6-prenylnaringenin and 8-prenylnaringenin, Laboratory of Food Chemistry, Wageningen University

[77] Dzoyem, J.P., Hamamoto, H., Ngameni, B., Ngadjui, B.T., and Sekimizu, K. (2013) Antimicrobial action mechanism of flavonoids from *Dorstenia* species. *Drug Discov Ther*, 7*(2)*: p. 66-72.

[78] Sato, M., Tanaka, H., Tani, N., Nagayama, M., and Yamaguchi, R. (2006) Different antibacterial actions of isoflavones isolated from *Erythrina poeppigiana* against methicillin-resistant *Staphylococcus aureus*. *Letters in Applied Microbiology*, 43*(3)*: p. 243-248.

[79] Wang, S.Y., Sun, Z.L., Liu, T., Gibbons, S., Zhang, W.J., and Qing, M. (2014) Flavonoids from *Sophora moorcroftiana* and their synergistic antibacterial effects on MRSA. *Phytotherapy Research*, 28*(7)*: p. 1071-1076.

[80] Fukai, T., Marumo, A., Kaitou, K., Kanda, T., Terada, S., and Nomura, T. (2002) Antimicrobial activity of licorice flavonoids against methicillin-resistant *Staphylococcus aureus*. *Fitoterapia*, 73*(6)*: p. 536-539.

[81] Fang, Y.J., Lu, Y.L., Zang, X.X., Wu, T., Qi, X.J., Pan, S.Y., and Xu, X.Y. (2016) 3D-QSAR and docking studies of flavonoids as potent *Escherichia coli* inhibitors. *Scientific Reports*, 6.

[82] Chen, R.D., Liu, X., Zou, J.H., Yin, Y.Z., Ou, B., Li, J.H., Wang, R.S., Xie, D., Zhang, P.C., and Dai, J.G. (2013) Regio- and stereospecific prenylation of flavonoids by *Sophora flavescens* prenyltransferase. *Advanced Synthesis & Catalysis*, 355*(9)*: p. 1817-1828.

[83] Sasaki, K., Mito, K., Ohara, K., Yamamoto, H., and Yazaki, K. (2008) Cloning and characterization of naringenin 8-prenyltransferase, a flavonoid-specific prenyltransferase of *Sophora flavescens*. *Plant Physiology*, 146*(3)*: p. 1075-1084.

[84] Wang, R.S., Chen, R.D., Li, J.H., Liu, X., Xie, K.B., Chen, D.W., Yin, Y.Z., Tao, X.Y., Xie, D., Zou, J.H., Yang, L., and Dai, J.G. (2014) Molecular characterization and phylogenetic analysis of two novel regio-specific flavonoid prenyltransferases from *Morus alba* and *Cudrania tricuspidata*. *Journal of Biological Chemistry*, 289*(52)*: p. 35815-35825.

[85] Yang, T.H., Fang, L.L., Sanders, S., Jayanthi, S., Rajan, G., Podicheti, R., Thallapuranam, S.K., Mockaitis, K., and Medina-Bolivar, F. (2018) Stilbenoid prenyltransferases define key steps in the diversification of peanut phytoalexins. *Journal of Biological Chemistry*, 293*(1)*: p. 28-46.

[86] Sopade, P.A. and Obekpa, J.A. (1990) Modeling water-absorption in soybean, cowpea and peanuts at 3 temperatures using peleg's equation. *Journal of Food Science*, 55*(4)*: p. 1084-1087.
[87] Simons, R., Vincken, J.-P., Bakx, E.J., Verbruggen, M.A., and Gruppen, H. (2009) A rapid screening method for prenylated flavonoids with ultra-high-performance liquid chromatography/electrospray ionisation mass spectrometry in licorice root extracts. *Rapid Communications in Mass Spectrometry*, 23*(19)*: p. 3083-3093.
[88] Søltoft, M., Jørgensen, L.N., Svensmark, B., and Fomsgaard, I.S. (2008) Benzoxazinoid concentrations show correlation with Fusarium Head Blight resistance in Danish wheat varieties. *Biochemical Systematics and Ecology*, 36*(4)*: p. 245-259.
[89] Marston, A. (2007) Role of advances in chromatographic techniques in phytochemistry. *Phytochemistry*, 68*(22-24)*: p. 2786-2798.
[90] Tanwir, F., Fredholm, M., Gregersen, P.L., and Fomsgaard, I.S. (2013) Comparison of the levels of bioactive benzoxazinoids in different wheat and rye fractions and the transformation of these compounds in homemade foods. *Food Chemistry*, 141*(1)*: p. 444-450.
[91] Araya-Cloutier, C., Martens, B., Schaftenaar, G., Leipoldt, F., Gruppen, H., and Vincken, J.-P. (2017) Structural basis for non-genuine phenolic acceptor substrate specificity of *Streptomyces roseochromogenes* prenyltransferase CloQ from the ABBA/PT-barrel superfamily. *Plos One*, 12*(3)*: p. e0174665.
[92] Haug-Schifferdecker, E., Arican, D., Brückner, R., and Heide, L. (2010) A new group of aromatic prenyltransferases in fungi, catalyzing a 2,7-dihydroxynaphthalene 3-dimethylallyl-transferase reaction. *Journal of Biological Chemistry*, 285*(22)*: p. 16487-16494.
[93] Haagen, Y., Unsöld, I., Westrich, L., Gust, B., Richard, S.B., Noel, J.P., and Heide, L. (2007) A soluble, magnesium-independent prenyltransferase catalyzes reverse and regular C-prenylations and O-prenylations of aromatic substrates. *Febs Letters*, 581*(16)*: p. 2889-2893.
[94] Bonitz, T., Zubeil, F., Grond, S., and Heide, L. (2013) Unusual N-prenylation in diazepinomicin biosynthesis: The farnesylation of a benzodiazepine substrate is catalyzed by a new member of the ABBA prenyltransferase superfamily. *Plos One*, 8*(12)*.
[95] Sasaki, K., Tsurumaru, Y., and Yazaki, K. (2009) Prenylation of flavonoids by biotransformation of yeast expressing plant membrane-bound prenyltransferase SfN8DT-1. *Bioscience Biotechnology and Biochemistry*, 73*(3)*: p. 759-761.
[96] Koopman, F., Beekwilder, J., Crimi, B., van Houwelingen, A., Hall, R.D., Bosch, D., van Maris, A.J.A., Pronk, J.T., and Daran, J.M. (2012) De novo production of the flavonoid naringenin in engineered Saccharomyces cerevisiae. *Microbial Cell Factories*, 11.
[97] Dong, X.W., Fan, Y.J., Yu, L.J., and Hu, Y.Z. (2007) Synthesis of four natural prenylflavonoids and their estrogen-like activities. *Archiv der Pharmazie*, 340*(7)*: p. 372-376.
[98] Khupse, R.S., Sarver, J.G., Trendel, J.A., Bearss, N.R., Reese, M.D., Wiese, T.E., Boué, S.M., Burow, M.E., Cleveland, T.E., Bhatnagar, D., and Erhardt, P.W. (2011) Biomimetic syntheses and antiproliferative activities of racemic, natural (-), and unnnatural (+) Glyceollin I. *Journal of Medicinal Chemistry*, 54*(10)*: p. 3506-3523.
[99] Uchihashi, K., Nakayashiki, H., Okamura, K., Ishihara, A., Tosa, Y., Park, P., and Mayama, S. (2011) *In situ* localization of avenanthramide A and its biosynthetic enzyme in oat leaves infected with the crown rust fungus, *Puccinia coronata* f. sp. *avenae*. *Physiological and Molecular Plant Pathology*, 76*(3-4)*: p. 173-181.
[100] Neves, M.P., Cidade, H., Pinto, M., Silva, A.M.S., Gales, L., Damas, A.M., Lima, R.T., Vasconcelos, M.H., and Nascimento, M.D.J. (2011) Prenylated derivatives of baicalein and 3,7-dihydroxyflavone: Synthesis and study of their effects on

tumor cell lines growth, cell cycle and apoptosis. *European Journal of Medicinal Chemistry*, 46*(6)*: p. 2562-2574.

[101] Smith, M.B. and March, J., Aliphatic substitution: Nucleophilic and organometallic, in *March's advanced organic chemistry*. 2006, John Wiley & Sons, Inc. p. 425-656.

[102] Hoarau, C. and Pettus, T.R.R. (2003) Strategies for the preparation of differentially protected *ortho*-prenylated phenols. *Synlett*, *(1)*: p. 127-137.

[103] Asioli, D., Aschemann-Witzel, J., Caputo, V., Vecchio, R., Annunziata, A., Naes, T., and Varela, P. (2017) Making sense of the "clean label" trends: A review of consumer food choice behavior and discussion of industry implications. *Food Research International*, 99: p. 58-71.

[104] The Plant List (2013) The Plant List > Angiosperms > Poaceae. Version 1.1, http://www.theplantlist.org/1.1/browse/A/Poaceae/ accessed 18-04-2018.

[105] Food and Agriculture Organization of the United Nations (2012) Crops, national. *FAOSTAT*, Rome, Italy.

[106] Du Fall, L.A. and Solomon, P.S. (2011) Role of cereal secondary metabolites involved in mediating the outcome of plant-pathogen interactions. *Metabolites*, 1*(1)*: p. 64-78.

[107] Bollina, V., Kumaraswamy, G.K., Kushalappa, A.C., Choo, T.M., Dion, Y., Rioux, S., Faubert, D., and Hamzehzarghani, H. (2010) Mass spectrometry-based metabolomics application to identify quantitative resistance-related metabolites in barley against *Fusarium* head blight. *Molecular Plant Pathology*, 11*(6)*: p. 769-782.

[108] Dinelli, G., Segura-Carretero, A., Di Silvestro, R., Marotti, I., Arráez-Román, D., Benedettelli, S., Ghiselli, L., and Fernadez-Gutierrez, A. (2011) Profiles of phenolic compounds in modern and old common wheat varieties determined by liquid chromatography coupled with time-of-flight mass spectrometry. *Journal of Chromatography A*, 1218*(42)*: p. 7670-7681.

[109] Schmelz, E.A., Huffaker, A., Sims, J.W., Christensen, S.A., Lu, X., Okada, K., and Peters, R.J. (2014) Biosynthesis, elicitation and roles of monocot terpenoid phytoalexins. *Plant Journal*, 79*(4)*: p. 659-678.

[110] Ejike, C.E.C.C., Gong, M., and Udenigwe, C.C. (2013) Phytoalexins from the Poaceae: Biosynthesis, function and prospects in food preservation. *Food Research International*, 52*(1)*: p. 167-177.

[111] Peters, R.J. (2006) Uncovering the complex metabolic network underlying diterpenoid phytoalexin biosynthesis in rice and other cereal crop plants. *Phytochemistry*, 67*(21)*: p. 2307-2317.

[112] Schmelz, E.A., Kaplan, F., Huffaker, A., Dafoe, N.J., Vaughan, M.M., Ni, X.Z., Rocca, J.R., Alborn, H.T., and Teal, P.E. (2011) Identity, regulation, and activity of inducible diterpenoid phytoalexins in maize. *Proceedings of the National Academy of Sciences of the United States of America*, 108*(13)*: p. 5455-5460.

[113] Zhou, K., Xu, M.M., Tiernan, M., Xie, Q., Toyomasu, T., Sugawara, C., Oku, M., Usui, M., Mitsuhashi, W., Chono, M., Chandler, P.M., and Peters, R.J. (2012) Functional characterization of wheat *ent*-kaurene(-like) synthases indicates continuing evolution of labdane-related diterpenoid metabolism in the cereals. *Phytochemistry*, 84: p. 47-55.

[114] Aach, H., Bose, G., and Graebe, J.E. (1995) *Ent*-kaurene biosynthesis in a cell-free system from wheat (*Triticum aestivum* L.) seedlings and the localization of *ent*-kaurene synthetase in plastids of 3 species. *Planta*, 197*(2)*: p. 333-342.

[115] Niemeyer, H.M. (2009) Hydroxamic acids derived from 2-hydroxy-2*H*-1,4-benzoxazin-3(4*H*)-one: Key defense chemicals of cereals. *Journal of Agricultural and Food Chemistry*, 57*(5)*: p. 1677-1696.

[116] Macías, F.A., Marín, D., Oliveros-Bastidas, A., Castellano, D., Simonet, A.M., and Molinillo, J.M.G. (2005) Structure-activity relationships (SAR) studies of benzoxazinones, their degradation products and analogues. Phytotoxicity on

standard target species (STS). *Journal of Agricultural and Food Chemistry*, 53*(3)*: p. 538-548.
[117] Adhikari, K.B., Tanwir, F., Gregersen, P.L., Steffensen, S.K., Jensen, B.M., Poulsen, L.K., Nielsen, C.H., Høyer, S., Borre, M., and Fomsgaard, I.S. (2015) Benzoxazinoids: Cereal phytochemicals with putative therapeutic and health-protecting properties. *Molecular Nutrition & Food Research*, 59*(7)*: p. 1324-1338.
[118] Gleńsk, M., Gajda, B., Franiczek, R., Krzyżanowska, B., Biskup, I., and Włodarczyk, M. (2016) In vitro evaluation of the antioxidant and antimicrobial activity of DIMBOA [2,4-dihydroxy-7-methoxy-2*H*-1,4-benzoxazin-3(4*H*)-one]. *Natural Product Research*, 30*(11)*: p. 1305-1308.
[119] Fang, L., Zuo, H., Li, Z.B., He, X.Y., Wang, L.Y., Tian, X., Zhao, B.X., Miao, J.Y., and Shin, D.S. (2011) Synthesis of benzo[b][1,4]oxazin-3(4*H*)-ones via smiles rearrangement for antimicrobial activity. *Medicinal Chemistry Research*, 20*(6)*: p. 670-677.
[120] Macoy, D.M., Kim, W.Y., Lee, S.Y., and Kim, M.G. (2015) Biotic stress related functions of hydroxycinnamic acid amide in plants. *Journal of Plant Biology*, 58*(3)*: p. 156-163.
[121] Collins, F.W. (1989) Oat phenolics - avenanthramides, novel substituted N-cinnamoylanthranilate alkaloids from oat groats and hulls. *Journal of Agricultural and Food Chemistry*, 37*(1)*: p. 60-66.
[122] Meydani, M. (2009) Potential health benefits of avenanthramides of oats. *Nutrition Reviews*, 67*(12)*: p. 731-735.
[123] Bird, C.R. and Smith, T.A. (1981) The biosynthesis of coumarylagmatine in barley seedlings. *Phytochemistry*, 20*(10)*: p. 2345-2346.
[124] Jin, S. and Yoshida, M. (2000) Antifungal compound, feruloylagmatine, induced in winter wheat exposed to a low temperature. *Bioscience Biotechnology and Biochemistry*, 64*(8)*: p. 1614-1617.
[125] Mayama, S., Matsuura, Y., Iida, H., and Tani, T. (1982) The role of avenalumin in the resistance of oat to crown rust, *Puccinia coronata* f. sp. *avenae*. *Physiological Plant Pathology*, 20*(2)*: p. 189-199.
[126] von Röpenack, E., Parr, A., and Schulze-Lefert, P. (1998) Structural analyses and dynamics of soluble and cell wall-bound phenolics in a broad spectrum resistance to the powdery mildew fungus in barley. *Journal of Biological Chemistry*, 273*(15)*: p. 9013-9022.
[127] Muroi, A., Ishihara, A., Tanaka, C., Ishizuka, A., Takabayashi, J., Miyoshi, H., and Nishioka, T. (2009) Accumulation of hydroxycinnamic acid amides induced by pathogen infection and identification of agmatine coumaroyltransferase in arabidopsis thaliana. *Planta*, 230*(3)*: p. 517-527.
[128] Stoessl, A. and Unwin, C.H. (1970) The antifungal factors in barley. V. Antifungal activity of the hordatines. *Canadian Journal of Botany*, 48*(3)*: p. 465-470.
[129] Corcuera, L.J. (1993) Biochemical basis for the resistance of barley to aphids. *Phytochemistry*, 33*(4)*: p. 741-747.
[130] Liu, D.L. and Lovett, J.V. (1993) Biologically-active secondary metabolites of barley. II. Phytotoxicity of barley allelochemicals. *Journal of Chemical Ecology*, 19*(10)*: p. 2231-2244.

CHAPTER 2

Antibacterial prenylated stilbenoids from peanut

Stilbenoids are a class of secondary metabolites with a stilbene backbone that can be produced by peanut (*Arachis hypogaea*) as defence metabolites. Six monomeric prenylated stilbenoids, including the compound arachidin-6 (**4**), were isolated from extracts of fungus-elicited peanuts using preparative liquid chromatography. Their structures were confirmed by MS^n, HRMS and NMR spectroscopy and their antibacterial activity was evaluated against methicillin-resistant *Staphylococcus aureus* (MRSA). Similarly to other phenolic compounds, prenylated derivatives of stilbenoids were more active than their non-prenylated precursors piceatannol, resveratrol, and pinosylvin. Chiricanine A (**6**), a chain-prenylated pinosylvin derivative, was the most potent compound tested, with a minimum inhibitory concentration (MIC) of 12.5 μg mL^{-1}. Arachidin-6 (**4**), a ring-prenylated piceatannol derivative, had moderate potency (MIC 50-75 μg mL^{-1}). A pool of dimeric prenylated stilbenoids, including arahypin-6, had an MIC of 25 μg mL^{-1}. In conclusion, prenylated stilbenoids represent a group of potential natural antibacterials which show promising activity against MRSA.

Adapted from: Wouter J. C. de Bruijn, Carla Araya-Cloutier, Judith Bijlsma, Anne de Swart, Mark G. Sanders, Pieter de Waard, Harry Gruppen, and Jean-Paul Vincken (2018) Antibacterial prenylated stilbenoids from peanut (*Arachis hypogaea*), *Phytochemistry Letters*, 28: p. 13-18.

2.1. Introduction

Stilbenoids, a class of secondary metabolites with a stilbene backbone (**Figure 2.1A**), can be produced by peanut (*Arachis hypogaea*) as defence metabolites.[1] Analogous to phenolic metabolites of other members of the *Leguminosae* family, e.g. soy bean and lmung bean,[2,3] the production of stilbenoids and, in particular, their prenylated derivatives can be stimulated by fungal elicitation of germinating peanut seeds.[4-6] Prenylation refers to the attachment of a prenyl-moiety (i.e. 3,3-dimethylallyl) by a prenyltransferase and in the case of peanut stilbenoids occurs mainly at the 4-position[7] as in, for example, arachidin-2 (**Figure 2.1B,** compound **2**).[5]

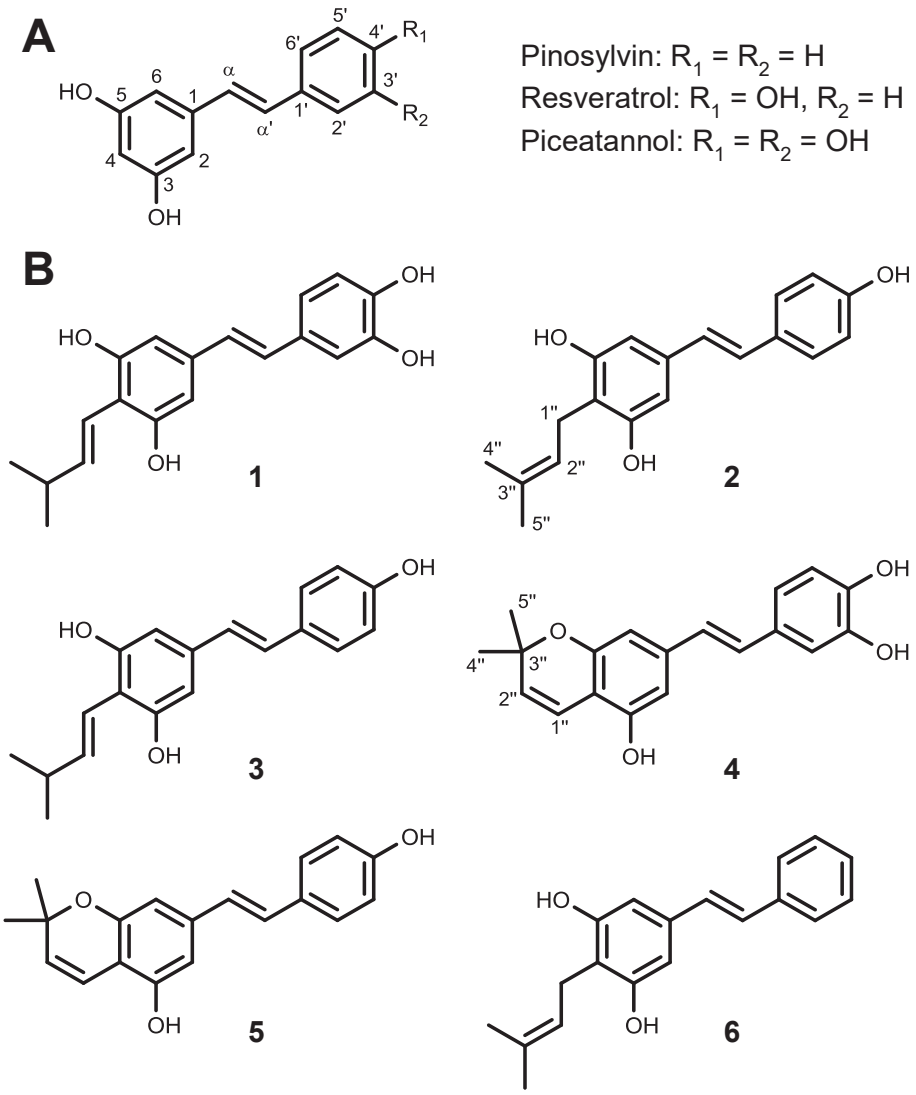

Figure 2.1. A, natural stilbenoids with a stilbene backbone. **B**, prenylated stilbenoids isolated in this work: **1**, arachidin-1; **2**, arachidin-2; **3**, arachidin-3; **4**, arachidin-6; **5**, arahypin-5; and **6**, chiricanine A.

Prenylation of phenolic compounds has been shown to increase their antibacterial activity, which is exemplified by the minimum inhibitory concentrations (MICs) of genistein (MIC >128 µg mL^{-1}), 6-prenyl-genistein (MIC 32 µg mL^{-1}), and 6,8-diprenyl-genistein (MIC 8 µg mL^{-1}) against methicillin-resistant *Staphylococcus aureus* (MRSA).[8] More generally, prenylated (iso)flavonoids have been shown to possess antibacterial activity against antibiotic-resistant strains of *S. aureus* and other pathogenic gram-positive bacteria.[9-11] An extract from fungus (*Rhizopus*) elicited peanut seedlings, enriched in prenylated stilbenoids, already showed promising antibacterial activity against *E. coli*, *L. monocytogenes* and MRSA.[9,12] In this study, we have isolated and characterized several prenylated compounds with different stilbenoid precursors and prenyl configurations from an extract of *Rhizopus*-elicited peanut seedlings and assessed their antibacterial activity against MRSA. In analogy with other phenolic compounds, we hypothesize that prenylation of stilbenoids will enhance their antibacterial activity.

2.2. Materials and methods

2.2.1. General experimental procedures

NMR Spectra were recorded on a Bruker Avance-III-600 spectrometer, equipped with a cryo-probe. Compounds **1**, **2**, **4**, and **5** were dissolved in 0.5 mL methanol-d_4 (99.9 atom%, Isotec); compounds **3** and **6** were dissolved in 0.5 mL chloroform-d (99.9 atom%, Isotec). ^{1}H and ^{13}C NMR spectra were recorded at a probe temperature of 300 K. Chemical shifts are expressed in ppm relative to internal TMS at 0.00 ppm, but were actually measured to the residual solvent signals of methanol (δC = 49.00 ppm, δH = 3.31 ppm) or chloroform (δC = 77.16 ppm, δH = 7.26 ppm). For all compounds, 1D ^{1}H spectra were acquired. For compound **4**, additional 1D ^{13}C and 2D COSY, HMBC, and HMQC spectra were acquired. ESI-IT-MS^n spectra were acquired on an LTQ Velos Pro linear ion trap mass spectrometer (Thermo Scientific, San Jose, CA, USA) equipped with a heated ESI probe coupled *in-line* to the Accela RP-UHPLC system (Thermo Scientific). The Accela UHPLC system was used in the same configuration as previously described.[13] The flow rate was 300 µL min^{-1} at a column temperature of 35 °C. Eluents used were water (A) and MeOH (B), both with 0.1% (*v/v*) formic acid. The elution profile can be found in the supplementary information. Detection wavelengths for UV−Vis were set to the range of 200-600 nm and data were recorded at 20 Hz. High resolution mass data were acquired on a Thermo Q Exactive Focus hybrid quadrupole-orbitrap mass spectrometer (Thermo Scientific) equipped with a heated ESI probe (ESI-FTMS) coupled *in-line* to the Vanquish RP-UHPLC system. The Vanquish UHPLC system (Thermo Scientific) in the same configuration and with the same column as described previously.[13] The samples were eluted with water (A) and ACN (B), both with 0.1% (*v/v*) formic acid with a flow rate of 400 µL min^{-1} at 45 °C. The elution profile can be found in the supplementary information. A Waters Acquity BEH C18 2.1 × 150 mm, 1.7 µm particle size column with a Waters VanGuard 2.1

× 5 mm guard column of the same material was used for all analytical RP-UHPLC separations. Flash chromatography was performed on a Reveleris Flash chromatography system (Grace, Columbia, MD, USA). A Reveleris C18 RP 80 g cartridge (particle size 40 µm) was eluted with water (A) and MeOH (B), both with 1% (*v/v*) formic acid, at room temperature at a flow rate of 60 mL min^{-1}. Preparative chromatography was performed on a Waters preparative RP-HPLC-MS system (Waters, Milford, MA, USA) as previously described.[14] The column used was a Waters XBridge Prep C18 OBD column (19 × 250 mm, 5 µm particle size) and was eluted with water (A) and ACN (B), both with 1% (*v/v*) formic acid, at room temperature at a flow rate of 17 mL min^{-1}.

2.2.2. Chemicals

Sodium hypochlorite 47/50% (*w/v*) solution (~13% active Cl) was obtained from Chem-Lab (Zedelgem, Belgium). Technical grade *n*-hexane 98% (*v/v*) was obtained from VWR International (Radnor, PA, USA). UHPLC-MS grade solvents and HPLC grade ACN (for preparative chromatography) were purchased from Biosolve (Valkenswaard, The Netherlands). *trans*-Piceatannol >98% (*w/w*) and *trans*-resveratrol ≥98% (*w/w*) were purchased from Cayman Chemical (Ann Arbor, MI, USA). *trans*-Pinosylvin ≥97% (*w/w*) and *tert*-butanol ≥98% (*w/w*) were purchased from Sigma-Aldrich (St. Louis, MO, USA). Water (MQ) for other purposes than UHPLC was prepared using a Milli-Q water purification system (Merck Millipore, Billerica, MA, USA). Ethanol absolute ≥99.9% (*v/v*) was purchased from Merck Millipore.

2.2.3. Plant and fungal material

Peeled peanuts (*Arachis hypogaea*) with skin for feed purposes were purchased locally. Dried *Rhizopus* culture was purchased as tempeh starter culture from TopCultures (Zoersel, Belgium).

2.2.4. Peanut germination and elicitation with *Rhizopus*

Peanuts were surface-sterilized by soaking in a 1% (*w/v*) hypochlorite solution (5 L kg^{-1} seeds) for 15 min at room temperature and were then rinsed with demineralized water. Surface-sterilized peanuts were germinated in the dark in a pilot-scale two-tank steep germinator (Custom Laboratory Products, Keith, UK). The cleaning procedure, trays, and setup of the germinator were the same as described previously.[13] In total 3 kg of peanuts were germinated in two identical experiments. Approximately 300 g peanuts were placed in each of the five tray compartments that were lined with disinfected cellulose filter paper (Whatman 595 ½, folded, 320 mm). The program set in the germinator was as follows: soaking for 16 h at 25 °C (aeration 1 min every 10 min), followed by germination for 48 h at 25 °C. The germinating peanuts were then inoculated by pouring the *Rhizopus* starter culture (0.2 L kg^{-1} peanuts equalling approximately 2 × 10^5 CFU g^{-1} peanuts) over them. Prior to application, the starter culture was rehydrated with

peptone physiological salt solution (Tritium Microbiologie, Eindhoven, The Netherlands) (100 mg mL^{-1}) and incubated for 1 h at 37 °C. After fungal inoculation, peanuts were incubated for 72 h at 30 °C. During the entire process, relative humidity (RH) was controlled by periodical aeration with humidified air, RH of the air supplied to the tanks was maintained between 60-83% (monitored by germinator), resulting in RH of 82-95% inside the tanks (measured externally). The described conditions proved to be effective to ensure germination of the seeds as well as growth of the fungus. At the end of the experiment, the peanuts were frozen and stored at -20 °C until further processing.

2.2.5. Extraction and isolation

Peanut seedlings were extracted according to a method adapted from Sobolev and co-workers.[15] In short, the elicited peanut seedlings were defatted by continuous Soxhlet extraction with *n*-hexane for 5 h. The defatted peanut seedlings were then extracted with MeOH in a blender for 1 min (1 L MeOH per 200 g seedlings). The suspension was filtered over a paper filter under reduced pressure and the retentate peanut pulp was subjected to one more identical extraction. The methanolic extracts were combined and defatted once more by liquid-liquid partitioning with *n*-hexane (hexane:MeOH, 1:3). The defatted methanolic extract was filtered over cellulose filter paper (Whatman 595 ½, folded, 320 mm) and the MeOH was evaporated under reduced pressure to yield the crude extract. Exposure to light was avoided where possible during further sample preparation and purification. In order to remove polar impurities, the dried crude extract was then suspended in ethyl acetate (33 mg mL^{-1}), subjected to an ultrasonic bath for 10 min, and centrifuged (10 min, 4,000 × *g*). The supernatant, containing the prenylated stilbenoids, was collected while the pellet, containing mostly polar impurities, was discarded. The supernatant was evaporated to dryness under reduced pressure, recollected using *tert*-butanol and lyophilised to yield the cleaned extract. Cleaned extracts were pre-purified using Flash chromatography. The sample was solubilised in MeOH acidified with 1% (*v/v*) FA (final sample concentration 300-500 mg mL^{-1}) and was manually injected (1.0-2.5 g per run). The elution profile used can be found in the supplementary information. The collected fractions were analysed by RP-UHPLC-PDA-ESI-IT-MS^n and those containing similar compounds were pooled. The MeOH was removed under reduced pressure and the remaining water was removed by lyophilisation.

The pools obtained from Flash chromatography were further purified using a Waters preparative RP-HPLC system (Waters, Milford, MA, USA) as previously described.[14] Pools were solubilised at 2 mg mL^{-1} in 50% (*v/v*) aqueous MeOH and injected (2.0-2.5 mL) on a Waters XBridge Prep C18 OBD column (19 × 250 mm, 5 µm particle size) and were eluted with water (A) and ACN (B), both with 1% (*v/v*) formic acid, at room temperature at a flow rate of 17 mL min^{-1}. The elution profile used for each compound can be found in the supplementary information. Data was acquired and analysed by MassLynx (version 4.1, Waters). The collected

fractions were analysed by RP-UHPLC-PDA-ESI-IT-MS^n. Based on the analysis, fractions containing the same compound were pooled and the ACN was evaporated under a stream of N_2. The remaining water phase was immediately frozen and lyophilised.

2.2.6. Micro-broth dilution assay

Compounds **1**-**6** were tested for their antibacterial activity against the gram-positive bacterium methicillin-resistant *Staphylococcus aureus* (MRSA) (18HN, spa type t034; RIVM, Bilthoven, The Netherlands), according to a previously described method.[9] The final inoculum size used was 4.2 ± 0.2 $\log_{10}$ CFU mL^{-1}. Final concentrations tested ranged from 6.25 to 200 µg mL^{-1}, depending on the amount of material available, with a maximum of 2.1% (*v/v*) ethanol in the final solution. Stock solutions of the tested compounds were prepared in 70% (*v/v*) aqueous ethanol. Prior to the micro-broth dilution assay, the stocks were diluted in tryptone soy broth (TSB) (Oxoid, Basingstoke, UK). Equal volumes (100 µL) of the diluted compound and of inoculum were transferred to each well of a 96-well plate. Inoculum with vancomycin (VWR International) (final concentration of 4 µg mL^{-1}) was used as a positive control. Inoculum with sterile TSB containing 2.1% (*v/v*) ethanol was used as a negative control. All compounds were tested in at least two independent biological replicates. The 96-well plate was covered with a gas-permeable imaging seal (4Titude, Wotton, UK) and incubated in a SpectraMax M2e (Molecular Devices, Sunnyvale, CA, USA) at 37 °C for 24 h with constant linear shaking. The optical density at 600 nm (OD_{600}) was measured every 5 min. Time-to-detection (TTD) was defined as the time (h) to reach a difference of 0.05 units from the initial OD_{600}.[9,12] If no measurable increase in OD_{600} was observed, the TTD was defined as >24 h and the tested concentration was considered to be inhibitory. The minimum inhibitory concentration (MIC) was defined as the lowest concentration of each compound that was found to be inhibitory. The TTD of the negative control with 2.1% (*v/v*) ethanol was 5.6 h (standard deviation ± 0.1 h) (average of four independent biological replicates, each with triplicates). For comparison of the compounds, TTD at concentrations of 25 and 50 µg mL^{-1}, respectively TTD_{25} and TTD_{50}, were determined.

2.3. Results and discussion

2.3.1. Sample clean-up, pre-purification and purification by preparative RP-HPLC

The crude extract of *Rhizopus*-elicited peanut seedlings showed a chromatographic profile on RP-UHPLC comparable to what was described previously.[4] The clean-up with ethyl acetate effectively removed the majority of polar impurities in the extract, yielding the cleaned extract which contained mainly prenylated stilbenoids (**Figure S2.1**, supplementary information, 6-19 min) and apolar impurities

(**Figure S2.1**, 19-28 min) which, based on LC-MS analysis, were mostly lipids like oxylipins and free fatty acids.[16] After pre-purification by Flash chromatography, most of the apolar impurities were removed and several pools were obtained enriched in mixtures of prenylated stilbenoids and some oxylipins (**Figure S2.1**). After subjecting these pools to preparative RP-HPLC separation, six purified compounds were obtained.

2.3.2. Structure elucidation of the prenylated stilbenoids

The six compounds that were isolated were first analysed by UHPLC-PDA-ESI-IT-MS, the corresponding spectrometric and spectroscopic data of which is shown in **Table 2.1**. Based on the comparison of this data to literature,[4,15,17] the compounds were tentatively annotated. For most purified compounds, the *trans* isomer was most abundant but the *cis* isomer was also present. The two isomers were distinguished by their λ_{max}, and the peak with the higher λ_{max} was assigned as the *trans* isomer, in accordance with previously reported data.[18] Based on UV_{310} area compound **1** was approximately 60% *trans*, compound **3** was approximately 88% *trans*, and compounds **2**, **4**, **5** and **6** were all more than 97% *trans*. Spectrometric and spectroscopic data provided is based on the *trans* isomer.

In ESI-IT-MS (**Table 2.1**), the most abundant fragments observed for compounds **1**-**3** and **6** in negative ionisation mode were those with a neutral loss (NL) of 56 u (C_4H_8) and NL of 69 or 70 u, corresponding to complete loss of the prenyl chain (as C_5H_8 or C_5H_9). In positive ionisation mode the main fragments were also related to the prenyl-moiety, resulting in a NL of 56 u (C_4H_8), as described previously for chain-prenylated (iso)flavonoids.[19] For compounds **4** and **5** the main fragment observed in positive ionisation mode, *m/z* 201, corresponded to loss of the catechol (NL 110 u, $C_6H_4O_2$) or phenol (NL 94 u, C_6H_4O) moiety, respectively. Fragments corresponding to neutral losses of 56 u and 42 u were also observed. For compound **4** the fragment at *m/z* 269 (NL 42 u, rel. abundance 25) was more intense than the fragment at *m/z* 255 (NL 56 u, rel. abundance 13, not shown in **Table 2.1**).

HMBC and HMQC were performed in order to elucidate the structure of compound **4** (see **Table 2.2** for the ^1H and ^{13}C NMR spectroscopic data). The ^{13}C NMR spectrum showed signals identical to those described for the catechol moiety of arachidin-1.[20] These signals were thereby assigned as aromatic carbons C-1′ to C-6′. Based on the HMBC and HMQC cross peaks of these carbons, the three ^1H NMR signals at δ_H 6.974 (d, *J* = 2.0 Hz, H-2′), 6.737 (d, *J* = 8.2 Hz, H-5′), and 6.835 (dd, *J* = 8.2 and 2.0 Hz, H-6′) were assigned as the corresponding protons. The olefin carbons C-α (δ_C 126.75) and C-α′ (δ_C 129.69) showed HMQC cross peaks with two doublet proton signals at δ_H 6.721 (*J* = 16.2 Hz, H-α) and 6.889 (*J* = 16.2 Hz, H-α′), whose coupling constants confirmed the *trans*-olefin. Both of these protons showed cross peaks with aromatic carbons C-1′ and C-1 (δ_C 140.23). Proton H-α also showed HMBC cross peaks with ^{13}C NMR signals δ_C 106.47 (C-6) and 106.79 (C-2). The ^1H NMR signals δ_H 6.418 (bs, H-2) and 6.475 (d, *J* = 1.3 Hz, H-6) were assigned by their HMQC cross peaks to C-2 and C-6, respectively.

Table 2.1. Spectrometric and spectroscopic data of purified compounds as determined by UHPLC-PDA coupled to ESI-IT-MS and ESI-FTMS.

			IT-MS				FTMS	
Comp. [a]	λ_{max} (nm)	Ionisation	*m/z* precursor	MS^2 product ions (relative abundance) [b]	Molecular formula	*m/z* calc.	*m/z* obs. [c]	Error (ppm)
1	339	$[M-H]^-$	311	241, 242 (93), 312 (76), 255 (46), 267 (45), 311 (31), 293 (25), 224 (20), 172 (16)	$C_{19}H_{20}O_4$	311.12888	311.12907	0.60
		$[M+H]^+$	313	257				
2	322	$[M-H]^-$	295	239, 296 (55), 240 (43), 226 (42), 295 (38)	$C_{19}H_{20}O_3$	295.13397	295.13388	-0.30
		$[M+H]^+$	297	241				
3	338	$[M-H]^-$	295	239, 240 (48), 226 (31), 295 (26), 227 (25), 251 (18)	$C_{19}H_{20}O_3$	295.13397	295.13402	0.18
		$[M+H]^+$	297	241				
4	342	$[M-H]^-$	309	309, 310 (63), 265 (60), 291 (24), 294 (21), 281 (18)	$C_{19}H_{18}O_4$	309.11323	309.11334	0.35
		$[M+H]^+$	311	201, 283 (55), 135 (50), 187 (40), 177 (30), 293 (29), 123 (28), 269 (25), 175 (22), 183 (20), 173 (19), 265 (17), 189 (16), 202 (16)				
5	339	$[M-H]^-$	293	293, 278 (47), 294 (35)	$C_{19}H_{18}O_3$	293.11832	293.11847	0.52
		$[M+H]^+$	295	201, 267 (93), 253 (51), 175 (37), 107 (37), 277 (32), 183 (28), 225 (24), 239 (23), 173 (19), 159 (18), 119 (18), 249 (15)				
6	312	$[M-H]^-$	279	224, 223 (85), 279 (66), 280 (50), 211 (15)	$C_{19}H_{20}O_2$	279.13905	279.13914	0.31
		$[M+H]^+$	281	225				

[a] Data provided based on the *trans* isomer. [b] Most abundant fragment is underlined, only fragment ions with a relative abundance of at least 15 are shown. [c] Based on the average of 5 spectra in negative ionisation mode.

These chemical shifts and their HMBC cross peaks were comparable to those described for arahypin-5.[15] Analogous to arahypin-5 and arachidin-1 the carbon signal δ_C 110.23 (C-4) showed HMBC cross peaks with H-2 and H-6 and did not have any HMQC cross peaks, indicating that the prenyl was attached at C-4. The remaining ^{13}C NMR signals were consistent with spectroscopic data of C-3 (δ_C 155.26), C-5 (δ_C 154.42) and the five carbons of the prenyl group reported for arahypin-5.[15] The signal of C-3″ (δ_C 76.77) was downfield compared to arachidin-1, which indicated that the prenyl was cyclised to a pyran as in arahypin-5. The remaining ^{1}H NMR signals and their HMBC cross peaks corresponded to those described for arahypin-5.[15] To the best of our knowledge the elucidated structure, a ring-prenylated piceatannol derivative, has not been previously reported. Consequently, compound **4** was identified as the new compound**,** 7-[(*E*)-2-(3,4-dihydroxyphenyl)ethenyl]-2,2-dimethylchromen-5-ol, herein named arachidin-6. The structures of compounds **1**-**6** are shown in **Figure 2.1B**.

Table 2.2. 1H (600 MHz) and 13C (150 MHz) NMR Spectroscopic data of arachidin-6 (**4**) recorded in methanol-d4 at 300K (δ in ppm, J in Hz).

Arachidin-6 **(4)**		
Position	**δ_C, type**	**δ_H, mult. (*J* in Hz) [a]**
1	140.23, C	
2	106.79, CH	6.418, bs
3	155.26, C	
4	110.23, C	
5	154.42, C	
6	106.47, CH	6.475, d (1.3)
α	126.75, CH	6.721, d (16.2)
α′	129.69, CH	6.889, d (16.2)
1′	131.02, C	
2′	113.83, CH	6.974, d (2.0)
3′	146.51, C	
4′	146.60, C	
5′	116.43, CH	6.737, d (8.2)
6′	120.27, CH	6.835, dd (8.2, 2.0)
1″	118.23, CH	6.626, d (9.9)
2″	129.10, CH	5.568, d (9.8)
3″	76.77, C	
4″	28.01, CH_3	1.391, s
5″	28.01, CH_3	1.391, s

[a] bs, broad singlet; d, doublet; dd, doublet of doublets; s, singlet.

Prenyl chains in (iso)flavonoids and chalcones have been described to be liable to cyclisation under acidic conditions.[21,22] Thus, it might be argued compound **4** might be an artefact formed due to the addition of 1% (*v/v*) formic acid in the preparative chromatography eluent. Acid-catalysed cyclisation of a prenyl chain,

however, typically yields a dihydropyran,[21,22] whereas the prenyl in compound **4** is present as a pyran as evidenced by the structure elucidation. It was, therefore, concluded that the compound as such was present in the elicited peanut seedlings.

2.3.3. Stability and antibacterial activity of prenylated stilbenoids

During the purification process, the prenylated stilbenoids were prone to both *trans-cis* isomerisation, as was previously reported,[18] and dimerization. The compounds' reactivity could potentially be of influence on their antimicrobial activity. Therefore, the stability of the compounds during the antibacterial assay was assessed by incubating them under normal assay conditions. Under these conditions, no further *trans* to *cis* isomerisation or dimerization was observed for compounds **2**-**6** (**Figure S2.2**, supplementary information). Arachidin-1 (**1**) was not included due to low amounts of available material. However, we assumed its stability during the assay would be similar to that of the other five compounds. Thus, we did not expect any influence of isomerization or dimerization on the antibacterial assay results.

The antibacterial activity of arachidin-1 (**1**), arachdin-2 (**2**), arachidin-3 (**3**), arachidin-6 (**4**), arahypin-5 (**5**), and chiricanine A (**6**) against MRSA was assessed. For reference, non-prenylated stilbenoids piceatannol (precursor of arachidin-1 (**1**) and -6 (**4**)), resveratrol (precursor of arachidin-2 (**2**) and -3 (**3**) and arahypin-5 (**5**)), and pinosylvin (precursor of chiricanine A (**6**)) were also tested. The resulting MIC and TTD values are shown in **Table 2.3**, together with some structural properties of these molecules. For resveratrol and piceatannol, no MIC was found below 200 μg mL^{-1}. Therefore, they were considered not to be active antibacterials. The attachment of a prenyl-moiety to these precursors increased the resulting molecule's antibacterial activity, as expected. For example, resveratrol had an MIC of > 200 μg mL^{-1} (> 877 μM) and its ring-prenylated derivative arahypin-5 (**5**) had an MIC of 25-50 μg mL^{-1} (85-170 μM), thus the prenyl group enhanced activity by up to ten fold in this case. No MIC was found below 50 μg mL^{-1} for arachidin-1 (**1**), arachidin-2 (**2**), or arachidin-3 (**3**). Based on the TTD_{50} (time-to-detection at 50 μg mL^{-1}) values of these compounds, arachidin-2 (**2**) was the most active of the three. In addition, the TTD_{50} and TTD_{25} values obtained for these compounds indicated that they were less active than compounds **4**-**6** and, especially arachidin-1 (**1**) and arachidin-3 (**3**), were only marginally more active than non-prenylated resveratrol and piceatannol. The new compound, arachidin-6 (**4**), showed moderate activity with MIC at 50-75 μg mL^{-1}. The prenylated pinosylvin derivative, chiricanine A (**6**), was the most active compound tested in this work with an observed MIC of 12.5 μg mL^{-1} (44 μM) against MRSA, which is quite promising and in range of that of some traditional antibiotics.[23]

Table 2.3. Structural characteristics, purity, and antibacterial activity of piceatannol, resveratrol, pinosylvin and the purified prenylated stilbenoids against MRSA.

Compound	Precursor	Prenyl configuration, type	No. of H-bond donors	$LogD_{7.2}$ [a]	Purity (%) [b]			MIC (µg mL^{-1})	TTD_{25} (± StDev) (h) [c]	TTD_{50} (± StDev) (h) [c]
					UV_{310}	MS (NI)	^1H NMR			
Piceatannol	n.a.	n.a.	n.a.	3.06	99	99	n.d.	>200	5.4 (± 0.1)	6.3 (± 0.3)
Resveratrol	n.a.	n.a.	n.a.	3.38	≥99	98	n.d.	>200	6.0 (± 0.1)	6.9 (± 0.7)
Pinosylvin	n.a.	n.a.	n.a.	3.69	≥99	≥99	n.d.	≤100 [d]	n.d. [d]	n.d. [d]
Arachidin-1	pice	chain, 3m1b	4	4.93	87	88	80	>50	6.1 (± 0.6)	8.4 (± 0.5)
Arachidin-2	resv	chain, 3m2b	3	5.10	98	89	95	>50	7.4 (± 0.5)	17.1 (± 3.0)
Arachidin-3	resv	chain, 3m1b	3	5.23	80	63	60	>50	6.6 (± 1.2)	8.6 (± 1.8)
Arachidin-6	pice	ring	3	4.27	96	96	n.d.	50-75 [e]	11.5 (± 2.2)	21.5 (± 0.5) - >24 [e]
Arahypin-5	resv	ring	2	4.58	99	94	80	25-50 [e]	9.6 (± 4.2) - >24 [e]	>24 (± n.a.)
Chiricanine A	pino	chain, 3m2b	2	5.40	99	98	99	12.5 [e]	>24 (± n.a.)	>24 (± n.a.)

n.a., not applicable; n.d., not determined; resv., resveratrol; pice, piceatannol; pino, pinosylvin; 3m1b, 3-methyl-1-butene, 3m2b; 3-methyl-2-butene. [a] $LogD_{7.2}$, calculated octanol-water partitioning coefficient at pH 7.2, as calculated using MarvinSketch 17.2.27 with default settings. [b] Combined purity of the *trans* and *cis* isomers of the purified compounds. UV_{310}, based on total peak area in UHPLC-PDA at 310 nm; MS (NI), based on total peak area in UHPLC-ESI-MS negative ionisation mode (*m/z* range 200-1500); ^1H NMR, based on the aromatic region in proton NMR spectroscopy. [c] TTD_{25}, time-to-detection at 25 µg mL^{-1}; TTD_{50}, time-to-detection at 50 µg mL^{-1}. [d] Pinosylvin was only tested in the concentration range 100-400 µg mL^{-1} (one biological experiment, triplicate measurement). [e] Determined in four independent biological replicates, ranges indicate that MIC and TTD varied between experiments.

2.3.4. Structure-activity relationships of prenylated stilbenoid monomers against MRSA

The antimicrobial activity of prenylated phenolics has been related to the increased hydrophobicity conferred by the addition of the prenyl-group.[24] Chiricanine A (**6**) possessed the highest $LogD_{7.2}$ of the six purified compounds. The anti-MRSA activity of compounds **1**-**6** (expressed as TTD_{25}, using 24 h if TTD > 24 h) was, however, not correlated to their $LogD_{7.2}$ (r = 0.002). The lack of a correlation between activity and hydrophobicity has been previously described for prenylated phenolic compounds.[12] The configuration of the prenyl-moiety (chain or ring) seems to have an effect on the observed antibacterial activity. Ring prenylation was found to be more effective than chain prenylation, as demonstrated when comparing molecules with the same stilbenoid precursor: arachidin-1 (**1**) (chain, TTD_{25} 6.1 h) vs. arachidin-6 (**4**) (ring, TTD_{25} 11.5 h) and arachidin-2 (**2**) or -3 (**3**) (chain, TTD_{25} 7.4 or 6.6 h, respectively) vs. arahypin-5 (**5**) (ring, TTD_{25} 9.6 – >24 h) (**Table 2.3**). This was in contrast with previous results which indicated that chain-prenylated (iso)flavonoids were generally more active than ring-prenylated ones.[11,12] The effect of a 3-methyl-1-butene (arachidin-1 (**1**) and -3 (**3**)) or a 3-methyl-2-butene (arachidin-2 (**2**)) type prenyl chain was not completely clear but the higher TTD_{50} of arachidin-2 indicated that a 3-methyl-2-butene chain might result in better activity than a 3-methyl-1-butene chain.

The stilbenoid precursor of the prenylated compounds might also affect their activity. So far, our results indicated that the order of activity for the three tested precursors is pinosylvin > resveratrol > piceatannol. Within the group of compounds **1**-**6**, the number of hydrogen bond donors is negatively correlated with TTD_{25} (r = -0.89), i.e. having less hydrogen bond donors seems to result in better anti-MRSA activity. This matches previously described results for pterostilbene (i.e. 3,5-dimethyl-resveratrol, MIC 78 µM) which was found to be up to 16 times more active against MRSA than resveratrol in that study (MIC 1,250 µM).[25]

The structure-antibacterial activity relationships described above indicate that prenylated stilbenoids from the pinosylvin precursor seem to be most potent. In addition, ring prenylation seems to confer more antibacterial potential than chain prenylation. A candidate anti-MRSA molecule reported in literature would be arahypin-13 (ring-prenylated pinosylvin).[5] This molecule might show similar or even more potent activity than chiricanine A. To establish quantitative structure-activity relationships, evaluation of a larger set of compounds will be necessary.

2.3.5. Structure elucidation and antibacterial activity of dimeric prenylated stilbenoids

During the purification process, three pools containing mainly dimeric prenylated stilbenoids were obtained (**Figure S2.3**, supplementary information). Spectrometric and spectroscopic properties of the main compound in each of these pools, as determined by UHPLC-PDA coupled to ESI-IT-MS and ESI-FTMS, are

shown in **Table S2.1** (supplementary information). Tentative annotations of the main compounds in pool **D1** and **D2** were based on previously reported fragmentation data of arahypin-7 (arachidin-1 homodimer) and arahypin-6 (arachidin-1 and -3 heterodimer).[6] The structures of these compounds are shown in **Figure S2.4** (supplementary information). The accurate mass of the main compound in the third dimer pool (**D3**) matched the molecular formula $C_{38}H_{36}O_7$ (**Table S2.1**), which might correspond to arahypin-12.[26] No fragmentation spectrum of arahypin-12 has been reported in literature. The main fragments in both negative and positive mode, *m/z* 509 and 511 respectively, corresponded to a neutral loss of a phenol moiety (94 u)(**Figure S2.4**). Arahypin-12, however, does not have an unsubstituted phenol moiety and, therefore, cannot yield this fragment (**Figure S2.4**). Similarly, no such fragment is detected for arahypin-7, which also does not have an unsubstituted phenol moiety, whereas arahypin-6, which does possess an unsubstituted phenol moiety, yields the NL of 94 u detected at *m/z* 511 and 513 in negative and positive ionisation modes, respectively (**Table S2.1**). Thus, the pool **D3** dimer most likely possessed an unsubstituted phenol moiety and conforms to the formula $C_{38}H_{36}O_7$. We therefore hypothesize that this compound is a dimer of arachidin-1 and arachidin-3 (further referred to as: ara-1+3 dimer) linked via the prenyl-moieties, similar to the linkages in arahypin-12. A putative structure of ara-1+3 dimer is shown in **Figure S2.4**. Such a structure is also more likely than arahypin-12 as most monomeric precursors (compounds **1**-**6**, **Figure 2.1**) were prenylated at the C4 position[27] rather than at the C3′ or C5′ position like the 3,5,4′-trihydroxy-5′-isopentenylstilbene subunit of arahypin-12. Whether the proposed ara-1+3 dimer is a natural product or the result of dimerization of arachidin-1 and arachidin-3 during the purification process remains unclear. Despite their low yield and purity, some preliminary experiments to assess the antibacterial activity of the dimeric compounds could be performed. The results of the antibacterial assay of the pools against MRSA are shown in **Table 2.4**. The pools were observed to possess promising anti-MRSA activity.

Table 2.4. Anti-MRSA activity of pools enriched in prenylated dimeric stilbenoids.

Dimer pool	Main constituent	Estimated purity MS (NI) (%) [a]	MIC (μg mL^{-1})	TTD_{25} (± StDev) (h) [b]
D1	Arahypin-7	48	>50	6.9 (± 0.6)
D2	Arahypin-6	69	25	>24 (± n.a.)
D3	Ara-1+3 dimer	52	25-50 [c]	22.0 (± 1.1) - >24 [c]

n.a., not applicable. [a] Based on total peak area in UHPLC-ESI-MS negative ionisation mode (*m/z* range 200-1500). [b] Time-to-detection at 25 μg mL^{-1}. [c] Determined in two independent biological replicates, in one of the biological replicates MIC was found at 25 μg mL^{-1} (TTD_{25} >24 h), in the other at 50 μg mL^{-1}.

In particular, Pool **D2** which contained an estimated 69% of arahypin-6 (heterodimer of arachidin-1 and -3) was found to be active with an MIC at 25 μg mL^{-1} against MRSA. Dimer pool **D3**, containing an estimated 52% of the putative

ara-1+3 dimer, seemed to have activity in the same range (**Table 2.4**). Considering that the monomers arachidin-1 and arachidin-3 themselves were not found to be antibacterial below 50 μg mL^{-1}, it seems that dimerization has a positive effect on anti-MRSA activity. Other research suggests that even non-prenylated dimeric stilbenoids, e.g. ε-viniferin, a homodimer of resveratrol found in grapes, function as defence metabolites.[28] This dimer, ε-viniferin, was reported to possess moderate to low activity against MRSA with MICs reported between 50 and 400 μg mL^{-1}.[29,30] Comparing this activity to the values observed from our prenylated dimer pools, it might be speculated that, like for stilbenoid monomers, dimers benefit from prenylation to enhance activity against MRSA. Some non-prenylated oligomeric stilbenoids, for example the resveratrol trimer gnetin E (MIC 12.5 μg mL^{-1}) and tetramer gnemonol B (MIC 6.25 μg mL^{-1}), show more potential against MRSA.[31] Possibly, prenylation of these molecules could make them even more potent. The preliminary findings presented here warrant further research into prenylated dimeric and possibly prenylated oligomeric stilbenoids as potential antibacterials.

2.4. Conclusion

Similarly to other phenolic compounds, prenylation of stilbenoids enhances their antibacterial activity. Prenylated stilbenoids represent a group of natural potential antibacterials with activity against the antibiotic-resistant gram-positive bacterium MRSA. The newly discovered prenylated stilbenoid, arachidin-6, was moderately potent with an MIC of 50-75 μg mL^{-1} against MRSA, whereas the activity of chiricanine A, with its MIC of 12.5 μg mL^{-1}, is in range with some traditional antibiotics. Within the set of stilbenoids assessed in this work prenylation enhanced antimicrobial activity. Hydrophobicity was not correlated with antimicrobial activity, whereas ring-prenylation seems to convey a larger increase in activity than chain-prenylation. Additionally, preliminary results showed that dimers of the prenylated stilbenoids (e.g. arahypin-6) are also promising in terms of their effectiveness against MRSA.

2.5. References

[1] Sobolev, V.S. (2013) Production of phytoalexins in peanut (*Arachis hypogaea*) seed elicited by selected microorganisms. *Journal of Agricultural and Food Chemistry*, 61*(8)*: p. 1850-1858.

[2] Simons, R., Vincken, J.-P., Roidos, N., Bovee, T.F.H., van Iersel, M., Verbruggen, M.A., and Gruppen, H. (2011) Increasing soy isoflavonoid content and diversity by simultaneous malting and challenging by a fungus to modulate estrogenicity. *Journal of Agricultural and Food Chemistry*, 59*(12)*: p. 6748-6758.

[3] Aisyah, S., Gruppen, H., Andini, S., Bettonvil, M., Severing, E., and Vincken, J.-P. (2016) Variation in accumulation of isoflavonoids in Phaseoleae seedlings elicited by *Rhizopus*. *Food Chemistry*, 196: p. 694-701.

[4] Aisyah, S., Gruppen, H., Slager, M., Helmink, B., and Vincken, J.-P. (2015) Modification of prenylated stilbenoids in peanut (*Arachis hypogaea*) seedlings by the same fungi that elicited them: The fungus strikes back. *Journal of Agricultural and Food Chemistry*, 63*(42)*: p. 9260-9268.

[5] Sobolev, V.S., Krausert, N.M., and Gloer, J.B. (2016) New monomeric stilbenoids from peanut (*Arachis hypogaea*) seeds challenged by an *Aspergillus flavus* strain. *Journal of Agricultural and Food Chemistry*, 64*(3)*: p. 579-584.

[6] Sobolev, V.S., Neff, S.A., and Gloer, J.B. (2010) New dimeric stilbenoids from fungal-challenged peanut (*Arachis hypogaea*) seeds. *Journal of Agricultural and Food Chemistry*, 58*(2)*: p. 875-881.

[7] Yang, T., Fang, L., Rimando, A.M., Sobolev, V., Mockaitis, K., and Medina-Bolivar, F. (2016) A stilbenoid-specific prenyltransferase utilizes dimethylallyl pyrophosphate from the plastidic terpenoid pathway. *Plant Physiology*, 171*(4)*: p. 2483-2498.

[8] Hatano, T., Shintani, Y., Aga, Y., Shiota, S., Tsuchiya, T., and Yoshida, T. (2000) Phenolic constituents of licorice. VIII. Structures of glicophenone and glicoisoflavanone, and effects of licorice phenolics on methicillin-resistant *Staphylococcus aureus*. *Chemical & Pharmaceutical Bulletin*, 48*(9)*: p. 1286-1292.

[9] Araya-Cloutier, C., den Besten, H.M.W., Aisyah, S., Gruppen, H., and Vincken, J.-P. (2017) The position of prenylation of isoflavonoids and stilbenoids from legumes (Fabaceae) modulates the antimicrobial activity against Gram positive pathogens. *Food Chemistry*, 226: p. 193-201.

[10] Gibbons, S. (2004) Anti-staphylococcal plant natural products. *Natural Product Reports*, 21*(2)*: p. 263-277.

[11] Araya-Cloutier, C., Vincken, J.-P., van de Schans, M.G.M., Hageman, J., Schaftenaar, G., den Besten, H.M.W., and Gruppen, H. (2018) QSAR-based molecular signatures of prenylated (iso)flavonoids underlying antimicrobial potency against and membrane-disruption in Gram positive and Gram negative bacteria. *Scientific Reports*, 8*(1)*: p. 9267.

[12] Araya-Cloutier, C., Vincken, J.-P., van Ederen, R., den Besten, H.M.W., and Gruppen, H. (2018) Rapid membrane permeabilization of *Listeria monocytogenes* and *Escherichia coli* induced by antibacterial prenylated phenolic compounds from legumes. *Food Chemistry*, 240: p. 147-155.

[13] de Bruijn, W.J.C., Vincken, J.-P., Duran, K., and Gruppen, H. (2016) Mass spectrometric characterization of benzoxazinoid glycosides from *Rhizopus*-elicited wheat (*Triticum aestivum*) seedlings. *Journal of Agricultural and Food Chemistry*, 64*(32)*: p. 6267-6276.

[14] van de Schans, M.G.M., Vincken, J.-P., de Waard, P., Hamers, A.R.M., Bovee, T.F.H., and Gruppen, H. (2016) Glyceollins and dehydroglyceollins isolated from soybean act as SERMs and ER subtype-selective phytoestrogens. *Journal of Steroid Biochemistry and Molecular Biology*, 156: p. 53-63.

[15] Sobolev, V.S., Neff, S.A., and Gloer, J.B. (2009) New stilbenoids from peanut (*Arachis hypogaea*) seeds challenged by an *Aspergillus caelatus* strain. *Journal of Agricultural and Food Chemistry*, 57*(1)*: p. 62-68.
[16] Murphy, R.C., Chapter 1: Fatty acids, in *Tandem mass spectrometry of lipids: Molecular analysis of complex lipids*, R.C. Murphy, Editor. 2014, The Royal Society of Chemistry: Cambridge, UK. p. 1-39.
[17] Sobolev, V.S., Potter, T.L., and Horn, B.W. (2006) Prenylated stilbenes from peanut root mucilage. *Phytochemical Analysis*, 17*(5)*: p. 312-322.
[18] Trela, B.C. and Waterhouse, A.L. (1996) Resveratrol: Isomeric molar absorptivities and stability. *Journal of Agricultural and Food Chemistry*, 44*(5)*: p. 1253-1257.
[19] Simons, R., Vincken, J.-P., Bakx, E.J., Verbruggen, M.A., and Gruppen, H. (2009) A rapid screening method for prenylated flavonoids with ultra-high-performance liquid chromatography/electrospray ionisation mass spectrometry in licorice root extracts. *Rapid Communications in Mass Spectrometry*, 23*(19)*: p. 3083-3093.
[20] Chang, J.C., Lai, Y.H., Djoko, B., Wu, P.L., Liu, C.D., Liu, Y.W., and Chiou, R.Y.Y. (2006) Biosynthesis enhancement and antioxidant and anti-inflammatory activities of peanut (*Arachis hypogaea* L.) arachidin-1, arachidin-3, and isopentadienylresveratrol. *Journal of Agricultural and Food Chemistry*, 54*(26)*: p. 10281-10287.
[21] Singhal, A.K., Sharma, R.P., Thyagarajan, G., Herz, W., and Govindan, S.V. (1980) New prenylated isoflavones and a prenylated dihydroflavonol from *Millettia pachycarpa*. *Phytochemistry*, 19*(5)*: p. 929-934.
[22] Popłoński, J., Turlej, E., Sordon, S., Tronina, T., Bartmańska, A., Wietrzyk, J., and Huszcza, E. (2018) Synthesis and antiproliferative activity of minor hops prenylflavonoids and new insights on prenyl group cyclization. *Molecules*, 23*(4)*.
[23] Braga, L.C., Leite, A.A.M., Xavier, K.G.S., Takahashi, J.A., Bemquerer, M.P., Chartone-Souza, E., and Nascimento, A.M.A. (2005) Synergic interaction between pomegranate extract and antibiotics against *Staphylococcus aureus*. *Canadian Journal of Microbiology*, 51*(7)*: p. 541-547.
[24] Botta, B., Vitali, A., Menendez, P., Misiti, D., and Delle Monache, G. (2005) Prenylated flavonoids: Pharmacology and biotechnology. *Current Medicinal Chemistry*, 12*(6)*: p. 713-739.
[25] Yang, S.C., Tseng, C.H., Wang, P.W., Lu, P.L., Weng, Y.H., Yen, F.L., and Fang, J.Y. (2017) Pterostilbene, a methoxylated resveratrol derivative, efficiently eradicates planktonic, biofilm, and intracellular MRSA by topical application. *Frontiers in Microbiology*, 8: p. Article 1103.
[26] Liu, Z.W., Wu, J.E., and Huang, D.J. (2013) New stilbenoids isolated from fungus-challenged black skin peanut seeds and their adipogenesis inhibitory activity in 3T3-L1 cells. *Journal of Agricultural and Food Chemistry*, 61*(17)*: p. 4155-4161.
[27] Yang, T., Fang, L., Rimando, A.M., Sobolev, V., Mockaitis, K., and Medina-Bolivar, F. (2016) A stilbenoid-specific prenyltransferase utilizes dimethylallyl pyrophosphate from the plastidic terpenoid pathway. *Plant Physiology*, 171*(4)*: p. 2483-2498.
[28] Pezet, R., Gindro, K., Viret, O., and Spring, J.L. (2004) Glycosylation and oxidative dimerization of resveratrol are respectively associated to sensitivity and resistance of grapevine cultivars to downy mildew. *Physiological and Molecular Plant Pathology*, 65*(6)*: p. 297-303.
[29] Basri, D.F., Luoi, C.K., Azmi, A.M., and Latip, J. (2012) Evaluation of the combined effects of stilbenoid from *Shorea gibbosa* and vancomycin against methicillin-resistant *Staphylococcus aureus* (MRSA). *Pharmaceuticals*, 5*(9)*: p. 1032-1043.
[30] Basri, D.F., Xian, L.W., Shukor, N.I.A., and Latip, J. (2014) Bacteriostatic antimicrobial combination: Antagonistic interaction between epsilon-viniferin and

vancomycin against methicillin-resistant *Staphylococcus aureus*. *Biomed Research International*, Article ID 461756.

[31] Sakagami, Y., Sawabe, A., Komemushi, S., Ali, Z., Tanaka, T., Iliya, I., and Iinuma, M. (2007) Antibacterial activity of stilbene oligomers against vancomycin-resistant enterococci (VRE) and methicillin-resistant *Staphylococcus aureus* (MRSA) and their synergism with antibiotics. *Biocontrol science*, 12*(1)*: p. 7-14.

2.6. Supplementary information

2.6.1. Elution profiles reversed-phase chromatography

2.6.1.1. Pre-purification by RP-flash chromatography

For Flash chromatography, samples were injected on a Reveleris C18 RP 80 g cartridge (particle size 40 µm) and eluents used were water (A) and MeOH (B), both with 1% (*v/v*) formic acid. Elution program: Isocratic at 48% B for 2.2 min, linear gradient to 80% B from 2.2-74.8 min, linear gradient to 100% B from 74.8-77.0 min, isocratic at 100% B from 77.0-88.0 min.

2.6.1.2. Preparative RP-HPLC-ESI-MS

For preparative HPLC, samples were injected on a Waters XBridge Prep C18 OBD column (19 × 250 mm, 5 µm particle size) (Waters, Milford, MA, USA) and eluents used were water (A) and ACN (HPLC-R grade) (B), both with 1% (*v/v*) formic acid. The elution programs for the different compounds were as follows:
Compound **1**: Isocratic at 37% B for 3.68 min, linear gradient to 47% B from 3.68-38.68 min, linear gradient to 100% B from 38.68-42.18 min, isocratic at 100%B from 42.18-59.69 min, linear gradient to 37% B from 59.69-63.19 min, isocratic at 37% B from 63.19-80.96 min.
Compounds **2**, **3**, **4** and **5**: Isocratic at 38% B for 3.68 min, linear gradient to 48% B from 3.68-38.68 min, linear gradient to 100% B from 38.68-42.18 min, isocratic at 100% B from 42.18-59.69 min, linear gradient to 38% B from 59.69-63.19 min, isocratic at 38% B from 63.19-80.96 min.
Compound **6**: Isocratic at 42% B for 3.68 min, linear gradient to 52% B from 3.68-38.68 min, linear gradient to 100% B from 38.68-42.18 min, isocratic at 100% B from 42.18-59.69 min, linear gradient to 52% B from 59.69-63.19 min, isocratic at 52% B from 63.19-80.96 min.

2.6.1.3. Analytical RP-UHPLC-PDA-ESI-IT-MS^n

For analytical UHPLC coupled to ESI-IT-MS^n, samples were injected on a Waters Acquity BEH C18 2.1 × 150 mm, 1.7 µm particle size column with a Waters VanGuard 2.1 × 5 mm guard column of the same material. Eluents used were water (A) and MeOH (B), both with 0.1% (*v/v*) formic acid. Elution program: Isocratic at 48% B for 1.45 min, linear gradient to 80% B from 1.45-16.96 min, linear gradient to 100% B from 16.96-18.42 min, isocratic at 100% B from 18.42-25.96 min. The eluent was adjusted to its starting composition in 1.18 min, followed by equilibration for 7.27 min.

2.6.1.4. Analytical RP-UHPLC-PDA-ESI-FTMS

For analytical UHPLC coupled to ESI-FTMS, samples were injected on a Waters Acquity BEH C18 2.1 × 150 mm, 1.7 µm particle size column with a Waters VanGuard 2.1 × 5 mm guard column of the same material. Eluents used were water (A) and ACN (B), both with 0.1% (*v/v*) formic acid. Elution program: Isocratic at

20% B for 0.58 min, linear gradient to 100% B from 0.58-47.18 min, isocratic at 100% B from 47.18-50.10 min.

2.6.2. Supplementary figures and tables

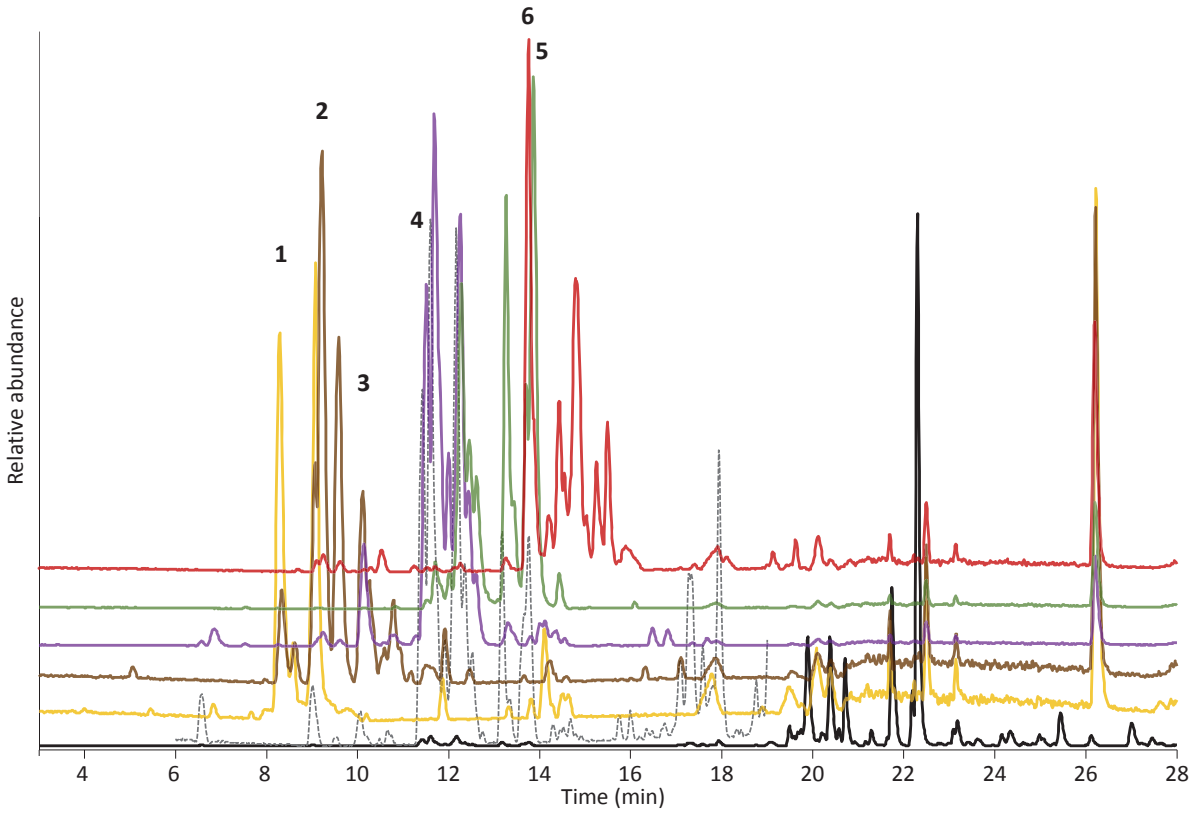

Figure S2.1. UHPLC-ESI-IT-MS negative mode (*m/z* 250-1000) chromatograms of cleaned peanut extract (black, full chromatogram; grey-dashed, zoom of 6-19 min) and pools obtained after Flash chromatography. Yellow, pool with compound **1**; brown, pool with compounds **2** and **3**; purple, pool with compound **4**; green, pool with compound **5**; and red, pool with compound **6**.

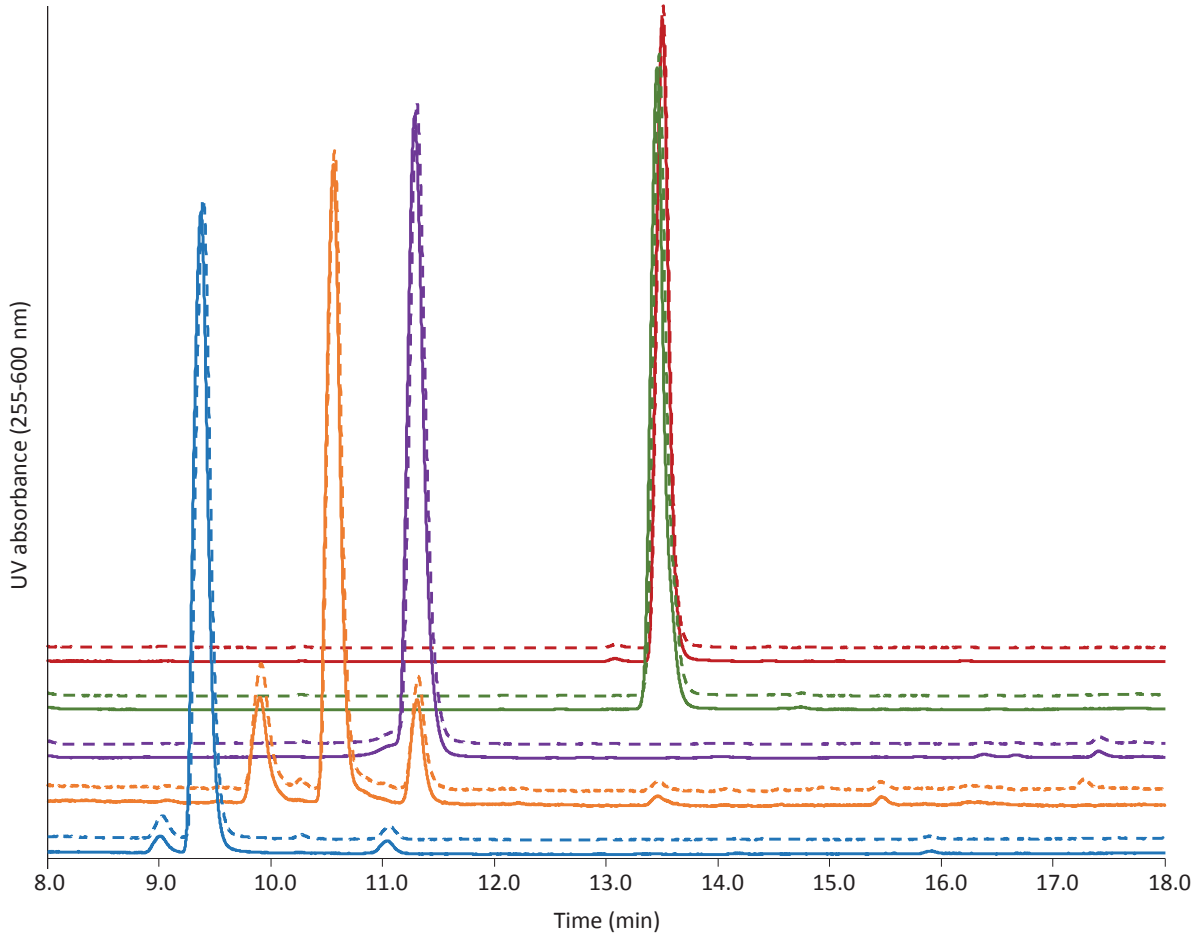

Figure S2.2. UHPLC-PDA (255-600 nm) chromatograms of compounds **2**, **3**, **4**, **5** and **6** before (solid line) and after (dashed line) incubation for 24 h under antimicrobial assay conditions. Blue, arachidin-2 (**2**); orange, arachidin-3 (**3**); purple, arachidin-6 (**4**); green, arahypin-5 (**5**); and red, chiricanine A (**6**).

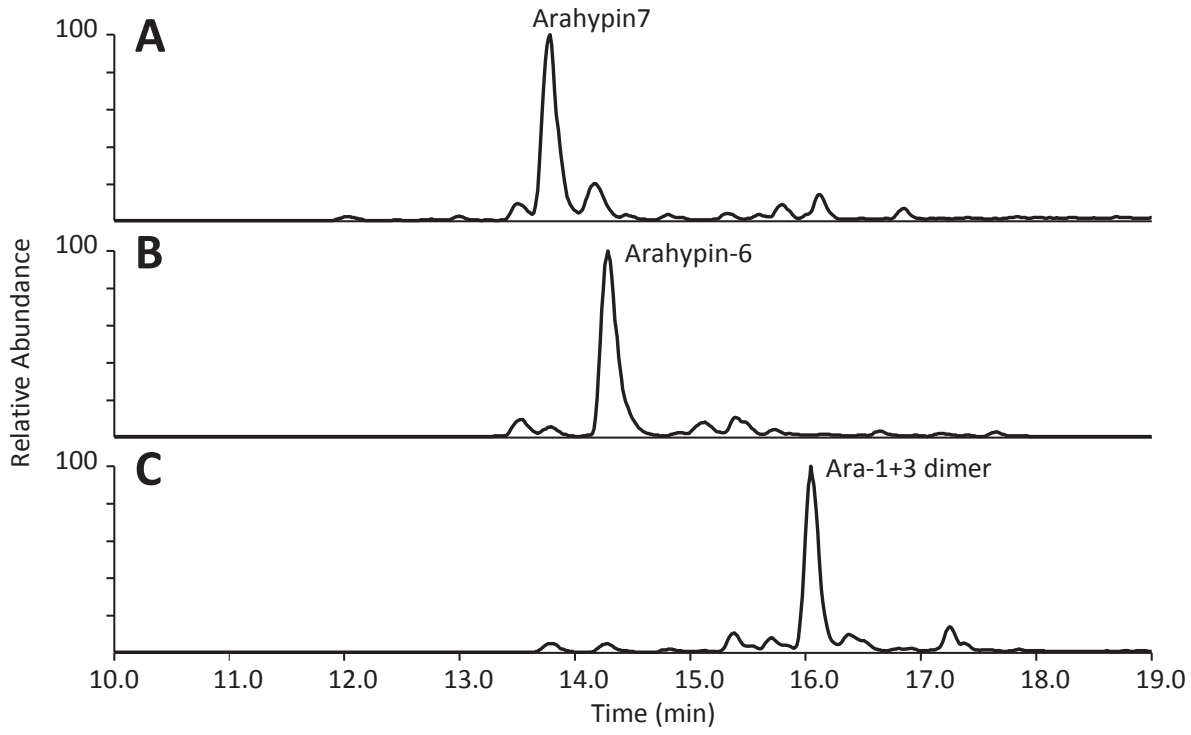

Figure S2.3. UHPLC-ESI-IT-MS negative mode (*m/z* range 450-1,000) chromatograms of dimeric stilbenoid pools: pool D1, D2, and D3. Main peaks tentatively annotated as arahypin-7, arahypin-6 and ara-1+3 dimer. Corresponding spectral data can be found in **Table S2.1**.

Table S2.1. Spectrometric and spectroscopic data of the main compounds in the prenylated dimeric stilbenoid pools as determined by UHPLC-PDA coupled to ESI-IT-MS and ESI-FTMS.

				IT-MS				FTMS	
Pool	**Tentative annotation**	**λ_{max} (nm)**	**Ionisation**	***m/z* precursor**	**MS^2 product ions (relative abundance) [b]**	**Molecular formula**	***m/z* calc.**	***m/z* obs. [c]**	**Error (ppm)**
D1	Arahypin-7 [a]	264, 328	$[M-H]^-$	621	<u>511</u>, 622 (26), 512 (21)	$C_{38}H_{38}O_8$	621.24939	621.24944	0.08
			$[M+H]^+$	623	<u>501</u>, 513 (74), 391 (60), 445 (29), 499 (29), 567 (28), 299 (23), 335 (19)				
D2	Arahypin-6 [a]	263, 313	$[M-H]^-$	605	<u>511</u>, 606 (85), 495 (29), 309 (25), 483 (23), 512 (19), 414 (16)	$C_{38}H_{38}O_7$	605.25448	605.25529	1.34
			$[M+H]^+$	607	<u>501</u>, 429 (89), 513 (85), 551 (74), 299 (68), 497 (62), 589 (60), 391 (54), 533 (47), 445 (42), 283 (41), 485 (29), 441 (28), 335 (27), 215 (27), 373 (25), 457 (22), 323 (21), 502 (20), 243 (18), 552 (18), 590 (16), 514 (16), 477 (15), 430 (15)				
D3	Ara-1+3 dimer	287, 317	$[M-H]^-$	603	<u>509</u>, 604 (65), 307 (28), 510 (24), 493 (19), 414 (19)	$C_{38}H_{36}O_7$	603.23883	603.23967	1.40
			$[M+H]^+$	605	<u>511</u>, 499 (91), 429 (90), 587 (82), 495 (76), 297 (60), 389 (57), 531 (50), 281 (50), 549 (49), 483 (35), 373 (26), 443 (26), 588 (24), 295 (22), 439 (21), 333 (19), 500 (18), 215 (17), 427 (17), 512 (16), 496 (16), 323 (15)				

[a] Tentative annotations based on previously reported spectrometric data.[6] Only the data of the main peak is shown, see also **Figure S2.3**.
[b] Most abundant fragment is underlined, only fragment ions with a relative abundance of at least 15 are shown. [c] Based on the average of 5 spectra in negative ionisation mode.

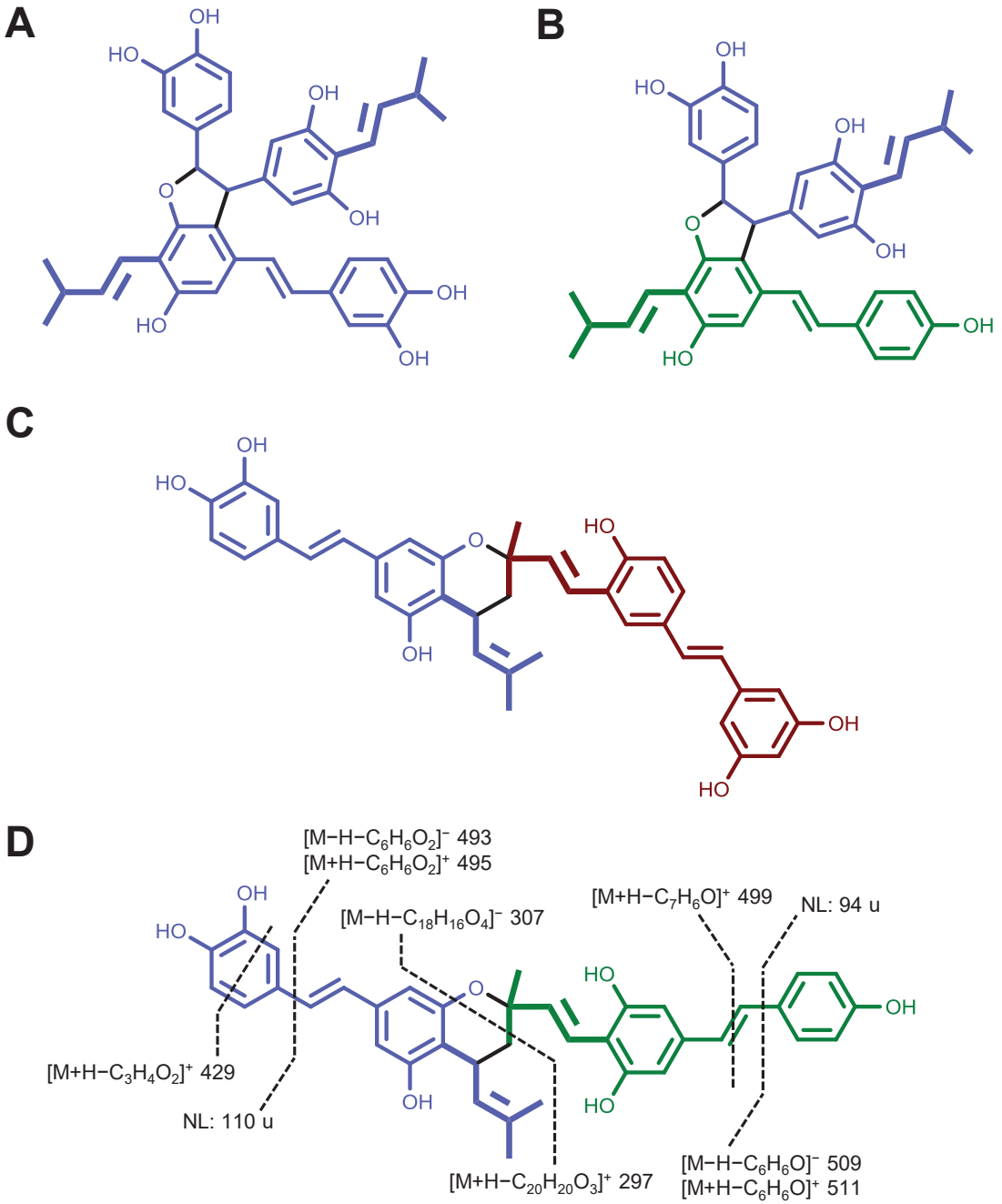

Figure S2.4. Structures of the tentatively annotated main dimeric stilbenoids in pools D1, D2 and D3. Arahypin-7 (A), arahypin-6 (B), arahypin-12, which was not detected in this work (C),[26] and the putative structure of the ara-1+3 dimer with some of its most abundant fragments (D). Blue indicates the arachidin-1 monomer, green the arachidin-3 monomer and red the 3,5,4′-trihydroxy-5′-isopentenylstilbene monomer. Prenyl chains are indicated in bold.

CHAPTER 3

Mass spectrometric characterization of benzoxazinoid glycosides from *Rhizopus*-elicited wheat seedlings

Benzoxazinoids function as defence compounds and have been suggested to possess health promoting effects. In this work, the mass spectrometric behaviour of benzoxazinoids from the classes benzoxazin-3-one (with subclasses lactams, hydroxamic acids, and methyl derivatives) and benzoxazolinones was studied. Wheat seeds were germinated with simultaneous elicitation by *Rhizopus*. The seedling extract was screened for the presence of benzoxazinoid (glycosides) using RP-UHPLC-PDA-MS^n. Benzoxazin-3-ones from the different subclasses showed distinctly different ionization and fragmentation behaviour. These features were incorporated into a newly proposed decision guideline to aid the classification of benzoxazinoids. Glycosides of the methyl derivative 2-hydroxy-4-methoxy-1,4-benzoxazin-3-one were tentatively identified for the first time in wheat. We conclude that wheat seedlings germinated with simultaneous fungal elicitation contain a diverse array of benzoxazinoids, mainly constituted by benzoxazin-3-one glycosides.

Based on: Wouter J. C. de Bruijn, Jean-Paul Vincken, Katharina Duran, and Harry Gruppen (2016) Mass spectrometric characterization of benzoxazinoid glycosides from *Rhizopus*-elicited wheat (*Triticum aestivum*) seedlings, *Journal of Agricultural and Food Chemistry*, 64(32): p. 6267-6276.

3.1. Introduction

Wheat (*Triticum aestivum*) is a member of the plant family Poaceae and is one of world's most consumed staple foods, contributing about 20% to dietary energy and protein intake world-wide.[1] Wheat, in particular germinated wheat, has recently gained interest because of its micro-nutrient content. Micro-nutrients, such as vitamin E, carotenoids, and other phytochemicals possessing antioxidative properties, accumulate during germination. These micro-nutrients are suggested to be responsible for a variety of health-promoting effects.[2] The health benefits of wheat (seedlings) have been associated partly with benzoxazinoids, a group of secondary metabolites found in several species of the family Poaceae. Health promoting effects suggested for benzoxazinoids comprise anti-inflammatory, anticancer and antimicrobial properties.[2-4] Potential adverse health effects, such as genotoxicity, on the other hand, have also been reported for benzoxazinoids.[5] Benzoxazinoids are divided into two classes: benzoxazin-3-ones (1,4-benzoxazin-3-one) and benzoxazolinones (1,3-benzoxazol-2-one). These metabolites play a role in allelopathic plant-plant interactions and as defence compounds against (micro)biological threats.[3,6,7] The class of benzoxazin-3-ones can be divided into three subclasses, based on their *N*-substitution: lactams (-H), hydroxamic acids (-OH) and methyl derivatives (-OCH_3) (**Figure 3.1**). Inside plant cells, benzoxazin-3-ones are glycosylated and stored in vacuoles in order to prevent self-toxicity.[8,9] Glycosylation of benzoxazin-3-ones in plants, generally with hexoses, is always reported to be on the hydroxyl moiety at *C*2.

Elicitation is frequently used as a way to stimulate changes in secondary metabolism of plants.[10,11] To this end abiotic (e.g. light, wounding, chemicals) and biotic (e.g. fungi, insects) stresses have been used.[12] Germination of seeds and simultaneous elicitation with fungus (*Rhizopus oryzae*) has been shown to successfully alter the secondary metabolite profile of members of the family Leguminosae (e.g. soybean).[11,13] The resulting seedling extracts showed modulated biological activity.[14] We aimed to use a similar fungal elicitation procedure to stimulate the production of a diverse benzoxazinoid profile in wheat seedlings.

Liquid chromatography combined with mass spectrometry has been shown to be a suitable method for detection and identification of benzoxazinoid glycosides and aglycones.[8,15,16] Mass spectrometric behaviour of benzoxazin-3-one and benzoxazolinone aglycones has been studied in detail previously.[16,17] In mass spectrometric analysis of benzoxazin-3-one glycosides, the main fragments reported are related to loss of the glycosyl moiety. It has not been studied systematically how the fragments originating from the benzoxazin-3-one glycosides can be used to classify these molecules into the three subclasses. Therefore, there is currently no way to easily differentiate structural isomers derived from the different benzoxazin-3-one subclasses (e.g. DHBOA and DIBOA, **Figure 3.1**).

Benzoxazin-3-ones	R_1	R_2	Name	Abbreviation	Molecular mass: *a* (R_3=H)	Molecular mass: M (R_3=hex)	Molecular mass: D (R_3=hex-hex)
Lactams							
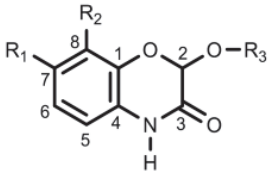	H	H	2-hydroxy-1,4-benzoxazin-3-one	HBOA	165	327	489
	OH	H	2,7-dihydroxy-1,4-benzoxazin-3-one	DHBOA	181	343	505
	OCH_3	H	2-hydroxy-7-methoxy-1,4-benzoxazin-3-one	HMBOA	195	357	519
	OCH_3	OCH_3	2-hydroxy-7,8-dimethoxy-1,4-benzoxazin-3-one	HM_2BOA	225	387	549
Hydroxamic acids							
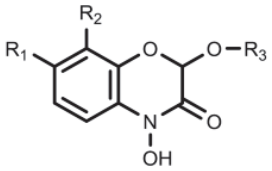	H	H	2,4-dihydroxy-1,4-benzoxazin-3-one	DIBOA	181	343	505
	OCH_3	H	2,4-dihydroxy-7-methoxy-1,4-benzoxazin-3-one	DIMBOA	211	373	535
	OCH_3	OCH_3	2,4-dihydroxy-7,8-dimethoxy-1,4-benzoxazin-3-one	DIM_2BOA	241	403	565
Methyl derivatives							
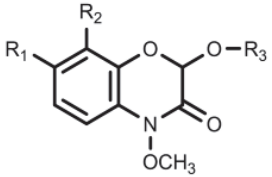	H	H	2-hydroxy-4-methoxy-1,4-benzoxazin-3-one	4-*O*-Me-DIBOA	195	357	519
	OCH_3	H	2-hydroxy-4,7-dimethoxy-1,4-benzoxazin-3-one	HDMBOA	225	387	549
	OCH_3	OCH_3	2-hydroxy-4,7,8-trimethoxy-1,4-benzoxazin-3-one	HDM_2BOA	255	417	579
Benzoxazolinones							
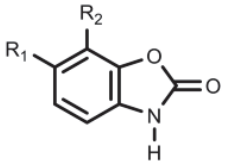	H	H	2-benzoxazolinone	BOA	135	n.a.	n.a.
	OH	H	6-hydroxy-2-benzoxazolinone	BOA-6-OH	151	n.a.	n.a.
	OCH_3	H	6-methoxy-2-benzoxazolinone	MBOA	165	n.a.	n.a.

Figure 3.1. Overview of the basic skeletons of benzoxazin-3-one lactams, hydroxamic acids, methyl derivatives and their glycosides, and benzoxazolinones, based on reports in literature.[3,8,10] Substitution at R_3 is not applicable for benzoxazolinones, molecular mass is only shown for aglycones. a, aglycone; D, dihexoside; hex, hexose; hex-hex, dihexose; M, monohexoside; n.a., not applicable.

In this work, the aglycone fragment formed in MS^2 was further characterized in MS^3 to establish clear rules in fragmentation of benzoxazin-3-one glycosides. Our hypothesis is that benzoxazin-3-one glycosides of each of the three subclasses yield diagnostic aglycone fragment ions that enable classification of these molecules.
Our objectives were to characterize benzoxazin-3-one glycosides and benzoxazolinones in wheat seedlings germinated with simultaneous elicitation by *Rhizopus* and to establish a decision guideline to facilitate the future identification of these molecules.

3.2. Materials and Methods

3.2.1. Seeds and chemicals

Wheat seeds, *Triticum aestivum* L., were purchased from Vreeken's Zaden (Dordrecht, The Netherlands). 2*H*-1,4-Benzoxazin-3(4*H*)-one (99%) and 2-benzoxazolinone (98%) were purchased from Sigma Aldrich (St. Louis, MO). L-Tryptophan (≥99.0%) was purchased from Fluka BioChemika (Sigma Aldrich, St. Louis, MO). UHPLC-MS grade acetonitrile and water, both acidified with 0.1% (*v/v*) formic acid (FA), were obtained from Biosolve (Valkenswaard, The Netherlands). Sodium hypochlorite 47/50% (*w/v*) solution (±13% active Cl) was obtained from Chem-Lab (Zedelgem, Belgium). Ethanol absolute (>99.5%) was purchased from VWR International (Amsterdam, The Netherlands). Other chemicals were purchased from Merck Millipore (Billerica, MA). The fungus *Rhizopus oryzae* LU 581 was kindly provided by the Laboratory of Food Microbiology, Wageningen University (Wageningen, The Netherlands). Water was prepared using a Milli-Q water purification system (Millipore, Billerica, MA).

3.2.2. Wheat germination and elicitation with Rhizopus

Wheat seeds were surface-sterilized by soaking in a 1.3% (*w/v*) hypochlorite solution (5 L kg^{-1} seeds) for 45 min at 20 ˚C. Subsequently, seeds were rinsed with demineralized water (8 L kg^{-1}). Seeds were germinated in the dark in a pilot-scale two-tank steep germinator (Custom Laboratory Products, Keith, UK). Prior to use, the germinator tanks (50 L per tank), containing the metal trays used to hold the seeds, were filled with water completely and sterilized for at least 1 h by adding 1 L of commercial bleach (1-5% (*w/v*) sodium hypochlorite) per tank. External surfaces of the germinator were sterilized with 70% (*v/v*) ethanol. Approximately 400 g seeds were distributed equally over two of the five compartments (90 x 195 x 100 mm) of custom-made rectangular perforated metal trays (450 x 195 x 100 mm). The program set in the germinator was as follows: soaking for 20 h at 20 ˚C, followed by germination for 7 d at 25 ˚C (± 3 ˚C). Seeds were inoculated at the start of the 4th day of germination. The fungal spore suspension was prepared according to the method described elsewhere.[11] Pure plate cultures of *R. oryzae* were grown on malt extract agar (CM59) (Oxoid, Basingstoke, UK). Sporangia were

collected from a total of 21 plates by scraping them off and suspending them in 0.95% (*w/v*) NaCl solution (10 mL per plate). Wheat seedlings (approximately 400 g) were inoculated by soaking them in the spore solution for 50 min. This spore preparation and application procedure proved sufficient to achieve growth of fungus over all seedlings. All other parameters were maintained identical to the process without elicitation.

During the germination process, relative humidity (RH) was controlled by periodical aeration with humidified air and was maintained above 70% (mean RH 84%). This protocol proved effective in ensuring germination of the seeds as well as growth of the fungus. After 8 days, seeds were removed from the germinator and frozen (-25 ˚C) immediately until further processing.

3.2.3. Extraction

Wheat seedlings were freeze-dried and milled into a fine powder using a Retsch MM400 Beadmill (Haan, Germany) equipped with two 50 mL grinding jars, each containing one bead (20 mm diam.). Seedlings were milled for 240 s, during the first 30 s the frequency was increased from 13 to 30 s^{-1}, which was maintained during the remaining 210 s. Powdered samples were extracted with chilled (4 ˚C) 80% (*v/v*) aqueous ethanol (20 mL g^{-1}). Samples were subjected to sonication for 15 min followed by centrifugation (10 min, 5000 *g*, 20 ˚C). The supernatant was collected and the pellet was subjected to two additional identical extraction steps. The three supernatants were pooled and the ethanol was evaporated under reduced pressure. Subsequently, the water was removed by freeze drying and dried samples were resolubilized in 80% (*v/v*) aqueous methanol to a concentration of 20 mg mL^{-1}. Samples were centrifuged (5 min, 16000 *g*, 20 ˚C) prior to RP-UHPLC analysis.

3.2.4. Reversed phase liquid chromatography (RP-UHPLC)

Samples were separated on an Accela UHPLC system (Thermo Scientific, San Jose, CA) equipped with a pump, degasser, autosampler, and photodiode array (PDA) detector. The column used was a 150 mm x 2.1 mm i.d., 1.7 µm, Acquity UPLC BEH C18 with a 5 mm x 2.1 mm i.d., VanGuard guard column of the same material (Waters, Milford, MA). The injection volume was 1.5 µL. The flow rate was 300 µL min^{-1} at a column temperature of 45 °C. Eluents used were: water (A) and acetonitrile (B), both containing 0.1% (*v/v*) formic acid. The elution program was started by running isocratically at 5% B for 2.6 min, followed by 2.6-16.0 min linear gradient to 26% B, 16.0-17.0 min linear gradient to 100% B, 17.0-24.0 min isocratic at 100% B. The eluent was adjusted to its starting composition in 1 min, followed by equilibration for 7 min. Detection wavelengths for UV-Vis were set to the range of 200-600 nm. Data were recorded at 20 Hz.

3.2.5. Electrospray ionization ion trap mass spectrometry (ESI-IT-MS^n)

Benzoxazinoids were characterized based on their MS^n fragmentation in electrospray ionization ion trap mass spectrometry. Mass spectrometric data were acquired using an LTQ Velos Pro linear ion trap mass spectrometer (Thermo Scientific) equipped with a heated ESI probe coupled in-line to the Accela RP-UHPLC system. Nitrogen was used both as sheath gas (15 arbitrary units) and auxiliary gas (10 arbitrary units). Data were collected in negative ionization mode over the range *m/z* 125-750. Data-dependent MS^n analyses were performed by collision-induced dissociation with a normalized collision energy of 35%. MS^2 analyses were performed at an activation Q of 0.200 with wideband activation. For MS^3 analyses, different settings were used: an activation Q of 0.250 without wideband activation. MS^n fragmentation was performed on the most intense product ion in the MS^{n-1} spectrum. Dynamic exclusion, with a repeat count of 5, repeat duration of 5.0 s and an exclusion duration of 5.0 s, was used to obtain MS^2 spectra of multiple different ions present in full MS at the same time. In addition, full MS data were recorded in positive ionization mode over the range *m/z* 125-750. Most settings were optimized by automatic tuning using LTQ Tune Plus 2.7 (Thermo Scientific) upon direct injection of 1,4-benzoxazin-3-one or 2-benzoxazolinone at a flow rate of 3 µL min^{-1}, in positive and negative mode, respectively. The ion transfer tube temperature was 275 °C, the source heater temperature 40 °C, and the source voltage 4.0 kV. Data were processed using Xcalibur 2.2 (Thermo Scientific).

3.2.6. Electrospray ionization hybrid quadrupole-orbitrap mass spectrometry (ESI-IT-FTMS)

For determination of accurate mass, samples were separated on a Vanquish UHPLC system (Thermo Scientific). Prior to injection, samples were diluted to 100 µg mL^{-1} (in 80% (*v/v*) aqueous methanol). The injection volume was 1 µL. The column, mobile phases, and elution program were identical to those described above for RP-UHPLC. The column compartment heater was operated in still air mode at 45 °C, the eluent preheater was set to 45 °C and the post column cooler to 40 °C. Accurate mass data were acquired using a Thermo Q Exactive Focus hybrid quadrupole-orbitrap mass spectrometer (Thermo Scientific) equipped with a heated ESI probe coupled in-line to the Vanquish RP-UHPLC system. Half of the flow from the RP-UHPLC system (150 µL min^{-1}) was directed toward the MS. Full MS data were collected in negative ionization mode over the range *m/z* 150-600 at 70,000 resolution. Prior to analysis the mass spectrometer was calibrated in negative ionization mode using Tune 2.6 software (Thermo Scientific) by injection of Pierce negative ion calibration solution (Thermo Scientific). Nitrogen was used both as sheath gas (35 arbitrary units) and auxiliary gas (20 arbitrary units). The capillary temperature was 275 °C, the auxiliary gas heater temperature 150 °C,

the S-lens RF level 55, and the source voltage 3.5 kV. Data were processed using Xcalibur 2.2 (Thermo Scientific) and FreeStyle 1.1 (Thermo Scientific). Molecular formulas of benzoxazinoids were calculated using CambridgeSoft ChemBioDraw Ultra 13.0.0.3015 (PerkinElmer, Waltham, MA).

3.3. Results & Discussion

3.3.1. Secondary metabolite profile of Rhizopus-elicited wheat seedlings

Seedlings that were germinated with simultaneous fungal elicitation were found to contain a wide variety of secondary metabolites (**Figure 3.2**). The main peaks (≥20% maximum intensity) observed were vii, 6, 11, 14, 17, and 21. The focus will be on the identification of benzoxazinoids from elicited seedlings.

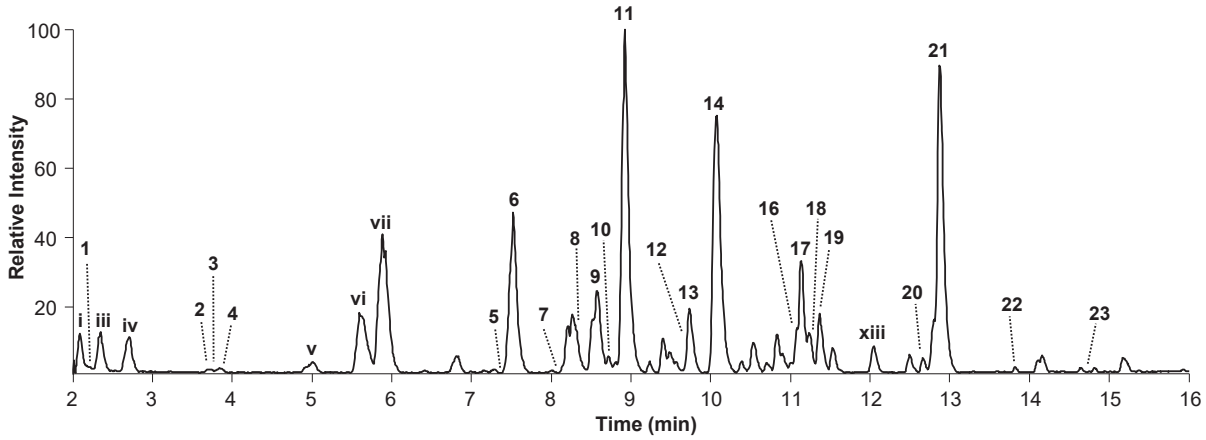

Figure 3.2. UHPLC-MS base peak chromatogram (*m/z* 200-750, negative ionization mode) of the extract from *Rhizopus*-elicited wheat seedlings. Peaks 1-23 correspond to benzoxazinoids (**Table 3.1**), peaks i-xiii correspond to miscellaneous compounds (**Table S3.1**, supplementary information). Labels of peaks ii and x-xii not shown for purpose of clarity.

3.3.2. Characterization of benzoxazin-3-one glycosides

Peaks potentially corresponding to benzoxazin-3-one glycosides in elicited the wheat seedling extract (**Figure 3.2**) were selected using the following three criteria. Firstly, an even mass-to-charge ratio in full MS (within the range *m/z* 300-600), which could indicate an odd number of nitrogen atoms. Secondly, a UV spectrum with a primary maximum between 250 to 265 nm, combined with a secondary maximum between 275 to 290 nm.[15] Lastly, neutral losses of 162, 180, 324 or 342 Da in MS^2, which indicate the presence of monohexosyl (hex) or dihexosyl (hex-hex) moieties.[8,15] Although these criteria provided a crude screening for potential benzoxazin-3-ones glycosides, further mass spectrometric characterization was necessary for peak identification.

Table 3.1. Spectral properties of benzoxazinoids in the wheat seedling extract, tentatively identified by UHPLC-PDA-ESI-IT-MS.

Peak no.	Rt. (min)	compound	UV_{max} (nm)	Ratio $\frac{[M-H]^-}{[M-H+FA]^-}$	Ionisation	*m/z*	MS^2 product ions (relative intensity) [a]								MS^3 product ions (relative intensity) [a,b]							
							I	II	III	IV	V	VI	IX	Misc. [c]	I	II	III	IV	VII	VIII	IX	Misc. [c]
Benzoxazinones																						
Lactams																						
2	4.04	DHBOA-hex	262, 281	1.85	$[M-H]^-$	342	**180**	162(6)	n.d.	152(3)	n.a.	n.a.	n.d.		n.a.	n.d.	134(11)	n.d.	n.a.	**152**	124(15)	
					$[M-H+FA]^-$	388	n.d.	n.d.	n.d.	n.d.	n.d.	**342**	n.d.		**180**	162(7)	n.d.	152 (6)	n.d.	n.d.	124(4)	
3	4.08	DHBOA-hex-hex	265, 286	1.71	$[M-H]^-$	504	**180**	162(33)	n.d.	152(10)	n.a.	n.a.	124(10)		n.a.	n.d.	134(10)	n.d.	n.a.	**152**	124(11)	
					$[M-H+FA]^-$	550	X [d]															
4	4.48	DHBOA-hex	264, 282	1.89	$[M-H]^-$	342	**180**	162(8)	n.d.	152(3)	n.a.	n.a.	n.d.		n.a.	n.d.	134(12)	n.d.	n.a.	**152**	124(15)	
					$[M-H+FA]^-$	388	n.d.	n.d.	n.d.	n.d.	n.a.	**342**	n.d.		**180**	162(13)	n.d.	152 (5)	n.a.	n.d.	124(5)	
5	7.50	HBOA-hex-hex	253, 278	>>20 [e]	$[M-H]^-$	488	**164**	n.d.	118(3)	136(5)	n.a.	n.a.	n.d.		n.a.	n.d.	118(27)	n.d.	n.a.	**136**	108(31)	
					$[M-H+FA]^-$	n.d.																
7	8.09	HBOA-hex-hex	264, 277	2.00	$[M-H]^-$	488	**164**	n.d.	118(3)	136(4)	n.a.	n.a.	n.d.		n.a.	n.d.	118(29)	n.d.	n.a.	**136**	108(29)	
					$[M-H+FA]^-$	534	X [d]															
8	8.38	HBOA-hex	256, 279	>>20 [e]	$[M-H]^-$	326	**164**	n.d.	n.d.	136(2)	n.a.	n.a.	n.d.		n.a.	n.d.	118(29)	n.d.	n.a.	**136**	108(30)	
					$[M-H+FA]^-$	n.d.																
10	8.71	HMBOA-hex-hex	260, 283	20.00	$[M-H]^-$	518	**194**	n.d.	n.d.	166(8)	n.a.	n.a.	138(10)		n.a.	n.d.	148(15)	n.d.	179 (2)	**166**	138(24)	
					$[M-H+FA]^-$	564	X [d]															
13	9.74	HMBOA-hex	265, 280	25.00	$[M-H]^-$	356	**194**	n.d.	n.d.	166(2)	n.a.	n.a.	n.d.		n.a.	n.d.	148(15)	n.d.	n.d.	**166**	138(25)	
					$[M-H+FA]^-$	402	X [d]															
16	11.02	HBOA-hex-ac	n.d. [f]	n.d.	$[M-H]^-$	368	**164**,	n.d.	n.d.	136(5)	n.a.	n.a.	108(5)		n.a.	n.d.	118(20)	n.d.	n.a.	**136**	108(34)	
22	13.86	HBOA-hex-ac	n.d. [f]	n.d.	$[M-H]^-$	368	**164**,	n.d.		136(3)	n.a.	n.a.	108(5)		n.a.	n.d.	118(21)	n.d.	n.a.	**136**	108(30)	
23	14.82	HMBOA-hex-ac	n.d. [f]	n.d.	$[M-H]^-$	398	**194**,	n.d.	n.d.	166(5)	n.a.	n.a.	138(3)		n.a.	n.d.	148(15)	n.d.	n.d.	**166**	138(23)	
Hydroxamic acids																						
6	7.59	DIBOA-hex-hex	254, 278	14.29	$[M-H]^-$	504	180(7)	162(72)	**134**	n.d.	n.a.	n.a.	n.d.	426(10)	X [d]							
					$[M-H+FA]^-$	550	X [d]															
9	8.60	DIBOA-hex	n.d. [f]	0.95	$[M-H]^-$	342	180(44)	162(25)	**134**	n.d.	n.a.	n.a.	n.d.		X [d]							
					$[M-H+FA]^-$	388	n.d.	n.d.	n.d.	n.d.	n.d.	**342**	n.d.		180(31)	162(23)	**134**	n.d.	n.a.	n.d.	n.d.	
11	8.90	DIMBOA-hex-hex	265, 285	6.25	$[M-H]^-$	534	210(7)	**192**	164(99)	n.d.	n.a.	n.a.	n.d.	149(78), 456(14)	n.d.	n.d.	n.d.	n.d.	n.d.	**164**	n.d.	
					$[M-H]^-$	534	210(11)	192(88)	**164**	n.d.	n.a.	n.a.	n.d.	149(77), 456(10)	n.d.	n.d.	n.d.	n.d.	**149**	n.d.	n.d.	
					$[M-H+FA]^-$	580	X [d]															
14	10.07	DIMBOA-hex	265, 286	0.72	$[M-H]^-$	372	210(39)	192(20)	**164**	n.d.	n.a.	n.a.	n.d.	149(51)	n.d.	n.d.	n.d.	n.d.	**149**	n.d.	n.d.	
					$[M-H+FA]^-$	418	n.d.	n.d.	n.d.	n.d.	n.d.	**372**	n.d.		210(50)	192(23)	**164**	n.d.	n.d.	n.d.	n.d.	149 (95)
18	11.28	DIBOA-hex-ac	n.d. [f]	n.d.	$[M-H]^-$	384	180(27)	162(32)	**134**	n.d.	n.a.	n.a.	n.d.		X [d]		.					

Methyl derivatives																					
12	9.71	4-O-Me-DIBOA-hex-hex	n.d. [f]	0.05	$[M-H]^-$	518	X [d]														
					$[M-H+FA]^-$	564	n.d.	n.d.	194(4)	n.d.	488	518 (61)	n.d.	486(68)	n.d.	n.d.	164	n.d.	n.a.	n.d.	n.d.	
17	11.17	HDMBOA-hex-hex	265, 282	0.03	$[M-H]^-$	548	224	n.d.	n.d.	n.d.	n.a.	n.a.	n.d.	386(23), 164(18), 149(14), 488(10)	n.d.	n.d.	n.d.	n.d.	n.d.	196 (3)	168(2)	164, 192 (19)
					$[M-H+FA]^-$	594	n.d.	n.d.	224(7)	n.d.	518	548 (85)	n.d.	516(72), 192(19), 323(11)	194	n.d.	n.d.	166 (6)	n.d.	n.d.	n.d.	
19	11.39	4-O-Me-DIBOA-hex	258, 279	<<0.05 [g]	$[M-H]^-$	n.d.															
					$[M-H+FA]^-$	402	n.d.	n.d.	194(9)	n.d.	326	356(7)	n.d.	134(15), 164(11)	164	n.d.	118(4)	136 (4)	n.a.	n.d.	108(9)	
20	12.69	HDMBOA-hex	273, 282	<<0.05 [g]	$[M-H]^-$	n.d.															
					$[M-H+FA]^-$	432	n.d.	n.d.	224(13)	n.d.	356	386(3)	n.d.	322(70), 401(70), 164(40), 194(17), 149(17)	194	n.d.	n.d.	166 (5)	n.d.	n.d.	138(3)	
21	12.89	HDMBOA-hex	264, 284	<<0.05 [g]	$[M-H]^-$	n.d.															
					$[M-H+FA]^-$	432	n.d.	n.d.	224(11)	n.d.	356	n.d.	n.d.	401(30), 322(27), 164(17), 194(13)	194	n.d.	n.d.	166 (4)	n.d.	n.d.	138(3)	
12	9.71	4-O-Me-DIBOA-hex-hex	n.d. [f]	0.05	$[M-H]^-$	518	X [d]														
Benzoxazolinones																					
1	2.36	BOA-6-O-hex	n.d. [f]	n.d.	$[M-H]^-$	312	150	n.d.	n.a.	n.a.	n.a.	n.a.	n.a.	192(13), 149(9), 151(3), 222(3)	n.d.	n.d.	n.d.	n.d.	n.d.	122	n.d.	106 (21)
15	10.92	MBOA	264, 284	n.d.	$[M-H]^-$	164	n.a.	n.a.	n.a.	n.a.	n.a.	n.a.	n.a.	149 [h]	n.d.	n.d.	n.d.	n.d.	121	n.d.	n.d.	

ac, acetyl; FA, formic acid; hex, hexose; hex-hex, dihexose; n.a., not applicable; n.d., not detected. a Intensity relative to the most abundant ion (as indicated in bold), only ions with minimum relative intensity of 2% are shown. Roman numerals refer to specific cleavages, as shown in Figure 3, the corresponding neutral losses are shown in **Table 3.3**. b Precursor ion is the most abundant ion of the MS2 spectrum. c Miscellaneous fragments, not corresponding to any (single) numbered cleavage. Only fragments with minimum relative intensity of 10% are shown. d No clear MSn spectrum was obtained either due to low intensity of the precursor or to low stability of the precursor or its fragments in the ion trap. e The formic acid adduct was not detected. Hence, calculating a ratio was not possible, indicated here with >>20. f No clear UV spectrum could be obtained due to low signal intensity or co-elution. g The deprotonated ion was not detected. Hence, calculating a ratio was not possible, indicated here with <<0.05. h Fragment generated with activation Q 0.250, neutral loss corresponds to cleavage VII (loss of •CH3).

The presence in negative mode full MS of peaks at an *m/z* value 46 Da higher than that of the deprotonated ions of benzoxazin-3-one glycosides, based on literature and calculated molecular masses (**Figure 3.1**), indicated formation of formic acid adducts, $[M+FA-H]^-$. This is in accordance with previous results.[8] If necessary, full MS spectra in positive ionization mode were analyzed to confirm the molecular mass.

Fragmentation behavior of peaks 2-14 and 16-23 can be delineated to tentative identification of lactam, hydroxamic acid, and methyl derivative glycosides. The ratio between the intensity of the deprotonated ion and the formic acid adduct was calculated for each peak (**Table 3.1**). Capitalized roman numerals were assigned to mass spectrometric cleavages as shown in **Figure 3.3** with the corresponding neutral losses shown in **Table 3.2**.

Table 3.2. Neutral losses and fragment ions associated with the diagnostic cleavages of benzoxazin-3-one glycosides.

Cleavage no. [a]	Parent ion [a]	Neutral fragment	NL (Da)	Fragment ion
I	**M**	hex	162	$[M-H-hex]^-$
	D	hex-hex	324	$[M-H-hex-hex]^-$
II	**M**	hex + H_2O	180	$[M-H-hex-H_2O]^-$
	D	hex-hex + H_2O	342	$[M-H-hex-hex-H_2O]^-$
III	**a**	CH_2O_2 [b]	46	$[M-H-CH_2O_2]^-$
	M	hex + CH_2O_2 [b]	208	$[M-H-hex-CH_2O_2]^-$
	D	hex-hex + CH_2O_2 [b]	370	$[M-H-hex-hex-CH_2O_2]^-$
IV	**M**	hex + CO	190	$[M-H-hex-CO]^-$
	D	hex-hex + CO	352	$[M-H-hex-hex-CO]^-$
V	**FA adduct of methyl derivative**	FA + OCH_3	76	$[M-H-OCH_3]^-$
VI	**FA adduct**	FA	46	$[M-H]^-$
VII	**Methylated**	$^{\bullet}CH_3$	15	$[M-H-CH_3]^-$
VIII	**all**	CO	28	$[M-H-CO]^-$
IX	**a**	2 CO	56	$[M-H-2CO]^-$
	M	hex + 2 CO	218	$[M-H-hex-2CO]^-$
	D	hex-hex + 2 CO	380	$[M-H-hex-hex-2CO]^-$

a, aglycone fragment; D, dihexoside; FA, formic acid; hex, hexose; hex-hex, dihexose; M, monohexoside; NL, neutral loss. [a] As shown in **Figure 3.3**. [b] H_2O + CO.

3.3.3. Lactams

Fragmentation of benzoxazin-3-one aglycones has been studied systematically.[16,17] Fragmentation of the deprotonated HBOA aglycone (*m/z* 164) typically yields fragments at *m/z* 136, 118 and 108, corresponding to neutral losses of CO (28 Da), CH_2O_2 (46 Da), and 2 CO (56 Da), respectively.[16] Similar neutral losses were described for the deprotonated HMBOA aglycone (*m/z* 194) yielding

fragments at *m/z* 166, 148, and 138 with an additional peak at *m/z* 179 corresponding to loss of a methyl radical $^{\bullet}CH_3$ (15 Da).[16] These fragments are similar to what we observed in MS^3 fragmentation of deprotonated aglycones after loss of mono- or dihexose in MS^2 (neutral loss of 162 or 324 Da, respectively)(**Table 3.1**). For example, MS^3 fragmentation of the $[M-H-hex]^-$ ion (*m/z* 164) from peak 5, 7, or 8 resulted in fragments at *m/z* 136, 118, and 108 (**Table 3.1**). In the case of lactam aglycones, the main losses corresponded to CO (**VIII**), 2 CO (**IX**), and CH_2O_2 (**III**) resulting from ring cleavages (**Figure 3.3**, **Table 2**). The deprotonated aglycone fragment, originating from **I** (**Figure 3.3**, **Table 2**), was by far the most abundant in the MS^2 spectrum of lactam glycosides, which is similar to literature data on HBOA hexosides.[15] We systematically extended the acquired knowledge on lactam fragmentation patterns to other peaks, which showed similar fragmentation behavior in MS^2 and MS^3. Peaks 2, 3, 4, 7, 10, and 13 were identified as lactams accordingly (**Table 3.1**).

Peaks 16, 22 and 23 showed fragmentation behavior similar to that of lactam hexosides, although the main neutral loss observed was 204 Da. We hypothesize that this loss corresponds to an acetyl-hexose (42 + 162 Da) (**I**). The MS^3 spectrum of the resulting ion $[M-H-hex-ac]^-$ was identical to that of the $[M-H-hex]^-$ ion observed in fragmentation of lactam non-acetylated monohexosides (**Table 3.1**). The mass spectrometric characterization of acetyl-hexosides of benzoxazin-3-ones has not been described previously.

3.3.4. Hydroxamic acids

Hydroxamic acid aglycones were often detected as $[M-OH]^-$, losing the hydroxyl group attached at the N atom.[16,17] Typical fragments described for the $[M-OH]^-$ ion of DIMBOA (*m/z* 194) are *m/z* 166, 164 and 149 with neutral losses of CO_2 (44 Da), CH_2O_2 (46 Da), and $CH_2O_2 + {}^{\bullet}CH_3$ (61 Da), respectively.[16,17] Although we detected the $[M-H]^-$ rather than the $[M-OH]^-$ ion, MS^2 fragmentation of peak 11 or 14 resulted in main fragments at *m/z* 192 and 164, originating from neutral loss of (di)hexose plus CH_2O_2 (208 or 307 Da, **III**) and (di)hexose plus H_2O (180 or 342 Da, **II**), respectively. Additionally, the diagnostic fragment at *m/z* 149, resulting from a neutral loss of hex or hex-hex with $CH_2O_2 + {}^{\bullet}CH_3$ (208 + 15 Da), and a fragment at *m/z* 210 (originating from **I**), which matches the deprotonated DIMBOA aglycone, were detected. Due to the nature of the MS^2 fragmentation, which was in accordance with data reported for hydroxamic acid glycosides in literature[8,15], no intact aglycone was obtained for further fragmentation. MS^3 fragmentation of the $[M-H-hex\text{-}hex-H_2O]^-$ ion (*m/z* 192) from peak 11 yielded the typical fragment at *m/z* 164 (neutral loss of CO, **VIII**). MS^3 fragmentation of the $[M-H-hex\text{-}hex-CH_2O_2]^-$ or $[M-H-hex-CH_2O_2]^-$ ion (*m/z* 164) from peak 11 or 14 yielded the diagnostic fragment at *m/z* 149 (neutral loss of $^{\bullet}CH_3$, **VII**).

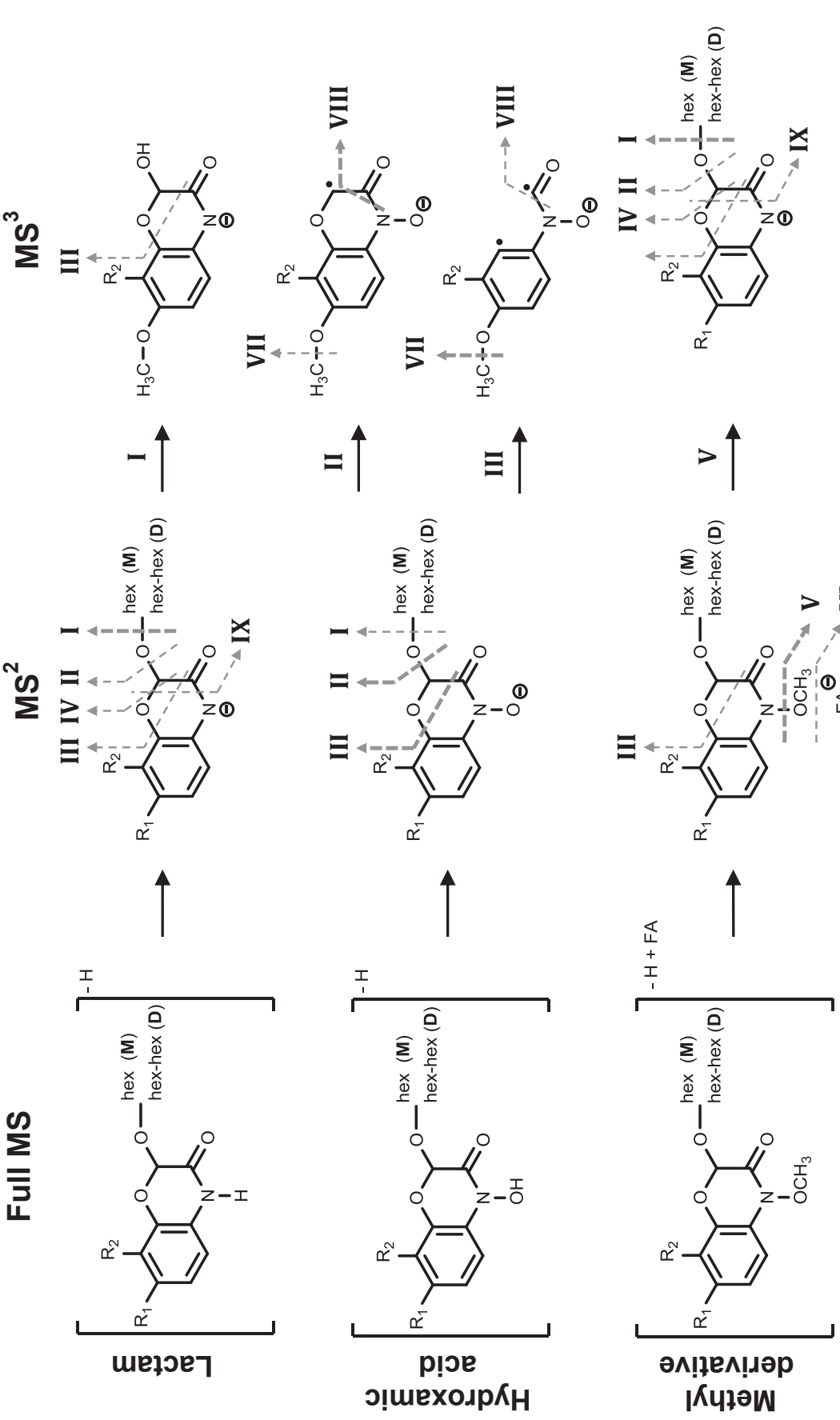

Figure 3.3. Putative fragmentation pathways of benzoxazin-3-one glycosides in mass spectrometry. The bold dashed line indicates a diagnostic cleavage with the highest observed intensity, for hydroxamic acids either **II** or **III** was the most intense. **VII** is only possible in methoxylated benzoxazin-3-ones. Therefore, a 6-methoxy derivative is used as an example in MS^3. Neutral losses associated with these cleavages are shown in **Table 3.2**. M. monohexoside: D. dihexoside: FA. formic acid.

Peaks 6, 9, 11, and 14 complied with the signatures described above and could readily be identified as hydroxamic acids. Based on these results, we conclude that fragmentation behaviour of hydroxamic acid glycosides differs distinctly from that of lactam glycosides.[8,15] In the case of hydroxamic acid glycosides, fragments associated with cleavages **II** and **III** (**Figure 3.3**) were the most abundant whereas for lactam glycosides the aglycone fragment, associated with cleavage **I** was always detected at the highest intensity.

Peak 18 was tentatively identified as an acetyl-hexoside of DIBOA, which was not previously described. The fragmentation found for this peak was similar to that of non-acetylated DIBOA hexosides. The main neutral loss of 250 Da corresponded to the tandem loss of the acetyl-hexose moiety (204 Da) and CH_2O_2 (46 Da)(**III**).

3.3.5. Methyl derivatives

Contrary to lactams and hydroxamic acids, no typical fragmentation behaviour of methyl derivatives could be identified from literature. In a previous study[8] two methyl derivative monohexosides (HDMBOA-hex and HDM_2BOA-hex) from maize were identified by LC-MS, but fragmentation data were not shown.

In our analyses we observed several peaks matching the screening criteria and calculated masses of benzoxazin-3-one glycosides, based on literature, (**Figure 3.1**) but showing ionization and fragmentation behaviour different from lactam and hydroxamic acid glycosides. It was deemed likely that these would be methyl derivatives. For most of these peaks, the deprotonated ion was detected at very low intensity or not at all. In these cases, formation of formic acid adducts, at an *m/z* value 46 Da higher than the expected $[M-H]^-$, enabled the detection of the suspected methyl derivative glycosides in ESI-MS. In order to confirm that these were indeed formic acid adducts, full MS spectra in positive ionization mode were analysed. Thereby, the nominal mass of the compounds was confirmed, establishing that the precursor ions in negative ionization mode were formic acid adducts. This was further corroborated by the presence of a MS^2 fragment ion corresponding to a neutral loss of FA (46 Da, **VI**). The MS^2 base peak corresponded to a neutral loss of 76 Da (**Table 3.1**). We hypothesize this to be a tandem loss of formic acid and the N-substituted methoxyl moiety (**V**)(**Figure 3.3**, **Table 3.2**). Similar behaviour has been suggested previously for acetic acid adducts.[8] To further support this hypothesis, MS^3 fragmentation of this ion (e.g. peak 21, MS^2 fragment at *m/z* 356) was performed, which produced a spectrum almost identical to the MS^2 spectrum of the corresponding lactam (**Figure 3.5**). Thus, the resulting fragment $[M-H-OCH_3]^-$ should be structurally equal to a deprotonated lactam (**Figure 3.5**). Other neutral losses from the $[M-H+FA]^-$ precursor in MS^2 were 208 or 370 Da, which were related to loss of mono- or dihexose plus CH_2O_2 (**III**), respectively. The neutral loss of 78 Da observed at relatively high intensity, especially in methyl derivative and hydroxamic acid dihexosides (e.g. HDMBOA-hex-hex fragment *m/z* 516), is possibly related to a neutral fragment originating from ring cleavage of the hexosyl moiety. Several other fragments were observed

in the MS^2 spectrum that did not correspond to any of the numbered cleavages, but which included typical benzoxazin-3-one fragments such as *m/z* 192, 164, 149, and 134 (**Table 1**).

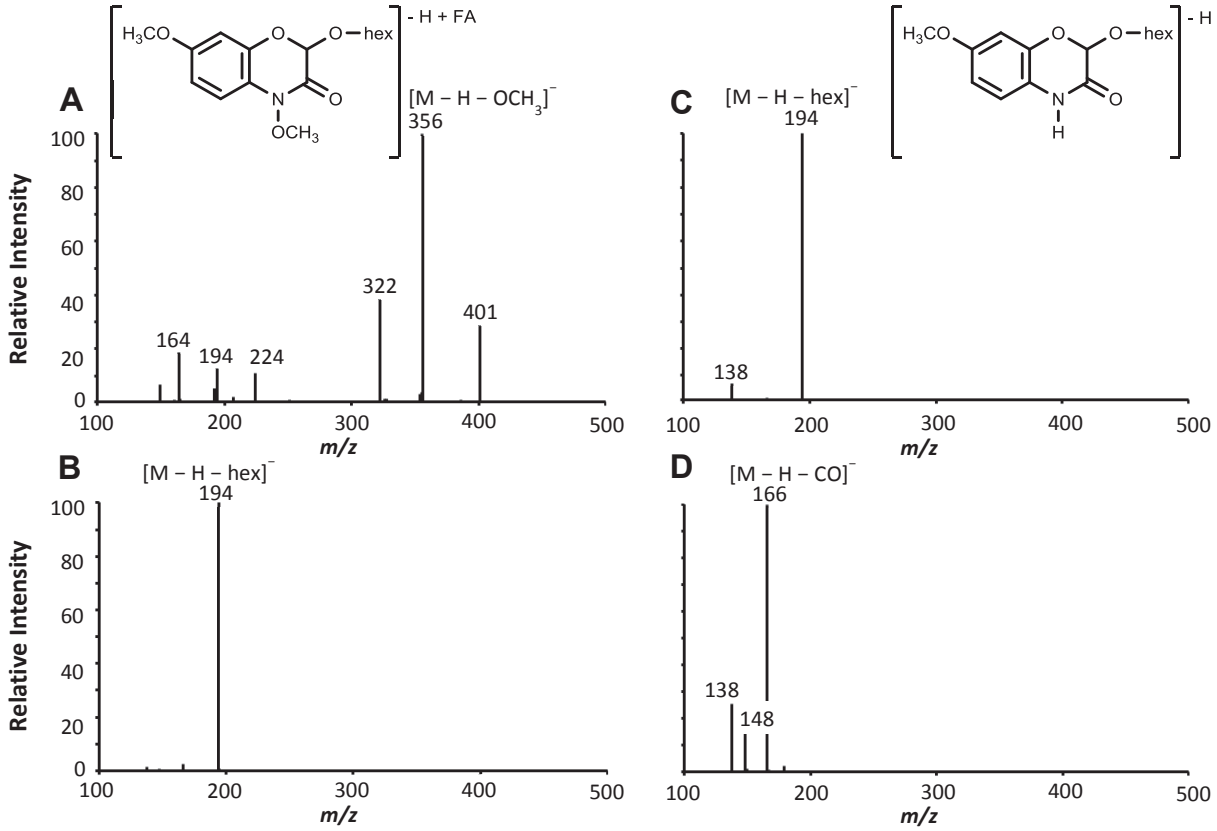

Figure 3.4. Fragmentation spectra of (A) the formic acid adduct of HDMBOA-hex *m/z* 432, a methyl derivative, in MS^2; (B) its most intense product ion *m/z* 356 in MS^3; (C) the deprotonated molecule HMBOA-hex *m/z* 356, a lactam, in MS^2; and (D) its most intense product ion *m/z* 194 in MS^3. hex, hexose.

Five peaks (12, 17, 19, 20 and 21) were identified as benzoxazin-3-one methyl derivatives. HDMBOA has been previously found in species of Poaceae[8,18], whereas 4-*O*-Me-DIBOA had only been detected upon *in vitro* incubations of DIBOA with a 4-*O*-methyltransferase but not in plant tissues from this family.[10] 4-*O*-Me-DIBOA was identified based on its fragmentation behaviour, which was similar to that of HDMBOA.

3.3.6. Subclassification of benzoxazin-3-one glycosides

Following these tentative identifications, the ratio between the deprotonated ion and the formic acid adduct was found to be indicative for the presence of the different subclasses of benzoxazin-3-one glycosides. The $[M-H]^-$:$[M+FA-H]^-$ ratio was found to be larger than 1.0 for all lactams. For hydroxamic acids the $[M-H]^-$:$[M+FA-H]^-$ ratio was generally found to be lower than that of lactams, between 0.5 and 1.0 for monohexosides, and above 1.0 for dihexosides. Low

intensity of the deprotonated ion in the case of methyl derivatives resulted in $[M-H]^-$:$[M+FA-H]^-$ ratios of 0.05 or below. Therefore, this ratio can be used to quickly discriminate benzoxazin-3-one methyl derivatives, from lactams and hydroxamic acids. On its own, the ratio is insufficient to clearly differentiate between the latter two subclasses. Screening the MS^2 fragmentation spectra for diagnostic fragments of lactam (162 or 324) and hydroxamic acid (208 and 180 or 342 and 370) mono- or dihexosides should efficiently confirm peak tentative peak identifications (**Table 3.2** and **Table 3.3**).

3.3.7. Characterization of benzoxazolinones

Peak 15, a benzoxazolinone aglycone, was identified as 6-methoxy-2-benzoxazolinone (MBOA), detected at 260 nm but not visible in **Figure 3.2**, based on its spectrometric properties matching those published previously[16] (**Table 3.1**). Peak 1 was tentatively assigned as a monohexoside of 6-hydroxy-2-benzoxazolinone (BOA-6-OH). Mass spectrometric data of benzoxazolinone hexosides has not been reported before, but fragmentation behaviour of this peak was similar to that observed for benzoxazin-3-one lactam hexosides. The main neutral loss of 162 Da (hexose) resulted in a fragment at *m/z* 150, matching the deprotonated BOA-6-OH aglycone fragment. Further fragmentation in MS^3 resulted in neutral losses of CO and CO_2, similar to what was observed for benzoxazin-3-ones (**Figure S3.1**, supplementary information). This compound, BOA-6-*O*-hex, is the detoxification product of MBOA, which is formed via demethylation of MBOA to BOA-6-OH, and subsequent glycosylation.[19]

3.3.8. Classification of benzoxazinoids

Peaks 1 to 23 (**Figure 3.2**, **Table 3.1**) were found to correspond to benzoxazinoids, as described in the previous sections. Our observations regarding their mass spectrometric behaviour were summarized in a decision guideline to aid future identification of benzoxazin-3-one glycosides and benzoxazolinones using mass spectrometry (**Figure 3.5**).

It has been reported[8,10] that in case of monoglycosides in Poaceae mainly glucose is present, however in other plant species galactosides have also been reported[20]. Thus, we cannot state with certainty that the hexosides represent glucosides. Regarding diglycosides, we can state that the second saccharide unit must have been a hexose, but no further conclusions could be made regarding its identity or the nature of the glycosidic bond between the two hexoses (α or β configuration, linkage type). For some benzoxazin-3-one glycosides two peaks were detected with similar spectral properties (e.g. peaks 2 and 4, 16 and 22, 20 and 21). In the case of dihexosides, the peaks are possibly isomers with different type or position of the second hexosyl moiety. Alternatively, the position of hydroxyl or methoxyl moieties on the aromatic ring might vary between isomers, but this was not investigated further. Glycosylation of benzoxazin-3-one at a position other than *C*-2 has not been reported.

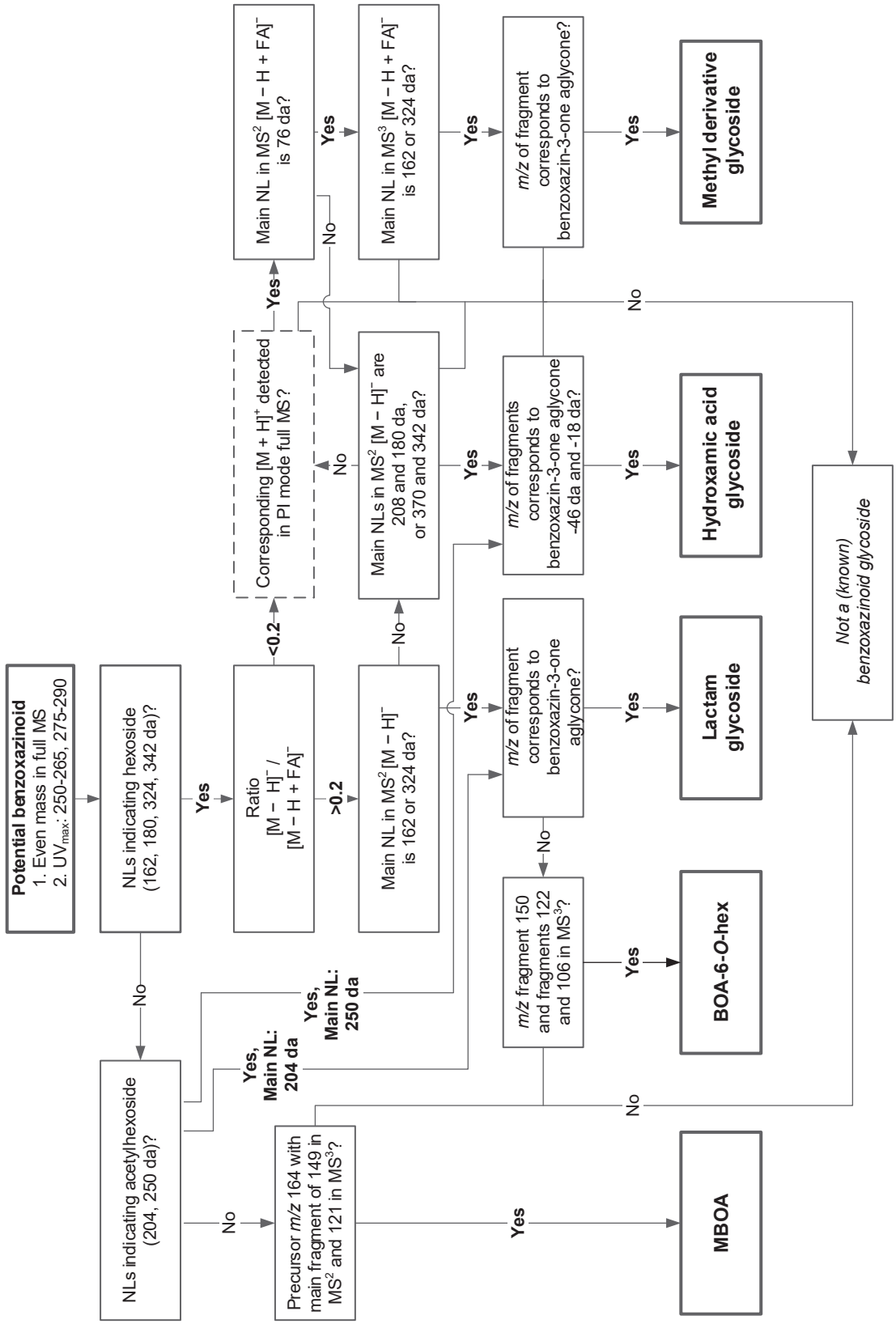

Figure 3.5. Decision guideline for the classification of benzoxazinoids. All decisions apply to analyses in negative ionization mode, except for the one delineated by dashed lines. $[M-H]^-$, deprotonated ion; $[M+FA-H]^-$, formic acid adduct; $[M+H]^+$, protonated ion; NL, neutral loss.

3.3.9. Accurate mass of benzoxazinoids by HRMS

All previously described data and identifications were based on MS^n fragmentation as determined on a low resolution mass spectrometer (ESI-IT-MS^n). To confirm the tentative identification of all benzoxazinoids (peaks 1-23), accurate mass data was acquired on a high resolution (max. mass error 2.3 ppm) mass spectrometer (ESI-IT-FTMS), therewith corroborating the expected elemental composition (**Table 3.3**).

Table 3.3. Accurate mass data as determined by UHPLC-ESI-IT-FTMS.

Peak no. [a]	Compound	Ionisation [b]	*m/z* observed	Molecular formula	*m/z* calculated	Error (ppm)
1	BOA-6-*O*-hex	$[M-H]^-$	312.0734	$C_{13}H_{15}NO_8$	312.0725	-2.3
2	DHBOA-hex	$[M-H]^-$	342.0836	$C_{14}H_{17}NO_9$	342.0831	-1.6
3	DHBOA-hex-hex	$[M-H]^-$	504.1370	$C_{20}H_{27}NO_{14}$	504.1359	-2.0
4	DHBOA-hex	$[M-H]^-$	342.0835	$C_{14}H_{17}NO_9$	342.0831	-1.6
5	HBOA-hex-hex	$[M-H]^-$	488.1418	$C_{20}H_{27}NO_{13}$	488.1410	-1.5
6	DIBOA-hex-hex	$[M-H]^-$	504.1367	$C_{20}H_{27}NO_{14}$	504.1359	-1.6
7	HBOA-hex-hex	$[M-H]^-$	488.1419	$C_{20}H_{27}NO_{13}$	488.1410	-1.2
8	HBOA-hex	$[M-H]^-$	326.0886	$C_{14}H_{17}NO_8$	326.0881	-1.3
9	DIBOA-hex	$[M-H]^-$	342.0834	$C_{14}H_{17}NO_9$	342.0831	-1.2
10	HMBOA-hex-hex	$[M-H]^-$	518.1522	$C_{21}H_{29}NO_{14}$	518.1515	-1.4
11	DIMBOA-hex-hex	$[M-H]^-$	534.1471	$C_{21}H_{29}NO_{15}$	534.1464	-1.1
12	4-*O*-Me-DIBOA-hex-hex	$[M-H+FA]^-$	564.1579	$C_{21}H_{29}NO_{14}$ + CHOOH [c]	564.1570	-1.6
13	HMBOA-hex	$[M-H]^-$	356.0993	$C_{15}H_{19}NO_9$	356.0987	-1.5
14	DIMBOA-hex	$[M-H]^-$	372.0940	$C_{15}H_{19}NO_{10}$	372.0936	-1.2
15	MBOA	$[M-H]^-$	164.0344	$C_8H_7NO_3$	164.0353	-1.6
16	HBOA-hex-ac	$[M-H]^-$	368.0991	$C_{16}H_{19}NO_9$	368.0987	-1.2
17	HDMBOA-hex-hex	$[M-H+FA]^-$	594.1686	$C_{22}H_{31}NO_{15}$ + CHOOH [c]	594.1676	-1.9
18	DIBOA-hex-ac	$[M-H]^-$	384.0942	$C_{16}H_{19}NO_{10}$	384.0936	-1.8
19	4-*O*-Me-DIBOA-hex	$[M-H+FA]^-$	402.1053	$C_{15}H_{19}NO_9$ + CHOOH [c]	402.1042	-1.5
20	HDMBOA-hex	$[M-H+FA]^-$	432.1154	$C_{16}H_{21}NO_{10}$ + CHOOH [c]	432.1148	-1.2
21	HDMBOA-hex	$[M-H+FA]^-$	432.1153	$C_{16}H_{21}NO_{10}$ + CHOOH [c]	432.1148	-1.1
22	HBOA-hex-ac	$[M-H]^-$	368.0990	$C_{16}H_{19}NO_9$	368.0987	-1.0
23	HMBOA-hex-ac	$[M-H]^-$	398.1096	$C_{17}H_{21}NO_{10}$	398.1093	-1.3

[a] Numbers refer to benzoxazinoid peaks (**Figure 2**) and corresponding spectral data from LC-ESI-IT-MS^n (**Table 1**). [b] Only the type of ionization with the highest intensity is shown. [c] Molecular formula CHOOH corresponds to formic acid.

3.3.10. Identification of miscellaneous peaks

Peaks labelled with lower case roman numerals (i to xiv) correspond to miscellaneous compounds (**Figure 3.2**, **Table S3.1**, supplementary information). By comparison to the authentic standard, the relatively large peak vii was found to be tryptophan (**Figure 3.2**, **Table S3.1**). Tryptophan is synthesized from indole-3-glycerol phosphate, which also serves as the starting point in the biosynthetic pathway of benzoxazinoids.[3,21]

Wheat seedlings elicited with *Rhizopus* during germination contain a wide variety of secondary metabolites mainly constituted by benzoxazin-3-one glycosides and benzoxazolinones. The systematic study of these benzoxazinoids using mass spectrometry described in this work will facilitate their future identification.

3.4. References

[1] Shiferaw, B., Smale, M., Braun, H.J., Duveiller, E., Reynolds, M., and Muricho, G. (2013) Crops that feed the world 10. Past successes and future challenges to the role played by wheat in global food security. *Food Security*, 5*(3)*: p. 291-317.

[2] Andersson, A.A.M., Dimberg, L., Aman, P., and Landberg, R. (2014) Recent findings on certain bioactive components in whole grain wheat and rye. *Journal of Cereal Science*, 59*(3)*: p. 294-311.

[3] Niemeyer, H.M. (2009) Hydroxamic acids derived from 2-hydroxy-2*H*-1,4-benzoxazin-3(4*H*)-one: Key defense chemicals of cereals. *Journal of Agricultural and Food Chemistry*, 57*(5)*: p. 1677-1696.

[4] Adhikari, K.B., Tanwir, F., Gregersen, P.L., Steffensen, S.K., Jensen, B.M., Poulsen, L.K., Nielsen, C.H., Hoyer, S., Borre, M., and Fomsgaard, I.S. (2015) Benzoxazinoids: Cereal phytochemicals with putative therapeutic and health-protecting properties. *Molecular Nutrition & Food Research*, 59*(7)*: p. 1324-1338.

[5] Buchmann, C.A., Nersesyan, A., Kopp, B., Schauberger, D., Darroudi, F., Grummt, T., Krupitza, G., Kundi, M., Schulte-Hermann, R., and Knasmueller, S. (2007) Dihydroxy-7-methoxy-1,4-benzoxazin-3-one (DIMBOA) and 2,4-dihydroxy-1,4-benzoxazin-3-one (DIBOA), two naturally occurring benzoxazinones contained in sprouts of Gramineae are potent aneugens in human-derived liver cells (HepG2). *Cancer Letters*, 246*(1-2)*: p. 290-299.

[6] Ahmad, S., Veyrat, N., Gordon-Weeks, R., Zhang, Y.H., Martin, J., Smart, L., Glauser, G., Erb, M., Flors, V., Frey, M., and Ton, J. (2011) Benzoxazinoid metabolites regulate innate immunity against aphids and fungi in maize. *Plant Physiology*, 157*(1)*: p. 317-327.

[7] Sicker, D., Frey, M., Schulz, M., and Gierl, A. (2000) Role of natural benzoxazinones in the survival strategy of plants. *International Review of Cytology - A Survey of Cell Biology*, 198: p. 319-346.

[8] Cambier, V., Hance, T., and de Hoffmann, E. (1999) Non-injured maize contains several 1,4-benzoxazin-3-one related compounds but only as glucoconjugates. *Phytochemical Analysis*, 10*(3)*: p. 119-126.

[9] von Rad, U., Huttl, R., Lottspeich, F., Gierl, A., and Frey, M. (2001) Two glucosyltransferases are involved in detoxification of benzoxazinoids in maize. *Plant Journal*, 28*(6)*: p. 633-642.

[10] Oikawa, A., Ishihara, A., and Iwamura, H. (2002) Induction of HDMBOA-Glc accumulation and DIMBOA-Glc 4-*O*-methyltransferase by jasmonic acid in poaceous plants. *Phytochemistry*, 61*(3)*: p. 331-337.

[11] Aisyah, S., Gruppen, H., Madzora, B., and Vincken, J.-P. (2013) Modulation of isoflavonoid composition of *Rhizopus oryzae* elicited soybean (*Glycine max*) seedlings by light and wounding. *Journal of Agricultural and Food Chemistry*, 61*(36)*: p. 8657-8667.

[12] Ahuja, I., Kissen, R., and Bones, A.M. (2012) Phytoalexins in defense against pathogens. *Trends in Plant Science*, 17*(2)*: p. 73-90.

[13] Simons, R., Vincken, J.-P., Bohin, M.C., Kuijpers, T.F.M., Verbruggen, M.A., and Gruppen, H. (2011) Identification of prenylated pterocarpans and other isoflavonoids in *Rhizopus* spp. elicited soya bean seedlings by electrospray ionisation mass spectrometry. *Rapid Communications in Mass Spectrometry*, 25*(1)*: p. 55-65.

[14] Simons, R., Vincken, J.-P., Roidos, N., Bovee, T.F.H., van Iersel, M., Verbruggen, M.A., and Gruppen, H. (2011) Increasing soy isoflavonoid content and diversity by simultaneous malting and challenging by a fungus to modulate estrogenicity. *Journal of Agricultural and Food Chemistry*, 59*(12)*: p. 6748-6758.

[15] Hanhineva, K., Rogachev, I., Aura, A.M., Aharoni, A., Poutanen, K., and Mykkanen, H. (2011) Qualitative characterization of benzoxazinoid derivatives in

whole grain rye and wheat by LC-MS metabolite profiling. *Journal of Agricultural and Food Chemistry*, 59*(3)*: p. 921-927.

[16] Bonnington, L., Eljarrat, E., Guillamon, M., Eichhorn, P., Taberner, A., and Barcelo, D. (2003) Development of a liquid chromatography-electrospray-tandem mass spectrometry method for the quantitative determination of benzoxazinone derivatives in plants. *Analytical Chemistry*, 75*(13)*: p. 3128-3136.

[17] Bonnington, L.S., Barcelo, D., and Knepper, T.P. (2003) Utilisation of electrospray time-of-flight mass spectrometry for solving complex fragmentation patterns: Application to benzoxazinone derivatives. *Journal of Mass Spectrometry*, 38*(10)*: p. 1054-1066.

[18] Oikawa, A., Ishihara, A., Tanaka, C., Mori, N., Tsuda, M., and Iwamura, H. (2004) Accumulation of HDMBOA-Glc is induced by biotic stresses prior to the release of MBOA in maize leaves. *Phytochemistry*, 65*(22)*: p. 2995-3001.

[19] Schulz, M., Knop, M., Kant, S., Sicker, D., Voloshchuk, N., and Gryganski, A., Detoxification of allelochemicals - the case of bezoxazolin-2(3H)-one (BOA), in *Allelopathy: A physiological process with ecological implications*, M.J. Reigosa, N. Pedrol, and L. González, Editors. 2006, Springer: Dordrecht, The Netherlands. p. 157-170.

[20] Wu, W.H., Chen, T.Y., Lu, R.W., Chen, S., and Chang, C.C. (2012) Benzoxazinoids from *Scoparia dulcis* (sweet broomweed) with antiproliferative activity against the DU-145 human prostate cancer cell line. *Phytochemistry*, 83: p. 110-115.

[21] Frey, M., Schullehner, K., Dick, R., Fiesselmann, A., and Gierl, A. (2009) Benzoxazinoid biosynthesis, a model for evolution of secondary metabolic pathways in plants. *Phytochemistry*, 70*(15-16)*: p. 1645-1651.

[22] Bjarnholt, N., Rook, F., Motawia, M.S., Cornett, C., Jorgensen, C., Olsen, C.E., Jaroszewski, J.W., Bak, S., and Moller, B.L. (2008) Diversification of an ancient theme: Hydroxynitrile glucosides. *Phytochemistry*, 69*(7)*: p. 1507-1516.

[23] Zagrobelny, M., Motawia, M.S., Olsen, C.E., Bak, S., and Moller, B.L. (2013) Male-to-female transfer of 5-hydroxytryptophan glucoside during mating in *Zygaena filipendulae* (Lepidoptera). *Insect Biochemistry and Molecular Biology*, 43*(11)*: p. 1037-1044.

[24] Franks, T.K., Hayasaka, Y., Choimes, S., and van Heeswijck, R. (2005) Cyanogenic glucosides in grapevine: Polymorphism, identification and developmental patterns. *Phytochemistry*, 66*(2)*: p. 165-173.

[25] Wang, Y.L., Liu, Z.J., Liu, Q., Ma, J.N., Hattori, M., and Ma, C.M. (2014) Simultaneous quantification of secoisolariciresinol diglucoside and cyanogenic glycosides in flaxseed products by various processing methods. *Food Analytical Methods*, 7*(7)*: p. 1526-1529.

[26] Piraud, M., Vianey-Saban, C., Petritis, K., Elfakir, C., Steghens, J.P., Morla, A., and Bouchu, D. (2003) ESI-MS/MS analysis of underivatised amino acids: A new tool for the diagnosis of inherited disorders of amino acid metabolism. Fragmentation study of 79 molecules of biological interest in positive and negative ionisation mode. *Rapid Communications in Mass Spectrometry*, 17*(12)*: p. 1297-1311.

[27] Levandi, T., Pussa, T., Vaher, M., Ingver, A., Koppel, R., and Kaljurand, M. (2014) Principal component analysis of HPLC-MS/MS patterns of wheat (*Triticum aestivum*) varieties. *Proceedings of the Estonian Academy of Sciences*, 63*(1)*: p. 86-92.

[28] Liu, Q., Qiu, Y., and Beta, T. (2010) Comparison of antioxidant activities of different colored wheat grains and analysis of phenolic compounds. *Journal of Agricultural and Food Chemistry*, 58*(16)*: p. 9235-9241.

3.5. Supplementary information

Table S3.1. Spectral properties of miscellaneous compounds in the wheat seedling extract, tentatively identified by UHPLC-PDA-ESI-IT-MS.

Peak no.	Rt. (min)	Compounds [a]	UV_{max} (nm)	Ionisation [a]	*m/z*	MS^2 product ions (relative intensity) [a, b]						Ref.
i	2.09	Unknown	n.d.	$[M+H]^+$	253	**n.d.** [c]						
				$[M+NH_4]^+$	270	**253** [c]	163(2)					
				$[M+Na]^+$	275	**n.d.** [c]						
				$[M-H]^-$	n.d.							
				$[M+FA-H]^-$	297	**251**						
ii	2.17	Unknown	283	$[M-H]^-$	625	**485** [c]	383(78)	221(51)	425(38)	323(29)	407(28)	
				$[M+FA-H]^-$	671	**625** [c]	650 (2)					
iii	2.35	Unknown	n.d.	$[M+H]^+$	253	**n.d.** [c]						
				$[M+NH_4]^+$	270	**253** [c]	163(2)					
				$[M+Na]^+$	275	**n.d.** [c]						
				$[M-H]^-$	251	**n.d.**						
				$[M+FA-H]^-$	297	**251**						
iv	2.71	Linamarin	n.d.	$[M+H]^+$	n.d.							[22-24]
				$[M+NH_4]^+$	265	**180** [c]	248(53)	163(48)	145(42)	221(6)	85(6)	
				$[M+Na]^+$	270	**n.d.** [c]						
				$[M-H]^-$	n.d.							
				$[M+FA-H]^-$	292	**246**	188(46)	161(13)	201(5)			
v	5.01	Neolinustatin	n.d.	$[M+H]^+$	424	**n.d.** [c]						[25]
				$[M+NH_4]^+$	441	**325** [c]	163(22)	145(19)	262(17)	289(13)	424(11)	
				$[M+Na]^+$	446	**n.d.** [c]						
				$[M-H]^-$	422	**323**	179(12)	221(8)	161(4)	263(2)	125(2)	
				$[M+FA-H]^-$	468	**422**						
vi	5.62	Tryptophan [d]	278	$[M-H]^-$	203	**159**	116(35)	142(12)				[26]
				$[M+H-NH_3]^+$	188	**146** [c]	144(11)	170(3)				
				$[M+H]^+$	205	**188** [c]						
vii	5.89	Lotaustralin	n.d.	$[M+H]^+$	262	**n.d.**						[22-24]
				$[M+NH_4]^+$	279	**180** [c]	262(69)	145(55)	163(52)	235(22)	85(9)	
				$[M+Na]^+$	284	**257** [c]	185(22)	212(3)				
				$[M-H]^-$	n.d.							
				$[M+FA-H]^-$	306	**260**	188(70)	161(18)	175(2)			
viii	10.73	Apigenin-	271,	$[M-H]^-$	563	**473**	443(98)	503(34)	383(26)	353(26)	474(24)	[27,28]
ix	10.99	Hex-hex-*N*-	n.d.	$[M-H]^-$	366	**186**	204(75)	246(17)	142(11)	187(4)		[27]
x	11.13	Unknown	n.d.	$[M-H]^-$	371	**249**	231(8)	121(5)	113(4)			
xi	11.27	Apigenin-	271,	$[M-H]^-$	563	**443**	473(63)	353(19)	444(18)	383(16)	474(14)	[27,28]
xii	11.42	Apigenin-	271,	$[M-H]^-$	563	**473**	443(81)	503(68)	383(37)	353(29)	474(20)	[27,28]
xiii	11.94	Unknown	n.d.	$[M-H]^-$	385	**267**	249 (11)					

[a] FA, formic acid; hex, hexose; n.d., not detected; pent, pentose. [b] Top six fragments with relative intensity >2 are shown. [c] Spectral data obtained from analysis with different MS settings (positive and negative ionisation mode, *m/z* range 125-1000, MS^2 fragmentation with activation Q 0.250). [d] Identification confirmed with authentic standard.

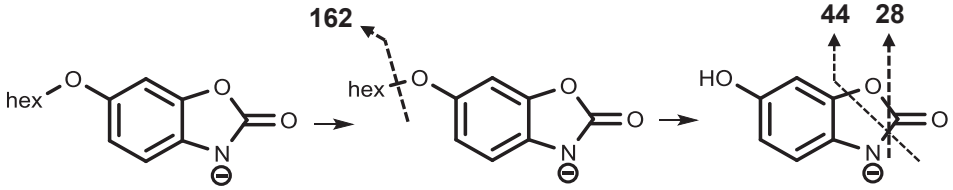

Figure S3.1. Proposed fragmentation of BOA-6-O-hex in ESI-IT-MS^n (negative ionisation mode).

CHAPTER 4

Structure and biosynthesis of benzoxazinoids: plant defence metabolites with potential as antimicrobial scaffolds

Benzoxazinoids, comprising the classes of benzoxazinones and benzoxazolinones, are a set of specialised metabolites produced by the plant family Poaceae (formerly Gramineae), and some dicots. The family Poaceae in particular contains several important crops like maize and wheat. Benzoxazinoids play a role in allelopathy and as defence compounds against (micro)biological threats. The effectivity of benzoxazinones in these functionalities is largely imposed by the subclasses (determined by *N* substituent). In this review, we provide an overview of all currently known natural benzoxazinoids and a summary of the current state of knowledge of their biosynthesis. We also evaluated their antimicrobial activity based on minimum inhibitory concentration (MIC) values reported in literature. Monomeric natural benzoxazinoids seem to lack potency as antimicrobial agents. The 1,4-benzoxazin-3-one backbone, however, has been shown to be a potential scaffold for designing new antimicrobial compounds. This has been demonstrated by a number of studies that report potent activity of synthetic derivatives of 1,4-benzoxazin-3-one, which possess MIC values down to 6.25 μg mL^{-1} against pathogenic fungi (e.g. *C. albicans*) and 16 μg mL^{-1} against bacteria (e.g. *S. aureus* and *E. coli*). Observations on the structural requirements for allelopathy, insecticidal, and antimicrobial activity suggest that they are not necessarily conferred by similar mechanisms.

Based on: Wouter J. C. de Bruijn, Harry Gruppen, and Jean-Paul Vincken (2018) Structure and biosynthesis of benzoxazinoids: plant defence metabolites with potential as antimicrobial scaffolds, *Phytochemistry*, 155: p. 233-243.

4.1. Introduction

Benzoxazinoids are a set of specialised metabolites that are prominently described in species of the monocot plant family Poaceae. Benzoxazinoids have also been reported to be present in dicots of the families Acanthaceae, Calceolariaceae, Lamiaceae, Plantaginaceae, and Ranunculaceae.[1-3] Due to the agricultural importance of the crops in Poaceae such as wheat (*Triticum aestivum*) and maize (*Zea mays*), benzoxazinoids of this plant family will be our main focus. These specialised metabolites play a role in allelopathic plant-plant interactions, as defence compounds against (micro)biological threats, and as defence regulatory signals.[3-6] Their allelopathic and defence functionalities, which are discussed in more detail in **Section 4.5**, suggest that benzoxazinoids could be potentially interesting leads for antimicrobial compounds. Promising lead structures might also be further modified to optimize their antimicrobial activity, as has been done for allelopathic activity.[7,8]

In this review we aim to provide a comprehensive overview of the structures of natural benzoxazinoids and to investigate their biosynthesis and biofunctionality with an emphasis on their antimicrobial potential.

4.2. Structure of natural benzoxazinoids

4.2.1. Classification and subclassification

Benzoxazinoids are divided into two classes: benzoxazinones (1,4-benzoxazin-3-one) and benzoxazolinones (1,3-benzoxazol-2-one) (**Figure 4.1**). Benzoxazolinones were first reported in rye in the 1950s[9] and benzoxazinones shortly thereafter in the early 1960s, also in rye.[10,11]

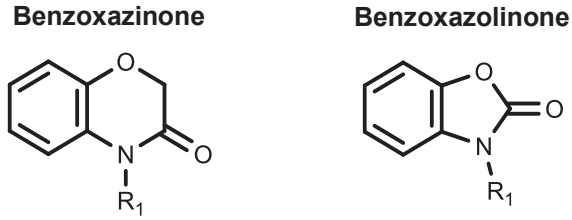

Figure 4.1. The backbones of the two classes of benzoxazinoids: benzoxazinones (1,4-benzoxazin-3-one) and benzoxazolinones (1,3-benzoxazol-2-one). R_1 substituent determines subclass, see **Table 4.1**.

Within these classes, several subclasses are formed by compounds with various *N* substituents.[3,12] The class of benzoxazinones is divided into three subclasses: lactams (*N*-hydro), hydroxamic acids (*N*-hydroxy), and methyl derivatives (*N*-methoxy) (**Table 4.1**). Within the class of benzoxazolinones, *N*-hydro derivatives are by far the most common due to loss of the *N* substituent in the transformation from benzoxazinone to benzoxazolinone (**Section 4.4.2**).

Table 4.1. Overview of monomeric natural benzoxazinoids of the classes benzoxazinones (1,4-benzoxazin-3-one backbone with *C*2 hydroxylation) and benzoxazolinones (1,3-benzoxazol-2-one backbone) reported in literature, with their systematic name and abbreviation. All benzoxazinones are displayed as their aglycones.

Benzoxazinones [a]	R_2	R_3	R_4	R_5	Systematic name	Abbreviation [b]	Natural source [c]	Ref.
***N*-hydro (R_1 = H): lactams**								
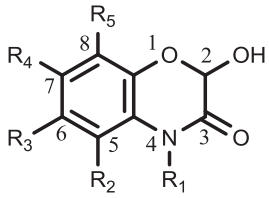	H	H	H	H	2-hydroxy-1,4-benzoxazin-3-one	HBOA	Poaceae Acanthaceae Calceolariaceae Plantaginaceae Lamiaceae	[13,14] [15,16] [17] [16] [18]
	H	H	OH	H	2,7-dihydroxy-1,4-benzoxazin-3-one	DHBOA	Poaceae Acanthaceae Calceolariaceae Lamiaceae	[19,20] [21] [17] [18]
	H	H	OCH_3	H	2-hydroxy-7-methoxy-1,4-benzoxazin-3-one	HMBOA	Poaceae Acanthaceae Plantaginaceae	[12,14] [15,16] [16]
	H	H	OCH_3	OCH_3	2-hydroxy-7,8-dimethoxy-1,4-benzoxazin-3-one	HM_2BOA	Poaceae	[12,22]
	Cl	H	OCH_3	H	5-chloro-2-hydroxy-7-methoxy-1,4-benzoxazin-3-one	Cl-HMBOA	Poaceae	[23]
	H	H	Cl	H	7-chloro-2-hydroxy-1,4-benzoxazin-3-one	n.a. [d]	Acanthaceae	[24]
	OH	H	H	H	2,5-dihydroxy-1,4-benzoxazin-3-one	n.a.	Acanthaceae	[24]
	H	OH	H	H	2,6-dihydroxy-1,4-benzoxazin-3-one	n.a.	Lamiaceae	[18]
***N*-hydroxy (R_1 = OH): hydroxamic acids**								
	H	H	H	H	2,4-dihydroxy-1,4-benzoxazin-3-one	DIBOA	Poaceae Acanthaceae Ranunculaceae Calceolariaceae Plantaginaceae Lamiaceae	[12,14] [15,21] [25] [17] [16] [18]
	H	H	OH	H	2,4,7-trihydroxy-1,4-benzoxazin-3-one	TRIBOA	Poaceae Acanthaceae	[19] [16]
	H	H	OCH_3	H	2,4-dihydroxy-7-methoxy-1,4-benzoxazin-3-one	DIMBOA	Poaceae Acanthaceae Plantaginaceae	[12,14] [15,16] [16]
	H	H	OH	OCH_3	2,4,7-trihydroxy-8-methoxy-1,4-benzoxazin-3-one	TRIMBOA	Poaceae	[26]
	H	H	OCH_3	OCH_3	2,4-dihydroxy-7,8-dimethoxy-1,4-benzoxazin-3-one	DIM_2BOA	Poaceae	[3,12]
	H	H	Cl	H	7-chloro-2,4-dihydroxy-1,4-benzoxazin-3-one	7-Cl-DIBOA	Acanthaceae	[27]
***N*-methoxy (R_1= OCH_3): methyl derivatives**								
	H	H	H	H	2-hydroxy-4-methoxy-1,4-benzoxazin-3-one	4-*O*-Me-DIBOA	Poaceae	[20,28]
	H	H	OCH_3	H	2-hydroxy-4,7-dimethoxy-1,4-benzoxazin-3-one	HDMBOA	Poaceae	[12,14]
	H	H	OCH_3	OCH_3	2-hydroxy-4,7,8-trimethoxy-1,4-benzoxazin-3-one	HDM_2BOA	Poaceae	[26,29]

Benzoxazolinones	R_2	R_3	R_4	R_5	Systematic name	Abbreviation [b]	Natural source [c]	Ref.
N-hydro **(R_1 = H)**								
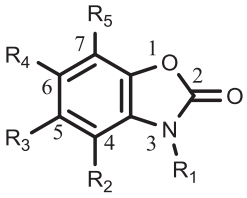	H	H	H	H	1,3-benzoxazol-2-one	BOA	Poaceae Acanthaceae Ranunculaceae Calceolariaceae Plantaginaceae	[12,30] [16,21] [25] [17] [16]
	H	H	OH	H	6-hydroxy-1,3-benzoxazol-2-one	BOA-6-OH	PDP [e]	[31,32]
	H	OH	H	H	5-hydroxy-1,3-benzoxazol-2-one	BOA-5-OH	PDP	[33]
	OH	H	H	H	4-hydroxy-1,3-benzoxazol-2-one	n.a.	Acanthaceae	[34,35]
	H	NO_2	OH	H	5-nitro-6-hydroxy-1,3-benzoxazol-2-one	Nitro-BOA-6-OH	MDP [e]	[36]
	H	H	OCH_3	H	6-methoxy-1,3-benzoxazol-2-one	MBOA	Poaceae Acanthaceae Plantaginaceae	[3,12] [16] [16]
	H	H	OCH_3	OCH_3	6,7-dimethoxy-1,3-benzoxazol-2-one	M_2BOA	Poaceae	[12,37]
	H	Cl	OCH_3	H	5-chloro-6-methoxy-1,3-benzoxazol-2-one	Cl-MBOA	Poaceae	[38]
	Cl	H	OCH_3	OCH_3	4-chloro-6,7-dimethoxy-1,3-benzoxazol-2-one	Cl-M_2BOA	Poaceae	[37]
	H	H	OGlc	H	6-*β*-D-glucopyranosyloxy-1,3-benzoxazol-2-one	BOA-6-*O*-Glc	PDP	[32,33]
	H	OGlc	H	H	5-*β*-D-glucopyranosyloxy-1,3-benzoxazol-2-one	BOA-5-*O*-Glc	PDP	[33]
	$COCH_3$	H	H	H	4-acetyl-1,3-benzoxazol-2-one	4-ABOA	Poaceae	[39]
N-hydroxy **(R_1 = OH)**								
	H	H	OCH_3	H	3-hydroxy-6-methoxy-1,3-benzoxazol-2-one	3-OH-MBOA	Plantaginaceae	[40]
N-methoxy **(R_1 = OCH_3)**								
	H	H	OCH_3	H	3,6-dimethoxy-1,3-benzoxazol-2-one	DMBOA	Plantaginaceae	[40]
N-glucosyl **(R_1 = Glc)**								
	H	H	OCH_3	H	3-*β*-D-glucopyranosyl-6-methoxy-1,3-benzoxazol-2-one	MBOA-*N*-Glc	IDP [e] PDP	[41] [32,33]

[a] Note that some of these compounds have, so far, only been detected as their 2-*O*-glycosides. [b] Most commonly used abbreviation reported in literature, for some compounds multiple different abbreviations are in use. [c] Natural source (plant family or detoxification product) in which the benzoxazinoid has been detected. Note that genera Scoparia and Calceolaria, formerly members of Scrophulariaceae, have been moved to Plantaginaceae and Calceolariaceae, respectively. [d] n.a., no abbreviation assigned in literature. [e] PDP, plant detoxification product; IDP, insect detoxification product; MDP, microbial detoxification product.

Nevertheless, benzoxazolinones with other *N* substituents have been reported: *N*-hydroxy and *N*-methoxy derivatives were found in *Scoparia dulcis*.[40] Possibly these compounds are formed enzymatically from *N*-hydro benzoxazolinones or by another yet to be discovered biosynthetic pathway. Additionally, *N*-glucosyl derivatives can be formed as detoxification products of benzoxazinoids (**Table 4.1**).[33,41,42]

Various properties of benzoxazinoids, such as stability and reactivity,[43,44] plant defence functionality,[3,45] effects on human health,[2] and fragmentation in mass spectrometry[20] were shown to be affected by *N* substitution.

4.2.2. Abbreviations and structural overview

The first benzoxazinoids were discovered over 50 years ago. Their systematic IUPAC names are long and inconvenient to use which led to the formulation of abbreviations based on the three letter code BOA. This code was complemented with prefixes of the letters H and M for hydroxy and methoxy substituents, respectively. BOA can refer to compounds with either a benzoxazinone or a benzoxazolinone backbone (**Figure 4.1**). Because this three letter code does not distinguish classes or subclasses, identification of compounds based on their abbreviation can be challenging, especially for newcomers in the benzoxazinoid field. To facilitate the correct use of these abbreviations and avoid inconsistency, this paper includes an overview of the presently known natural benzoxazinoids of different (sub)classes with their abbreviations (**Table 4.1**).

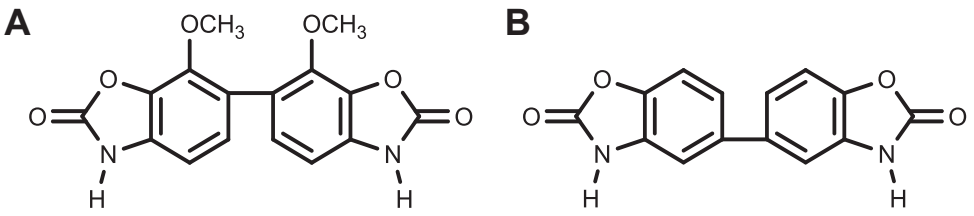

Figure 4.2. Zeaoxazolinone (**A**), a 7-methoxy-1,3-benzoxazol-2-one dimer from *Zea mays*[46], and 5,5′-bis-benzoxazoline-2,2′-dione (**B**), a 1,3-benzoxazol-2-one dimer from *Acanthus ilicifolius*.[47]

This overview does not include benzoxazinone *C*2 *O*-glycosides, which will be discussed in the following section. In addition to the benzoxazinoids in **Table 4.1**, zeaoxazolinone, a 7-methoxy-1,3-benzoxazol-2-one dimer from maize,[46] is displayed in **Figure 4.2A**. Another dimeric benzoxazolinone, 5,5′-bis-benzoxazoline-2,2′-dione (1,3-benzoxazol-2-one dimer) was found in *Acanthus ilicifolius*[47] (**Figure 4.2B**).

4.2.3. Glycosylation of benzoxazinones

Benzoxazinones are glycosylated in an early step of the biosynthesis (**Section 4.3.1**). Glycosylation is used as a mechanism to store benzoxazinones inside plant cells and to prevent self-toxicity.[12,48] Glycosides are unable to undergo ring-opening, limiting their reactivity (**Figure 4.3** and **Section 4.4**).

So far, glycosides reported in Poaceae are mainly glucosides, whereas in the family Plantaginaceae galactosides were also detected.[40] Recent studies also indicate the presence of dihexosides in wheat and rye (*Secale cereale*),[20,30] tri- and tetrahexosides in wheat and rye beers,[49] and acetylhexosides in wheat.[20] Upon metabolism by mammals, benzoxazinoids may also be conjugated with uronic

acids.[50] In addition, reglucosylation of aglycones, with inversion of stereochemistry (from 2*R* to 2*S*), is a mechanism of benzoxazinoid detoxification found in some insects.[51]

4.2.4. Substituents on the benzene moiety (R_2 to R_5)

The most common natural substituents at positions R_2 to R_5 are hydroxyl or methylated hydroxyl (methoxyl) groups.[3] Other substituents at these positions occurring more rarely in nature are chloro-, acetyl- or glucopyranosyloxy-groups (**Table 4.1**). Chloro-derivatives, for example, can be found in maize[37] and *A. ilicifolius* (Acanthaceae).[24]

4.3. Benzoxazinone biosynthesis and distribution in Poaceae

4.3.1. General biosynthesis of benzoxazinones

The basic biosynthetic pathway of benzoxazinones (up to DIBOA-Glc) was first studied and elucidated in maize,[52] and later also in wheat[53,54] and rye.[55,56] The biosynthesis starts from indole-3-glycerolphosphate (IGP), which is consecutively converted to HBOA, the first benzoxazinoid, in 4 steps by the enzymes BX1 to BX4 (**Figure 4.3**). A subsequent glucosylation and hydroxylation leads to DIBOA-Glc, which serves as the starting point for hydroxamic acid biosynthesis. All further downstream benzoxazinoids are synthesized as glucosides and most of the enzymes involved are unable to use the aglycones as substrates.[28,57] The formation of these downstream metabolites has mainly been studied in maize and to a lesser extent in wheat and rye.[26,57-61] A summary of the current state of knowledge on the biosynthetic pathways of benzoxazinones is shown in **Figure 4.3**. As shown on the right-hand side of this figure, benzoxazinones can be transformed to benzoxazolinones, which is further discussed in **Section 4.4.2**. Next to the Poaceae, benzoxazinoids have been reported in dicots of the families Acanthaceae, Calceolariaceae, Lamiaceae, Plantaginaceae, and Ranunculaceae (**Table 4.1**). The biosynthesis in these families might be similar to what has been reported in Poaceae, as indicated by analogues of the benzoxazinoid biosynthetic enzymes that have been found in dicots.[62,63] The overview in **Figure 4.3** indicates that several benzoxazinoid biosynthetic pathways require further investigation (dashed arrows). These aspects are discussed in the next section.

4.3.2. Tentative pathways in benzoxazinone biosynthesis

According to the generally accepted pathway, as shown in **Figure 4.3**, HBOA is converted to DIBOA by BX5, which is then glucosylated by BX8 or BX9. Whereas HBOA aglycons are relatively stable, DIBOA aglycons are reactive (**Section 4.4**) and phytotoxic (**Section 4.5**). Therefore, the formation of free DIBOA within the plant cell is likely omitted.

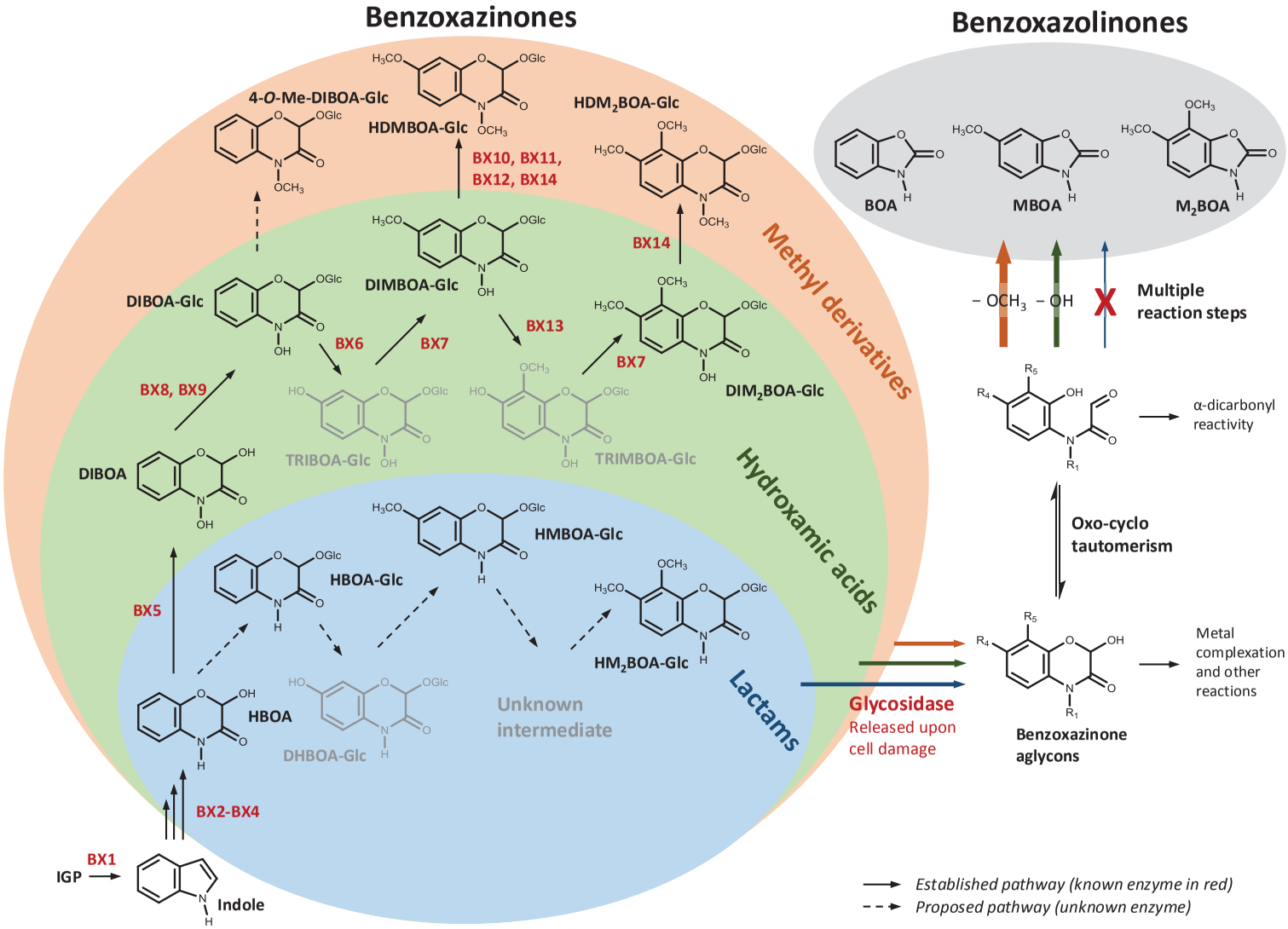

Figure 4.3. The biosynthetic pathway of the three subclasses of benzoxazinones in plants[26,28,52,57,59,60,64] and their transformation into benzoxazolinones.[44] Biosynthetic intermediates are shown in grey. Different mechanisms have been proposed for the multi-step degradation from the ring-opened configuration of benzoxazinones to the corresponding benzoxazolinone.[44] IGP, indole-3-glycerol phosphate.

One possibility could be the stabilisation and rapid glycosylation of DIBOA within a metabolon (i.e. a complex of sequential metabolic enzymes) by metabolic channelling. This would be similar to what has been demonstrated for toxic or labile intermediates in other secondary metabolic pathways (e.g. dhurrin biosynthesis in sorghum).[64] As an alternative, we propose a pathway in which HBOA is glycosylated prior to oxidation to form DIBOA-Glc. It was previously proposed that HBOA-Glc and DIBOA-Glc are in fact a redox pair,[13] which might present a mechanism for the possible interconversion of these compounds. The existence of an enzyme which catalyses the oxidation of HBOA-Glc to DIBOA-Glc has not been thoroughly explored in literature.

Maize BX8 and BX9 were both shown to be able to glycosylate HBOA albeit at a much lower conversion rate than DIBOA and DIMBOA.[48] The glycosylation of DIMBOA, however, does not seem to serve a function within the biosynthetic pathway, as it is already formed as a glycoside. The formation of HBOA-Glc would be a logical starting point for the biosynthesis of lactams. Further hydroxylation and methylation to produce DHBOA-Glc, HMBOA-Glc, and HM_2BOA-Glc might be performed by the same or similar enzymes as those involved in hydroxamic acid biosynthesis (BX6, BX7, and BX13) or by a yet to be discovered part of the BX enzyme-cluster. The compounds TRIBOA-Glc and TRIMBOA-Glc are intermediates of the biosynthesis and are not typically accumulated and detected in maize tissues.[12,26] Possibly, DHBOA-Glc serves a similar role as an intermediate in HMBOA-Glc synthesis. An analogue of TRIMBOA-Glc as an intermediate for the biosynthesis of HM_2BOA-Glc is not yet known. The biosynthetic pathway of benzoxazinone lactams presents a gap in our current knowledge. Lactams are the least prevalent subclass of benzoxazinones in maize explaining the lack of research on their biosynthesis, however, lactams are more prominent in other species, such as rye.[14]

The methyl derivative equivalent of DIBOA, 4-*O*-Me-DIBOA-Glc, was annotated in wheat seedlings exposed to fungal stress based on LC-MS analysis.[20] Thus far, its biosynthesis has not yet been fully elucidated. It was shown that a DIMBOA-Glc 4-*O*-methyltransferase from wheat was also able to convert DIBOA-Glc to 4-*O*-Me-DIBOA-Glc *in vitro*, but the latter compound was not detected *in planta* in that study.[28]

4.3.3. Distribution of benzoxazinones in Poaceae

Several recent reviews have addressed the genetic background of benzoxazinoid production between the different species within the Poaceae family.[60,61] Three agriculturally important crops that produce benzoxazinoids are maize, wheat, and rye. The profile of benzoxazinones produced between these species varies (**Figure 4.4**). Overall, maize produces the most diverse profile of benzoxazinones, whereas rye possesses the lowest diversity. Based on the biosynthetic pathways involved (**Figure 4.3**), it seems like wheat does not possess an active BX14-like enzyme to perform the conversion of DIM_2BOA-Glc into HDM_2BOA-Glc. It is, however, able to

produce HDMBOA-Glc which indicates the presence of an active BX10-like enzyme. Rye has not been shown to produce HDMBOA-Glc and other methyl derivatives.

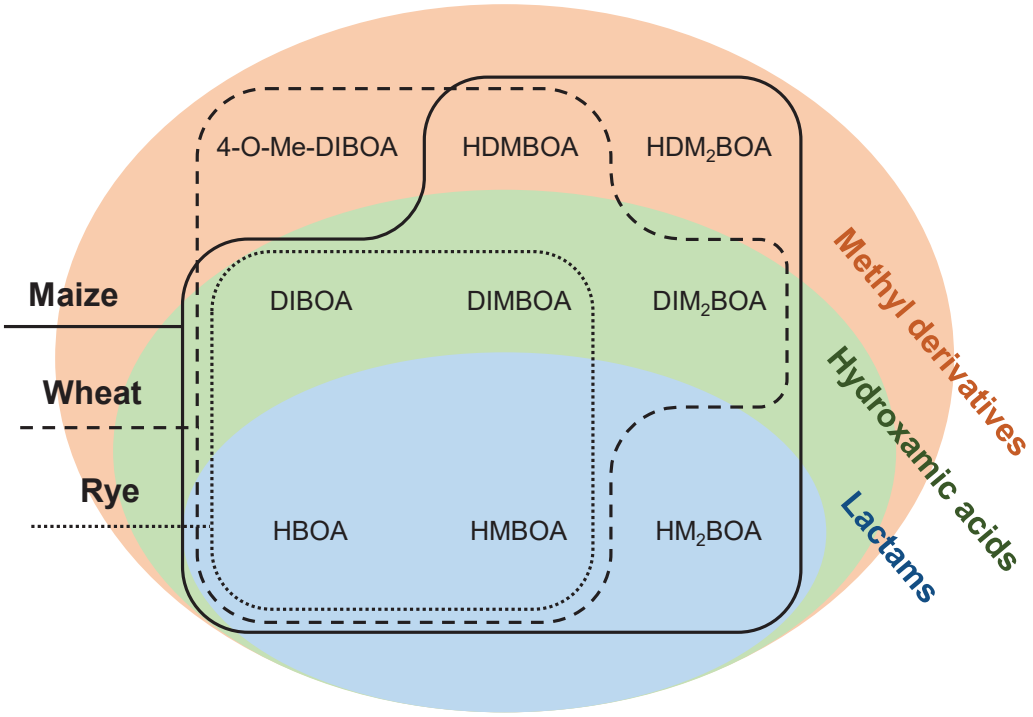

Figure 4.4. Distribution of individual benzoxazinones amongst the three major benzoxazinoid producing species of the family Poaceae.[12,14,19,20,23,65] The biosynthetic intermediates DHBOA, TRIBOA, and TRIMBOA are not included.

Several other well-known species from the Poaceae family, such as rice (*Oryza sativa*), oat (*Avena sativa*), and barley (*Hordeum vulgare*) do not produce benzoxazinoids. Interestingly, some other members of the genus *Hordeum*, e.g. *Hordeum lecheri*, have been found to produce benzoxazinoids.[66] There have also been some reports of benzoxazinoid production in sorghum.[67,68] Several other less well-known species in the Poaceae (e.g. *Aegilops speltoides*) have been reported to produce benzoxazinoids.[60] As shown by the phylogenetic trees presented by Dutartre and co-workers, the development of the benzoxazinoid biosynthetic cluster does not necessarily follow the general phylogenetic relationships between the different species, as is exemplified by the genus *Hordeum*.[60]

For a more in-depth perspective of benzoxazinoid phylogenomics, we would like to refer readers to the aforementioned reviews (focussed on Poaceae).[60,61] In addition, there are several studies that provide more information about benzoxazinoids in dicots.[1,62,63] The main benzoxazinoids produced by dicots are similar to those produced by Poaceae (**Table 4.1**). In **Section 4.2** and **Table 4.1**, several notable molecules unique to dicots are shown such as chloro-derivatives of HBOA and DIBOA, and the production of benzoxazinone galactosides rather than glucosides.

4.3.4. Benzoxazinoid content and induction *in planta*

The main benzoxazinoid in maize and wheat is DIMBOA (and its glycosides),[29,69] whereas in rye this is DIBOA (and its glycosides).[28,55] Reported values for the total quantities of benzoxazinoids in tissues of different species are highly variable. They range from 4.8 and 95 μg g^{-1} dry weight in wheat and rye grains,[14] respectively, to over 1900 μg g^{-1} dry weight in rye shoots,[70] and to several mg g^{-1} fresh weight in maize.[29,59] Comparing individual or total benzoxazinoid content from different literature sources is not straightforward. One of the underlying causes is that many papers focus solely on the analysis of a select number of benzoxazinones (usually DIMBOA and DIBOA) whereas in other works total benzoxazinoid content might include glycosides, other benzoxazinones, and benzoxazolinones. Secondly, the quantitative analysis of these molecules is challenging and has been addressed in multiple publications.[71-73] This is mainly due to the activity of glycosidases during sample treatment and the reactivity of the resulting benzoxazinone aglycons (**Section 4.4**).[12,43] Furthermore, there are several factors which can have a large effect on the total content and composition of benzoxazinoids reported in plants: (i) plant species and cultivar,[70,72,74,75] (ii) plant age,[12,29,58] (iii) tissue type (e.g. root, shoot),[12,69,74] and (iv) growth conditions (e.g. fertilization).[76]

Several induction methods have been described to elicit *in planta* production or diversification of benzoxazinoids. Abiotic elicitation methods include treatment with jasmonic acid,[28] *cis*-jasmone,[77] chitin and chitosan oligomers, or copper chloride.[78] Biotic elicitation methods include exposure to fungi,[4,45] bacteria,[76] insects, or insect larvae.[4,45]

4.4. Reactivity of benzoxazinoids

As previously described, benzoxazinones are stored as stable glycosides in the plant (**Sections 4.2.3** and **4.3.1**, and **Figure 4.3**). Upon cell damage or when exuded from roots, the glycosides come into contact with glycosidases which leads to the release of the less stable and more reactive benzoxazinone aglycones. The storage of defence compounds as glycosidic precursors which are released under stress conditions by glycosidase action is also observed in plants of other families. In Brassicaceae, for example, glucosinolates (precursors) are deglycosylated leading to the formation of isothiocyanates, which can react with thiols or amines contributing to antimicrobial functionality and other bioactivities.[79] Benzoxazinone aglycones can undergo a variety of reactions, as described in the following sections.

4.4.1. Oxo-cyclo tautomerism of benzoxazinone aglycons

Several mechanisms for the reactivity of ring-closed benzoxazinone aglycones have been suggested, such as metal-complexation by hydroxamic acids.[80] Another proposed mechanism is based on the electrophilicity of the nitrenium (N^+) ion

which is formed when the *N* substituent acts as a leaving group.[44,81] Additionally, benzoxazinone aglycones can undergo oxo-cyclo tautomerism in which the heterocycle assumes its ring-opened configuration. In the ring-opened configuration, benzoxazinones possess an α-dicarbonyl moiety which can react with thiols and amines.[44] In addition, ring-opening can lead to transformation of benzoxazinones to benzoxazolinones, which is discussed in the next section.

4.4.2. Transformation benzoxazinones to benzoxazolinones

One of the possible follow-up reactions of ring-opening of benzoxazinone aglycones is the spontaneous transformation into the corresponding benzoxazolinone (**Figure 4.3**).[44] Several different multi-step mechanisms have been proposed for this transformation, all of which involve a deprotonation step and eventually lead to loss of the *N* substituent (R_1).[44] The reactivity of aglycones towards this transformation is mainly determined by their *N* substituent which acts as the leaving group. Methyl derivatives (*N*-methoxy) are more reactive than hydroxamic acids (*N*-hydroxy), whereas lactams (*N*-hydro) are practically unreactive because H is not a suitable leaving group.[43,44] Due to the deprotonation step, the reaction is pH dependent. It proceeds rapidly around neutral pH and even more quickly in alkaline conditions. Below pH 7, the degradation rate decreases, with a rate constant at pH 4 which is approximately 150-fold lower than that at pH 7, as demonstrated for DIBOA.[82]

Whether alternative pathways exist to produce benzoxazolinones *in planta* is unknown. The detection of benzoxazolinones, especially those with *N*-hydroxy and *N*-methoxy substituents (**Section 4.2.1**, **Table 4.1**),[40] in some plants might indicate the existence of pathways dedicated to the production of specific benzoxazolinones.

4.4.3. Transformation products of benzoxazolinones

As demonstrated by the discovery of zeaoxazolinone in maize[46] (**Figure 2A**) and 5,5′-bis-benzoxazoline-2,2′-dione in *A. ilicifolius*[47] (**Figure 2B**), benzoxazolinones can form dimers *in planta*. Surprisingly, zeaoxazolinone consists of two 7-methoxy-1,3-benzoxazol-2-one subunits, although the monomeric 7-methoxy derivative has not yet been found (**Table 4.1**). The exact mechanism of dimer formation and the enzymes involved needs to be further elucidated.

Benzoxazolinones can be detoxified by plants or insects using various mechanisms, e.g. hydroxylation, and *O* or *N* glycosylation (**Table 4.1**).[32,33,41,83] Furthermore, in soil, benzoxazolinones can undergo microbial transformations.[44,70,84] In the presence of bacteria or fungi, benzoxazolinones are converted to aminophenol intermediates (e.g. 2-aminophenol), which can subsequently react to aminophenoxazinones (e.g. 2-amino-phenoxazin-3-one).[84,85] Besides aminophenoxazinones, other transformation products formed via aminophenol intermediates are acetamides and malonamic acids.[70,84] These transformation

products, however, have lost their benzoxazinoid structural motif and are therefore not considered in more detail in this work.

4.5. *In planta* functionality of benzoxazinoids

Allelopathic functionality of benzoxazinoids has been well-established and is one of the main functions of these compounds. Benzoxazinoid levels are especially high in roots and root exudates of young maize, wheat, and rye, as they compete with other plants during early growth.[3,70] General structure-activity relationships observed for allelopathic or phytotoxic activity are that hydroxamic acids (usually represented by DIBOA and DIMBOA) are more potent than lactams (usually represented by HBOA and HMBOA). The benzoxazolinones BOA and MBOA are in between hydroxamic acids and lactams in terms of allelopathic potency. DIBOA and DIBOA-Glc typically seem to be the most potent allelopathic natural benzoxazinoids, exhibiting significant root length inhibition at concentrations between 10^{-3} to 10^{-4} M (depending on target species).[86,87] Interestingly, glycosylation of DIBOA does not seem to affect its activity.[44,86,87] It was also shown to be possible to enhance selectivity and potency of the phytotoxic activity by chemical modification of 4-hydroxy-1,4-benzoxazin-3-one.[7,8]

Besides allelopathy, benzoxazinoids also play a role as defence compounds against insects and microorganisms. In general, accumulation of benzoxazinoids is positively correlated with resistance against disease and insects in maize, wheat, and rye.[3,4,59,65,74] As with allelopathy, hydroxamic acids seem to be more potent than lactams.[44] Moreover, benzoxazinones with increased methylation (i.e. *N*-OCH_3 or *C*7-OCH_3) were found to be correlated with disease resistance.[65] In another study, it was suggested that methylation of DIMBOA-Glc to HDMBOA-Glc might be a mechanism by which MBOA production is accelerated, as HDMBOA will more quickly transform to MBOA than DIMBOA.[45] In that study, they observed increased concentrations of HDMBOA-Glc in maize upon fungal infection and larval feeding. Additionally, MBOA was shown to be more effective at inhibiting fungal germination than its precursors.[45]

Wouters and co-workers postulated that the capacity to undergo ring-opening increased activity of benzoxazinones against insects. Consequently, glycosides were found to be less active than aglycons.[44] The toxicity of MBOA to insects was lower than that of DIMBOA,[44] suggesting that insecticidal activity is probably conferred by benzoxazinones via another mechanism (**Section 4.4**) than antifungal activity.

These defence functionalities associated with benzoxazinoids indicate that they might be potentially interesting leads for antimicrobial compounds. As an example, the antibiotic ofloxacin shares structural features (1,4-benzoxazin ring system) with natural benzoxazinoids.[88]

4.6. Potential of natural benzoxazinoids as antimicrobials

One of the first reports on the antimicrobial potential of benzoxazinoids described the inhibition of the gram-negative bacterium *Xanthomonas stewartii* (i.e. *Pantoea stewartii*), the causal agent of Stewart's wilt, by MBOA from maize.[89] A more recent study indicated that DIMBOA also possesses antibacterial properties against the pathogenic bacterium *Staphylococcus aureus*, albeit at high concentrations.[90] The novel benzoxazinoid zeaoxazolinone (**Figure 4.2A**) showed fungal inhibition comparable to clotriamazole against amongst others *Aspergillus flavus* and *Candida albicans*.[46] Unfortunately, no MIC values were reported for this dimeric benzoxazinoid. The antifungal and possibly antibacterial potential of this promising compound should be further investigated. The antimicrobial activity of 5,5′-bis-benzoxazoline-2,2′-dione (**Figure 4.2B**) has not yet been evaluated.

Despite the extensive research on benzoxazinoids, only a limited number of papers evaluated activity of these compounds against human pathogens, commonly represented by *S. aureus* (gram-positive bacterium), *Escherichia coli* (gram-negative bacterium), and *C. albicans* (yeast, fungus). Three papers by Bravo, Lazo and co-workers[91-93] and one other paper[90] reported minimum inhibitory concentration (MIC) values of benzoxazinoids against these three pathogens (**Table 4.2**). The antifungal activity of these compounds has been studied more extensively than their antibacterial activity. MBOA and DIMBOA (MIC 450 and 500 µg mL^{-1}, respectively) are most effective against fungi. As expected, the antifungal activity of benzoxazinoid glucosides (i.e. detoxified derivatives) is very limited (MIC >1000 µg mL^{-1}).[91] MIC values against bacteria have only been reported for the most common natural benzoxazinoids, namely the benzoxazinone aglycons DIMBOA and DIBOA, and the benzoxazolinones BOA and MBOA. Overall, DIMBOA is the natural benzoxazinoid with the lowest reported MIC values (**Table 4.2**).

Table 4.2. Antimicrobial activity of natural benzoxazinoids against the pathogens *S. aureus* (gram-positive bacterium), *E. coli* (gram-negative bacterium) and *C. albicans* (yeast, fungus). Colour of abbreviation indicates benzoxazinone subclass, green is hydroxamic acid whereas blue is lactam.

		Antimicrobial activity, MIC (µg mL^{-1})[a]			
Abbreviation	**Class**	***S. aureus***	***E. coli***	***C. albicans***	**Ref.**
DIMBOA	Benzoxazinone	250 - 500	666	500	[90-92]
DIBOA	Benzoxazinone	500	1250	666	[91,92]
MBOA	Benzoxazolinone	>1000	>1000	450	[93]
BOA	Benzoxazolinone	>1000	>1000	650	[93]
DIBOA-2-*O*-Glc	Benzoxazinone	n.a.	n.a.	>1000	[91]
DIMBOA-2-*O*-Glc	Benzoxazinone	n.a.	n.a.	>1000	[91]
HMBOA	Benzoxazinone	n.a.	n.a.	1000	[91]
HBOA	Benzoxazinone	n.a.	n.a.	>1000	[91]

n.a., no data available. [a] Minimum inhibitory concentration, range indicates that different values were reported in literature.

Our general observations regarding antimicrobial activity of monomeric natural benzoxazinoids are that: (i) hydroxamic acids are more active than lactams, (ii) hydroxylation at *C*7 increases activity, and (iii) glycosylation decreases activity. This is in accordance with a previous review.[44] Interestingly, the second and third observation are in contrast with findings for allelopathy (phytotoxicity) where these factors do not seem to affect activity (**Section 4.5**). This suggests that allelopathy, antimicrobial, and insecticidal activity are not necessarily conferred by the same structural motifs. Nevertheless, it seems that hydroxamic acids are more active than lactams with regard to all three of these functionalities. Even DIMBOA, the most antimicrobial monomeric natural benzoxazinoid, has relatively poor activity (lowest reported MIC 250 μg mL^{-1} against *S. aureus*)[90] compared to other natural compounds, such as flavonoids (e.g. MIC 3.9-15.6 μg mL^{-1} of apigenin against *S. aureus*)[94] and prenylated isoflavonoids (e.g. MIC 3.13 μg mL^{-1} of licoricidin against *S. aureus*).[94]

Interestingly, the benzoxazolinone transformation product 2-amino-phenoxazin-3-one was selectively very potent as an antimicrobial compound against the species *Helicobacter pylori* (MIC 1 μg mL^{-1}),[95] some *Mycobacterium* spp. (MIC 2.8 – 11.3 μg mL^{-1}),[96] and *Chlamydia pneumoniae* (MIC 2.1 μg mL^{-1}).[97] Activity of this compound against many other bacteria (e.g. *E. coli* and *S. aureus*) was limited.[96,98]

Overall, the antimicrobial potential of monomeric natural benzoxazinoids seems to be limited, yet several known antifungals such as carbendazim and boscalid contain the NHCO structure (in open chain configuration) coupled to an aromatic system.[99] This suggests that structural modification of benzoxazinoids might enhance their antimicrobial activity.

4.7. Potential of the 1,4-benzoxazin-3-one scaffold

In addition to their work on natural benzoxazinoids, Bravo and Lazo also evaluated some synthetic derivatives of these compounds. They showed that some synthetic 1,4-benzoxazin-3-one hydroxamic acids lacking the *C*2 hydroxyl group possessed more antifungal potential against *C. albicans* than DIMBOA.[91,92] These studies first demonstrated the potential of benzoxazinoids as scaffolds for the design of antimicrobial compounds. The 1,4-benzoxazin-3-one scaffold in particular, typically without the hydroxamic acid motif conferred by the *N*-OH group, was further utilized in several other studies in which more extensive modifications were applied.

One study showed that three synthetic benzoxazinones, with a combination of a *C*8 chloro and a *C*2 alkane (*n*-propyl, *n*-butyl, *n*-pentyl) substituent, had antifungal activity comparable to fluconazole.[100] Another study found two other benzoxazinone derivatives, namely a *C*2 ethyl and *N*-acetyl benzoxazinone, with promising antifungal activity against a variety of phytopathogenic fungi.[99] Unfortunately, no MIC values were determined in these studies. Several other

studies do, however, report MIC values for synthetic 1,4-benzoxazin-3-ones and these values are up to 40-fold lower than those reported for DIMBOA (**Figure 4.5**).

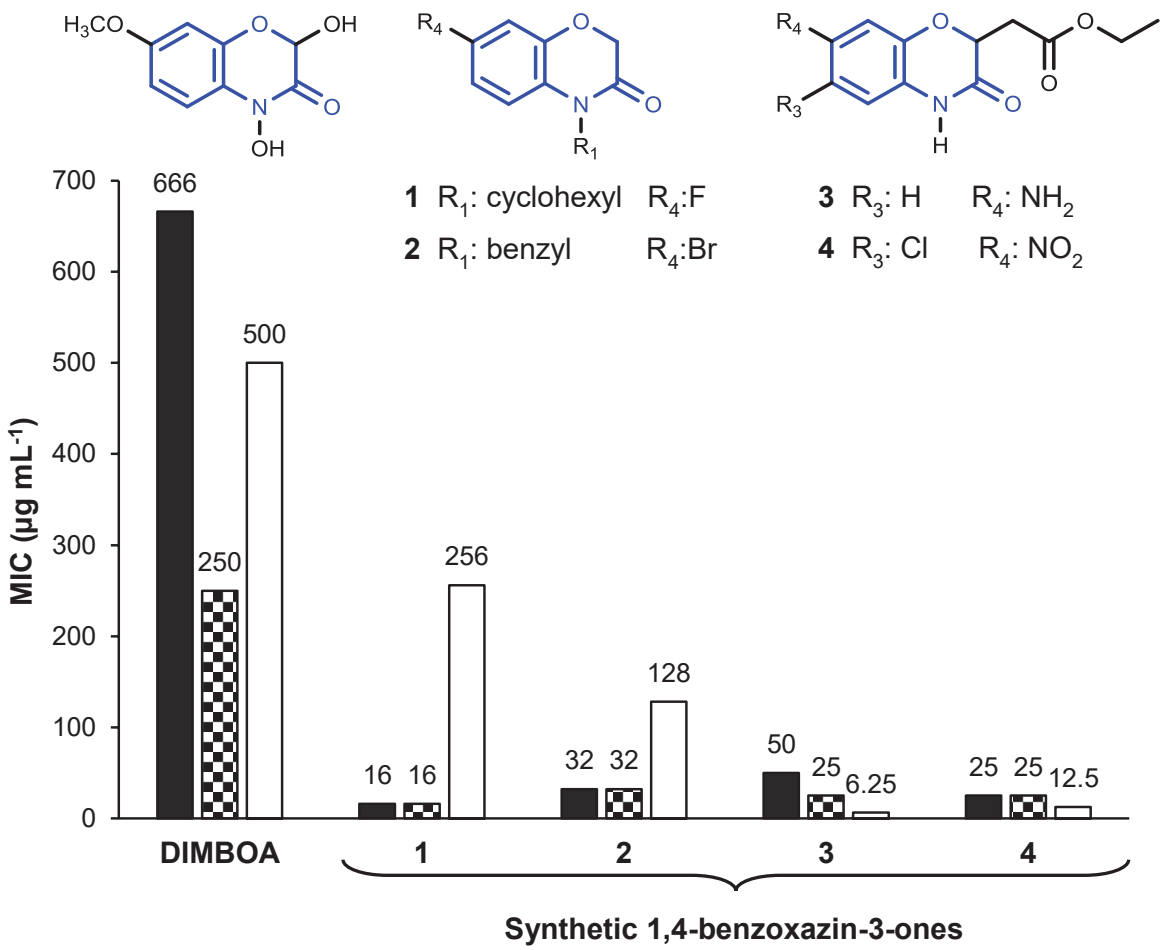

Figure 4.5. Antimicrobial activity of the most potent monomeric natural benzoxazinone DIMBOA[90,92] compared to four synthetic benzoxazinones.[101,102] The 1,4-benzoxazin-3-one scaffold is shown in blue. Minimum inhibitory concentration (MIC) displayed in µg mL^{-1} against gram-negative bacterium *E. coli* (black), gram-positive bacterium *S. aureus* (checkered), and fungus *C. albicans* (white).

For example, a number of compounds with *N*-alkyl and *C*7 halogen substituents were found to possess good activity against several pathogenic bacteria but limited antifungal activity.[102] In addition, two other studies describe multiple compounds with good activity against pathogenic bacteria as well as fungi.[101,103] An example of an all-round active molecule is 2-(2-ethyloxy-2-oxo-ethyl)-6-chloro-7-nitro-1,4-benzoxazin-3-one with MIC 12.5 µg mL^{-1} against *C. albicans,* and MIC 25 µg mL^{-1} against *S. aureus* and *E. coli* (**Figure 4.5**).[101] Most of the antimicrobial synthetic 1,4-benzoxazin-3-one derivatives do not possess a hydroxyl-moiety at *C*2 and can therefore not undergo ring-opening. Neither is the formation of a nitrenium ion or metal complexation very likely, considering their structure. Establishing structure-

activity relationships for these antimicrobial compounds might help in elucidating their antimicrobial mode-of-action.
Overall, synthetic benzoxazinoids based on a 1,4-benzoxazin-3-one scaffold show promising antimicrobial activity which might be further enhanced by targeted modifications based on previously reported findings. Considering the general observation that hydroxamic acids are more reactive and bioactive than lactams, perhaps its 4-hydroxy derivative would be an even more potent scaffold which was already used to produce synthetic allelopathic compounds.[8]

4.8. Conclusion

In this review, we provided an overview of all 32 currently known natural benzoxazinoids (excluding *C*2 glycosides), which includes one dimeric benzoxazolinone. The current state of knowledge on the biosynthesis of these compounds in Poaceae was summarised and a gap in the knowledge on the pathways responsible for lactam biosynthesis was identified. Within the family Poaceae, maize, wheat, and rye are the major benzoxazinoid producers, differences in the benzoxazinoid diversity between these species suggests a more advanced development of the biosynthesis in maize than in the other two species. The subclass (*N* substituent) of benzoxazinones amongst others affects their allelopathy and defence functionality.
We evaluated the antimicrobial activity of natural benzoxazinoids based on MIC values reported in literature. Even though these compounds play an important role in plant defence and allelopathy, monomeric natural benzoxazinoids seem to lack potency as antimicrobial agents. Observations on the structural requirements for allelopathy, insecticidal, and antimicrobial activity suggest that they are not necessarily conferred by similar mechanisms.
The 1,4-benzoxazin-3-one backbone has been shown to be a potential scaffold for designing new antimicrobial compounds with activity against pathogenic bacteria and fungi. This has been demonstrated by a number of studies that report potent activity (MIC down to 6.25-16 µg mL^{-1} against *C. albicans*, *E.coli,* and *S. aureus*) of synthetic derivatives of 1,4-benzoxazin-3-one.

4.9. References

[1] Frey, M., Schullehner, K., Dick, R., Fiesselmann, A., and Gierl, A. (2009) Benzoxazinoid biosynthesis, a model for evolution of secondary metabolic pathways in plants. *Phytochemistry*, 70*(15-16)*: p. 1645-1651.

[2] Adhikari, K.B., Tanwir, F., Gregersen, P.L., Steffensen, S.K., Jensen, B.M., Poulsen, L.K., Nielsen, C.H., Høyer, S., Borre, M., and Fomsgaard, I.S. (2015) Benzoxazinoids: Cereal phytochemicals with putative therapeutic and health-protecting properties. *Molecular Nutrition & Food Research*, 59*(7)*: p. 1324-1338.

[3] Niemeyer, H.M. (2009) Hydroxamic acids derived from 2-hydroxy-2*H*-1,4-benzoxazin-3(4*H*)-one: Key defense chemicals of cereals. *Journal of Agricultural and Food Chemistry*, 57*(5)*: p. 1677-1696.

[4] Ahmad, S., Veyrat, N., Gordon-Weeks, R., Zhang, Y.H., Martin, J., Smart, L., Glauser, G., Erb, M., Flors, V., Frey, M., and Ton, J. (2011) Benzoxazinoid metabolites regulate innate immunity against aphids and fungi in maize. *Plant Physiology*, 157*(1)*: p. 317-327.

[5] Sicker, D., Frey, M., Schulz, M., and Gierl, A. (2000) Role of natural benzoxazinones in the survival strategy of plants. *International Review of Cytology - A Survey of Cell Biology*, 198: p. 319-346.

[6] Neal, A.L., Ahmad, S., Gordon-Weeks, R., and Ton, J. (2012) Benzoxazinoids in root exudates of maize attract *Pseudomonas putida* to the rhizosphere. *Plos One*, 7*(4)*.

[7] Macías, F.A., Marín, D., Oliveros-Bastidas, A., and Molinillo, J.M.G. (2006) Optimization of benzoxazinones as natural herbicide models by lipophilicity enhancement. *Journal of Agricultural and Food Chemistry*, 54*(25)*: p. 9357-9365.

[8] Macías, F.A., Chinchilla, N., Arroyo, E., Molinillo, J.M.G., Marín, D., and Varela, R.M. (2010) Combined strategy for phytotoxicity enhancement of benzoxazinones. *Journal of Agricultural and Food Chemistry*, 58*(3)*: p. 2047-2053.

[9] Virtanen, A.I. and Hietala, P.K. (1955) 2(3)-Benzoxazolinone, an anti-Fusarium factor in rye seedlings. *Acta Chemica Scandinavica*, 9*(9)*: p. 1543-1544.

[10] Hietala, P.K. and Virtanen, A.I. (1960) Precursors of benzoxazolinone in rye plants II. Precursor I, the glucoside. *Acta Chemica Scandinavica*, 14*(2)*: p. 502-504.

[11] Honkanen, E. and Virtanen, A.I. (1960) The synthesis of precursor II of benzoxazolinone formed in rye plants, and the enzymic hydrolysis of precursor I, the glucoside. *Acta Chemica Scandinavica*, 14*(2)*: p. 504-507.

[12] Cambier, V., Hance, T., and de Hoffmann, E. (1999) Non-injured maize contains several 1,4-benzoxazin-3-one related compounds but only as glucoconjugates. *Phytochemical Analysis*, 10*(3)*: p. 119-126.

[13] Hofman, J. and Hofmanová, O. (1969) 1,4-Benzoxazine derivatives in plants - Sephadex fractionation and identification of a new glucoside. *European Journal of Biochemistry*, 8*(1)*: p. 109-112.

[14] Tanwir, F., Fredholm, M., Gregersen, P.L., and Fomsgaard, I.S. (2013) Comparison of the levels of bioactive benzoxazinoids in different wheat and rye fractions and the transformation of these compounds in homemade foods. *Food Chemistry*, 141*(1)*: p. 444-450.

[15] Baumeler, A., Hesse, M., and Werner, C. (2000) Benzoxazinoids-cyclic hydroxamic acids, lactams and their corresponding glucosides in the genus *Aphelandra* (Acanthaceae). *Phytochemistry*, 53*(2)*: p. 213-222.

[16] Pratt, K., Kumar, P., and Chilton, W.S. (1995) Cyclic hydroxamic acids in dicotyledonous plants. *Biochemical Systematics and Ecology*, 23*(7-8)*: p. 781-785.

[17] Bravo, H.R., Copaja, S.V., Figueroa-Duarte, S., Lamborot, M., and Martín, J.S. (2005) 1,4-benzoxazin-3-one, 2-benzoxazolinone and gallic acid from *Calceolaria*

thyrsilora Graham and their antibacterial activity. *Zeitschrift fur Naturforschung C: Journal of Biosciences*, 60*(5-6)*: p. 389-393.

[18] Alipieva, K.I., Taskova, R.M., Evstatieva, L.N., Handjieva, N.V., and Popov, S.S. (2003) Benzoxazinoids and iridoid glucosides from four *Lamium* species. *Phytochemistry*, 64*(8)*: p. 1413-1417.

[19] Woodward, M.D., Corcuera, L.J., Schnoes, H.K., Helgeson, J.P., and Upper, C.D. (1979) Identification of 1,4-benzoxazin-3-ones in maize extracts by gas-liquid chromatography and mass spectrometry. *Plant Physiology*, 63*(1)*: p. 9-13.

[20] de Bruijn, W.J.C., Vincken, J.-P., Duran, K., and Gruppen, H. (2016) Mass spectrometric characterization of benzoxazinoid glycosides from *Rhizopus*-elicited wheat (*Triticum aestivum*) seedlings. *Journal of Agricultural and Food Chemistry*, 64*(32)*: p. 6267-6276.

[21] Bravo, H.R., Copaja, S.V., and Martín, J.S. (2004) Contents of 1,4-benzoxazin-3-ones and 2-benzoxazolinone from *Stenandrium dulce* (Nees). *Zeitschrift fur Naturforschung C: Journal of Biosciences*, 59*(3-4)*: p. 177-180.

[22] Hofman, J. and Masojídková, M. (1973) 1,4-Benzoxazine glucosides from *Zea mays*. *Phytochemistry*, 12*(1)*: p. 207-208.

[23] Le-Van, N. and Wratten, S.J. (1984) Compound 30.4, an unusual chlorinated 1,4-benzoxazin-3-one derivative from corn (*Zea mays*). *Tetrahedron Letters*, 25*(2)*: p. 145-148.

[24] Kanchanapoom, T., Kamel, M.S., Kasai, R., Picheansoonthon, C., Hiraga, Y., and Yamasaki, K. (2001) Benzoxazinoid glucosides from *Acanthus ilicifolius*. *Phytochemistry*, 58*(4)*: p. 637-640.

[25] Özden, S., Özden, T., Attila, I., Küçükislamoglu, M., and Okatan, A. (1992) Isolation and identification via high-performance liquid chromatography and thin-layer chromatography of benzoxazolinone precursors from *Consolida orientalis* flowers. *Journal of Chromatography*, 609*(1-2)*: p. 402-406.

[26] Handrick, V., Robert, C.A.M., Ahern, K.R., Zhou, S.Q., Machado, R.A.R., Maag, D., Glauser, G., Fernandez-Penny, F.E., Chandran, J.N., Rodgers-Melnik, E., Schneider, B., Buckler, E.S., Boland, W., Gershenzon, J., Jander, G., Erb, M., and Köllner, T.G. (2016) Biosynthesis of 8-O-methylated benzoxazinoid defense compounds in maize. *Plant Cell*, 28*(7)*: p. 1682-1700.

[27] Kanchanapoom, T., Kasai, R., Picheansoonthon, C., and Yamasaki, K. (2001) Megastigmane, aliphatic alcohol and benzoxazinoid glycosides from *Acanthus ebracteatus*. *Phytochemistry*, 58*(5)*: p. 811-817.

[28] Oikawa, A., Ishihara, A., and Iwamura, H. (2002) Induction of HDMBOA-Glc accumulation and DIMBOA-Glc 4-*O*-methyltransferase by jasmonic acid in poaceous plants. *Phytochemistry*, 61*(3)*: p. 331-337.

[29] Köhler, A., Maag, D., Veyrat, N., Glauser, G., Wolfender, J.L., Turlings, T.C.J., and Erb, M. (2015) Within-plant distribution of 1,4-benzoxazin-3-ones contributes to herbivore niche differentiation in maize. *Plant Cell and Environment*, 38*(6)*: p. 1081-1093.

[30] Hanhineva, K., Rogachev, I., Aura, A.M., Aharoni, A., Poutanen, K., and Mykkänen, H. (2011) Qualitative characterization of benzoxazinoid derivatives in whole grain rye and wheat by LC-MS metabolite profiling. *Journal of Agricultural and Food Chemistry*, 59*(3)*: p. 921-927.

[31] Schulz, M. and Wieland, I. (1999) Variation in metabolism of BOA among species in various field communities - biochemical evidence for co-evolutionary processes in plant communities? *Chemoecology*, 9*(3)*: p. 133-141.

[32] Wieland, I., Kluge, M., Schneider, B., Schmidt, J., Sicker, D., and Schulz, M. (1998) 3-*β*-d-glucopyranosyl-benzoxazolin-2(3*H*)-one - a detoxification product of benzoxazolin-2(3*H*)-one in oat roots. *Phytochemistry*, 49*(3)*: p. 719-722.

[33] Hofmann, D., Knop, M., Hao, H., Hennig, L., Sicker, D., and Schulz, M. (2006) Glucosides from MBOA and BOA detoxification by *Zea mays* and *Portulaca oleracea*. *Journal of Natural Products*, 69*(1)*: p. 34-37.

[34] Zhao, D., Xie, L.J., Yu, L., An, N., Na, W., Chen, F., Li, Y.B., Tan, Y.F., and Zhang, X.P. (2015) New 2-benzoxazolinone derivatives with cytotoxic activities from the roots of *Acanthus ilicifolius*. *Chemical & Pharmaceutical Bulletin*, 63*(12)*: p. 1087-1090.

[35] Huo, C.H., An, D.G., Wang, B., Zhao, Y.Y., and Lin, W.H. (2005) Structure elucidation and complete NMR spectral assignments of a new benzoxazolinone glucoside from *Acanthus ilicifolius*. *Magnetic Resonance in Chemistry*, 43*(4)*: p. 343-345.

[36] Schulz, M., Sicker, D., Schackow, O., Hennig, L., Hofmann, D., Disko, U., Ventura, M., and Basyuk, K. (2017) 6-Hydroxy-5-nitrobenzo[*d*]oxazol-2(3*H*)-one - A degradable derivative of natural 6-hydroxybenzoxazolin-2(3*H*)-one produced by *Pantoea ananatis*. *Commun Integr Biol*, 10*(3)*: p. e1302633.

[37] Anai, T., Aizawa, H., Ohtake, N., Kosemura, S., Yamamura, S., and Hasegawa, K. (1996) A new auxin-inhibiting substance, 4-Cl-6,7-dimethoxy-2-benzoxazolinone, from light-grown maize shoots. *Phytochemistry*, 42*(2)*: p. 273-275.

[38] Kato-Noguchi, H., Kosemura, S., and Yamamura, S. (1998) Allelopathic potential of 5-chloro-6-methoxy-2-benzoxazolinone. *Phytochemistry*, 48*(3)*: p. 433-435.

[39] Fielder, D.A., Collins, F.W., Blackwell, B.A., Bensimon, C., and Apsimon, J.W. (1994) Isolation and characterization of 4-acetyl-benzoxazolin-2-one (4-ABOA), a new benzoxazolinone from *Zea mays*. *Tetrahedron Letters*, 35*(4)*: p. 521-524.

[40] Wu, W.H., Chen, T.Y., Lu, R.W., Chen, S., and Chang, C.C. (2012) Benzoxazinoids from *Scoparia dulcis* (sweet broomweed) with antiproliferative activity against the DU-145 human prostate cancer cell line. *Phytochemistry*, 83: p. 110-115.

[41] Maag, D., Dalvit, C., Thevenet, D., Köhler, A., Wouters, F.C., Vassão, D.G., Gershenzon, J., Wolfender, J.L., Turlings, T.C.J., Erb, M., and Glauser, G. (2014) 3-*β*-D-Glucopyranosyl-6-methoxy-2-benzoxazolinone (MBOA-*N*-Glc) is an insect detoxification product of maize 1,4-benzoxazin-3-ones. *Phytochemistry*, 102: p. 97-105.

[42] Sicker, D., Schneider, B., Hennig, L., Knop, M., and Schulz, M. (2001) Glycoside carbamates from benzoxazolin-2(3*H*)-one detoxification in extracts and exudates of corn roots. *Phytochemistry*, 58*(5)*: p. 819-825.

[43] Grambow, H.J., Lückge, J., Klausener, A., and Müller, E. (1986) Occurrence of 2-(2-hydroxy-4,7-dimethoxy-2*H*-1,4-benzoxazin-3-one)-*β*-D-glucopyranoside in *Triticum aestivum* leaves and its conversion into 6-methoxy-benzoxazolinone. *Zeitschrift fur Naturforschung C: Journal of Biosciences*, 41*(7-8)*: p. 684-690.

[44] Wouters, F.C., Gershenzon, J., and Vassão, D.G. (2016) Benzoxazinoids: Reactivity and modes of action of a versatile class of plant chemical defenses. *Journal of the Brazilian Chemical Society*, 27*(8)*: p. 1379-1397.

[45] Oikawa, A., Ishihara, A., Tanaka, C., Mori, N., Tsuda, M., and Iwamura, H. (2004) Accumulation of HDMBOA-Glc is induced by biotic stresses prior to the release of MBOA in maize leaves. *Phytochemistry*, 65*(22)*: p. 2995-3001.

[46] Mohamed, G.A., Ibrahim, S.R.M., Abdelkader, M.S.A., Al-Musayeib, N.M., Ghoneim, M., and Ross, S.A. (2014) Zeaoxazolinone, a new antifungal agent from *Zea mays* roots. *Medicinal Chemistry Research*, 23*(10)*: p. 4627-4630.

[47] D'Souza, L., Wahidulla, S., and Mishra, P.D. (1997) Bisoxazolinone from the mangrove *Acanthus illicifolius*. *Indian Journal of Chemistry Section B-Organic Chemistry Including Medicinal Chemistry*, 36*(11)*: p. 1079-1081.

[48] von Rad, U., Hüttl, R., Lottspeich, F., Gierl, A., and Frey, M. (2001) Two glucosyltransferases are involved in detoxification of benzoxazinoids in maize. *Plant Journal*, 28*(6)*: p. 633-642.

[49] Pihlava, J.M. and Kurtelius, T. (2016) Determination of benzoxazinoids in wheat and rye beers by HPLC-DAD and UPLC-QTOF MS. *Food Chemistry*, 204: p. 400-408.

[50] Adhikari, K.B., Lærke, H.N., Mortensen, A.G., and Fomsgaard, I.S. (2012) Plasma and urine concentrations of bioactive dietary benzoxazinoids and their glucuronidated conjugates in rats fed a rye bread-based diet. *Journal of Agricultural and Food Chemistry*, 60*(46)*: p. 11518-11524.

[51] Wouters, F.C., Reichelt, M., Glauser, G., Bauer, E., Erb, M., Gershenzon, J., and Vassão, D.G. (2014) Reglucosylation of the benzoxazinoid DIMBOA with inversion of stereochemical configuration is a detoxification strategy in lepidopteran herbivores. *Angewandte Chemie-International Edition*, 53*(42)*: p. 11320-11324.

[52] Frey, M., Chomet, P., Glawischnig, E., Stettner, C., Grün, S., Winklmair, A., Eisenreich, W., Bacher, A., Meeley, R.B., Briggs, S.P., Simcox, K., and Gierl, A. (1997) Analysis of a chemical plant defense mechanism in grasses. *Science*, 277*(5326)*: p. 696-699.

[53] Nomura, T., Ishihara, A., Imaishi, H., Endo, T.R., Ohkawa, H., and Iwamura, H. (2002) Molecular characterization and chromosomal localization of cytochrome P450 genes involved in the biosynthesis of cyclic hydroxamic acids in hexaploid wheat. *Molecular Genetics and Genomics*, 267*(2)*: p. 210-217.

[54] Nomura, T., Ishihara, A., Imaishi, H., Ohkawa, H., Endo, T.R., and Iwamura, H. (2003) Rearrangement of the genes for the biosynthesis of benzoxazinones in the evolution of Triticeae species. *Planta*, 217*(5)*: p. 776-782.

[55] Rakoczy-Trojanowska, M., Orczyk, W., Krajewski, P., Bocianowski, J., Stochmal, A., and Kowalczyk, M. (2017) *ScBx* gene based association analysis of hydroxamate content in rye (*Secale cereale* L.). *Journal of Applied Genetics*, 58*(1)*: p. 1-9.

[56] Bakera, B., Makowska, B., Groszyk, J., Niziołek, M., Orczyk, W., Bolibok-Bragoszewska, H., Hromada-Judycka, A., and Rakoczy-Trojanowska, M. (2015) Structural characteristics of *ScBx* genes controlling the biosynthesis of hydroxamic acids in rye (*Secale cereale* L.). *Journal of Applied Genetics*, 56*(3)*: p. 287-298.

[57] Jonczyk, R., Schmidt, H., Osterrieder, A., Fiesselmann, A., Schullehner, K., Haslbeck, M., Sicker, D., Hofmann, D., Yalpani, N., Simmons, C., Frey, M., and Gierl, A. (2008) Elucidation of the final reactions of DIMBOA-glucoside biosynthesis in maize: Characterization of *Bx6* and *Bx7*. *Plant Physiology*, 146*(3)*: p. 1053-1063.

[58] Tanwir, F., Dionisio, G., Adhikari, K.B., Fomsgaard, I.S., and Gregersen, P.L. (2017) Biosynthesis and chemical transformation of benzoxazinoids in rye during seed germination and the identification of a rye *Bx6*-like gene. *Phytochemistry*, 140: p. 95-107.

[59] Meihls, L.N., Handrick, V., Glauser, G., Barbier, H., Kaur, H., Haribal, M.M., Lipka, A.E., Gershenzon, J., Buckler, E.S., Erb, M., Köllner, T.G., and Jander, G. (2013) Natural variation in maize aphid resistance is associated with 2,4-dihydroxy-7-methoxy-1,4-benzoxazin-3-one glucoside methyltransferase activity. *Plant Cell*, 25*(6)*: p. 2341-2355.

[60] Dutartre, L., Hilliou, F., and Feyereisen, R. (2012) Phylogenomics of the benzoxazinoid biosynthetic pathway of Poaceae: Gene duplications and origin of the *Bx* cluster. *BMC Evolutionary Biology*, 12.

[61] Makowska, B., Bakera, B., and Rakoczy-Trojanowska, M. (2015) The genetic background of benzoxazinoid biosynthesis in cereals. *Acta Physiologiae Plantarum*, 37*(9)*.

[62] Dick, R., Rattei, T., Haslbeck, M., Schwab, W., Gierl, A., and Frey, M. (2012) Comparative analysis of benzoxazinoid biosynthesis in monocots and dicots: Independent recruitment of stabilization and activation functions. *Plant Cell*, 24*(3)*: p. 915-928.

[63] Schullehner, K., Dick, R., Vitzthum, F., Schwab, W., Brandt, W., Frey, M., and Gierl, A. (2008) Benzoxazinoid biosynthesis in dicot plants. *Phytochemistry*, 69*(15)*: p. 2668-2677.

[64] Jørgensen, K., Rasmussen, A.V., Morant, M., Nielsen, A.H., Bjarnholt, N., Zagrobelny, M., Bak, S., and Møller, B.L. (2005) Metabolon formation and metabolic channeling in the biosynthesis of plant natural products. *Current Opinion in Plant Biology*, 8*(3)*: p. 280-291.

[65] Søltoft, M., Jørgensen, L.N., Svensmark, B., and Fomsgaard, I.S. (2008) Benzoxazinoid concentrations show correlation with Fusarium Head Blight resistance in Danish wheat varieties. *Biochemical Systematics and Ecology*, 36*(4)*: p. 245-259.

[66] Grün, S., Frey, M., and Gierl, A. (2005) Evolution of the indole alkaloid biosynthesis in the genus Hordeum: Distribution of gramine and DIBOA and isolation of the benzoxazinoid biosynthesis genes from *Hordeum lechleri*. *Phytochemistry*, 66*(11)*: p. 1264-1272.

[67] Niemeyer, H.M. (1988) Hydroxamic acids (4-hydroxy-1,4-benzoxazin-3-ones), defense chemicals in the Gramineae. *Phytochemistry*, 27*(11)*: p. 3349-3358.

[68] Malan, C., Visser, J.H., and van de Venter, H.A. (1984) Screening for DIMBOA (benzoxazinone) concentration among South African inbred maize lines and sorghum cultivars. *South African Journal of Plant and Soil*, 1*(4)*: p. 99-102.

[69] Villagrasa, M., Guillamón, M., Labandeira, A., Taberner, A., Eljarrat, E., and Barceló, D. (2006) Benzoxazinoid allelochemicals in wheat: Distribution among foliage, roots, and seeds. *Journal of Agricultural and Food Chemistry*, 54*(4)*: p. 1009-1015.

[70] Schulz, M., Marocco, A., Tabaglio, V., Macías, F.A., and Molinillo, J.M.G. (2013) Benzoxazinoids in rye allelopathy - from discovery to application in sustainable weed control and organic farming. *Journal of Chemical Ecology*, 39*(2)*: p. 154-174.

[71] Bonnington, L., Eljarrat, E., Guillamón, M., Eichhorn, P., Taberner, A., and Barceló, D. (2003) Development of a liquid chromatography-electrospray-tandem mass spectrometry method for the quantitative determination of benzoxazinone derivatives in plants. *Analytical Chemistry*, 75*(13)*: p. 3128-3136.

[72] Eljarrat, E. and Barceló, D. (2001) Sample handling and analysis of allelochemical compounds in plants. *Trac-Trends in Analytical Chemistry*, 20*(10)*: p. 584-590.

[73] Pedersen, H.A., Heinrichson, K., and Fomsgaard, I.S. (2017) Alterations of the benzoxazinoid profiles of uninjured maize seedlings during freezing, storage, and lyophilization. *Journal of Agricultural and Food Chemistry*, 65*(20)*: p. 4103-4110.

[74] Copaja, S.V., Villarroel, E., Bravo, H.R., Pizarro, L., and Argandona, V.H. (2006) Hydroxamic acids in *Secale cereale* L. and the relationship with their antifeedant and allelopathic properties. *Zeitschrift fur Naturforschung C: Journal of Biosciences*, 61*(9-10)*: p. 670-676.

[75] Zasada, I.A., Rice, C.P., and Meyer, S.L.F. (2007) Improving the use of rye (*Secale cereale*) for nematode management: Potential to select cultivars based on *Meloidogyne incognita* host status and benzoxazinoid content. *Nematology*, 9: p. 53-60.

[76] Walker, V., Couillerot, O., Von Felten, A., Bellvert, F., Jansa, J., Maurhofer, M., Bally, R., Moenne-Loccoz, Y., and Comte, G. (2012) Variation of secondary metabolite levels in maize seedling roots induced by inoculation with *Azospirillum*, *Pseudomonas* and *glomus* consortium under field conditions. *Plant and Soil*, 356*(1-2)*: p. 151-163.

[77] Moraes, M.C.B., Birkett, M.A., Gordon-Weeks, R., Smart, L.E., Martin, J.L., Pye, B.J., Bromilow, R., and Pickett, J.A. (2008) *cis*-Jasmone induces accumulation of defence compounds in wheat, *Triticum aestivum*. *Phytochemistry*, 69*(1)*: p. 9-17.

[78] Oikawa, A., Ishihara, A., Hasegawa, M., Kodama, O., and Iwamura, H. (2001) Induced accumulation of 2-hydroxy-4,7-dimethoxy-1,4-benzoxazin-3-one glucoside (HDMBOA-Glc) in maize leaves. *Phytochemistry*, 56*(7)*: p. 669-675.

[79] Dufour, V., Stahl, M., and Baysse, C. (2015) The antibacterial properties of isothiocyanates. *Microbiology*, 161: p. 229-243.
[80] Tipton, C.L. and Buell, E.L. (1970) Ferric iron complexes of hydroxamic acids from maize. *Phytochemistry*, 9*(6)*: p. 1215-1217.
[81] Hashimoto, Y. and Shudo, K. (1996) Chemistry of biologically active benzoxazinoids. *Phytochemistry*, 43*(3)*: p. 551-559.
[82] Bredenberg, J.B., Honkanen, E., and Virtanen, A.I. (1962) Kinetics and mechanism of decomposition of 2,4-dihydroxy-1,4-benzoxazin-3-one. *Acta Chemica Scandinavica*, 16*(1)*: p. 135-&.
[83] Schulz, M., Filary, B., Kühn, S., Colby, T., Harzen, A., Schmidt, J., Sicker, D., Hennig, L., Hofmann, D., Disko, U., and Anders, N. (2016) Benzoxazolinone detoxification by N-glucosylation: The multi-compartment-network of *Zea mays* L. *Plant Signaling & Behavior*, 11*(1)*.
[84] Fomsgaard, I.S., Mortensen, A.G., and Carlsen, S.C.K. (2004) Microbial transformation products of benzoxazolinone and benzoxazinone allelochemicals - a review. *Chemosphere*, 54*(8)*: p. 1025-1038.
[85] Macías, F.A., Marín, D., Oliveros-Bastidas, A., and Molinillo, J.M.G. (2009) Rediscovering the bioactivity and ecological role of 1,4-benzoxazinones. *Natural Product Reports*, 26*(4)*: p. 478-489.
[86] Macías, F.A., Marín, D., Oliveros-Bastidas, A., Castellano, D., Simonet, A.M., and Molinillo, J.M.G. (2005) Structure-activity relationships (SAR) studies of benzoxazinones, their degradation products and analogues. Phytotoxicity on standard target species (STS). *Journal of Agricultural and Food Chemistry*, 53*(3)*: p. 538-548.
[87] Macías, F.A., Marín, D., Oliveros-Bastidas, A., Castellano, D., Simonet, A.M., and Molinillo, J.M.G. (2006) Structure-activity relationship (SAR) studies of benzoxazinones, their degradation products, and analogues. Phytotoxicity on problematic weeds *Avena fatua* L. and *Lolium rigidum* Gaud. *Journal of Agricultural and Food Chemistry*, 54*(4)*: p. 1040-1048.
[88] Hayakawa, I., Atarashi, S., Yokohama, S., Imamura, M., Sakano, K.I., and Furukawa, M. (1986) Synthesis and antibacterial activities of optically-active ofloxacin. *Antimicrobial Agents and Chemotherapy*, 29*(1)*: p. 163-164.
[89] Whitney, N.J. and Mortimore, C.G. (1961) Effect of 6-methoxybenzoxazolinone on growth of *Xanthomonas stewartii* (Erw. Smith) Dowson and its presence in sweet corn (*Zea mays* var. *Saccharata* bailey). *Nature*, 189*(476)*: p. 596-597.
[90] Gleńsk, M., Gajda, B., Franiczek, R., Krzyżanowska, B., Biskup, I., and Włodarczyk, M. (2016) In vitro evaluation of the antioxidant and antimicrobial activity of DIMBOA [2,4-dihydroxy-7-methoxy-2*H*-1,4-benzoxazin-3(4*H*)-one]. *Natural Product Research*, 30*(11)*: p. 1305-1308.
[91] Bravo, H.R. and Lazo, W. (1996) Antialgal and antifungal activity of natural hydroxamic acids and related compounds. *Journal of Agricultural and Food Chemistry*, 44*(6)*: p. 1569-1571.
[92] Bravo, H.R. and Lazo, W. (1993) Antimicrobial activity of cereal hydroxamic acids and related compounds. *Phytochemistry*, 33*(3)*: p. 569-571.
[93] Bravo, H.R., Copaja, S.V., and Lazo, W. (1997) Antimicrobial activity of natural 2-benzoxazolinones and related derivatives. *Journal of Agricultural and Food Chemistry*, 45*(8)*: p. 3255-3257.
[94] Gibbons, S. (2004) Anti-staphylococcal plant natural products. *Natural Product Reports*, 21*(2)*: p. 263-277.
[95] Hanawa, T., Osaki, T., Manzoku, T., Fukuda, M., Kawakami, H., Tomoda, A., and Kamiya, S. (2010) *In vitro* antibacterial activity of Phx-3 against *Helicobacter pylori*. *Biological & Pharmaceutical Bulletin*, 33*(2)*: p. 188-191.
[96] Shimizu, S., Suzuki, M., Tomoda, A., Arai, S., Taguchi, H., Hanawa, T., and Kamiya, A. (2004) Phenoxazine compounds produced by the reactions with

bovine hemoglobin show antimicrobial activity against non-tuberculosis mycobacteria. *Tohoku Journal of Experimental Medicine*, 203*(1)*: p. 47-52.

[97] Uruma, T., Yamaguchi, H., Fukuda, M., Kawakami, H., Goto, H., Kishimoto, T., Yamamoto, Y., Tomoda, A., and Kamiya, S. (2005) *Chlamydia pneumoniae* growth inhibition in human monocytic THP-1 cells and human epithelial HEp-2 cells by a novel phenoxazine derivative. *Journal of Medical Microbiology*, 54*(12)*: p. 1143-1149.

[98] Atwal, A.S., Teather, R.M., Liss, S.N., and Collins, F.W. (1992) Antimicrobial activity of 2-aminophenoxazin-3-one under anaerobic conditions. *Canadian Journal of Microbiology*, 38*(10)*: p. 1084-1088.

[99] Śmist, M., Kwiecień, H., and Krawczyk, M. (2016) Synthesis and antifungal activity of 2*H*-1,4-benzoxazin-3(4*H*)-one derivatives. *Journal of Environmental Science and Health Part B-Pesticides Food Contaminants and Agricultural Wastes*, 51*(6)*: p. 393-401.

[100] Özden, S., Özturk, A.M., Göker, H., and Altanlar, N. (2000) Synthesis and antimicrobial activity of some new 4-hydroxy-2*H*-1,4-benzoxazin-3(4*H*)-ones. *Farmaco*, 55*(11-12)*: p. 715-718.

[101] Alper-Hayta, S., Akı-Sener, E., Tekiner-Gulbas, B., Yıldız, I., Temiz-Arpacı, O., Yalcın, I., and Altanlar, N. (2006) Synthesis, antimicrobial activity and QSARs of new benzoxazine-3-ones. *European Journal of Medicinal Chemistry*, 41*(12)*: p. 1398-1404.

[102] Fang, L., Zuo, H., Li, Z.B., He, X.Y., Wang, L.Y., Tian, X., Zhao, B.X., Miao, J.Y., and Shin, D.S. (2011) Synthesis of benzo[b][1,4]oxazin-3(4*H*)-ones via smiles rearrangement for antimicrobial activity. *Medicinal Chemistry Research*, 20*(6)*: p. 670-677.

[103] Yalcin, I., Tekiner, B.P., Oren, I.Y., Arpaci, O.T., Aki-Sener, E., and Altanlar, N. (2003) Synthesis and antimicrobial activity of some novel 2,6,7-trisubstituted-2*H*-3,4-dihydro-1,4-benzoxazin-3-one derivatives. *Indian Journal of Chemistry Section B-Organic Chemistry Including Medicinal Chemistry*, 42*(4)*: p. 905-909.

CHAPTER 5

QSAR of 1,4-benzoxazin-3-one antimicrobials and their drug design perspectives

Synthetic derivatives of 1,4-benzoxazin-3-ones have been shown to possess promising antimicrobial activity, whereas their natural counterparts were found lacking in this respect. In this work, quantitative structure-activity relationships (QSAR) of natural and synthetic 1,4-benzoxazin-3-ones as antimicrobials were established. Data published in literature were curated into an extensive dataset of 111 compounds. Descriptor selection was performed by a genetic algorithm. QSAR models revealed differences in requirements for activity against fungi, gram-positive and gram-negative bacteria. Shape, VolSurf, and H-bonding property descriptors were frequently picked in all models. The models obtained for gram-positive and gram-negative bacteria showed good predictive power (Q2Ext 0.88 and 0.85, respectively). Based on the models generated, an additional set of 1,4-benzoxazin-3-ones, for which no antimicrobial activity had been determined in literature, were evaluated in silico. Additionally, newly designed lead compounds with a 1,4-benzoxazin-3-one scaffold were generated in silico by varying the positions and combinations of substituents. Two of these were predicted to be up to 5 times more active than any of the compounds in the current dataset. The 1,4-benzoxazin-3-one scaffold was concluded to possess potential for the design of new antimicrobial compounds with potent antibacterial activity, a multitarget mode of action, and possibly reduced susceptibility to gram negatives' efflux pumps.

Based on: Wouter J.C. de Bruijn, Jos A. Hageman, Carla Araya-Cloutier, Harry Gruppen, and Jean-Paul Vincken (2018) QSAR of 1,4-benzoxazin-3-one antimicrobials and their drug design perspectives, *Bioorganic & Medicinal Chemistry*, 26: p. 6105-6114.

5.1. Introduction

Benzoxazinoids are secondary metabolites that are prominently, but not exclusively, described in species of the plant family Poaceae (formerly Gramineae).[1-3] Their role in plant defence could be an indication for antimicrobial potential. In a recent review, however, we concluded that natural benzoxazinoids are not very potent as antimicrobial compounds. Even the overall most active natural benzoxazinoid, 2,4-dihydroxy-7-methoxy-1,4-benzoxazin-3-one (DIMBOA) (**Figure 5.1A**), lacks antimicrobial potency when compared to other natural products.[1]

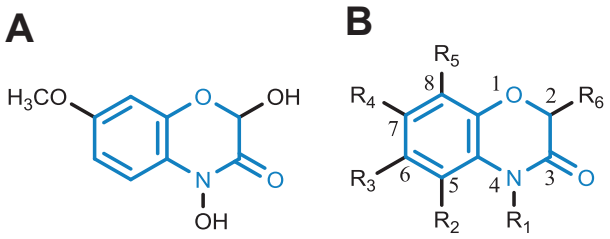

Figure 5.1. The natural benzoxazinoid 2,4-dihydroxy-7-methoxy-1,4-benzoxazin-3-one (DIMBOA) (A) and the core structure of 1,4-benzoxazin-3-one (blue) with its possibilities for substitutions (B).

Several known antimicrobials, however, share structural features with benzoxazinones such as a secondary amide (NHC=O) or an aromatic ring fused to an *N*- or *O*-containing heterocycle. The fluoroquinolones ciprofloxacin and ofloxacin, for example, both possess a core structure of an aromatic ring fused to an *N*-containing heterocycle, a 1-quinolin-4-one and 1,4-benzoxazine, respectively (**Figure S5.1**, supplementary information). The 1,4-benzoxazin-3-one backbone (**Figure 5.1B**) can, therefore, be used as a scaffold for designing new antimicrobial compounds.[1,4,5] It has been demonstrated by multiple studies that 1,4-benzoxazin-3-ones are well suited for further structural optimisation by organic synthesis.[6-8] Six positions on this backbone, indicated with R_1 to R_6 in **Figure 5.1B**, are suitable for substitution which enables the generation of a wide variety of derivatives. Thus, substitution of 1,4-benzoxazin-3-one is a promising approach to synthesize antimicrobial lead compounds. To this end, a wide variety of substituents has been reported. Common small substituents include ethyl acetate on *C*2,[9-11] alkyl or aromatic moieties on *N*4,[5,10] and halogen atoms on *C*5 through *C*8.[5,10] Besides these small substituents, the 1,4-benzoxazin-3-one scaffold has also been decorated with substructures inspired by existing antibiotics. Firstly, *N*4 has been substituted with imidazole or triazole moieties[12-14] inspired by ketoconazole or fluconazole (**Figure S5.2**, supplementary information). Secondly, C6 has been decorated with sulfonamide substituents[15] based on combined features of i.a. ofloxacin (**Figure S5.1**) and sulfadoxine (**Figure A.2**), Thirdly, *C*5 through *C*8 were decorated with linezolid-like (**Figure S5.2**) moieties.[16]

The mode of action of most antibiotics is through interaction with a protein target. For example, fluoroquinolones act on the structurally similar DNA gyrase or topoisomerase IV. Both enzymes belong to a group of heterotetrameric enzymes, the members of which consist of the subunits, GyrA and GyrB or ParC and ParE, repectively. Fluoroquinolones main mode of action is stabilisation of the DNA cleavage-complex in either GyrA or ParC, which makes them multitarget antibiotics.[17-19] Typically, the intracellular target of the above-mentioned antibiotics is the same in gram positives and gram negatives. Compared to most known antibiotics, however, 1,4-benzoxazin-3-one (149 g mol^{-1}) and DIMBOA (181 g mol^{-1}) possess a lower molecular weight[20] and lack halogen atoms (**Figure S5.1** and **Figure S5.2**). A certain minimum size might be required for successful binding to and inhibition of protein targets. Additionally, halogen atoms can form non-covalent bonds (i.e. halogen bonding), which can contribute to interactions with protein targets.[21] We expected to find that halogen substituents and large substituents which increase the M_w of benzoxazinones have a positive effect on antimicrobial activity, both of these characteristics are common in antibiotic-inspired substituents. Besides interaction with a protein target, cell entry of antimicrobial compounds is an essential requirement for their activity. In this respect, the differences in the cell envelopes of fungi, gram-positive, and gram-negative bacteria[22-24] were expected to result in differences in structural requirements for activity against these three separate groups of microorganisms.
In this work, we aimed to establish quantitative structure-activity relationships (QSAR) of 1,4-benzoxazin-3-one derivatives as antimicrobials, based on minimum inhibitory concentration (MIC) values reported in literature. To this end, natural and synthetic 1,4-benzoxazin-3-one structures and MICs were extracted from various publications. Additionally, we aimed to employ the models generated in this work to predict the antimicrobial activity of existing 1,4-benzoxazin-3-ones and new compounds designed *in silico*, to further explore the drug design potential of this scaffold.

5.2. Methods

5.2.1. Dataset curation

Two overall criteria were used to select literature data to be included in the dataset: the core structure should contain the 1,4-benzoxazin-3-one motif (**Figure 5.1B**) and minimum inhibitory concentration (MIC) values should be determined by broth dilution methodologies. In total, this led to the inclusion of 11 different studies, published between 1993 and 2017, and 111 unique molecules.[5,9-16,25,26] Structures and antimicrobial activity data for each of the molecules were extracted from these studies. The overall workflow of the dataset curation is summarized in **Figure 5.2**.

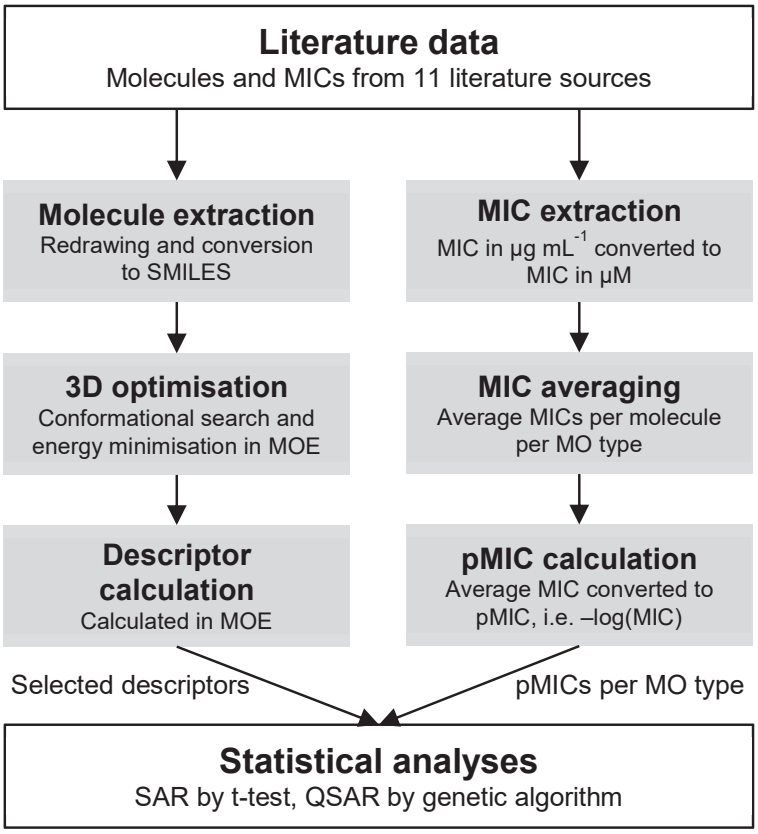

Figure 5.2. Summarized workflow for dataset curation used in this study. Molecular optimisation and descriptor calculation were performed in Molecular Operating Environment (MOE). MIC, minimum inhibitory concentration; MO, microorganism.

5.2.1.1. Molecule extraction and molecular descriptor calculation

The structures of molecules reported in the selected studies were redrawn in Cambridgesoft ChemDraw (PerkinElmer Informatics, Waltham, MA, USA) and converted to SMILES using ChemDraw for Excel (PerkinElmer Informatics). Molecules were numbered **1** to **111**, as shown in the supplementary information (**Table S5.1**-**Table S5.4** and **Figure S5.3**-**Figure S5.5**). Molecules were imported as SMILES in Molecular Operating Environment (MOE) (Chemical Computing Group, Montreal, Canada). A conformational search was performed using the LowModeMD method with a rejection limit of 100, iteration limit of 500, and RMS gradient of 0.005 kcal/mol. The lowest energy conformation was selected and refined using energy minimization under the MMFF94 force-field with MOE default settings. In total, 156 molecular descriptors were calculated for the energy minimized structures from the default list of descriptors available in MOE. A list of these descriptors, which were all included in the final dataset for QSAR modelling, is shown in the supplementary information (**Table A.6**, Supplement A).

5.2.1.2. Activity data

The final dataset included MICs determined against a wide variety of microorganisms (MOs), which was divided in three MO types: fungi (5 species, one

mould and four yeasts), gram-positive bacteria (5 species), and gram-negative bacteria (6 species). All statistical analyses were performed separately for each MO type. For some compounds, MIC values were only reported against one or two of the three MO types. In total, there were 94 compounds in the dataset for gram positives, 91 in the dataset for gram negatives, and 88 in the dataset for fungi. Several of the studies reported MIC values against resistant strains or clinical isolates. These data were not included in our dataset. MIC values from literature were converted from μg mL^{-1} to μM where necessary. To obtain unique MIC values per compound for each MO type, multiple reported MIC values for the same compound against the same MO type were averaged; larger than (">") or smaller than ("<") were not included. Furthermore, if within one study for a specific MO the MIC values for at least two compounds were reported as ">" or "<", then all MIC values related to that specific MO were not included. The reason for this is illustrated by the following example: A compound with reported MICs of 0.49, 15.60, 7.80, and 250 would get an average MIC of 68, whereas a compound with reported MICs of 0.49, 15.60, 15.60, and >500 would get an average MIC of 11, falsely representing the latter molecule as the more active of the two. **Table S5.5** (supplementary information) gives an overview of the MIC values reported for compounds **1-111** (for full MIC overview see **Table A.5**, Supplement A).
Amongst the literature included in the dataset, it was observed that the methodology used to determine antifungal activity was highly heterogeneous. Different combinations of incubation time (24 or 48 h) and temperature (ranging from 25 to 35 °C) were used for the broth dilution assay. Such a variety in methodology was not observed for the determination of antibacterial activity.

5.2.2. Statistical analyses

For all statistical analyses, the MIC values were expressed as pMIC, i.e. –log(MIC). MIC values (in μM) were averaged prior to calculating pMIC.

5.2.2.1. SAR study

To investigate the effect of different types of substituents, including antibiotic-inspired substructures, on the antimicrobial activity of 1,4-benzoxazin-3-one derivatives, independent samples t-tests were used. These analyses were performed in SPSS Statistics (IBM, Armonk, NY, USA) with default settings. Substituents were divided in several groups, firstly, to investigate the effect of antibiotic-inspired substituents: linezolid-like, sulfonamide-like, and azole-like. Secondly, to investigate the effect of other substituents: hydroxy, aromatic, alkyl, halogen, nitro, ethyl acetate, bulky (M_w > 200), and miscellaneous. Other types of substituents were not sufficiently represented (n < 5) in the dataset for reliable statistical analysis. It was expected that antibiotic-inspired substituents would have a large influence on the antimicrobial activity. Therefore, in the first set of analyses, the effect of antibiotic-inspired substituents on antimicrobial activity was tested against having no antibiotic-inspired substituent. Secondly, the effect of

substituents on the different positions *C*2, *N*4, *C*6, and *C*7 were tested against no substitution (i.e. R_n = –H) on each of these positions. Very few cases of substituents on *C*5 and *C*8 were described, which made these positions unsuitable for statistical analyses.

5.2.2.2. QSAR modelling

For all three MO types, the available data was divided into two parts: a training set consisting of 80% of all molecules and an external validation set with the remaining 20% molecules. The division into training and validation set was performed using Kennard-Stone algorithm.[27] This algorithm finds a subset of molecules of a given size that best represents the complete data set. The remaining part automatically becomes the validation set. This procedure is deterministic, thereby preventing an overoptimistic division in training and validation set, something which commonly occurs in random divisions. An overview of the compounds in each of the training and validation sets can be found in the supplementary information (**Table A.7**, supplement A).

A genetic algorithm (GA) was used to select a small subset of predictors best able to predict the antibacterial activities using multiple linear regression with the descriptors calculated by MOE as predictors and pMIC as the response variable. The GA approach has been adapted from Araya-Cloutier and co-workers (2018).[28] Model accuracy for a given set of predictors was determined by a leave-one-out cross validation (LOOCV) procedure.[29] During each iteration of the LOOCV procedure a new optimal set of predictors was selected by the GA. This leads to as many models as there are molecules in the training set, each of which may include a different set of predictors. Using this sceheme each molecule is left out once and predicted by a model based on the remaining molecules. All LOOCV-models were stored. The prediction quality was summarised in a Q^2_{LOO} value. Lastly, the external validation set was predicted by taking the average of the predictions of each compound of the training set within all LOOCV-models. The prediction quality of the external validation set was summarised in Q^2_{Ext}.

To exclude lucky or unlucky GA runs, every run was repeated 10 times with different starting seeds. Combinations of predictors with a Variance Inflation Factor (VIF) > 5, indicating a strong inter-correlation, were effectively removed from the GA population by penalizing the fitness during the GA run. GA parameters were optimised using a full factorial experimental design and were found to be: population size = 200, cross-over rate = 0.6, mutation rate = 0.3. The maximum number of iterations was set to 200 and elitism set to 10. The number of predictors to be selected during a GA run was varied between 1 and 8.

For each compound in the training and validation sets, the fit within the applicability domain (AD) was calculated according to the method of Roy and co-workers (2015).[30] The calculations were performed separately for each of the models in the selected solution (e.g. the 75 models for the four-descriptor solution for gram-positive bacteria). Descriptor values were standardised and the maximum

value was recorded for each model within a solution and the average over all maxima was determined and compared to the threshold (3.0).[30]

5.3. Results and discussion

5.3.1. Most active compounds

The structures of compounds **1**-**111** are described in **Table S5.1**-**Table S5.4** and **Figure S5.3**-**Figure S5.5**. Natural benzoxazinoids (e.g. compounds **1**, **3**, and **15**) generally showed very poor activity with MIC values > 1000 µM (**Table S5.5**). The most active antibacterial compounds were **77** and **83** (**Figure 5.3**), reported by Deshmukh and Jain, which were more active than the antibiotic linezolid by which they were inspired.[16]

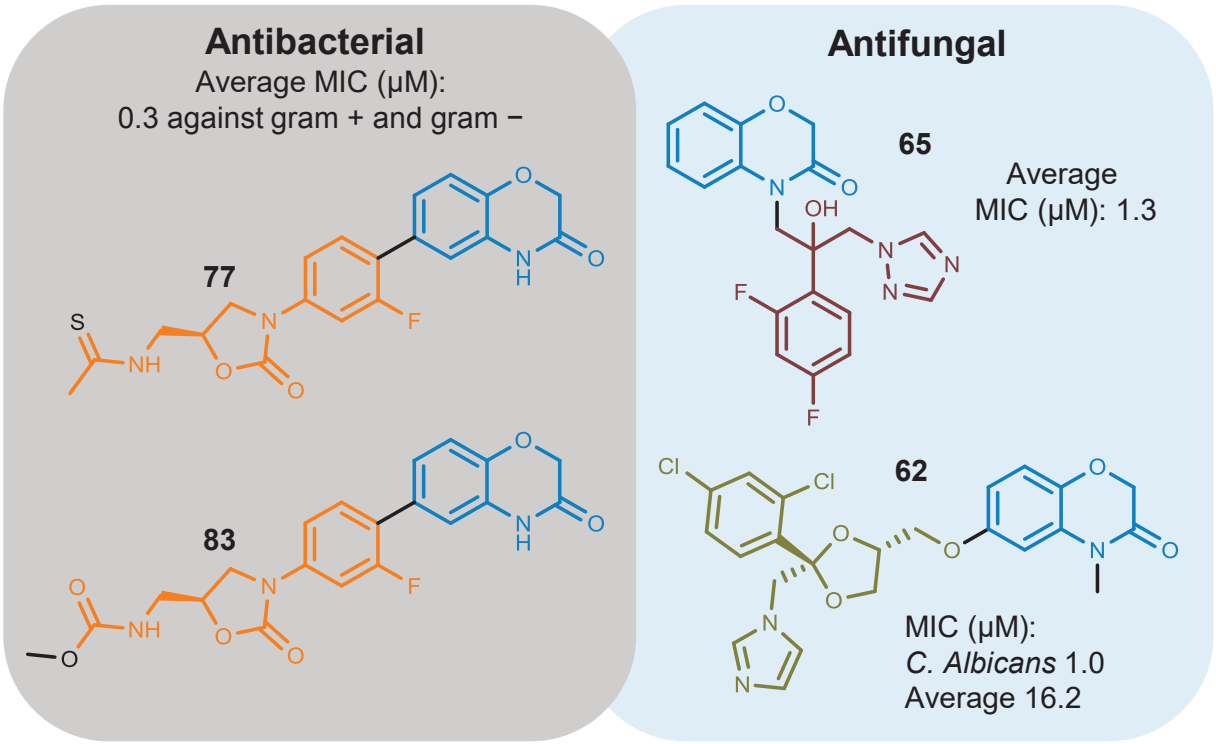

Figure 5.3. The most active molecules in the dataset: antibacterial compounds **77** and **83** with linezolid-like substituents (orange), and antifungal compounds **65** with a fluconazole-like substituent (brown) and **62** with a ketoconazole-like substituent (olive green).

The most active antifungal compound was **65** (**Figure 5.3**), reported by Borate and co-workers, which was found to be more active than fluconazole on which the main substituent was based.[14] Compounds **61**-**64** with a ketoconazole-like substituent, reported by Fringuelli and co-workers,[13] possessed slightly lower MICs against *C. albicans* than **65** (only tested against *C. albicans*), but their average activity was less potent (MICs ranging from 16.2 to 40.8 µM).

5.3.2. Structure-activity relationships (SAR)

Natural benzoxazinoids possess a hydroxy or glucopyranosyloxy moiety at *C*2, both of which negatively affect activity.[1] To gain more insight in the effect of common substituents on the antimicrobial activity, structure-activity relationships (SAR) were studied. This SAR study gives a quick impression of what types of substituents should be used or avoided for structural optimisation of benzoxazinones.

5.3.2.1. Antibiotic-inspired substituents

The effect of antibiotic-inspired substituents was tested against no substitution (H) or any other substituents (X) (**Figure S5.6**). Sulfonamide-like substituents did not significantly affect the antimicrobial activity against any of the MO types. The antibacterial activity was positively affected by linezolid-like substituents, whereas the antifungal activity was positively affected by azole-like substituents (**Figure S5.6**). Due to the strong effects of these linezolid- and azole-like substituents on the antimicrobial activity and the fact that these substituents strongly overruled the effect of non-antibiotic-like substituents, it was not possible to reliably study the effect of other substituents on *C*2, *N*4, *C*6, and *C*7. Therefore molecules containing linezolid- or azole-like substituents were excluded from further SAR studies. For these further SAR studies, substituents on positions *C*2, *N*4, *C*6, and *C*7 were tested against no substitution (i.e. –H) on the respective position.

5.3.2.2. Substitution of C2

Hydroxylation of *C*2, which is observed in all natural benzoxazinones, negatively affected antimicrobial activity against all three MO types (**Figure 5.4**). This might be related to the ring-opening of the hemiacetal, which can lead to subsequent degradation of natural benzoxazinones into even less active benzoxazolinones.[1,31] Substitution of *C*2 with an ethyl acetate moiety positively affected antifungal activity, whereas no effect on the antibacterial activity was observed.

5.3.2.3. Substitution of N4

N-alkylation and aromatic moieties positively affected activity against bacteria but not against fungi. Hydroxylation of *N*4, which was associated with a positive effect on biological activity (e.g. allelopathy) amongst natural benzoxazinones,[1,31] was unexpectedly shown to have a negative effect on antimicrobial activity for all three MO types.

5.3.2.4. Substitution of C6 or C7

Halogenation on *C*6 was not found to affect antibacterial activity, whereas halogenation on *C*7 only gave a modest positive effect against gram negatives. Conversely, against fungi halogenation of *C*6 had a strong positive effect, whereas halogenation on *C*7 had a negative effect.

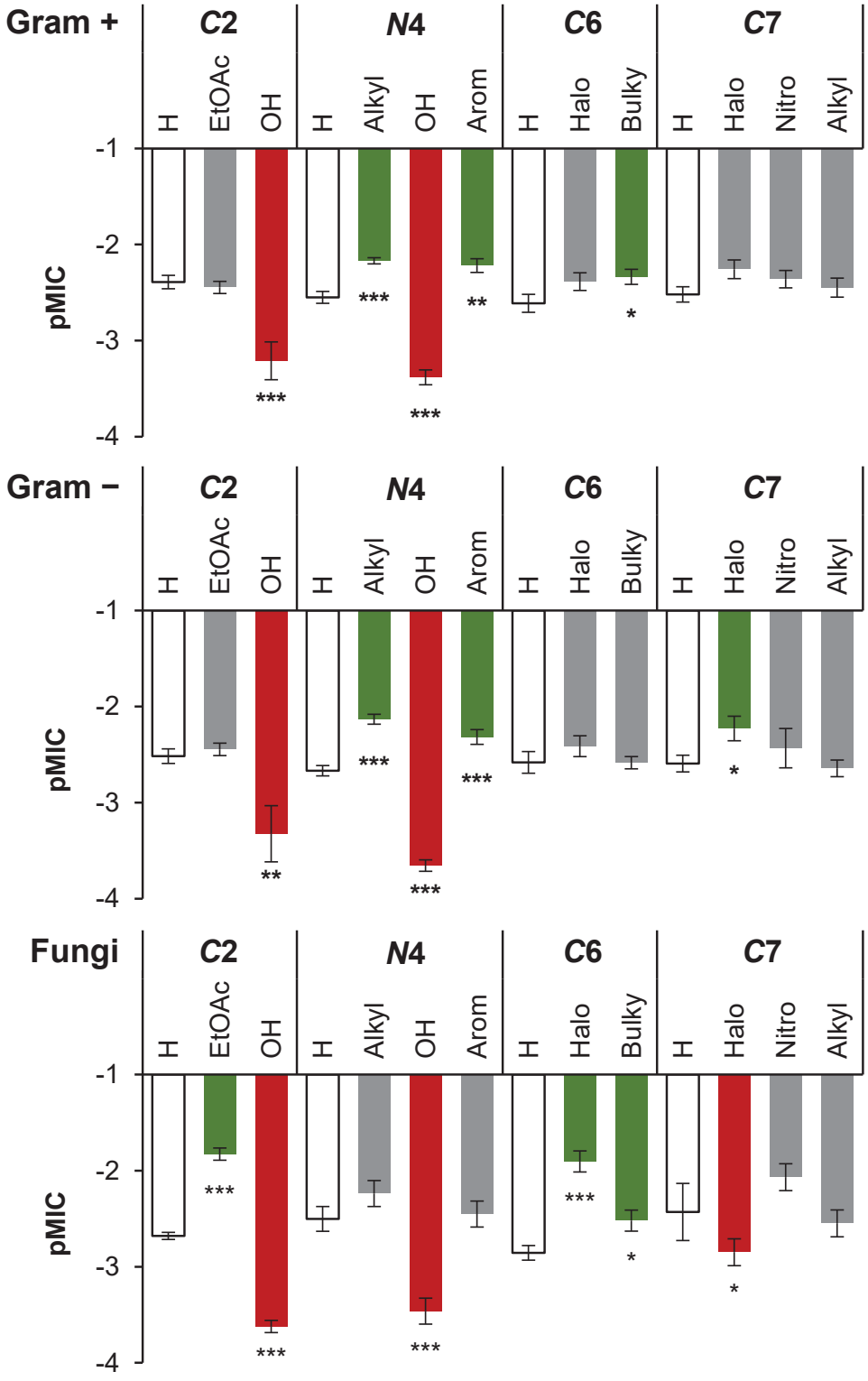

Figure 5.4. Effect of various substituents at *C*2, *N*4, *C*6, and *C*7 on the antimicrobial activity (pMIC) of 1,4-benzoxazin-3-ones. Higher pMIC corresponds to higher activity. Error bars indicate standard error, asterisks indicate significant difference compared to H on that position: *, p <0.05; **, p <0.01; ***, p <0.001. Red colour indicates decreased activity compared to H whereas green colour indicates increased activity compared to H, grey indicates no significant difference. Halo, halogen; Bulky, substituent > 200 Da; Arom, aromatic.

Bulky substituents on *C*6 had a moderate positive effect on activity against gram positives and fungi but no effect against gram negatives. Nitro or alkyl groups on *C*7 did not have a significant effect on the antimicrobial activity.

Interestingly, very little difference was observed between the structure-activity relationships of gram-positive and gram-negative bacteria despite differences in their cell envelopes, which will be discussed in more detail later. Results against fungi were quite different from what was observed for bacteria. The SAR results have to be considered in perspective as not all possible combinations of substituents on various positions were available in the dataset. Thus, synergistic or antagonistic effects between substituents are not yet clear.

5.3.3. QSAR models of 1,4-benzoxazin-3-ones

For each MO type, models were generated by multiple linear regression using a genetic algorithm (GA) for descriptor selection. The optimal number of descriptors in the solution was chosen based on the leave-one-out cross-validated Q^2 (Q^2_{LOO}) and a preference for simpler solutions (lower number of descriptors) was also considered. Both Q^2_{LOO} and the external validation Q^2_{Ext} should be higher than 0.5.

Table 5.1. Characteristics of the chosen solution with n_{train} number of models per solution.

MO type	n_{train}	k	Q^2_{LOO}	$Q^2_{LOO\ adj}$	R^2_{LOO}	$R^2_{LOO\ adj}$	n_{vali}	Q^2_{Ext}
Gram +	75	4	0.64	0.62	0.77	0.76	19	0.88
Gram –	73	4	0.60	0.58	0.77	0.76	18	0.85
Fungi	70	3	0.57	0.55	0.65	0.63	18	0.48
		5	0.46	0.41	0.72	0.70	18	0.68

n_{train}, number of objects in the training set; n_{vali}, number of objects in the validation set; k, number of descriptors in the solution; LOO, leave-one-out; Ext, external (based on validation set); adj, adjusted for n_{train} and k.

The complete output of the GA-generated modelling solutions with 1-8 descriptors for all three MO types can be found in the supplementary information: gram-positive bacteria (Supplement B), gram-negative bacteria (Supplement C), and fungi (Supplement D). The statistical characterisation of the chosen solution for each MO type is shown in **Table 5.1**. The approach used in this paper leads to a large number of models (n_{models}) within each solution, one model for each molecule in the training set ($n_{models} = n_{train}$). Identification of the most important descriptors from this multitude of models was based on the selection frequency: Important predictors were selected more often (**Table 5.2**). All of the compounds in the training and validation sets were found to fit within the AD of all models in the chosen solutions. In the text below the plus (+) or minus (−) signs in parentheses indicate the sign of the regression coefficient for that particular descriptor.

Table 5.2. Descriptors most frequently selected by the genetic algorithm to predict the antibacterial activity (expressed as pMIC).

	Descriptor	f [a]	Coef. [b]	Description	Ref.
Gram	vsurf_IW6	71	−	Hydrophilic integy moment at −4.0 kcal mol^{-1}	[32]
positive	vsurf_W1	45	+	Hydrophilic volume at −0.2 kcal mol^{-1}	[32]
n_{train} = 75	a_acc	43	−	Number of H-bond acceptor atoms	
k = 4	FCASA−	43	−	Fractional negative charge weighted surface area	
	h_pka	31	+	Acidity (pH = 7)	
	npr1	30	−	Normalized principal moment of inertia ratio 1 (pmi1 / pmi3)	[33,34]
	vsurf_Wp3	27	+	Polar volume at −1.0 kcal mol^{-1}	[32]
Gram	a_don	73	+	Number of H-bond donor atoms	
negative	h_pka	73	+	Acid dissociation constant	
n_{train} = 73	b_double	55	+	Number of double bonds	
k = 4	npr1	55	−	Normalized principal moment of inertia ratio 1 (pmi1 / pmi3)	[33,34]

n_{train}, number of objects in the training set; k, number of descriptors in the models. [a] Frequency with which this descriptor was selected. [b] Sign of the regression coefficient.

5.3.3.1. Gram-positive bacteria

The dataset for gram positives included MIC values determined against many different species, amongst which *Staphylococcus aureus* was most common (**Table A.5**, Supplement A). The solution with four descriptors in the models was chosen, which had good internal (Q^2_{LOO} = 0.64) and excellent external (Q^2_{Ext} = 0.88) validation results.

The most frequently selected descriptors are shown in **Table 5.2**. The descriptors vsurf_IW6 (−) and vsurf_W1 (+) represent the hydrophilic integy moment and hydrophilic volume. The former is a measure for the distribution of hydrophilic regions (low integy moment means that hydrophilic regions are equally distributed or close to the centre of mass).[32] The descriptor vsurf_W1 was exchanged for vsurf_Wp3 (+), i.e. polar volume, in some solutions. Furthermore, a_acc (−) and npr1 (−) represent the number of hydrogen-bond acceptors and the three-dimensional shape, respectively.[33,34] FCASA− (−), the fractional negative charge weighted surface area, and h_pka (+), the acid dissociation constant, were also frequently selected and were seemingly interchangeable with one another. This combination of descriptors suggests that molecules should possess some hydrophilic surface with equally distributed hydrophilic groups, possess limited H-bond acceptors. Additionally, negative charges on the molecular surface are undesirable and the molecular shape should not be sphere-like, i.e. a disc-like or rod-like shape is preferred.

5.3.3.2. Gram-negative bacteria

The dataset for gram negatives included MIC values determined against many different species, amongst which *Escherichia coli* was most common (**Table A.5**). The solution with four descriptors in the models was chosen, which had good internal (Q^2_{LOO} = 0.60) and excellent external (Q^2_{Ext} = 0.85) validation results.

The most frequently selected descriptors are shown in **Table 5.2**. The two most important descriptors were a_don (+), i.e. the number of hydrogen bond donors, and h_pKa (+), the acid dissociation constant (higher h_pKa means less acidic). This combination suggests that OH and NH groups as H-bond donors are preferred over acidic groups. Besides these descriptors, b_double (+) and npr1 (−) were frequently selected, representing the number of double bonds and rod- rather than sphere-like shape. Overall, H-bond donation in combination with a rod-like shape seemed to be important factors in activity against gram negatives. The number of double bonds did not include those in aromatic rings and was found to be mainly related to the number of (thio)ketones.

5.3.3.3. Fungi

The dataset for fungi mainly included MIC values determined against *Candida* species (**Table A.5**). The solution with three descriptors in the models was chosen because it resulted in the highest Q^2_{LOO} (0.57), although the external validation results (Q^2_{Ext} = 0.48) were lower than desirable. Alternatively, the solution with five descriptors in the models had a low Q^2_{LOO} (0.46) but a higher Q^2_{Ext} (0.68). Neither of these combinations of Q^2_{LOO} and Q^2_{Ext} was considered to be acceptable. The heterogeneity of the antifungal MIC values might be the underlying cause for the lower quality of the QSAR solutions for antifungal activity compared to the bacteria. Nevertheless, the descriptors selected by the QSAR models for fungi are briefly addressed. In the three-descriptor solution, Q_RPC+ (−), a_nH (−), and vsurf_CW1 (−) were almost exclusively selected. In the five-descriptor solution Q_RPC+ (−), vsurf_CW1 (−), vsa_acc (−), vsurf_IW7 (+), and b_double (+) were most frequently selected (see supplement D). The selection of these descriptors suggests that charged and polar surface is undesirable, whereas equal distribution of hydrophilic groups is desirable. Lack of flexibility might positively affect activity, as suggested by the negative correlation of a_nH and the positive correlation of b_double.

Considering the low quality of the QSAR models, the results of the modelling outcomes of the dataset for fungi are not considered further in this manuscript. Acquisition of a more uniform dataset will be essential to reliably establish antifungal QSAR of benzoxazinones.

5.3.4. *In silico* predictions of compounds with unknown activity

The models presented in this work can be used to evaluate compounds with unknown antibacterial activity *in silico* in order to find new leads for antimicrobial compounds. Prior to calculating the molecular descriptors, all compounds were subjected to the same preparation procedure as the dataset, as depicted on the left-hand side of **Figure 5.2**.

5.3.4.1. Compounds from literature

A subset of the compounds included in our dataset was only tested against fungi and no antibacterial activity was reported. These are compounds **59**-**64** reported by Fringuelli and co-workers[12,13] and compounds **65**-**71** reported by Borate and co-workers.[14] The results of the *in silico* evaluation of these molecules using all the models in the chosen solutions for gram-positive and gram-negative bacteria are presented in **Table A.8** (Supplement A). Except for compounds **61** and **62**, all compounds were inside the AD of the antibacterial activity models. None of the compounds were, however, predicted to possess very potent (< 1 μM) antibacterial activity. Moderate activity was predicted for compound **60** with MIC 21.7 μM against gram negatives and 35 μM against gram positives. Considering the structures of this set of molecules, these predictions indicate that azole substitution of 1,4-benzoxazin-3-ones is unlikely to result in compounds with good antibacterial activity. This is probably due to the large increase in hydrogen bond acceptors (higher a_acc), more disc- rather than rod-like shape (higher npr1), and an increase in partial negatively charged surface area (higher FCASA−) as a result of azole substitution.

In addition, several publications reporting substituted 1,4-benzoxazin-3-ones were not included in our dataset, because they did not determine antimicrobial activity of their compounds or the antimicrobial activity was assessed by other methods than broth dilution (thus no MICs reported). This set of compounds includes *C*2 alkyl derivatives with varying aromatic substituents,[4,35] *C*6 cinnamoyl derivatives,[8] *N*4 aryl-triazolyl derivatives,[36] and *C*6 aryl-imidazolyl derivatives.[37] To evaluate the potency of these molecules (**U1**-**U59**), their antibacterial activities were evaluated *in silico*. The results of these predictions are shown in **Table A.9** (Supplement A). All of these compounds were found to be within the AD of the models for bacteria. Interestingly, it seems that the compounds in this set are selectively active against either gram positives or gram negatives. Three compounds (**U1**, **U5**, and **U7**) were predicted to possess MIC values ranging from 24 to 26 μM against gram-positive bacteria and MIC values from 41 to 139 μM against gram-negative bacteria. Seven compounds were found which had predicted MIC ≤ 15 μM against gram-negative bacteria. Three of these compounds were reported by Reddy Sastry and co-workers (**U22**, **U23**, and **U25**)[37] and four others by Zhou and co-workers (**U54**, **U57, U58**, and **U59**)[8].

The lowest predicted MIC against gram positives amongst these seven compounds was 91 μM. This group of seven compounds might be suitable for further optimisation as selective antibacterials against gram negatives. The structures of the above-mentioned compounds are shown in **Figure S5.7**.

5.3.4.2. Molecular optimisation

Based on the outcomes of the SAR studies and the QSAR models, new compounds were generated and evaluated. This was done through an iterative process in which the effect of substituents was evaluated and adjustments were made to generate new series of compounds. Most of these substituents were based on those found in compounds in the dataset, whereas some were newly designed substituents. **Figure 5.5** gives an overview of the structural diversity of the substituents that were systematically explored.

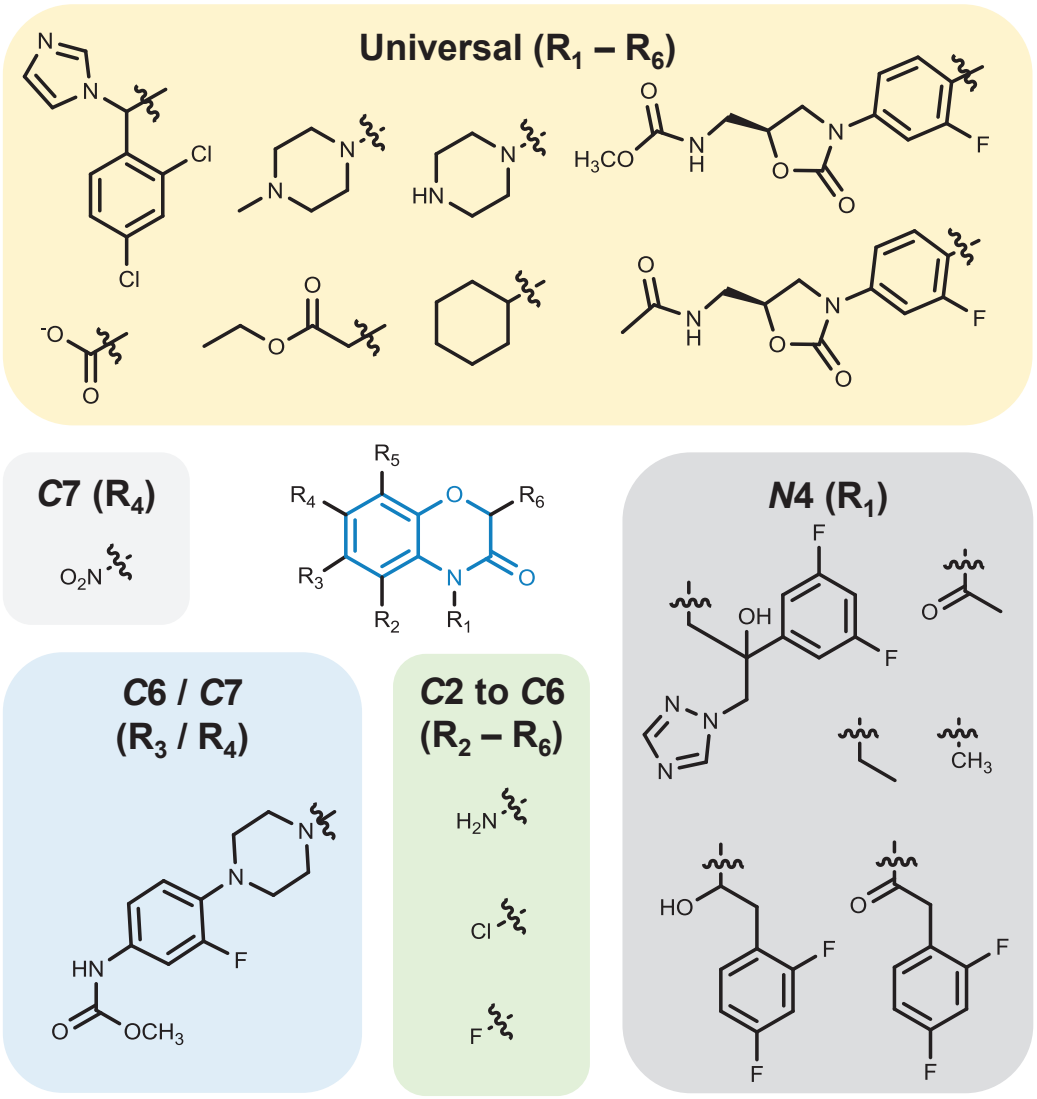

Figure 5.5. Structural diversity of substituents used for the generation of new lead compounds based on the 1,4-benzoxazin-3-one scaffold.

These substituents include: halogens, alkyl, aromatic, nitro, ethyl acetate, amino, azole-like (as in compounds **62** and **65**), and linezolid-like (as in compounds **77** and **83**) moieties. The use of amino groups was inspired by a report of 3-amino-3,4-dihydroquinolin-2-ones with high antibacterial activity.[38] Further inspiration for substituents was found from existing antibiotics, such as formic acid, (methyl)piperazinyl, or difluorophenyl-ethanoyl. Additionally, novel substituents were generated by modifying and combining promising structural elements of substituents reported in the dataset. Different positions (R_1 to R_6) were evaluated for most of these substituents (**Figure 5.5**). Theoretically, application of all substituents on all positions would yield thousands of possible structures. Therefore, not all substituents were combined (M_w maximum of 900 Da) and some substituents were limited to one or two positions, mainly based on chemical logic (e.g. amino groups or halogens were not attached on *N*4). In total, more than 500 new compounds were generated.

	Predicted activity									
	Gram positive (n_{models} = 75)			Gram negative (n_{models} = 73)			Lipinski's rules			
Comp.	pMIC	StDev	MIC (µM)	pMIC	StDev	MIC (µM)	H-bond don.	H-bond acc.	M_w	logD
L1	0.92	0.39	0.12	0.89	0.29	0.13	4	11	502	1.6
L2	0.30	0.23	0.50	0.68	0.07	0.21	4	9	414	1.8
L3	0.44	0.12	0.36	1.22	0.20	0.06	3	10	484	0.4
L4	1.03	0.23	0.09	1.30	0.19	0.05	4	10	459	1.6
L5	0.88	0.24	0.13	0.71	0.25	0.20	3	10	457	2.1

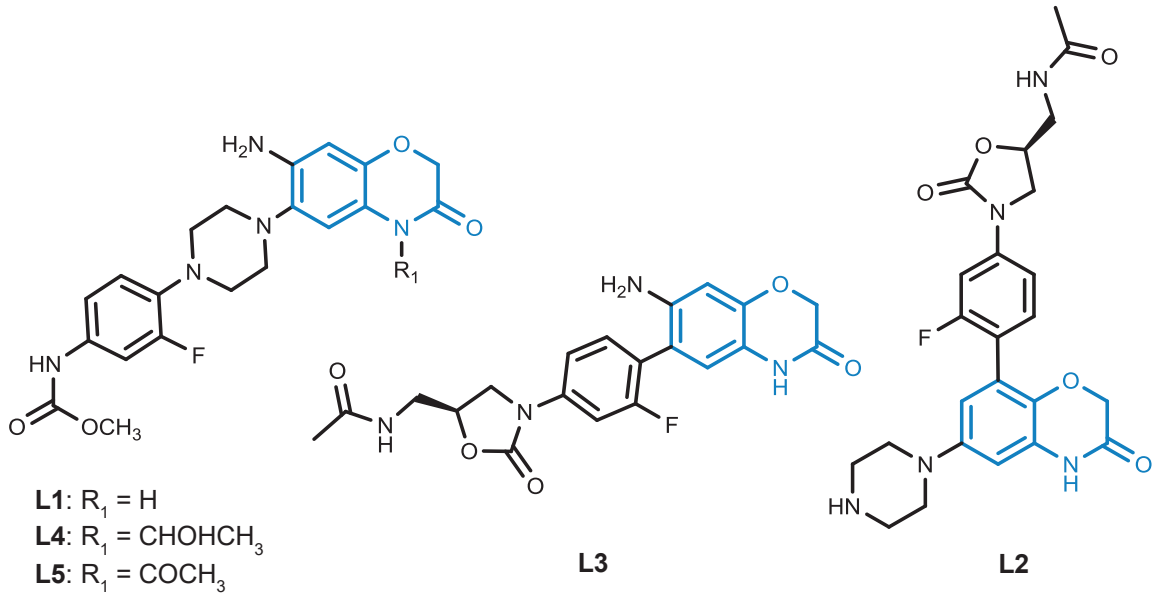

Figure 5.6. Predicted activity (average pMIC based on n_{models}) of newly designed lead compounds **L1**-**L5** and their characteristics with regard to Lipinksi's rules.[39] These characteristics were calculated by MOE (lip_don, lip_acc, weight, and h_logD descriptors). StDev, standard deviation of the pMIC as predicted by the different models.

Five compounds (**L1**-**L5**) from this set were selected as the most promising new lead compounds (**Figure 5.6**), based on their very potent predicted antibacterial activity and favourable characteristics with regard to Lipinski's rules.[39] Lipinski's 'rule of five' is a rule of thumb used in drug discovery and predicts that for good absorption or permeation a molecule should possess: H-bond donors ≤ 5, H-bond acceptors ≤ 10, molecular weight ≤ 500 g mol^{-1}, and calculated logP ≤ 5.
These compounds were all predicted to possess MIC values ≤ 0.5 μM against both gram positives and gram negatives, making them even more potent than the most active antibacterials in the modelling dataset (compounds **77** and **83**). **L1** and **L4** in particular were predicted to be highly potent with MICs below 0.15 μM against both types of bacteria. A common structural element found in four of the five newly-designed lead compounds was an amino group at *C*6, for example **L3** only differs from compound **75** by addition of this amino group and predicted activity was 3 to 10 times higher (**Figure 5.6** and **Table A.5**).
The positive effect of the amino group was, based on our QSAR findings, probably due to the associated increase in polar or hydrophilic surface area (higher vsurf_Wp3 or vsurf_W1), reduced acidity (higher h_pKa), and the addition of an extra hydrogen bond donor (higher a_don). Furthermore, compounds possessing the newly designed substituent (see **L1**, **L4**, and **L5**), which was inspired by both piperazinyl (like in fluoroquinolones) and fluorophenyl (like in linezolid), were predicted to be highly effective. The differences between compounds **77** and **83** and the newly-designed lead compounds with respect to several important descriptors are visualised in **Figure 5.7**.
Generally, the lead compounds possessed a greater hydrophilic and polar volume than **77** and **83** (higher vsurf_W1 or surf_Wp3), as well as more equally distributed hydrophilic groups than **83** (lower vsurf_IW6) (**Figure 5.7A** and **B**). The hydrophilic regions of the lead compounds were less pronounced and the hydrophobic regions in particular were less intensely concentrated at the core of the molecule than in **77** and **83**. In terms of molecular shape (npr1 and npr2), the lead compounds were similar to **77** and **83**, all these molecules possessed a rod-like shape (**Figure 5.7C**). The lead compounds possessed the same number of H-bond acceptors (except for **L3**), but generally a higher number of H-bond donors (except for **L5**) than **77** and **83** (**Figure 5.7D**). In addition to **Figure 5.7**, most lead compounds' FCASA– was found to be lower and h_pka was found to be higher than for compounds **77** and **83**.
The lead compounds' characteristics with respect to Lipinski's 'rule of five' were calculated (**Figure 5.6**). Except for **L1** (minor violations of lip_acc and weight), all the lead compounds comply with Lipinski's rules. These lead compounds need to be evaluated *in vitro* to verify their activity and then be further optimized with regards to their absorption and permeation characteristics if necessary.

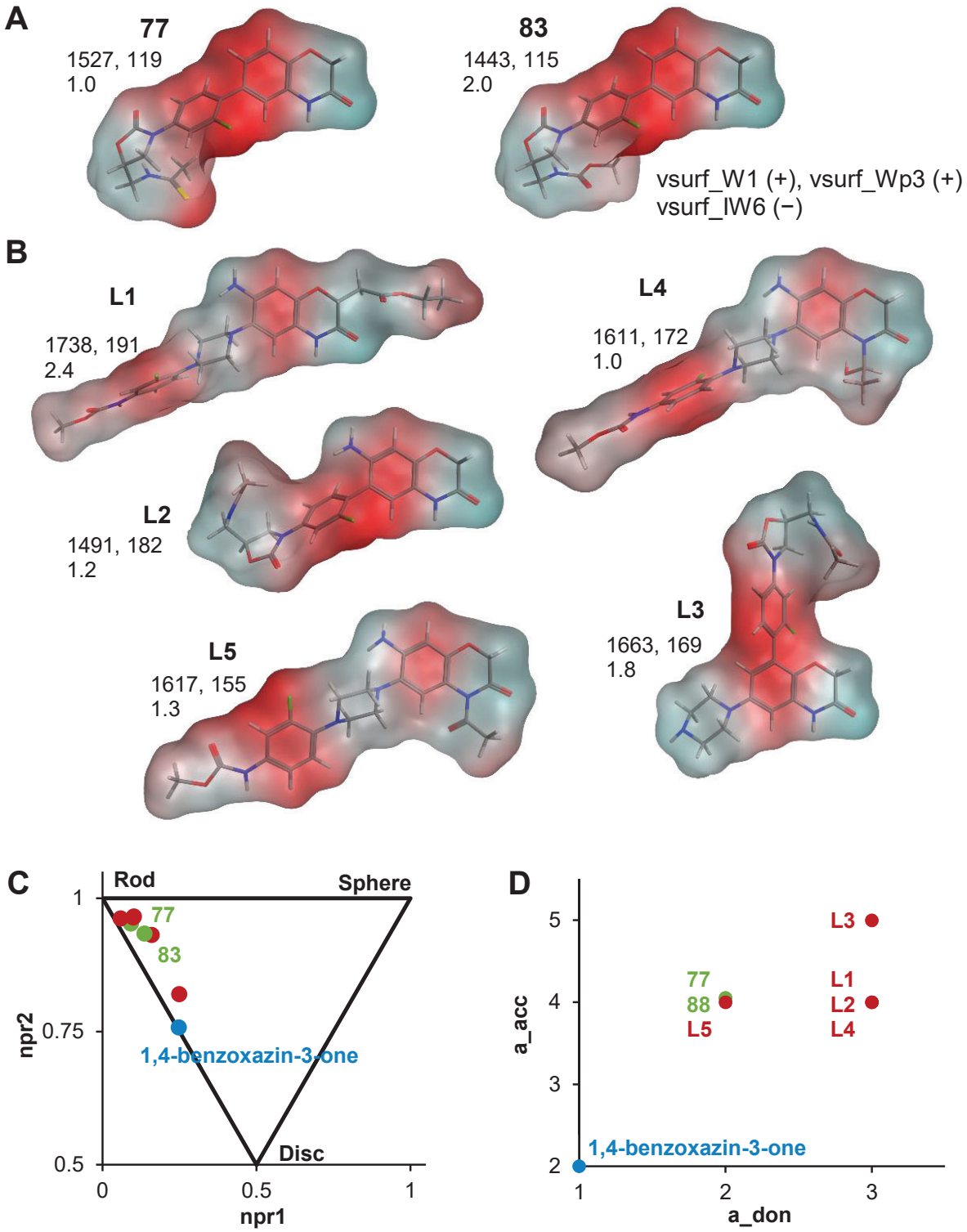

Figure 5.7. Visualisation of key descriptors for 1,4-benzoxazin-3-one, compounds **77** and **83**, and the lead compounds. Hydrophilicity surface maps of compounds **77** and **83** (A) and **L1**-**L5** (B) in which red indicates hydrophobic regions and light-blue hydrophilic regions, the numbers underneath the compound names indicate the calculated values for vsurf_W1, vsurf_Wp3, and vsurf_IW6. Plot of the three-dimensionality descriptors npr1 and npr2 (C) and the a_don and a_acc descriptors (D).

5.3.5. Cell entry and interaction with molecular target

In order for molecules to exert antimicrobial activity against microorganims, they have to meet three main requirements: entry into the microbial cell, accumulation in the cell, and interaction with the target.[40] Typically, the intracellular target of antibiotics is the same in gram positives and gram negatives, we therefore expected the same for our compounds. Differences in activity against both types of bacteria are most likely caused by differences in cell entry or intracellular accumulation. The former is mainly due to differences in their cell envelopes, whereas the latter is usually related to gram negatives' efflux pumps. A QSAR approach cannot distinguish the structural requirements for each of these aspects. Compounds with good antimicrobial activity must perform well on each aspect. Nevertheless, in the following sections we will try to address cell entry and interaction with the target of 1,4-benzoxazin-3-ones in relation to the modelling outcomes.

5.3.5.1. Cell entry

The bacteria studied here possess widely different cell envelopes. Between gram negatives and gram positives, the plasma membrane, which is a lipid bilayer, is accompanied by different types of cell walls. Penetration of an antimicrobial through the cell wall and plasma membrane is most likely determined by its physical character (charge, shape, hydrophobicity, and amphiphilicity), rather than specific structural elements.[40] This might explain why each of the models contains descriptors related to shape, charge, or surface polarity (e.g. npr1, vsurf descriptors).

Gram-positive bacteria possess a thick peptidoglycan cell wall which is hydrophobic and diffusion of apolar molecules is rather facile.[22] This can explain why surface charge (FCASA−) was negatively correlated with activity against gram-positive bacteria. Hydrophilicity-related descriptors (vsurf_W1 or vsurf_Wp3) were positively correlated with activity against gram positives, which seems to contradict the aforementioned. Possibly, hydrophilicity is necessary for later stages of activity (e.g. protein interaction) and does not limit cell entry for the compounds in the current dataset.

On the other hand, gram-negative bacteria possess a thin layer of peptidoglycan surrounded by an outer membrane.[22] The outer membrane severely limits permeation of hydrophobic molecules, but small hydrophilic molecules (<600 Da) can passively diffuse through porins to reach the cytoplasmic membrane.[40] Relating to the modelling outcomes, H-bond donors probably facilitate cell entry by H-bond formation with the porins themselves and the water molecules inside, as reported for other known antimicrobials.[41] Bulky substituents might negatively affect antimicrobial activity by reducing diffusion through porins, although very few molecules exceeded a molecular weight of 600 Da in the current dataset.

5.3.5.2. Interaction with the intracellular target

Benzoxazinones possess structural analogy with linezolid, aminocoumarins (e.g. novobiocin), and (fluoro)quinolone, such as ciprofloxacin and ofloxacin (**Table S5.1**). The modes of action of benzoxazinones might be the same or similar to these antibiotics.

Recently, Yilmaz and co-workers performed *in silico* docking of their set of 1,4-benzoxazin-3-ones with *C*2 ethyl acetate substituents (compounds **18**, **30**-**32**, and **34**-**42**) and their results indicated the ability of the compounds to interact with the GyrA-DNA breakage-complex in a similar way as the fluoroquinolone moxifloxacin.[11] On the other hand, Deshmukh and Jain (2017) evaluated the docking of compounds **75** and **83,** 1,4-benzoxazin-3-ones with linezolid-like substituents, in the 50S ribosomal unit and they concluded that the binding was similar to that of linezolid.[16] Linezolid acts by inhibiting the initiation phase of protein synthesis,[42,43] however, it possesses limited activity against gram negatives because they can quickly excrete this compound through their efflux pumps.[44] It seems like Deshmukh and Jain's 1,4-benzoxazin-3-one derivatives were less affected by efflux pumps (i.e. they were more active than linezolid against gram negatives), which may be a valuable advantage of the 1,4-benzoxazin-3-one scaffold in comparison with the original morpholine scaffold of linezolid. Furthermore, other 1,4-benzoxazin-3-ones in the dataset also exhibited comparable activity against both types of bacteria, supporting the hypothesis of reduced efflux of 1,4-benzoxazin-3-one based antimicrobials.

A cytoplasmic protein target, rather than the cell membrane, which is one of the proposed target sites of prenylated (iso)flavonoids,[28] would explain the selection of descriptors related to H-bond formation (**Table 5.2**), which is often essential for drug-protein interaction. Based on the structural analogies and the results discussed above, likely modes of action of 1,4-benzoxazin-3-ones are: stabilisation of the DNA cleavage-complex in GyrA or ParC, or inhibition of the 50S ribosomal unit, or a combination of these mechanisms. Dual inhibitors of GyrA and ParC are one of the promising options in this respect, as demonstrated by the success of fluoroquinolones.[18] The indication that 1,4-benzoxazin-3-ones might be able to act in such a way and might be less susceptible to gram negative efflux pumps makes this scaffold even more interesting for antimicrobial drug development. Antimicrobials which act via interactions with multiple targets (i.e. multitarget mechanism) are less likely to lead to short-term resistance development, thus preserving antimicrobial activity over longer periods of time.[18] Besides exerting antimicrobial activity, there are also indications that 1,4-benzoxazin-3-ones might be used in combination with existing antibiotics to restore activity of those antibiotics against resistant microorganisms, as shown against quinolone-resistant *Acinetobacter baumannii*.[11]

5.3.6. Future perspectives for 1,4-benzoxazin-3-one antimicrobials

The dataset curated in this work demonstrates that 1,4-benzoxazin-3-ones have successfully been used by various researchers as scaffolds for the design of antimicrobial agents. Depending on the (combination of) substituents, this scaffold has the potential to outperform existing antibiotic scaffolds,[14,16] not only in terms of potency (this study), but also considering their possible multitarget mechanism[11,16,18] and their presumed reduced susceptibility to gram negatives' efflux pumps.[16] The models presented here were built upon this diverse dataset, which included compounds of widely varying complexity and antimicrobial activity. These models provide a tool for further optimisation of 1,4-benzoxazin-3-ones to enhance their antimicrobial activity. The 1,4-benzoxazin-3-one scaffold offers flexibility for substitutions as it possesses five carbon atoms and one nitrogen atom which are suitable for a wide variety of substituents. The potential for further optimisation of antibacterial activity guided by the QSAR models was demonstrated with five newly designed lead compounds that were predicted to be highly potent. For future development of 1,4-benzoxazin-3-one derived antimicrobials, other drug requirements such as favourable absorption, distribution, metabolism, and excretion (ADME) characteristics need to be evaluated. In conclusion, 1,4-benzoxazin-3-one is a scaffold which offers flexibility in its substitution pattern and can be used to generate potent antimicrobial lead compounds.

5.4. References

[1] de Bruijn, W.J.C., Gruppen, H., and Vincken, J.-P. (2018) Structure and biosynthesis of benzoxazinoids: Plant defence metabolites with potential as antimicrobial scaffolds. *Phytochemistry*, 155: p. 233-243.

[2] Frey, M., Schullehner, K., Dick, R., Fiesselmann, A., and Gierl, A. (2009) Benzoxazinoid biosynthesis, a model for evolution of secondary metabolic pathways in plants. *Phytochemistry*, 70*(15-16)*: p. 1645-1651.

[3] Niemeyer, H.M. (2009) Hydroxamic acids derived from 2-hydroxy-2*H*-1,4-benzoxazin-3(4*H*)-one: Key defense chemicals of cereals. *Journal of Agricultural and Food Chemistry*, 57*(5)*: p. 1677-1696.

[4] Śmist, M., Kwiecień, H., and Krawczyk, M. (2016) Synthesis and antifungal activity of 2*H*-1,4-benzoxazin-3(4*H*)-one derivatives. *Journal of Environmental Science and Health, Part B: Pesticides, Food Contaminants, and Agricultural Wastes*, 51*(6)*: p. 393-401.

[5] Fang, L., Zuo, H., Li, Z.B., He, X.Y., Wang, L.Y., Tian, X., Zhao, B.X., Miao, J.Y., and Shin, D.S. (2011) Synthesis of benzo[*b*][1,4]oxazin-3(4*H*)-ones via smiles rearrangement for antimicrobial activity. *Medicinal Chemistry Research*, 20*(6)*: p. 670-677.

[6] Macías, F.A., Chinchilla, N., Arroyo, E., Molinillo, J.M.G., Marín, D., and Varela, R.M. (2010) Combined strategy for phytotoxicity enhancement of benzoxazinones. *Journal of Agricultural and Food Chemistry*, 58*(3)*: p. 2047-2053.

[7] Macías, F.A., Marín, D., Oliveros-Bastidas, A., and Molinillo, J.M.G. (2006) Optimization of benzoxazinones as natural herbicide models by lipophilicity enhancement. *Journal of Agricultural and Food Chemistry*, 54*(25)*: p. 9357-9365.

[8] Zhou, X.W., Ma, H.L., Zhang, X., Jing, S.Y., Miao, J.Y., and Zhao, B.X. (2014) Synthesis of 6-cinnamoyl-2*H*-benzo[*b*][1,4]oxazin-3(4*H*)-ones and their effects on A549 lung cancer cell growth. *European Journal of Medicinal Chemistry*, 79: p. 95-101.

[9] Yalcin, I., Tekiner, B.P., Oren, I.Y., Arpaci, O.T., Aki-Sener, E., and Altanlar, N. (2003) Synthesis and antimicrobial activity of some novel 2,6,7-trisubstituted-2*H*-3,4-dihydro-1,4-benzoxazin-3-one derivatives. *Indian Journal of Chemistry, Section B: Organic Chemistry Including Medicinal Chemistry*, 42*(4)*: p. 905-909.

[10] Alper-Hayta, S., Akı-Sener, E., Tekiner-Gulbas, B., Yıldız, I., Temiz-Arpacı, O., Yalcın, I., and Altanlar, N. (2006) Synthesis, antimicrobial activity and QSARs of new benzoxazine-3-ones. *European Journal of Medicinal Chemistry*, 41*(12)*: p. 1398-1404.

[11] Yilmaz, S., Yalcin, I., Okten, S., Onurdag, F.K., and Aki-Yalcin, E. (2017) Synthesis and investigation of binding interactions of 1,4-benzoxazine derivatives on topoisomerase IV in *Acinetobacter baumannii*. *SAR and QSAR in Environmental Research*, 28*(11)*: p. 941-956.

[12] Fringuelli, R., Pietrella, D., Schiaffella, F., Guarraci, A., Perito, S., Bistoni, F., and Vecchiarelli, A. (2002) Anti-*Candida albicans* properties of novel benzoxazine analogues. *Bioorganic & Medicinal Chemistry*, 10*(6)*: p. 1681-1686.

[13] Fringuelli, R., Giacchè, N., Milanese, L., Cenci, E., Macchiarulo, A., Vecchiarelli, A., Costantino, G., and Schiaffella, F. (2009) Bulky 1,4-benzoxazine derivatives with antifungal activity. *Bioorganic & Medicinal Chemistry*, 17*(11)*: p. 3838-3846.

[14] Borate, H.B., Maujan, S.R., Sawargave, S.P., Chandavarkar, M.A., Vaiude, S.R., Joshi, V.A., Wakharkar, R.D., Iyer, R., Kelkar, R.G., Chavan, S.P., and Kunte, S.S. (2010) Fluconazole analogues containing 2*H*-1,4-benzothiazin-3(4*H*)-one or 2*H*-1,4-benzoxazin-3(4*H*)-one moieties, a novel class of anti-*Candida* agents. *Bioorganic & Medicinal Chemistry Letters*, 20*(2)*: p. 722-725.

[15] Konda, S., Raparthi, S., Bhaskar, K., Munaganti, R.K., Guguloth, V., Nagarapu, L., and Akkewar, D.M. (2015) Synthesis and antimicrobial activity of novel

benzoxazine sulfonamide derivatives. *Bioorganic & Medicinal Chemistry Letters*, 25*(7)*: p. 1643-1646.
[16] Deshmukh, M.S. and Jain, N. (2017) Design, synthesis, and antibacterial evaluation of oxazolidinones with fused heterocyclic C-ring substructure. *ACS Medicinal Chemistry Letters*, 8*(11)*: p. 1153-1158.
[17] Collin, F., Karkare, S., and Maxwell, A. (2011) Exploiting bacterial DNA gyrase as a drug target: Current state and perspectives. *Applied Microbiology and Biotechnology*, 92*(3)*: p. 479-497.
[18] East, S.P. and Silver, L.L. (2013) Multitarget ligands in antibacterial research: Progress and opportunities. *Expert Opinion on Drug Discovery*, 8*(2)*: p. 143-156.
[19] Hiasa, H., DNA topoisomerases as targets for antibacterial agents, in *DNA topoisomerases: Methods and protocols*, M. Drolet, Editor. 2018, Springer New York: New York, NY. p. 47-62.
[20] Payne, D.J., Gwynn, M.N., Holmes, D.J., and Pompliano, D.L. (2007) Drugs for bad bugs: Confronting the challenges of antibacterial discovery. *Nature Reviews Drug Discovery*, 6*(1)*: p. 29-40.
[21] Wilcken, R., Zimmermann, M.O., Lange, A., Joerger, A.C., and Boeckler, F.M. (2013) Principles and applications of halogen bonding in medicinal chemistry and chemical biology. *Journal of Medicinal Chemistry*, 56*(4)*: p. 1363-1388.
[22] Silhavy, T.J., Kahne, D., and Walker, S. (2010) The bacterial cell envelope. *Cold Spring Harbor Perspectives in Biology*, 2*(5)*: p. a000414.
[23] Cabib, E., Roh, D.H., Schmidt, M., Crotti, L.B., and Varma, A. (2001) The yeast cell wall and septum as paradigms of cell growth and morphogenesis. *Journal of Biological Chemistry*, 276*(23)*: p. 19679-19682.
[24] Klis, F.M., Mol, P., Hellingwerf, K., and Brul, S. (2002) Dynamics of cell wall structure in *Saccharomyces cerevisiae*. *FEMS Microbiology Reviews*, 26*(3)*: p. 239-256.
[25] Bravo, H.R. and Lazo, W. (1993) Antimicrobial activity of cereal hydroxamic acids and related compounds. *Phytochemistry*, 33*(3)*: p. 569-571.
[26] Bravo, H.R. and Lazo, W. (1996) Antialgal and antifungal activity of natural hydroxamic acids and related compounds. *Journal of Agricultural and Food Chemistry*, 44*(6)*: p. 1569-1571.
[27] Kennard, R.W. and Stone, L.A. (1969) Computer aided design of experiments. *Technometrics*, 11*(1)*: p. 137-148.
[28] Araya-Cloutier, C., Vincken, J.-P., van de Schans, M.G.M., Hageman, J., Schaftenaar, G., den Besten, H.M.W., and Gruppen, H. (2018) QSAR-based molecular signatures of prenylated (iso)flavonoids underlying antimicrobial potency against and membrane-disruption in Gram positive and Gram negative bacteria. *Scientific Reports*, 8*(1)*: p. 9267.
[29] Hageman, J.A., Engel, B., de Vos, R.C.H., Mumm, R., Hall, R.D., Jwanro, H., Crouzillat, D., Spadone, J.C., and van Eeuwijk, F.A., Robust and confident predictor selection in metabolomics, in *Statistical analysis of proteomics, metabolomics, and lipidomics data using mass spectrometry*, S. Datta and B.J.A. Mertens, Editors. 2017, Springer International Publishing: Cham. p. 239-257.
[30] Roy, K., Kar, S., and Ambure, P. (2015) On a simple approach for determining applicability domain of QSAR models. *Chemometrics and Intelligent Laborary Systems*, 145: p. 22-29.
[31] Wouters, F.C., Gershenzon, J., and Vassão, D.G. (2016) Benzoxazinoids: Reactivity and modes of action of a versatile class of plant chemical defenses. *Journal of the Brazilian Chemical Society*, 27*(8)*: p. 1379-1397.
[32] Cruciani, C., Crivori, P., Carrupt, P.-A., and Testa, B. (2000) Molecular fields in quantitative structure-permeation relationships: The VolSurf approach. *Journal of Molecular Structure: THEOCHEM*, 503*(1-2)*: p. 17-30.
[33] Meyers, J., Carter, M., Mok, N.Y., and Brown, N. (2016) On the origins of three-dimensionality in drug-like molecules. *Future Medicinal Chemistry*, 8*(14)*.

[34] Sauer, W.H.B. and Schwarz, M.K. (2003) Molecular shape diversity of combinatorial libraries: A prerequisite for broad bioactivity. *Journal of Chemical Information and Computer Sciences*, 43*(3)*: p. 987-1003.
[35] Özden, S., Özturk, A.M., Göker, H., and Altanlar, N. (2000) Synthesis and antimicrobial activity of some new 4-hydroxy-2*H*-1,4-benzoxazin-3(4*H*)-ones. *Farmaco*, 55*(11-12)*: p. 715-718.
[36] Jiang, Y.Q., Mao, L.F., Zhu, L., Ren, B.Q., Li, W., and Xu, G.Q. (2014) Synthesis, characterization and antifungal evaluation of novel 2*H*-1,4-benzoxazin-3(4*H*)-one derivatives linked with a 1,2,3-triazole moiety. *Zeitschrift fur Naturforschung B: Journal of Chemical Sciences*, 69*(1)*: p. 103-108.
[37] Reddy Sastry, C.V., Srinivasa Rao, K., Rastogi, K., Jain, M.L., Reddi, G.S., Sudhakar, M., and Sudhakar Reddy, P. (1991) Synthesis and antimicrobial activity of 1-[(aryl)3-oxo-1, 4-benzoxazin-6-yl)methyl]-1*H*-imidazoles. *Indian Journal of Pharmaceutical Sciences*, 53*(2)*: p. 67-69.
[38] Davis, A.L., Hulme, K.L., Wilson, G.T., and McCord, T.J. (1978) In vitro antimicrobial activity of some cyclic hydroxamic acids and related lactams. *Antimicrobial Agents and Chemotherapy*, 13*(3)*: p. 542-544.
[39] Lipinski, C.A., Lombardo, F., Dominy, B.W., and Feeney, P.J. (2012) Experimental and computational approaches to estimate solubility and permeability in drug discovery and development settings. *Advanced Drug Delivery Reviews*, 64: p. 4-17.
[40] Denyer, S.P. and Maillard, J.-Y. (2002) Cellular impermeability and uptake of biocides and antibiotics in gram-negative bacteria. *Journal of Applied Microbiology*, 92: p. 35S-45S.
[41] Ziervogel, B.K. and Roux, B. (2013) The binding of antibiotics in OmpF porin. *Structure*, 21*(1)*: p. 76-87.
[42] Bozdogan, B. and Appelbaum, P.C. (2004) Oxazolidinones: Activity, mode of action, and mechanism of resistance. *International Journal of Antimicrobial Agents*, 23*(2)*: p. 113-119.
[43] Shinabarger, D.L., Marotti, K.R., Murray, R.W., Lin, A.H., Melchior, E.P., Swaney, S.M., Dunyak, D.S., Demyan, W.F., and Buysse, J.M. (1997) Mechanism of action of oxazolidinones: Effects of linezolid and eperezolid on translation reactions. *Antimicrobial Agents and Chemotherapy*, 41*(10)*: p. 2132-2136.
[44] Barbachyn, M.R. and Ford, C.W. (2003) Oxazolidinone structure-activity relationships leading to linezolid. *Angewandte Chemie-International Edition*, 42*(18)*: p. 2010-2023.

5.5. Supplementary information

The full supplementary information files (supplement A, B, C, and D) can be found on the publisher's website at https://doi.org/10.1016/j.bmc.2018.11.016. Selected parts of supplement A have been adapted and incorporated here. Table and figure numbers preceded by "A", "B", "C", or "D" (e.g. **Figure A.1**) refer to the corresponding full supplementary information file whereas **Figure S5.1**, for example, refers to the supplementary information below.

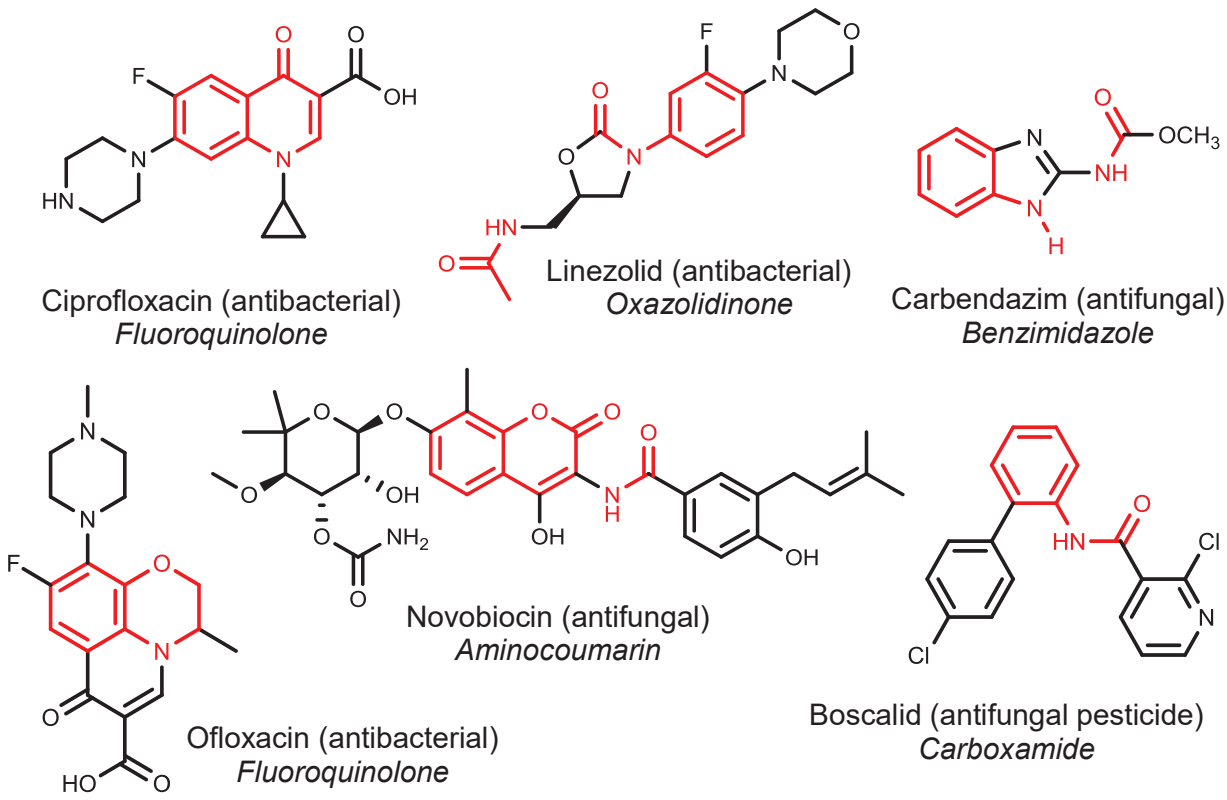

Figure S5.1. Known antimicrobials with (sub)structural features (in red) similar to benzoxazinoids, the class which they belong to is indicated in italics.

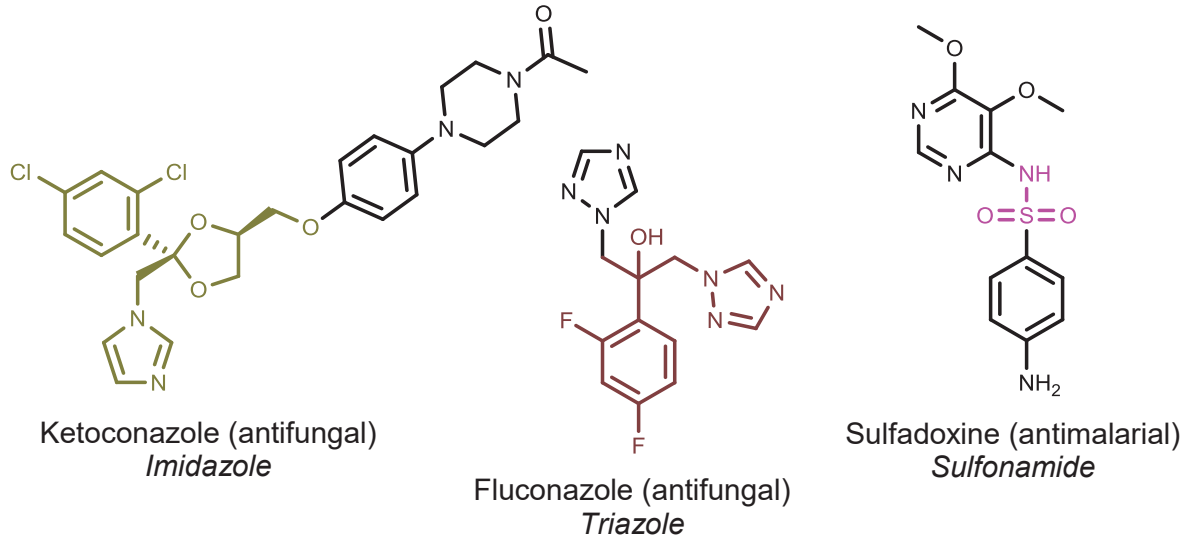

Figure S5.2. Two azole fungicides, which are used as antibiotics, and the antimalarial agent sulfadoxine. The coloured substructures have been used as substituents for 1,4-benzoxazin-3-ones in various studies.

Table S5.1. Structural features of compounds **1**-**17**, 1,4-benzoxazin-3-one derivatives.

Compound	R_1	R_4	R_6	Ref.
1	OH	H	OH	[25,26]
2	OH	CN	OH	[25]
3	OH	OCH_3	OH	[25,26]
4	OH	CH_3	OH	[25]
5	OH	NO_2	OH	[25]
6	OH	H	OCH_3	[25,26]
7	OH	H	H	[25,26]
8	OH	$COOCH_3$	H	[25]
9	OH	F	H	[25,26]
10	OH	OCH_3	H	[25,26]
11	OH	CH_3	H	[25,26]
12	H	H	H	[26]
13	OAc [a]	H	OH	[26]
14	H	$COOCH_3$	OH	[26]
15	H	OCH_3	OH	[26]
16	H	H	CH_2COOH	[9]
17	H	H	OH	[9,26]

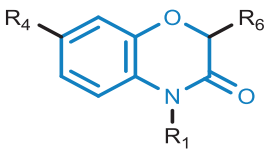

1,4-benzoxazin-3-one

[a] OAc, acetoxy.

Table S5.2. Structural features of compounds **18-42**, 2-(2-ethyloxy-2-oxo-ethyl)-1,4-benzoxazin-3-one derivatives.

Compound	R_1	R_2	R_3	R_4	Ref.
18	H	H	H	H	[9-11]
19	CH_3	H	CH_3	H	[10]
20	C_2H_5	H	H	H	[10]
21	C_2H_5	H	Cl	H	[10]
22	C_2H_5	H	Cl	NO_2	[10]
23	C_2H_5	H	H	NO_2	[10]
24	CH_3	H	H	H	[10]
25	CH_3	H	H	H	[10]
26	CH_3	H	Cl	H	[10]
27	CH_3	H	Cl	NO_2	[10]
28	CH_3	H	H	NO_2	[10]
29	H	H	$COOC_2H_5$	H	[10]
30	H	H	Cl	H	[9-11]
31	H	H	Cl	NO_2	[9-11]
32	H	H	CH_3	H	[9-11]
33	H	H	H	NH_2	[10]
34	H	H	H	NO_2	[9-11]
35	H	H	H	CH_3	[9,11]
36	H	CH_3	H	H	[11]
37	H	NO_2	H	H	[11]
38	H	H	$SO_2C_2H_5$	H	[11]
39	H	H	F	H	[11]
40	H	H	NO_2	H	[11]
41	H	H	Ph [a]	H	[11]
42	H	H	Cl	H	[11]

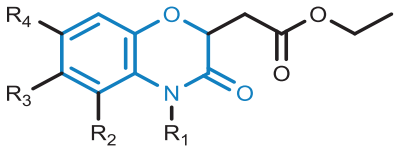

2-(2-ethyloxy-2-oxo-ethyl)-1,4-benzoxazin-3-one

[a] Ph, phenyl.

Table S5.3. Structural features of compounds **43-71**, 1,4-benzoxazin-3-one derivatives.

Compound	R_1	R_3	R_4	R_5	R_6	Ref.
43	CH_2Thf [a]	H	Br	H	H	[5]
44	CH_2Thf	H	Cl	H	H	[5]
45	CH_2Thf	H	F	H	H	[5]
46	C_2H_4Ph [a]	H	Cl	H	H	[5]
47	Bn [a]	Cl	H	H	H	[5]
48	Bn	H	Br	H	H	[5]
49	Bn	H	Cl	H	H	[5]
50	Bn	H	F	H	H	[5]
51	Cy [a]	Cl	H	H	H	[5]
52	Cy	H	Br	H	H	[5]
53	Cy	H	Cl	H	H	[5]
54	Cy	H	F	H	H	[5]
55	Cy	H	H	Cl	H	[5]
56	C_6H_{13}	H	Br	H	H	[5]
57	C_6H_{13}	H	Cl	H	H	[5]
58	C_6H_{13}	H	F	H	H	[5]
59	CH_3	X_1 [b]	H	H	H	[12]
60	CH_3	X_2	H	H	H	[12]
61	H	*cis*-X_3	H	H	C_4H_9	[13]
62	H	*cis*-X_3	H	H	H	[13]
63	H	*trans*-X_3	H	H	C_4H_9	[13]
64	H	*trans*-X_3	H	H	H	[13]
65	X_4	H	H	H	H	[14]
66	X_4	Br	H	H	H	[14]
67	X_4	Cl	H	H	H	[14]
68	X_4	NO_2	H	H	H	[14]
69	X_5	Ac	H	H	H	[14]
70	X_5	Cl	H	H	H	[14]
71	X_6	Cl	H	H	H	[14]

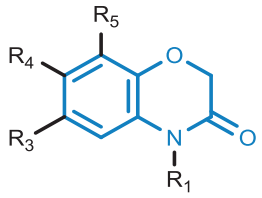

1,4-benzoxazin-3-one

[a] Thf, tetrahydrofuran-2-yl; Ph, phenyl; Bn, benzyl; Cy, cyclohexyl. [b] See **Figure S5.3** for substituents X_1 to X_6.

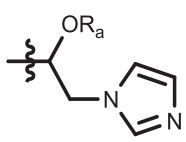

X_1: R_a = H
X_2: R_a = 4-chlorobenzyl

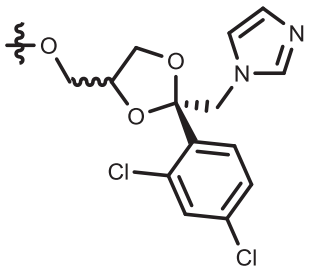

X_3

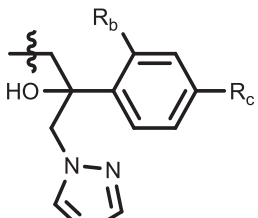

X_4: R_b = F, R_c = F
X_5: R_b = H, R_c = Br
X_6: R_b = H, R_c = F

Figure S5.3. Substituents X_1 to X_6 for compounds **59-71** (**Table S5.3**)

Table S5.4. Structural features of compounds **72-111**, 1,4-benzoxazin-3-one derivatives.

Compound	R_1	R_3	R_4	R_5	R_6	Ref.
72	H	X_7 [a]	H	H	di-CH_3 [b]	[16]
73	H	X_7	H	H	H	[16]
74	H	X_7	H	H	Scp [c]	[16]
75	H	X_8	H	H	H	[16]
76	H	X_9	H	H	H	[16]
77	H	X_{10}	H	H	H	[16]
78	H	X_{11}	H	H	H	[16]
79	H	X_{12}	H	H	H	[16]
80	H	X_{13}	H	H	H	[16]
81	H	X_{14}	H	H	H	[16]
82	H	X_{15}	H	H	H	[16]
83	H	X_{16}	H	H	H	[16]
84	H	H	X_7	H	H	[16]
85	H	H	H	X_7	H	[16]
86	H	X_{17}	CH_3	H	H	[15]
87	H	X_{18}	CH_3	H	H	[15]
88	H	X_{19}	CH_3	H	H	[15]
89	H	X_{20}	H	H	H	[15]
90	H	X_{20}	CH_3	H	H	[15]
91	H	X_{21}	H	H	H	[15]
92	H	X_{21}	CH_3	H	H	[15]
93	H	X_{22}	H	H	H	[15]
94	H	X_{22}	CH_3	H	H	[15]
95	H	X_{23}	H	H	H	[15]
96	H	X_{24}	H	H	H	[15]
97	H	X_{24}	CH_3	H	H	[15]
98	X_{25}	X_{19}	CH_3	H	H	[15]
99	X_{25}	X_{18}	CH_3	H	H	[15]
100	X_{26}	X_{18}	CH_3	H	H	[15]
101	X_{26}	X_{19}	CH_3	H	H	[15]
102	X_{27}	X_{18}	CH_3	H	H	[15]
103	X_{27}	X_{19}	CH_3	H	H	[15]
104	X_{28}	X_{19}	CH_3	H	H	[15]
105	X_{28}	X_{19}	CH_3	H	H	[15]
106	X_{29}	X_{18}	CH_3	H	H	[15]
107	X_{29}	X_{19}	CH_3	H	H	[15]
108	X_{30}	X_{18}	CH_3	H	H	[15]
109	X_{30}	X_{19}	CH_3	H	H	[15]
110	X_{31}	X_{18}	CH_3	H	H	[15]
111	X_{31}	X_{19}	CH_3	H	H	[15]

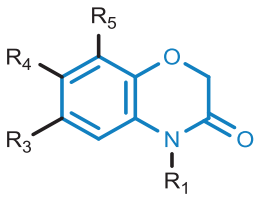

1,4-benzoxazin-3-one

[a] See **Figure S5.4** for substituents X_7 to X_{31}. [b] See **Figure S5.5A**; di-CH_3, dimethyl. [c] See **Figure S5.5B**; Scp, spirocyclopropan.

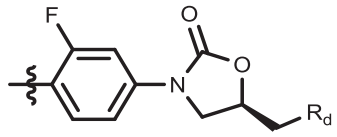

X$_7$: R$_d$ = OH
X$_8$: R$_d$ = NHAc
X$_9$: R$_d$ = NHSO$_2$CH$_3$
X$_{10}$: R$_d$ = NHCSCH$_3$

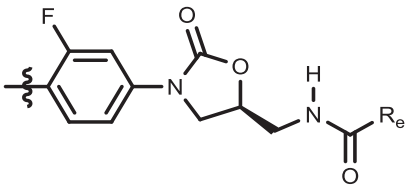

X$_{11}$: R$_e$ = C$_2$H$_5$
X$_{12}$: R$_e$ = CyBu
X$_{13}$: R$_e$ = CyPro
X$_{14}$: R$_e$ = CHF$_2$
X$_{15}$: R$_e$ = CH$_2$CH$_2$OH
X$_{16}$: R$_e$ = OCH$_3$

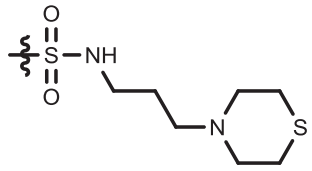

X$_{17}$

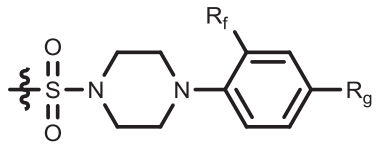

X$_{18}$: R$_f$ = OCH$_3$, R$_g$ = H
X$_{19}$: R$_f$ = H, R$_g$ = CF$_3$

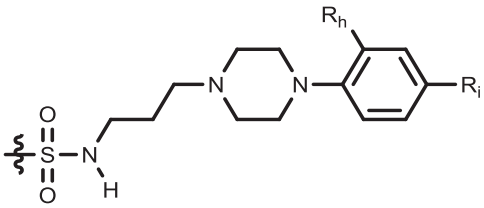

X$_{20}$: R$_h$ = OCH$_3$, R$_i$ = H
X$_{21}$: R$_h$ = H, R$_i$ = CF$_3$
X$_{22}$: R$_h$ = F, R$_i$ = H
X$_{23}$: R$_h$ = H, R$_i$ = F
X$_{24}$: R$_h$ = H, R$_i$ = H

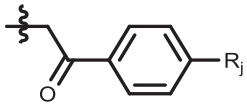

X$_{25}$: R$_j$ = NO$_2$
X$_{26}$: R$_j$ = H
X$_{27}$: R$_j$ = Cl
X$_{28}$: R$_j$ = OCH$_3$
X$_{29}$: R$_j$ = CH$_3$
X$_{30}$: R$_j$ = Ph

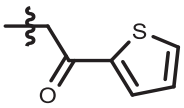

X$_{31}$

Figure S5.4. Substituents X$_7$ to X$_{31}$ for compounds **72**-**111** (**Table S5.4**).

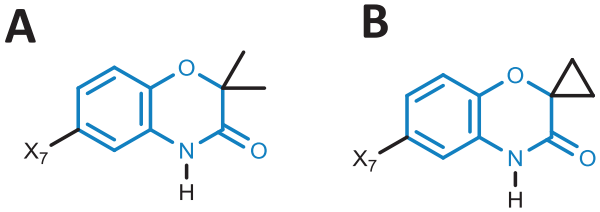

Figure S5.5. Structures of compound **72** (A), and compound **74** (B).

Table S5.5. Overview of average antimicrobial activity values (MIC in μM) of 1,4-benzoxazin-3-ones based on literature used to calculate pMIC for statistical analyses.

	Average MIC (μM) [a]					Average MIC (μM) [a]			
Comp.	**Fungi**	**Gram pos.**	**Gram neg.**	**Ref.**	**Comp.**	**Fungi**	**Gram pos.**	**Gram neg.**	**Ref.**
1	3676.6	2760.2	6900.5	[25,26	**57**	1912.2	119.5	99.6	[5]
2	7276.0	7276.0	n.a.	[25]	**58**	509.3	127.3	212.2	[5]
3	2367.7	1576.9	3153.8	[25,26	**59**	32.7	n.a.	n.a.	[12]
4	3412.3	2561.8	3412.3	[25]	**60**	647.9	n.a.	n.a.	[12]
5	6632.9	734.0	3683.5	[25]	**61**	21.7 [c]	n.a.	n.a.	[13]
6	3371.4	2561.8	n.a.	[25,26	**62**	16.2 [c]	n.a.	n.a.	[13]
7	2067.8	2016.4	7569.0	[25,26	**63**	40.8 [c]	n.a.	n.a.	[13]
8	n.a.	4480.6	n.a.	[25]	**64**	21.5 [c]	n.a.	n.a.	[13]
9	2730.2	1818.3	4548.5	[25,26	**65**	1.3	n.a.	n.a.	[14]
10	809.5	3412.3	6404.5	[25,26	**66**	34.4	n.a.	n.a.	[14]
11	1906.0	1858.5	2790.6	[25,26	**67**	19.0	n.a.	n.a.	[14]
12	6704.7	n.a.	n.a.	[26]	**68**	74.2	n.a.	n.a.	[14]
13	2984.1	n.a.	n.a.	[26]	**69**	67.9	n.a.	n.a.	[14]
14	4480.6	n.a.	n.a.	[26]	**70**	8.6	n.a.	n.a.	[14]
15	5123.6	n.a.	n.a.	[26]	**71**	39.7	n.a.	n.a.	[14]
16	79.7	432.4	487.3	[9-11]	**72**	n.a.	2.6	0.3	[16]
17	n.a. [b]	158.3	95.0	[10]	**73**	n.a.	1.4	1.4	[16]
18	95.0	95.0	379.8	[10]	**74**	n.a.	1.3	1.3	[16]
19	84.0	125.9	167.9	[10]	**75**	n.a.	1.3	0.6	[16]
20	72.9	182.4	291.8	[10]	**76**	n.a.	2.3	1.1	[16]
21	108.1	162.2	162.2	[10]	**77**	n.a.	0.3	0.3	[16]
22	50.1	167.2	150.4	[10]	**78**	n.a.	0.6	0.6	[16]
23	38.9	129.7	116.7	[10]	**79**	n.a.	1.1	2.3	[16]
24	117.5	176.2	132.2	[10]	**80**	n.a.	2.4	2.4	[16]
25	50.7	152.1	76.1	[10]	**81**	n.a.	1.1	1.1	[16]
26	42.5	169.9	127.4	[10]	**82**	n.a.	2.4	1.2	[16]
27	47.5	135.6	122.0	[10]	**83**	n.a.	0.3	0.3	[16]
28	57.9	390.4	486.3	[9-11]	**84**	n.a.	1.4	0.7	[16]
29	39.7	236.7	231.1	[9-11]	**85**	n.a.	11.2	2.8	[16]
30	62.7	422.4	497.5	[9-11]	**86**	648.5	324.2	1080.8	[15]
31	83.2	133.2	149.8	[10]	**87**	1197.6	598.8	1197.6	[15]
32	66.9	253.1	272.2	[9-11]	**88**	1097.8	548.9	914.8	[15]
33	100.3	613.8	696.4	[9,11]	**89**	135.7	67.9	361.9	[15]
34	120.7	181.0	181.0	[9]	**90**	526.8	526.8	1053.6	[15]
35	n.a.	302.8	151.4	[9]	**91**	250.7	125.4	501.5	[15]
36	n.a.	1027.0	1027.0	[11]	**92**	243.9	121.9	365.8	[15]
37	n.a.	685.1	456.8	[11]	**93**	278.7	69.7	185.8	[15]
38	n.a.	586.5	391.0	[11]	**94**	540.5	540.5	540.5	[15]
39	n.a.	1010.9	1010.9	[11]	**95**	557.4	557.4	510.9	[15]
40	n.a.	685.1	456.8	[11]	**96**	1161.4	580.7	1161.4	[15]
41	n.a.	308.3	411.1	[11]	**97**	562.4	562.4	562.4	[15]
42	n.a.	949.3	949.3	[11]	**98**	50.5	50.5	117.9	[15]
43	410.0	102.5	136.7	[5]	**99**	430.6	107.6	358.8	[15]
44	717.2	119.5	159.4	[5]	**100**	116.7	116.7	194.5	[15]
45	1018.9	127.4	233.5	[5]	**101**	435.8	435.8	435.8	[15]
46	444.8	222.4	74.1	[5]	**102**	438.5	438.5	365.5	[15]
47	175.4	175.4	350.7	[5]	**103**	822.3	411.2	822.3	[15]
48	402.3	100.6	83.8	[5]	**104**	55.2	55.2	92.1	[15]
49	467.6	175.4	175.4	[5]	**105**	414.2	103.5	345.1	[15]
50	746.3	186.6	82.9	[5]	**106**	113.7	227.4	151.6	[15]
51	120.4	301.0	260.9	[5]	**107**	425.4	212.7	124.1	[15]
52	825.3	103.2	68.8	[5]	**108**	817.4	102.2	476.8	[15]
53	722.5	240.8	160.6	[5]	**109**	192.4	192.4	256.5	[15]
54	641.8	96.3	64.2	[5]	**110**	461.6	923.1	461.6	[15]
55	722.5	180.6	100.3	[5]	**111**	53.9	53.9	161.7	[15]
56	410.0	102.5	85.4	[5]					

[a] Averages are calculated per compound per MO. n.a., not applicable. [b] The antifungal MIC of **17** was not included in the dataset due to large variation in reported MIC values.[9,26] [c] Fringuelli *et al* 2009 report antifungal MIC after 24 and 48 h, the values included are those after 24 h.

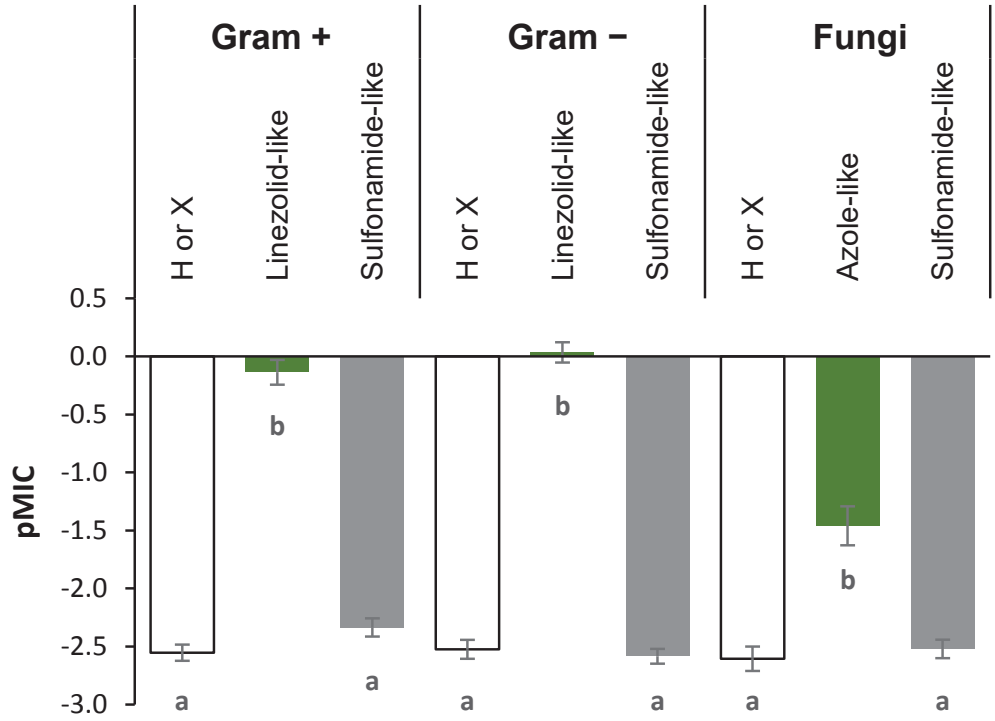

Figure S5.6. Effect of antibiotic-inspired substituents on the antimicrobial activity (pMIC) of 1,4-benzoxazin-3-ones. Higher pMIC corresponds to higher activity. Error bars indicate standard error, within the same MO type different letters indicate significant difference ($p < 0.001$). Green colour indicates increased activity compared to H or X. X, any non-antibiotic-like substituent.

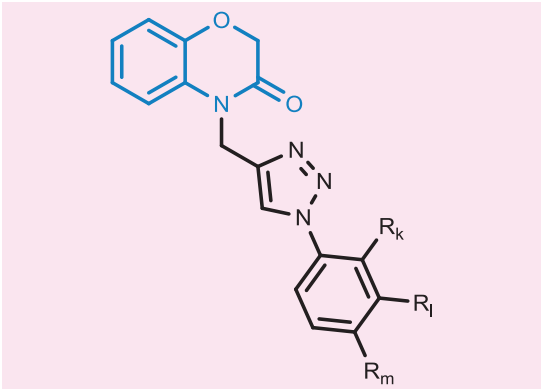

U1: R_k = CH_3, R_l = H, R_m = H
U5: R_k = H, R_l = H, R_m = CH_3
U7: R_k = H, R_l = NO_2, R_m = H

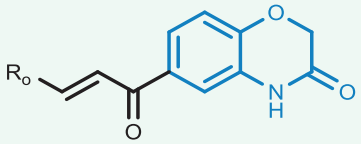

U54: R_o = benzene
U57: R_o = (4-benzyloxy)benzene
U58: R_o = 4-chlorobenzene
U59: R_o = napthalene

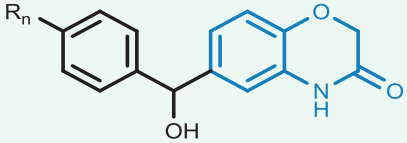

U22: R_n = H
U23: R_n = F
U25: R_n = Cl

Figure S5.7. Compounds from literature with the lowest predicted MIC values (**Table A.7**, Supplement A). Pink shading indicates compounds with activity against gram negatives, whereas mint-green shading indicates activity against gram positives.

CHAPTER 6

Mass spectrometric characterisation of avenanthramides and enhancing their production by germination of oat

Avenanthramides are amides with a phenylalkenoic acid (PA) and an anthranilic acid (AA) subunit, which are secondary metabolites of oat. Oat seeds were germinated, extracted, and the avenanthramides analysed by a combination of UHPLC with ion trap and high resolution ESI-MS. Typical fragmentation pathways with corresponding diagnostic fragments belonging to the PA and AA subunits were identified and summarised in a decision guideline. Based on these findings 28 unique avenanthramides were annotated in the oat seed(ling) extracts, including the new avenanthramide 6f (with a 4/5-methoxy AA subunit). Avenanthramide content increased by 25 times from seed to seedling. Avenanthramides 2p, 2c, and 2f, which are commonly described as the major avenanthramides, represented less than 20% of the total content in the seedlings. Future quantitative analyses should, therefore, include a wider range of avenanthramides to avoid underestimation of the total avenanthramide content.

Based on: Wouter J. C. de Bruijn, Sarah van Dinteren, Harry Gruppen, and Jean-Paul Vincken (2019) Mass spectrometric characterisation of avenanthramides and enhancing their production by germination of oat (*Avena sativa*), *Food Chemistry*, 277: p. 682-690.

6.1. Introduction

Avenanthramides are secondary metabolites most prominently found in oat (*Avena sativa*). These metabolites consist of a phenylalkenoic acid (PA) subunit linked to an anthranilic acid (AA) subunit via an amide bond. Even though these molecules belong to the class of hydroxycinnamic acid amides, the PA subunit can either be hydroxycinnamic or avenalumic acid derived (**Figure 6.1**).[1] Avenalumic acids are long-chained PAs produced by oat, which in analogy with hydroxycinnamic acids can possess additional hydroxy and methoxy substituents.[2] Avenanthramides were first characterised in oat and described to exhibit inhibition of fungal germination and to play a role in disease resistance of oat.[3-5] Collins and co-workers reported a wider variety of avenanthramides and started naming these compounds on an alphabetical basis.[6,7] Dimberg later introduced a more systemic nomenclature, resulting in a system where a number indicates the AA subunit and a letter the PA subunit (**Figure 6.1**).[8,9]

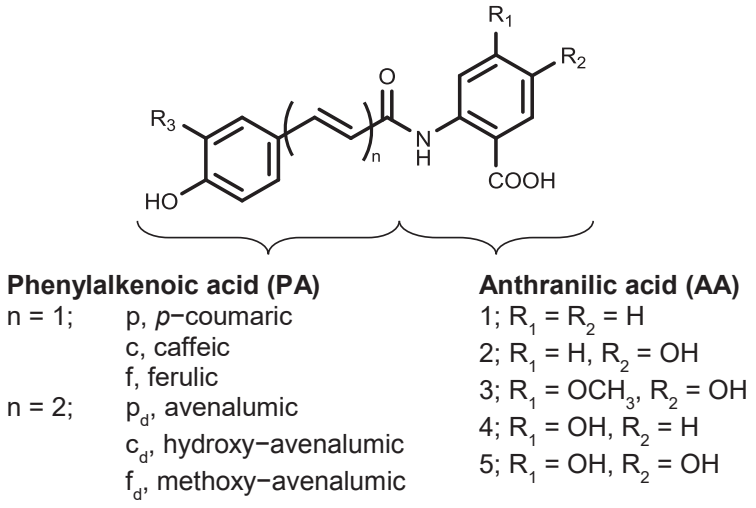

Figure 6.1. General structure of avenanthramides with their subunit based nomenclature as introduced by Dimberg.[8,9]

An additional subscripted d (e.g. $2p_d$) is used to indicate long-chained PA subunits. An overview of natural avenanthramides with their nomenclature according to both Collins and Dimberg is shown in **Table S6.1**, supplementary information. We will adhere to the Dimberg nomenclature (**Figure 6.1**) in this work. Due to their absorbance of ultra-violet (UV) light, with λ_{max} values generally ranging from 315 to 365 nm and molar extinction coefficients around 23,000-28,000 L mol^{-1} cm^{-1} (M^{-1} cm^{-1}), avenanthramides can be analysed by UV-Vis spectroscopy.[1,6] Their detection by mass spectrometry (MS) is possible in both positive and negative ionisation modes. These compounds can be separated and annotated by a combination of liquid chromatography with UV-Vis and ESI-MS detection.[1,10,11] Avenanthramides can be found in oat grains as well as commercial and processed oat products.[12-14] They have been shown to be bioavailable in humans and to

possess, amongst others, anti-oxidant and anti-inflammatory activity.[15,16] Their role in plant disease resistance[17,18] suggests that they also possess antifungal and possibly antibacterial activity. Considering their antimicrobial and anti-oxidant activity, avenanthramides or avenanthramide-rich oat extracts could potentially be applied as food preservatives in clean label products. In literature, the main focus has been on the three of the major avenanthramides, namely 2p, 2c, and 2f, which are in many cases the only compounds analysed.[17,19,20] The overview in **Table S6.1**, however, illustrates that many more avenanthramides can be formed.[1] As germination is known to increase the amount and variety of secondary metabolites in plant seedlings,[21,22] we expected oat seedlings to contain a wide variety of avenanthramides. In this work, we systematically approached the mass spectrometric analysis of avenanthramides to establish guidelines that facilitate annotation of unknown avenanthramides for which no standards are available. Our aim was to apply these findings to characterize the full spectrum of avenanthramides in oat seeds and seedlings. Additionally, germination was investigated as a method to enhance the content of potential anti-oxidative and antimicrobial avenanthramides in oat seeds.

6.2. Experimental

6.2.1. Seeds and chemicals

Oat seeds, *Avena sativa*, were purchased from Vreeken's Zaden (Dordrecht, The Netherlands). Sodium hypochlorite 14% Cl_2 (*w/v*) aqueous solution and technical grade *n*-hexane 98% (*v/v*) were obtained from VWR International (Radnor, PA, USA). Avenanthramide A (i.e. 2p) (≥98.0%), avenanthramide B (i.e. 2f) (≥98.0%), and avenanthramide C (i.e. 2c) (≥98.0%) were purchased from Sigma Aldrich (St. Louis, MO). ULC-MS grade formic acid (FA) 99% (*v/v*), methanol (MeOH), and water containing 0.1% (*v/v*) FA were purchased from Biosolve (Valkenswaard, The Netherlands). Water (MQ) for other purposes than UHPLC was prepared using a Milli-Q water purification system (Merck Millipore, Billerica, MA, USA). Ethanol absolute ≥99.9% (*v/v*) was purchased from Merck Millipore.

6.2.2. Methods

6.2.2.1. Oat germination

Oat seeds were first surface sterilized by washing with 70 % (*v/v*) ethanol (3.3 L kg^{-1}), rinsing with MQ (3.3 L kg^{-1}), immersion in a 1.4 % (*w/v*) hypochlorite solution (5 L kg^{-1}) for 20 min, and finally rinsing four times with MQ (3.3 L kg^{-1}). Oat seeds were germinated in the dark in a pilot-scale two-tank steep germinator (Custom Laboratory Products, Keith, UK). The cleaning procedure, trays, and setup of the germinator were the same as described previously.[23] Per experiment, approximately 150 g surface-sterilized oat seeds were placed in one of the five equally-sized compartments of the germinator trays that were lined with

disinfected cellulose filter paper (Whatman 595 ½, folded, 320 mm). The program set in the germinator was as follows: soaking for 20 h at 20 ˚C (aeration 1 min every 10 min), followed by germination for 72 h at 25 ˚C (RH ≥ 99%). After the first 72 h of germination, oat seedlings were incubated for another 96 h at 30 ˚C (RH 70-80%). The described conditions proved to be effective to ensure germination of the seeds. At the end of the experiment, the seedlings were frozen and stored at -20 ˚C until further processing.

6.2.2.2. Sample preparation and extraction

The frozen seed(ling)s were lyophilised prior to milling. Dry samples were placed in 50 mL grinding jars (filled approximately ⅓ with sample) together with six stainless steel beads (diameter 12 mm) and milled for 180 s at a frequency of 30 s^{-1} using an MM400 beadmill (Retsch, Haan, Germany). The resulting powdered sample was mixed with fat-free quartz sand (0.3-0.9 mm, Büchi) and extracted using an E916 speed extractor (Büchi, Flawil, Switzerland). The operating conditions were 100 bar and 40 ˚C. The samples (approximately 400 mg) were first defatted by two consecutive extraction cycles (10 min each) with *n*-hexane, subsequently phytochemicals were extracted by three consecutive extraction cycles (10 min each) with MeOH. Extracts were concentrated under reduced pressure and evaporated to dryness under nitrogen flow. Dried extract was resolubilized in MeOH to a concentration of 20 mg mL^{-1} aided by 20 min sonication. Prior to UHPLC analysis, samples were diluted with MQ to a final concentration of 10 mg mL^{-1} and centrifuged (16,000 *g*, 5 min, RT).

6.2.2.3. Analytical reversed phase liquid chromatography (RP-UHPLC)

For analytical purposes, samples were separated on a Thermo Accela UHPLC system (Thermo Scientific, San Jose, CA, USA) equipped with a pump, degasser, autosampler, and photodiode array (PDA) detector. The flow rate was 300 µL min^{-1} at a column temperature of 45 °C. Eluents used were water (A) and MeOH (B), both with 0.1% (*v/v*) formic acid. The column used was a Acquity UPLC BEH C18 (150 mm x 2.1 mm i.d., 1.7 µm) with a VanGuard (5 mm x 2.1 mm i.d., 1.7 µm) guard column of the same material (Waters, Milford, MA). The elution program was started by running isocratically at 35% B for 1.45 min, followed by 1.45−30.52 min linear gradient to 55% B, 30.52−31.97 min linear gradient to 100% B, 31.97−39.24 min isocratically at 100% B. The eluent was adjusted to its starting composition in 1.45 min, followed by equilibration for 7.31 min. Detection wavelengths for UV−Vis were set to the range of 200-600 nm and data were recorded at 20 Hz. Due to the unavailability of standards, all quantifications were based on a calibration curve of avenanthramide 2c (1.2-158.6 µM, R^2 = 0.9996). Expressing avenanthramide contents as molar equivalents of 2c should give a reasonable approximation, as molar extinction coefficients of various avenanthramides reported in literature are similar (e.g. 2p, 28,184 M^{-1} cm^{-1} at 339 nm; 1p, 29,512 M^{-1} cm^{-1} at 329 nm).[6] Means and standard deviations are

calculated based on two independent germination experiments which were each extracted in duplicate.

6.2.2.4. Electrospray ionisation ion trap mass spectrometry (ESI-IT-MS^n)

Mass spectrometric data were acquired using an LTQ Velos Pro linear ion trap mass spectrometer (Thermo Scientific) equipped with a heated ESI probe coupled in-line to the Accela RP-UHPLC system as previously described.[23] Nitrogen was used both as sheath gas (35 arbitrary units) and auxiliary gas (24 arbitrary units). Data were collected in both positive and negative ionisation mode over the *m/z* range 200-1,500. Data-dependent MS^n analyses were performed by collision-induced dissociation (CID) with a normalized collision energy of 35%. MS^n fragmentation was performed on the most intense product ion in the MS^{n-1} spectrum. Dynamic exclusion, with a repeat count of 2, repeat duration of 5.0 s and an exclusion duration of 5.0 s, was used to obtain MS^2 spectra of multiple different ions present in full MS at the same time. Most settings were optimized by automatic tuning using LTQ Tune Plus 2.7 (Thermo Scientific) upon direct injection of a mixture of avenanthramide standards 2p, 2c, and 2f. The ion transfer tube temperature was 325 °C, the source heater temperature 150 °C, and the source voltage 4.0 kV. Data were processed using Xcalibur 4.0 (Thermo Scientific).

6.2.2.5. Electrospray ionisation hybrid quadrupole-orbitrap mass spectrometry (ESI-FTMS)

Accurate mass data were acquired using a Thermo Q Exactive Focus hybrid quadrupole-Orbitrap Fourier Transform mass spectrometer (FTMS) (Thermo Scientific) equipped with a heated ESI probe. Prior to analysis the mass spectrometer was calibrated in positive and negative ionisation mode using Tune 2.9 software (Thermo Scientific) by injection of Pierce negative and positive ion calibration solutions (Thermo Scientific).

To study the ionisation and fragmentation of the standards 2p, 2c, and 2f, these compounds were analysed by direct infusion. The compounds were solubilised in 50% (*v/v*) aqueous MeOH with 0.1% (*v/v*) FA to a concentration of 10 µg mL^{-1} and infused at 8 µL min^{-1} using a syringe pump. Nitrogen was used both as sheath gas (50 arbitrary units) and auxiliary gas (13 arbitrary units). The source conditions used in negative ionisation mode were capillary temperature of 350 °C, probe heater temperature 150 °C, and a source voltage of 2.5 kV. The source conditions used in positive ionisation mode were capillary temperature of 320 °C, probe heater temperature 30 °C, and a source voltage of 4.0 kV. The S-Lens RF level was 50 and 25, respectively in negative and positive ionisation modes. Full MS and higher energy C-trap dissociation (HCD) fragmentation data were recorded at 70,000 resolution for 0.5 min (112 scans). Normalized collision energy (NCE) was varied to obtain spectra which provided maximal structural information.

For determination of accurate mass of avenanthramides in the germinated oat samples (injection volume 1 µL), they were first separated on a Thermo Vanquish UHPLC system (Thermo Scientific) in the same configuration as described previously.[23] The mobile phases, flow rate, column, and elution program were the same as used on the Accela UHPLC system. The column compartment heater was operated in still air mode at 45 °C and the post column cooler was set to 40 °C. Half of the flow from the RP-UHPLC system (150 µL min^{-1}) was directed toward the MS, which was coupled in-line to the Vanquish RP-UHPLC system. Full MS data were collected in positive and negative ionisation mode over the *m/z* range 200-1,000 at 70,000 resolution. The source conditions used were the same as for direct infusion in positive ionisation mode. Data were processed using Xcalibur 4.0 (Thermo Scientific).

6.3. Results & Discussion

6.3.1. Ionisation and fragmentation of avenanthramides

6.3.1.1. Systematic study of avenanthramides 2p, 2c, and 2f

The ionisation and fragmentation of avenanthramides (Av) was first studied with the authentic standards of 2p, 2c, and 2f. Typical MS and CID MS^2 spectra obtained are shown in **Figure 6.2**, with avenanthramide 2f as an example. Most of the avenanthramides were detected in full MS with several adducts besides their $[M_{Av}-H]^-$ and $[M_{Av}+H]^+$. In negative ionisation mode (NI) a peak was usually detected at 68 u higher than the $[M_{Av}-H]^-$, corresponding to a sodiated formic acid (FA) adduct $[M_{Av}+FA+Na-2H]^-$. In positive ionisation mode (PI) a peak was usually detected at 22 u higher than the $[M_{Av}+H]^+$, corresponding to a sodiated adduct $[M_{Av}+Na]^+$. Additionally, in-source dimerization was observed with $[2M_{Av}-H]^-$ and $[2M_{Av}+Na-2H]^-$ in NI and $[2M_{Av}+H]^+$ and $[2M_{Av}+Na]^+$ in PI. The identity of these adducts was confirmed by high resolution mass spectrometry (**Figure S6.2**, supplementary information). In both modes, the main fragment observed in CID MS^2 was typically already visible in full MS as an in-source fragment (**Figure 6.2**). Fragmentation in PI mode allowed the detection of the phenylalkenoic acid (PA) subunit as an acylium ion fragment $[M_{PA}+H-H_2O]^+$, which was always the main and usually the only fragment (**Figure 6.2**). Xie and co-workers reported a wider variety of fragments in positive ionisation mode, however, they used a triple-quadrupole MS with different settings.[11] The molecular formula of the PI MS^2 fragments was confirmed by high resolution MS with HCD fragmentation (**Figure S3**, supplementary information).

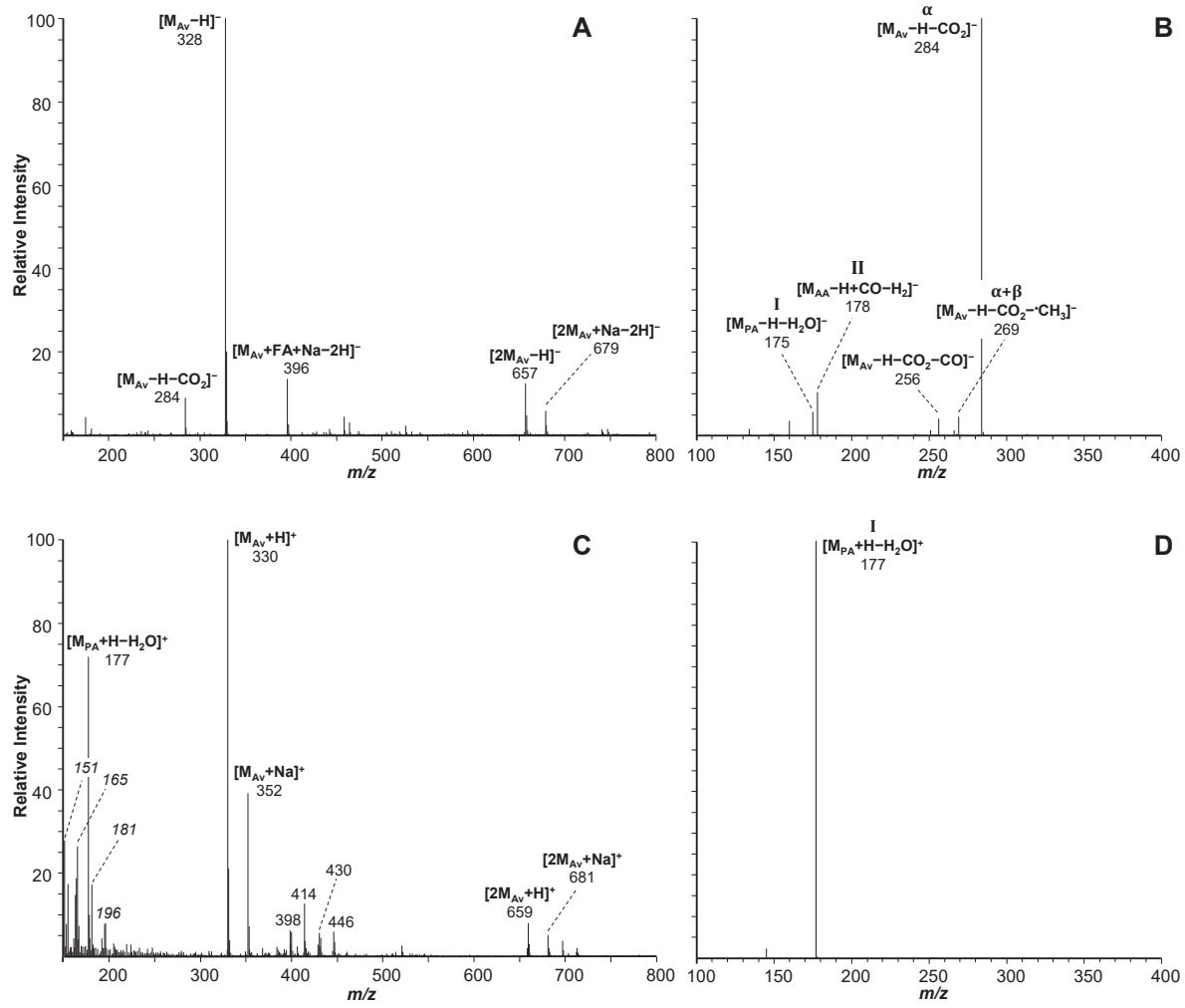

Figure 6.2. Typical ESI-IT-MS spectra of avenanthramides in negative mode full MS (A) and MS^2 (B), and positive mode full MS (C) and MS^2 (D), demonstrated with a standard of avenanthramide 2f. Peak labels show the corresponding fragmentation pathway, (fragment) adduct and *m/z*. Peaks labelled with *m/z* in italic are known background peaks from the LC-MS analysis. FA, formic acid; Av, avenanthramide; PA, phenylalkenoic acid; AA, anthranilic acid.

Fragmentation in NI mode provided more structural information by detection of the anthranilic acid (AA) subunit as an isocyanatobenzoate fragment $[M_{AA}-H+CO-H_2]^-$ and the PA as an oxo-indenolate fragment $[M_{PA}-H-H_2O]^-$, the latter usually at low intensity.[10] The loss of the carboxylic acid moiety as CO_2 (44 u) $[M_{Av}-H-CO_2]^-$ was also observed, often at high intensity (**Figure 6.2**). These observations were in agreement with previously reported data.[10] To confirm the molecular formulae of these fragments and to gain more insight in several other fragments, high resolution HCD fragmentation spectra were recorded (**Figure 6.3**). The relative intensity of the fragments in these spectra differed from what was observed in CID and a wider variety of fragments was obtained.

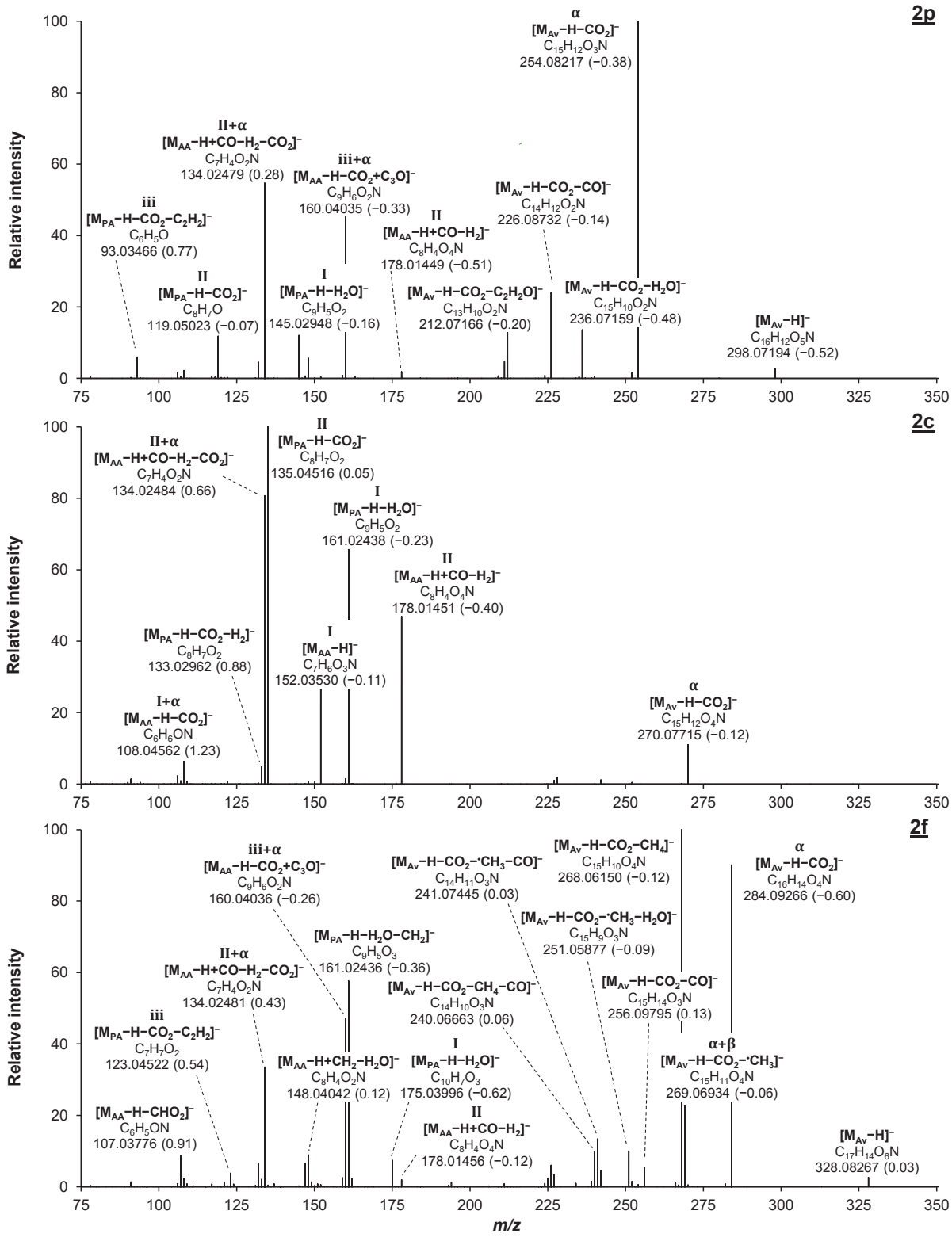

Figure 6.3. High resolution HCD fragmentation spectra (NCE = 35) of avenanthramide standards 2p, 2c, and 2f in negative ionisation mode obtained by direct infusion in FTMS. Peak labels show the corresponding fragmentation pathway (**Figure 6.4A**), the fragment adduct with its molecular formula, and its measured *m/z* with the error (in ppm) in parentheses. Av, avenanthramide; AA, anthranilic acid; PA, phenylalkenoic acid; NCE, normalized collision energy.

Based on these annotations and previously reported data,[10] several fragmentation pathways were proposed which are summarised in **Figure 6.4A**.

6.3.1.2. Long-chained avenanthramides

To gain additional insight in the fragmentation of avenanthramides with long-chained (avenalumic acid-derived) PA subunits, the oat seedling extract was screened for the presence of the long-chained equivalent of 2p, namely $2p_d$ ($C_{18}H_{15}NO_5$, $[M_{Av}-H]^-$ *m/z* calc. 324.08775). Annotation of the HCD fragmentation spectrum confirmed that similar fragmentations were observed as for short-chained avenanthramides, with the addition of several fragments related to the longer chain (**Figure S6.3** and **Figure S6.4**, supplementary information). Typically, fragmentation of the unsaturated bond closest to the amide linkage was not observed whereas a minor fragment corresponding to fragmentation of the further unsaturated bond was sometimes found (**Figure S6.4**).

6.3.1.3. Avenanthramide glycosides

In the seed(ling) extracts, glycosides of several avenanthramides were detected which, due to their higher polarity, always eluted before the aglycone (**Figure 6.5**). The glycosides were characterized in NI by a general fragment corresponding to a neutral loss of anhydrohexose (162 u) (**Figure 6.4A**), resulting in a fragment corresponding to the *m/z* of the aglycone $[M_{Av}-H]^-$. Other fragments corresponded to the isocyanatobenzoate fragment $[M_{AA}-H+CO-H_2]^-$ and the loss of CO_2, the latter of which was often observed in combination with the loss of the anhydrohexose $[M_{Av}-H-CO_2]^-$.

In PI, the acylium ion fragment resulting from the PA $[M_{PA}+H-H_2O]^+$ was almost always the main fragment. Combined with NI MS^3 spectra, this allowed the assignment of the PA and AA subunits of the aglycone (**Table S5**, supplementary information). In this work, only avenanthramide hexosides were detected, nevertheless, the possible occurrence of other types of glycosides cannot be excluded. Based on the work of Wu and co-workers majority of glycosides are *O*-glucosides attached on the aromatic ring of the PA subunit.[24] Comparison of spectral data with the glycosides for which Wu and co-workers confirmed the structure by NMR, leads us to believe that peak G2 is 2c-3′-*O*-glc (i.e. the glucoside is attached on the *meta* position of the caffeic ring).[24]

6.3.2. General fragmentation pathways of avenanthramides

In **Figure 4A**, an overview is given of the fragmentation pathways observed upon CID or HCD fragmentation of avenanthramides. We have assigned Roman numerals to the cleavages of the enamide chain between the two aromatic rings, with numbering going up from the amide linkage towards the aromatic ring of the PA subunit.

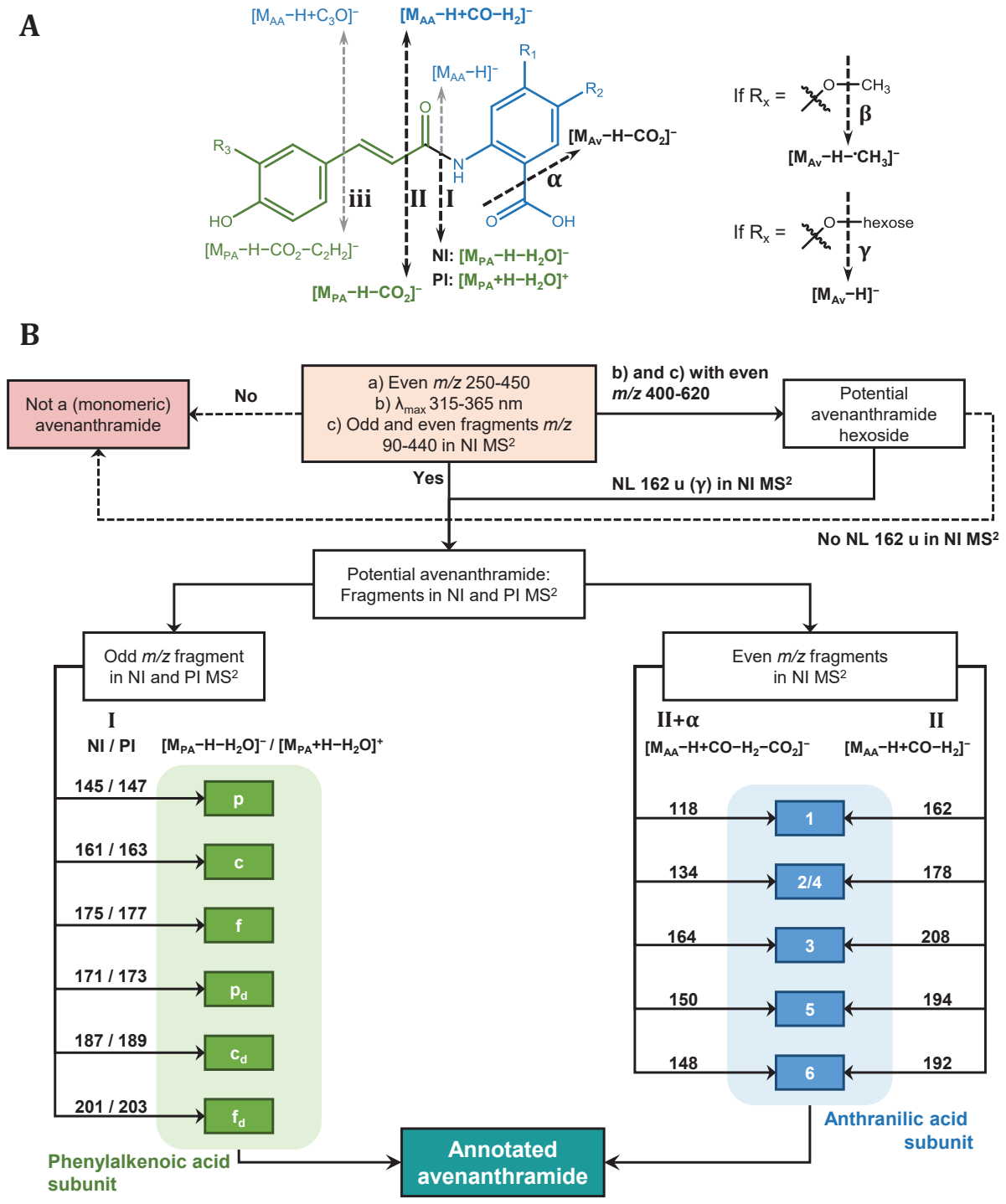

Figure 6.4. Overview of (A) General MS fragmentation pathways of avenanthramides in NI and PI with the observed fragments and (B) decision guideline for the annotation of avenanthramides using LC-ESI-MS with CID or HCD fragmentation. Diagnostic fragmentation pathways (bold arrows) are indicated with I and II and the resulting fragments in bold text. Minor fragmentation pathways are indicated with thin grey arrows and lower case roman numerals (iii, iv, and v)(**Figure S6.4**), whereas α, β, and γ indicate general cleavages. Combinations of I, II, or, iii with α or β are possible. Numbers and letters in green and blue boxes correspond to subunit codes, see **Figure 6.1** (6 = 4/5-methoxy anthranilic acid, **Section 6.3.3.2**, **Figure S6.5** and**Figure S6.6**). NI, negative ionisation mode; PI, positive ionisation mode; NL, neutral loss.

The major fragmentation pathways are associated with cleavages on either side of the amide carbonyl and are indicated with capital Roman numerals (I and II, **Figure 6.4A**). The fragments obtained via pathways I and II are diagnostic, i.e. they yield unique fragments related to the AA and PA subunits and can, therefore, be used to annotate unknown avenanthramides. Pathway I almost exclusively yields $[M_{PA}-H-H_2O]^-$ (NI) or $[M_{PA}+H-H_2O]^+$ (PI) with *m/z* corresponding to the anhydro-PA. The corresponding AA fragment $[M_{AA}-H]^-$ is rarely observed, indicating that the charge is preferentially located on the PA for this cleavage. Pathway II yields the isocyanatobenzoate fragment $[M_{AA}-H+CO-H_2]^-$ and the PA fragment $[M_{PA}-H-CO_2]^-$ with *m/z* corresponding to the decarboxy-PA (not to be confused with α, see below). Minor fragmentation pathways related to the enamide chain are indicated with lower case Roman numerals (iii to v) (**Figure 6.4A**), where iv and v are only applicable in long-chained derivatives (**Figure S6.4**). Long-chained avenanthramides can be annotated using the same diagnostic fragmentation pathways (I and II) as their short-chained equivalents.
In addition to the cleavages of the enamide chain, two general (non-diagnostic) fragments were commonly observed. These cleavages were assigned Greek letters: α for loss of the carboxylic acid moiety of the AA subunit as CO_2 and β for loss of a methyl group as $^{\bullet}CH3$. The latter only occurred if a methoxy-group was present. Loss of anhydrohexose from an avenanthramide glycoside was assigned the Greek letter γ. Combinations of enamide cleavages and general fragments (e.g. II + α) were commonly observed (**Figure 6.2**, **Figure 6.3** and **Figure 6.4A**). Nominal masses of the diagnostic fragments, corresponding to pathways I and II in **Figure 6.4A**, were calculated to facilitate further annotation (**Table S2**). Additionally, to facilitate the annotation of unknown avenanthramides by LC-ESI-MS with CID or HCD fragmentation without standards, we have defined a decision guideline (**Figure 6.4B**). Potential avenanthramide peaks can be recognized by: (a) even *m/z* in the range of 250 to 450, (b) λ_{max} between 315 and 365 nm, and (c) both even and odd fragments observed in NI MS^2 in the *m/z* range of 90 to 440. This guideline is based on the diagnostic fragments as described in this section and glycosides were also included. By following the guideline diagnostic fragments corresponding to both subunits are identified, leading to annotation of the avenanthramide.

6.3.3. Annotation of avenanthramides from oat seedlings

Using the established fragmentation pathways (**Figure 6.4A**), the calculated diagnostic fragments (**Table S2**), and the decision guideline (**Figure 6.4B**), avenanthramides detected in the oat seedling extract were annotated. Separation on RP-UHPLC was used in combination with ESI-IT-MS^n for CID fragmentation and ESI-FTMS for high resolution mass determination. Additionally, chromatograms of the oat seedling extracts were screened for masses of natural avenanthramides to identify any avenanthramide peaks of low abundance (**Table S2**). In general, NI provided higher signal and more structural information upon fragmentation than

PI. Primarily, CID Fragmentation spectra from ESI-IT-MS^n analyses in PI and NI were used to annotate the compounds. Additionally, the retention order of the compounds was taken into account. Generally, this order followed their expected hydrophobicity (e.g. caffeoyl (c) derivatives eluted before *p*-coumaroyl (p) or feruloyl (f) derivatives and short-chained derivatives eluted before their long-chained equivalents).

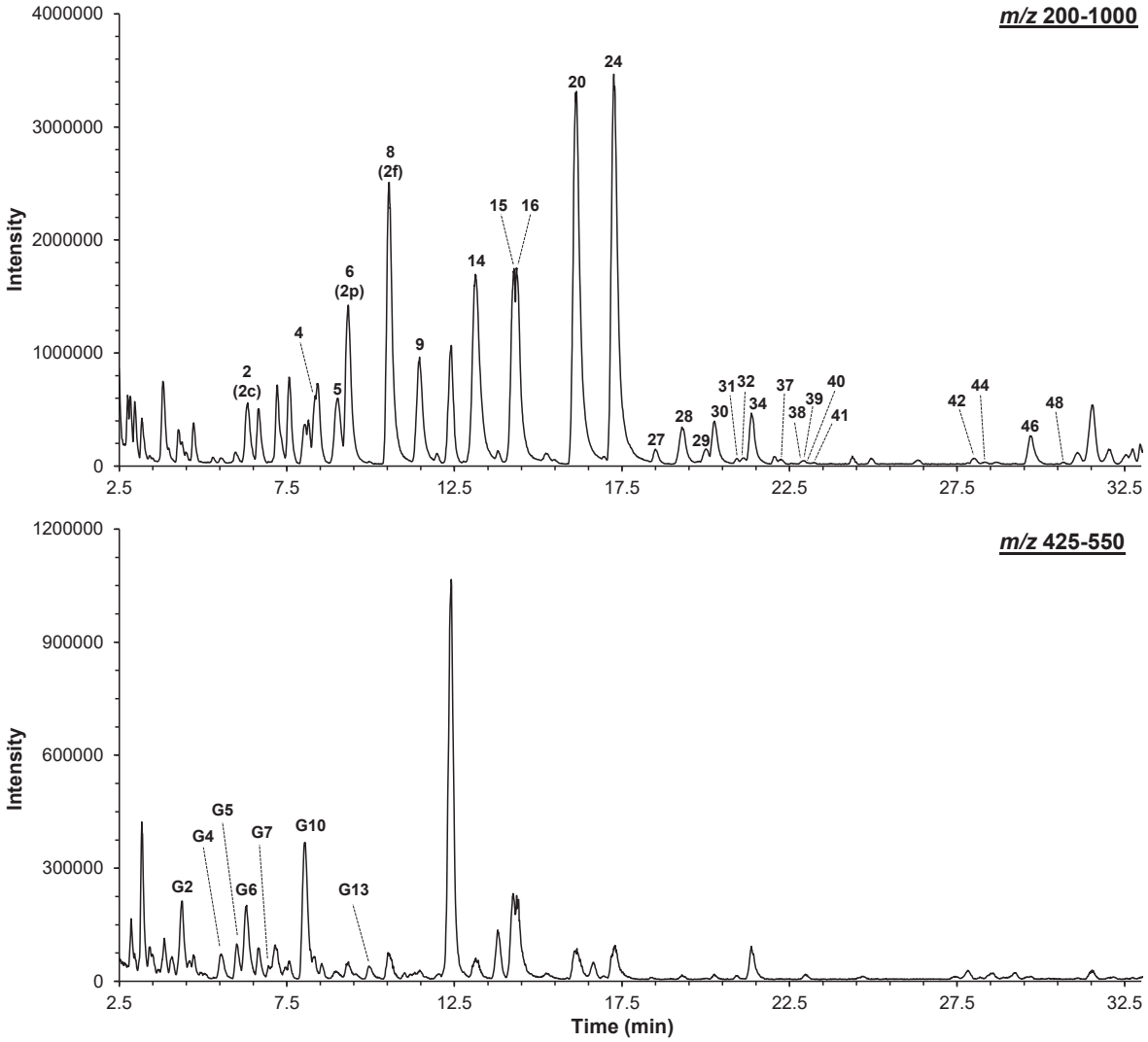

Figure 6.5. Negative mode UHPLC-ESI-IT-MS chromatograms of oat seedling extract in the ranges *m/z* 200-1,000 (top) and *m/z* 425-550 (bottom). Peaks labelled with a number indicate avenanthramide aglycones (**Table S6.2**, supplementary information) and those labelled with "G" plus a number indicate avenanthramide glycosides (**Table S5**, supplementary information). Not all detected peaks are visible in this figure.

Using this approach, 28 of the 30 (combinations of five AA with six PA) natural avenanthramides (**Table S6.1**)[1] were detected in the oat seedling extract (**Table S6.2**, **Figure 6.5**). Avenanthramides with a 5-hydroxy or 4-hydroxy anthranilic acid (i.e. 2 or 4, respectively) have the same mass and the same diagnostic

fragments. Based on the elution of the analytical standards used in this work and on previously reported data,[10,24,25] it was assumed that the 2 isomer always eluted before the 4.

6.3.3.1. Stereo-isomerisation of long-chained avenanthramides

Avenanthramides can undergo isomerisation from the naturally synthesized *E* (*trans*) isomer to the *Z* (*cis*) isomer upon exposure to UV or daylight.[7] In the oat extracts, *E*-*Z* isomerisation of the double bond in the PA subunit was only observed for the long-chained PA derivatives. Most likely, these isomers were formed upon exposure to daylight during extraction and sample treatment. The lack of isomerisation of short-chain PA derived avenanthramides under the influence of daylight is in accordance with previously reported data.[9] Theoretically, four different isomers of long-chained avenanthramides are possible, namely: *E*,*E*; *E*,*Z*; *Z*,*E*; and *Z*,*Z* (**Figure S6**, supplementary information). For most long-chained avenanthramides only three isomer peaks were observed. It was assumed that the most abundant peak, which usually eluted first, corresponded to the naturally occurring *E*,*E* isomer, this is in agreement with previous observations that *E* isomers of hydroxycinnamic acids eluted before their *Z* isomers.[9] Subsequent peaks with a similar *m/z* and fragmentation spectrum were most likely the isomers with one of the double bonds in the *Z* configuration. For the six peaks corresponding to $2p_d$ and $4p_d$ (each Av with three stereoisomers), *E*,*E*-$2p_d$ could be annotated with high confidence. The other five peaks were assumed to correspond to $4p_d$ and the *Z* isomers of both compounds, but these could not confidently be differentiated.

6.3.3.2. Avenanthramide with a 4/5-methoxy-anthranilic acid subunit

Extracts were screened for presence of avenanthramides with sinapic (s) or cinnamic (a) acid subunits, which were not previously detected in nature and were assumed to be non-natural.[1] No avenanthramides with s or a subunits could be detected in the oat extract. Upon screening the NI chromatogram of the extract for *m/z* 342 ($[M_{Av}-H]^-$ of 1s), however, a peak was observed with fragments which did not correspond to any of the calculated diagnostic fragments (**Figure S6.5**, supplementary information). The fragments indicated the presence of a ferulic acid subunit linked to an anthranilic acid subunit with only a methoxy substituent on the 4 or 5 position (**Figure S6.6**, supplementary information), the molecular formula of which was confirmed by HRMS (**Table S4**). Avenanthramides with a 4/5-methoxy-anthranilic acid subunit (hereby assigned subunit number 6 and incorporated in the decision guideline **Figure 6.4B**) have not been reported before. Thus, this observation could suggest a new variation in natural avenanthramide structure. This peak was, however, only detected at low intensity (**Figure S6.5**). The existence of this new subunit could lead to the expansion of the natural avenanthramide pool, although no other avenanthramides with a 6 subunit were detected in this work even after further screening. Future studies will have to

confirm this new subunit and its definitive structure (methoxy-group on the 4 or 5 position of the anthranilic acid).

6.3.4. Avenanthramide profile of oat seedlings

Annotation of the peaks in the oat extract (**Figure 6.5**, **Table S6.2**) led to the conclusion that besides the well-documented avenanthramides 2p, 2c, and 2f, many other avenanthramides are present in oat. The chromatographic profile also showed that several of these other avenanthramides were abundantly present in the oat seedling extract, especially $5p_d$, $5f_d$, 3f, $2p_d$, and $2f_d$, (peaks 14, 15, 16, 20, and 24, respectively). A recent publication on the avenanthramides of oat bran also indicated that a much wider variety of avenanthramides are commonly found in oat.[24] In our work, however, the long-chained avenanthramides $5p_d$, $5f_d$, $2p_d$, and $2f_d$ were found to be abundant in oat seedling extract, whereas no long-chained derivatives were reported in oat bran. These differences in composition between oat bran and oat seedlings indicate that the avenanthramide profile can vary between oat tissues.

To get an indication of the quantities of avenanthramides in the oat seedlings, avenanthramides were quantified using a calibration curve of 2c at 340 nm. A typical UHPLC-PDA 340 nm chromatogram of seed and seedling extract is shown in **Figure S9** (supplementary information). The oat seed extract contained only small quantities of avenanthramides mainly (>70%) represented by 2p, 2c, and 2f (**Figure 6.6**, **Table S6.3**, supplementary information). Avenanthramide content was boosted by germination, resulting in around 25 times larger quantities found in oat seedlings (**Figure 6.6**, **Table S6.3**). Previous studies also showed an increase in avenanthramide content upon germination, but to a lesser extent than in our current experiment.[26] Skoglund and co-workers used different growth conditions, namely a shorter soaking time (10-14 vs. 20 h) and their seed germination phase was performed at lower temperature and different time (120 h at 16 °C or 72 h at 20 °C vs 96 h at 30 °C).[26] These difference might have accounted for some of the observed differences. Addtionally, Skoglund and co-workers quantified avenanthramides 2p, 2c, 2f, and 3f but also observed a large number of unknown peaks in the UV 340 nm chromatogram. Based on wide variety of avenanthramides annotated in our work, many of these peaks probably corresponded to other avenanthramides but they were not identified and quantified as such.

In our seedling extract, avenanthramides 2p, 2c, and 2f, represented less than 20% of the total avenanthramide content. This is in contrast with previous reports in which these three avenanthramides usually represented a major part of the avenanthramide content of various oat samples.[8,10,14] Thus, depending on the type of oat sample, quantification of only avenanthramides 2p, 2c, and 2f, as the total avenanthramide content could lead to a major underestimation. Long-chained avenanthramides represented the majority of the avenanthramide content in oat seedlings. Ideally, future quantifications should be performed based on MS,

possibly with MRM[11] to limit influence of co-elution. This would enable more accurate quantification, at least when a wider variety of standards becomes commercially available.

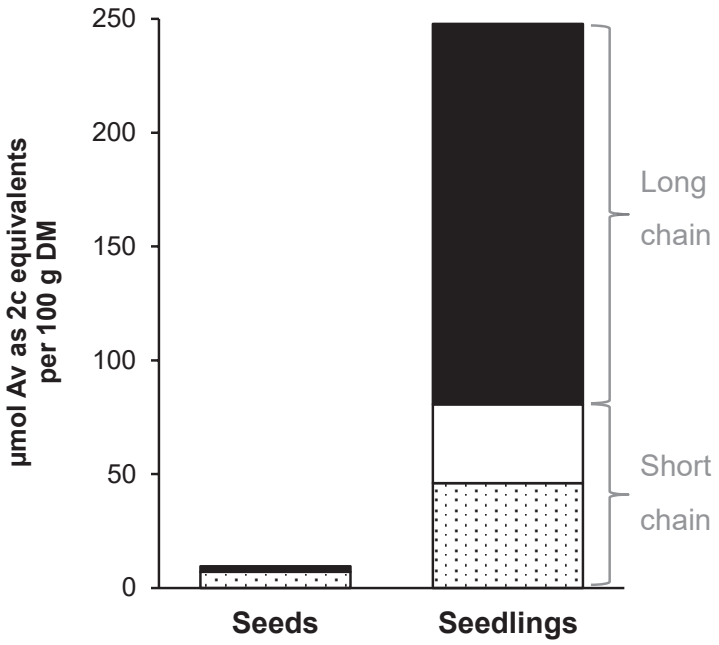

Figure 6.6. Avenanthramide content of oat seeds and seedlings in µmol avenanthramide per 100 g DM, based on area in UHPLC-PDA at 340 nm quantified using a calibration curve of 2c. Dotted, 2p + 2c + 2f; white, other short-chained avenanthramides; black, long-chained avenanthramides. Average quantities per avenanthramide with standard deviations are shown in **Table S6.3**. DM, dry matter.

Upon germination with simultaneous *Rhizopus*-elicitation, using a method described previously,[23] no significant changes in avenanthramide content or composition were observed (data not shown). Fungal stress as effected by *Rhizopus* does not seem to be an effective elicitor of oat, which is in contrast with what was observed for legume seedlings.[22,27,28] Perhaps another elicitation procedure, e.g. with benzothiadiazole[10] or N-acetylchitooligosaccharides,[29] would be more effective.

Up until recently, no reports of avenanthramide glycosides had been published, when Wu and co-workers reported several glycosides from oat bran.[24] Glycosylation is commonly used as a way for plants to store secondary metabolites, which is also observed in other grains, for example benzoxazinoid glycosides in wheat.[23] Glycosylation limits the reactivity of the secondary metabolites and prevents self-toxicity.[30] The abundance of avenanthramide glycosides observed in this work was less than 2% of the total avenanthramide content (**Table S6.3**), similarly avenanthramide glycosides in oat bran were also present in minor quantities compared the aglycones.[24] This might indicate that toxicity of avenanthramides to the oat seedlings is limited.

6.4. Conclusion

The ionisation and fragmentation of avenanthramides was systematically studied using a combination of ion trap mass spectrometry with CID fragmentation and high resolution FTMS with HCD fragmentation. With this, fragmentation pathways of avenanthramides were elucidated and diagnostic fragments were identified. A decision guideline was defined to facilitate future annotation of unknown avenanthramides by LC-ESI-MS. With this approach, 28 unique avenanthramides were annotated by UHPLC-MS analysis of an oat seedling extract. In addition, *Z* isomers and glycosides of avenanthramides were detected. Tentative annotation of the new avenanthramide 6f, with a novel anthranilic acid subunit (4/5-methoxy-anthranilic acid) might hint at a wider array of yet to be discovered natural avenanthramides. The avenanthramide content increased 25 times by germination of oat seeds. In the oat seedling extract, the avenanthramides 2p, 2c, and 2f, which are often referred to as the major avenanthramides, represented less than 20% of the total avenanthramide content. Thus, neglecting any but these three avenanthramides in quantification of the total avenanthramide content, likely results in an underestimation of total content.

6.5. References

[1] Wise, M.L., Avenanthramides: Chemistry and biosynthesis, in *Oats nutrition and technology*, Y. Chu, Editor. 2013, John Wiley & Sons Ltd. p. 195-226.

[2] Collins, F.W., McLachlan, D.C., and Blackwell, B.A. (1991) Oat phenolics - avenalumic acids, a new group of bound phenolic-acids from oat groats and hulls. *Cereal Chemistry*, 68*(2)*: p. 184-189.

[3] Mayama, S., Tani, T., Matsuura, Y., Ueno, T., and Fukami, H. (1981) The production of phytoalexins by oat in response to crown rust, *Puccinia coronata* f. sp. *avenae*. *Physiological Plant Pathology*, 19*(2)*: p. 217-&.

[4] Mayama, S., Tani, T., Ueno, T., Hirabayashi, K., Nakashima, T., Fukami, H., Mizuno, Y., and Irie, H. (1981) Isolation and structure elucidation of genuine oat phytoalexin, avenalumin-I. *Tetrahedron Letters*, 22*(22)*: p. 2103-2106.

[5] Mayama, S., Matsuura, Y., Iida, H., and Tani, T. (1982) The role of avenalumin in the resistance of oat to crown rust, *Puccinia coronata* f. sp. *avenae*. *Physiological Plant Pathology*, 20*(2)*: p. 189-199.

[6] Collins, F.W. (1989) Oat phenolics - avenanthramides, novel substituted N-cinnamoylanthranilate alkaloids from oat groats and hulls. *Journal of Agricultural and Food Chemistry*, 37*(1)*: p. 60-66.

[7] Collins, F.W. and Mullin, W.J. (1988) High-performance liquid-chromatographic determination of avenanthramides, N-aroylanthranilic acid alkaloids from oats. *Journal of Chromatography*, 445*(2)*: p. 363-370.

[8] Bratt, K., Sunnerheim, K., Bryngelsson, S., Fagerlund, A., Engman, L., Andersson, R.E., and Dimberg, L.H. (2003) Avenanthramides in oats (*Avena sativa* L.) and structure-antioxidant activity relationships. *Journal of Agricultural and Food Chemistry*, 51*(3)*: p. 594-600.

[9] Dimberg, L.H., Sunnerheim, K., Sundberg, B., and Walsh, K. (2001) Stability of oat avenanthramides. *Cereal Chemistry*, 78*(3)*: p. 278-281.

[10] Wise, M.L. (2011) Effect of chemical systemic acquired resistance elicitors on avenanthramide biosynthesis in oat (*Avena sativa*). *Journal of Agricultural and Food Chemistry*, 59*(13)*: p. 7028-7038.

[11] Xie, Z.H., Mui, T., Sintara, M., Ou, B.X., Johnson, J., Chu, Y.F., O'shea, M., Kasturi, P., and Chen, Y.M. (2017) Rapid quantitation of avenanthramides in oat-containing products by high-performance liquid chromatography coupled with triple quadrupole mass spectrometry (HPLC-TQMS). *Food Chemistry*, 224: p. 280-288.

[12] Mattila, P., Pihlava, J.M., and Hellstrom, J. (2005) Contents of phenolic acids, alkyl- and alkenylresorcinols, and avenanthramides in commercial grain products. *Journal of Agricultural and Food Chemistry*, 53*(21)*: p. 8290-8295.

[13] Dimberg, L.H., Molteberg, E.L., Solheim, R., and Frolich, W. (1996) Variation in oat groats due to variety, storage and heat treatment .1. Phenolic compounds. *Journal of Cereal Science*, 24*(3)*: p. 263-272.

[14] Dimberg, L.H., Theander, O., and Lingnert, H. (1993) Avenanthramides - a group of phenolic antioxidants in oats. *Cereal Chemistry*, 70*(6)*: p. 637-641.

[15] Meydani, M. (2009) Potential health benefits of avenanthramides of oats. *Nutrition Reviews*, 67*(12)*: p. 731-735.

[16] Sur, R., Nigam, A., Grote, D., Liebel, F., and Southall, M.D. (2008) Avenanthramides, polyphenols from oats, exhibit anti-inflammatory and anti-itch activity. *Archives of Dermatological Research*, 300*(10)*: p. 569-574.

[17] Wise, M.L., Doehlert, D.C., and McMullen, M.S. (2008) Association of avenanthramide concentration in oat (*Avena sativa* L.) grain with crown rust incidence and genetic resistance. *Cereal Chemistry*, 85*(5)*: p. 639-641.

[18] Uchihashi, K., Nakayashiki, H., Okamura, K., Ishihara, A., Tosa, Y., Park, P., and Mayama, S. (2011) In situ localization of avenanthramide A and its biosynthetic

enzyme in oat leaves infected with the crown rust fungus, *Puccinia coronata* f. sp. *avenae*. *Physiological and Molecular Plant Pathology*, 76*(3-4)*: p. 173-181.
[19] Jastrebova, J., Skoglund, M., Nilsson, J., and Dimberg, L.H. (2006) Selective and sensitive LC-MS determination of avenanthramides in oats. *Chromatographia*, 63*(9-10)*: p. 419-423.
[20] Bryngelsson, S., Ishihara, A., and Dimberg, L.H. (2003) Levels of avenanthramides and activity of hydroxycinnamoyl-CoA: Hydroxyanthranilate N-hydroxycinnamoyl transferase (HHT) in steeped or germinated oat samples. *Cereal Chemistry*, 80*(3)*: p. 356-360.
[21] Aisyah, S., Vincken, J.-P., Andini, S., Mardiah, Z., and Gruppen, H. (2016) Compositional changes in (iso)flavonoids and estrogenic activity of three edible Lupinus species by germination and *Rhizopus*-elicitation. *Phytochemistry*, 122: p. 65-75.
[22] Aisyah, S., Gruppen, H., Slager, M., Helmink, B., and Vincken, J.-P. (2015) Modification of prenylated stilbenoids in peanut (*Arachis hypogaea*) seedlings by the same fungi that elicited them: The fungus strikes back. *Journal of Agricultural and Food Chemistry*, 63*(42)*: p. 9260-9268.
[23] de Bruijn, W.J.C., Vincken, J.-P., Duran, K., and Gruppen, H. (2016) Mass spectrometric characterization of benzoxazinoid glycosides from *Rhizopus*-elicited wheat (*Triticum aestivum*) seedlings. *Journal of Agricultural and Food Chemistry*, 64*(32)*: p. 6267-6276.
[24] Wu, W., Tang, Y., Yang, J., Idehen, E., and Sang, S. (2018) Avenanthramide aglycones and glucosides in oat bran: Chemical profile, levels in commercial oat products, and cytotoxicity to human colon cancer cells. *Journal of Agricultural and Food Chemistry*, 66*(30)*: p. 8005-8014.
[25] Wise, M.L., Sreenath, H.K., Skadsen, R.W., and Kaeppler, H.F. (2009) Biosynthesis of avenanthramides in suspension cultures of oat (*Avena sativa*). *Plant Cell Tissue and Organ Culture*, 97*(1)*: p. 81-90.
[26] Skoglund, M., Peterson, D.M., Andersson, R., Nilsson, J., and Dimberg, L.H. (2008) Avenanthramide content and related enzyme activities in oats as affected by steeping and germination. *Journal of Cereal Science*, 48*(2)*: p. 294-303.
[27] Aisyah, S., Gruppen, H., Madzora, B., and Vincken, J.-P. (2013) Modulation of isoflavonoid composition of *Rhizopus oryzae* elicited soybean (*Glycine max*) seedlings by light and wounding. *Journal of Agricultural and Food Chemistry*, 61*(36)*: p. 8657-8667.
[28] Aisyah, S., Gruppen, H., Andini, S., Bettonvil, M., Severing, E., and Vincken, J.-P. (2016) Variation in accumulation of isoflavonoids in *Phaseoleae* seedlings elicited by *Rhizopus*. *Food Chemistry*, 196: p. 694-701.
[29] Ishihara, A., Ohtsu, Y., and Iwamura, H. (1999) Induction of biosynthetic enzymes for avenanthramides in elicitor-treated oat leaves. *Planta*, 208*(4)*: p. 512-518.
[30] Jones, P. and Vogt, T. (2001) Glycosyltransferases in secondary plant metabolism: Tranquilizers and stimulant controllers. *Planta*, 213*(2)*: p. 164-174.

6.6. Supplementary information

The full supplementary information file can be found on the publisher's website at https://doi.org/10.1016/j.foodchem.2018.11.013. Selected parts of the supplementary information have been adapted and incorporated here. Table and figure numbers preceded by "S" but without the chapter number (e.g. **Figure S1**) refer to the full supplementary information whereas **Figure S6.1**, for example, refers to the supplementary information below.

Table S6.1. Overview of natural avenanthramides with their Dimberg and Collins nomenclature, n and R groups are shown in **Figure 6.1**. Adapted from Wise (2013).[1]

Abbreviation Dimberg	Abbreviation Collins	n	R_1	R_2	R_3
1p	D	1	H	H	H
1c	F	1	H	H	OH
1f	E	1	H	H	OCH_3
$1p_d$	L	2	H	H	H
$1c_d$	N	2	H	H	OH
$1f_d$	M	2	H	H	OCH_3
2p	A	1	H	OH	H
2c	C	1	H	OH	OH
2f	B	1	H	OH	OCH_3
$2p_d$	O	2	H	OH	H
$2c_d$	Q	2	H	OH	OH
$2f_d$	P	2	H	OH	OCH_3
3p	X	1	OCH_3	OH	H
3c	Z	1	OCH_3	OH	OH
3f	Y	1	OCH_3	OH	OCH_3
$3p_d$	U	2	OCH_3	OH	H
$3c_d$	W	2	OCH_3	OH	OH
$3f_d$	V	2	OCH_3	OH	OCH_3
4p	G	1	OH	H	H
4c	K	1	OH	H	OH
4f	H	1	OH	H	OCH_3
$4p_d$	R	2	OH	H	H
$4c_d$	T	2	OH	H	OH
$4f_d$	S	2	OH	H	OCH_3
5p	AA	1	OH	OH	H
5c	CC	1	OH	OH	OH
5f	BB	1	OH	OH	OCH_3
$5p_d$	OO	2	OH	OH	H
$5c_d$	QQ	2	OH	OH	OH
$5f_d$	PP	2	OH	OH	OCH_3

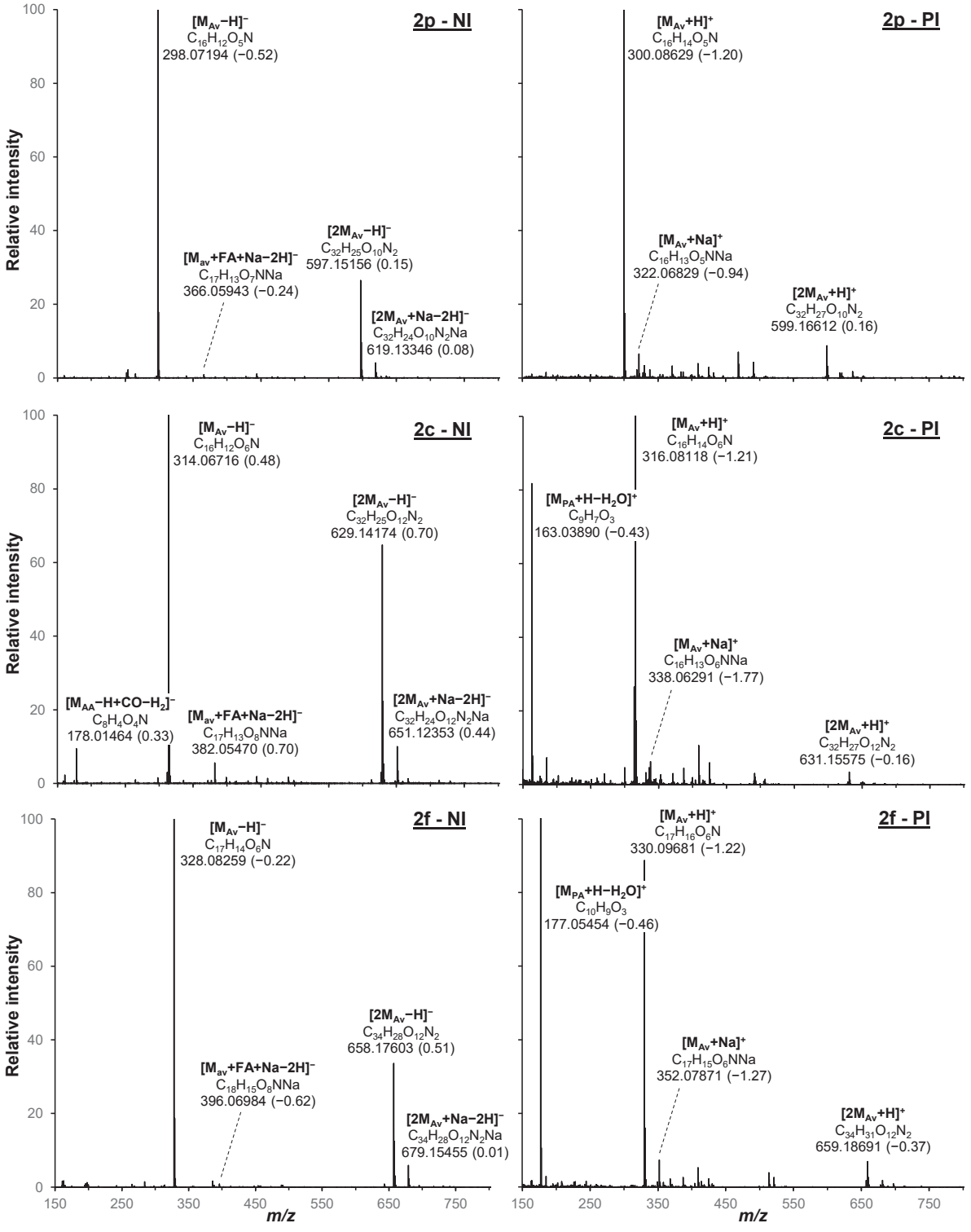

Figure S6.1. High resolution full MS spectra of avenanthramide standards 2p, 2c, and 2f in negative (NI, left) and positive (PI, right) ionisation mode obtained by direct infusion in FTMS. Peak labels show the adduct with its molecular formula, and its measured *m/z* with the error (in ppm) in the parentheses. Av, avenanthramide; AA, anthranilic acid; PA, phenylalkenoic acid; FA, formic acid (CHOOH).

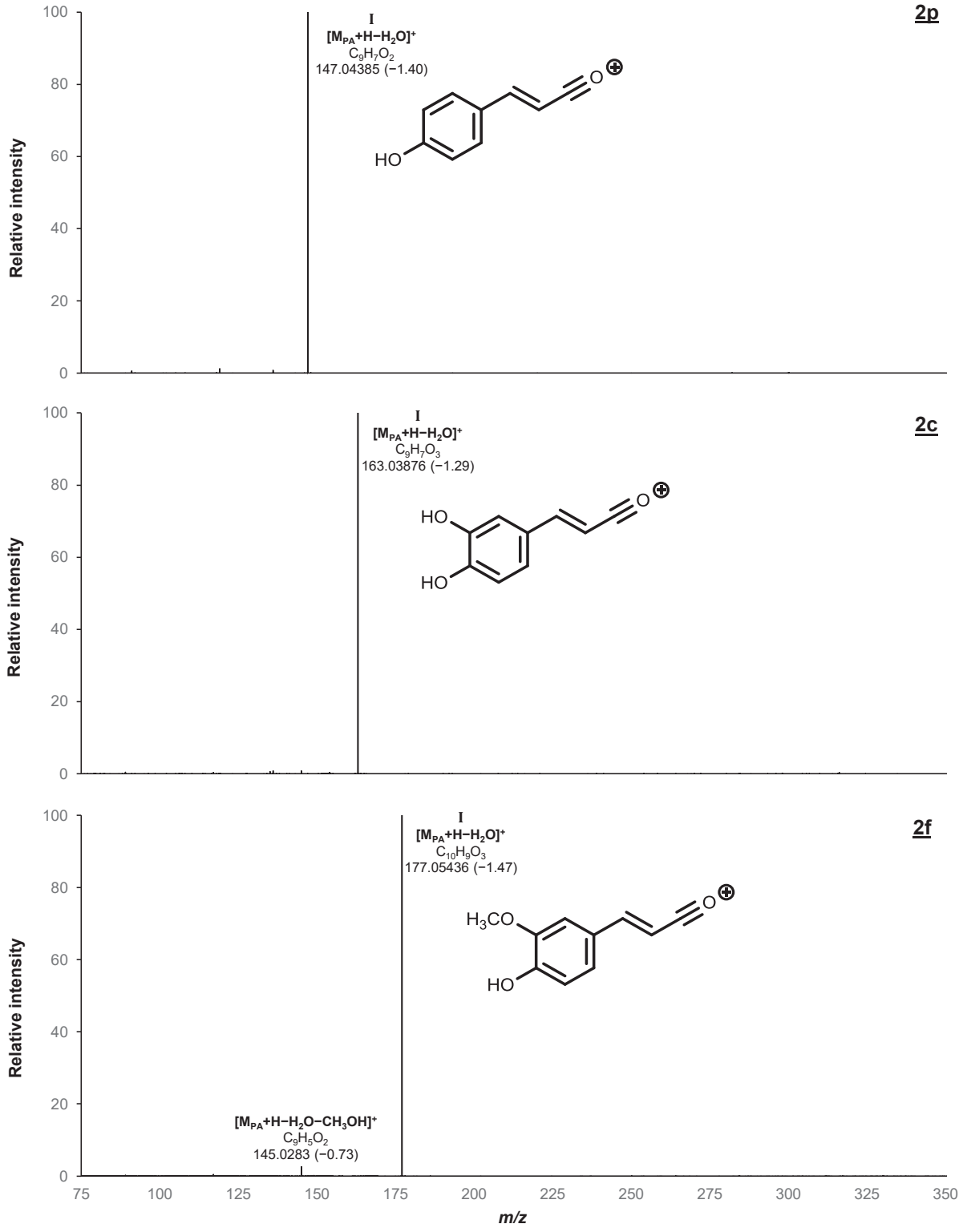

Figure S6.2. High resolution HCD fragmentation spectra (NCE = 10) of avenanthramide standards 2p, 2c, and 2f in positive ionisation mode obtained by direct infusion in FTMS. Peak labels show the corresponding fragmentation pathway (**Figure 6.4A**), the fragment adduct with its molecular formula, and its measured *m/z* with the error (in ppm) in parentheses. Inset shows the proposed structure of the main fragment. PA, phenylalkenoic acid; NCE, normalized collision energy.

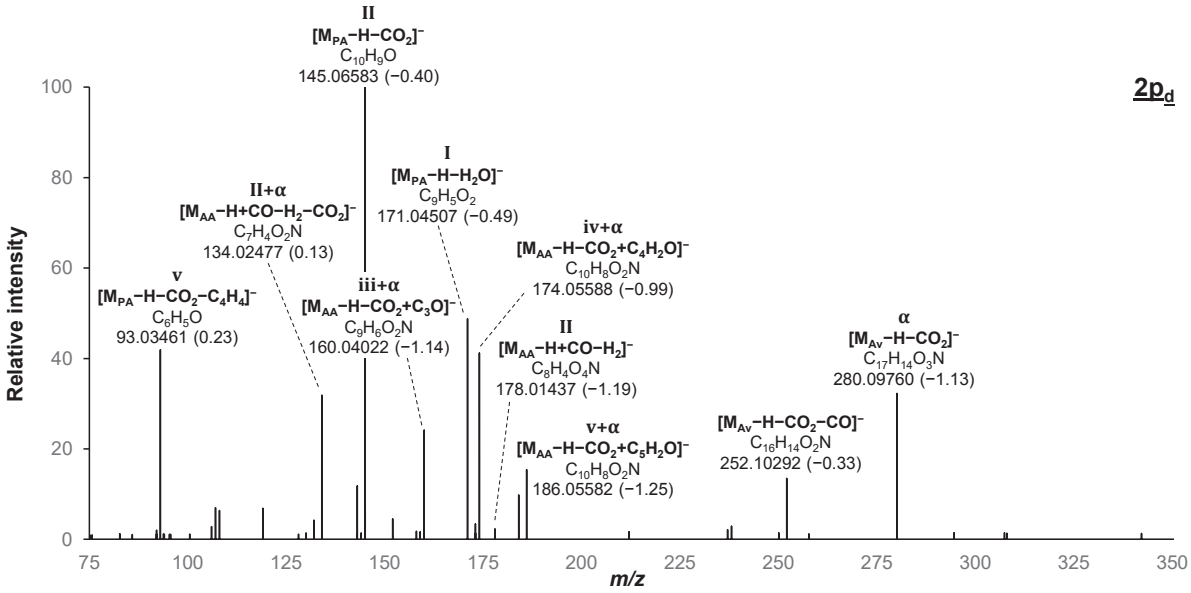

Figure S6.3. High resolution HCD fragmentation spectrum (NCE = 25) of *m/z* 324.08776 in negative mode, which was tentatively annotated as avenanthramide 2p$_d$. Peak labels show the corresponding fragmentation pathway (**Figure S6.4A**), the fragment adduct with its molecular formula, and its measured *m/z* with the error (in ppm) in parentheses. This spectrum was recorded at 35,000 resolution during a chromatographic run of the oat extract. Av, avenanthramide; AA, anthranilic acid; PA, phenylalkenoic acid.

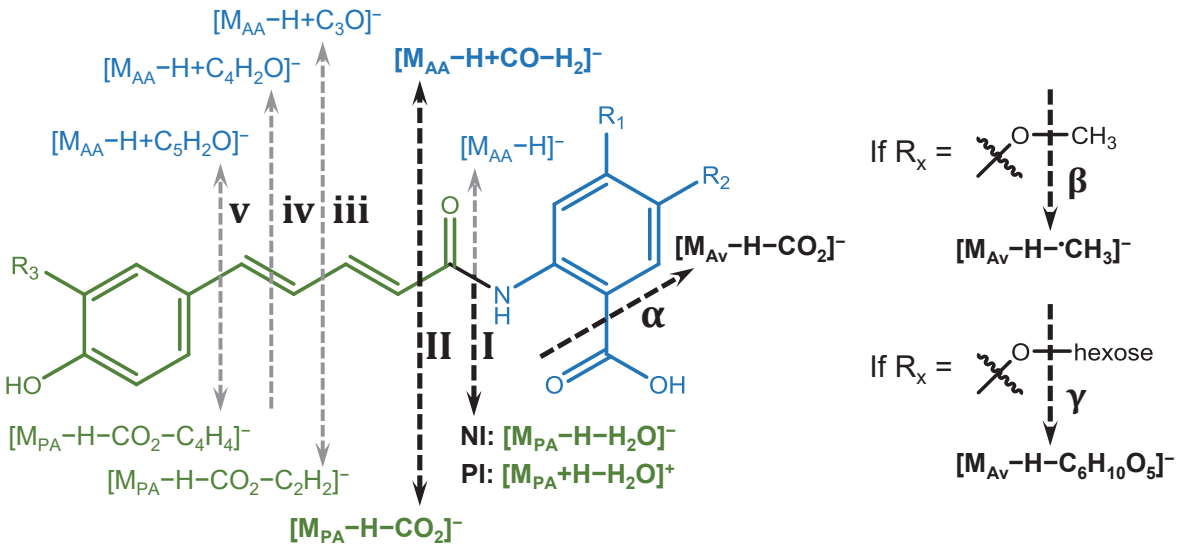

Figure S6.4. Fragmentations observed in long-chain avenanthramides in addition to the fragmentations described in **Figure S6.4A**. Combinations of I to v with α, β, or γ are possible.

Table S6.2. Tentative annotations of avenanthramide peaks (**Figure S6.5**) and the spectrometric data obtained using negative ionisation mode ESI-IT-MS^n. Additional spectrometric and spectroscopic data can be found in **Table S4**.

				Diagnostic fragments (relative intensity) [a]			Small NL Fragments (rel. int.)					Other fragments (rel. int.)		
				I	II	II+α	II	α	β	α+β	iii+α	v+α		
Peak no.	Rt (min)	Av.	$[M_{Av}-H]^-$	$[M_{PA}-H-H_2O]^-$	$[M_{AA}-H+CO-H_2]^-$	$[M_{AA}-H+CO-H_2-CO_2]^-$	$[M_{PA}-H-CO_2]^-$	$[M_{Av}-H-CO_2]^-$	$[M_{Av}-H-{}^{\bullet}CH_3]^-$	$[M_{Av}-H-CO_2-{}^{\bullet}CH_3]^-$	$[M_{AA}-H-CO_2+C_3O]^-$	$[M_{AA}-H-CO_2+C_5H_2O]^-$	Other fragments [b]	
1	4.92	5c	330	161 (2)	194	150 (8)	n.d.	286 (72)	n.a.	n.a.	176 (12)	n.a.	220 (10)	
2	6.33	2c [c]	314	161 (8)	178	134 (4)	135 (3)	n.d.	n.a.	n.a.	n.d.	n.a.		
3	7.28	5p	314	145 (5)	194	150 (25)	119 (1)	270 (94)	n.a.	n.a.	176 (6)	n.a.	242 (6)	
4	8.35	5f	344	175 (3)	194 (64)	150 (20)	149 (1)	300	n.d.	285 (3)	176 (2)	n.a.	168 (4), 164 (4)	
5	9.01	$5c_d$	356	187 (3)	194 (23)	150 (6)	161 (2)	312 (77)	n.a.	n.a.	176 (57)	202 (3)	220	
6	9.33	2p [c]	298	145 (15)	178 (39)	134 (4)	119 (1)	254	n.a.	n.a.	160 (14)	n.a.	226 (14), 236 (12)	
7	9.52	4c [d]	314	161 (2)	178	134 (5)	135 (1)	270 (10)	n.a.	n.a.	160 (1)	n.a.		
8	10.55	2f [c]	328	175 (6)	178 (10)	134 (2)	n.d.	284	<1	269 (4)	160 (4)	n.a.	256 (4)	
9	11.46	$2c_d$	340	187 (23)	178	134 (12)	161 (21)	296 (1)	n.a.	n.a.	n.d.	n.d.		
10	11.55	$5c_d$ *Z* iso.	356	187 (4)	194 (33)	150 (7)	161 (2)	312	n.a.	n.a.	176 (46)	202 (3)	220 (67), 338 (9)	
11	11.90	$5c_d$ *Z* iso.	356	187 (4)	194 (17)	150 (6)	161 (2)	312	n.a.	n.a.	176 (21)	202 (1)	220 (21)	
12	12.98	3p	328	145 (12)	208 (90)	164 (7)	149 (3)	284	313 (12)	269 (32)	190 (1)	n.a.	268 (24), 176 (19)	
13	12.99	4p [d]	298	145 (28)	178	134 (29)	119 (3)	254 (83)	n.a.	n.a.	160 (8)	n.a.	148 (6), 226 (11), 236 (9)	
14	13.12	$5p_d$	340	171 (2)	194 (16)	150 (5)	145 (1)	296	n.a.	n.a.	176 (6)	202 (6)		
15	14.28	$5f_d$	370	201 (1)	194 (9)	150 (4)	n.d.	326	n.d.	311 (2)	176 (2)	202 (3)		
16	14.35	3f	358	175 (8)	208 (38)	164 (3)	149 (5)	314	343 (15)	299 (39)	190 (1)	n.d.	176 (33), 298 (28)	
17	14.35	4f [d]	328	175 (15)	178 (38)	134 (15)	149 (2)	284	313 (2)	269 (8)	160 (7)	n.a.	256 (9), 148 (6)	
18	15.23	$3c_d$	370	187 (6)	208	164 (8)	161 (13)	326 (49)	n.d.	n.d.	190 (1)	n.d.	194 (4), 149 (4)	
19	15.47	$5p_d$ *Z* iso.	340	171 (1)	194 (19)	150 (5)	145 (1)	296	n.a.	n.a.	176 (4)	n.d.		
20	16.14	$2p_d$	324	171 (9)	178 (14)	134 (2)	145 (3)	280	n.a.	n.a.	160 (5)	186 (17)	174 (14)	
21	16.79	$5p_d$ *Z* iso.	340	171 (1)	194 (16)	150 (5)	145 (1)	296	n.a.	n.a.	176 (4)	202 (1)		
22	16.95	$5f_d$ *Z* iso.	370	201 (1)	194 (9)	150 (3)	175 (1)	326	n.d.	n.d.	176 (1)	n.d.	208 (6), 187 (4)	
23	17.09	1c	298	161 (10)	162	118 (2)	135 (5)	254 (1)	n.a.	n.a.	n.d.	n.a.	284 (8)	
24	17.26	$2f_d$	354	201 (7)	178 (9)	134 (2)	175 (3)	310	n.d.	295 (8)	160 (3)	186 (14)	174 (17)	
25	17.46	$5f_d$ *Z* iso.	370	201 (1)	194 (7)	150 (4)	175 (1)	326	n.d.	n.d.	176 (1)	202 (1)	187 (6), 338 (5)	
26	17.57	$2p_d$ / $4p_d$	324	171 (43)	178	134 (10)	145 (10)	280 (22)	n.a.	n.a.	160 (1)	186 (4)		
27	18.50	$2p_d$ / $4p_d$ iso.	324	171 (44)	178	134 (10)	145 (10)	280 (12)	n.a.	n.a.	160 (1)	186 (2)		
28	19.29	$4f_d$	354	201 (60)	178	134 (14)	175 (16)	310 (18)	n.d.	295 (2)	160 (4)	186 (4)	322 (9), 152 (4)	

				Diagnostic fragments (relative intensity) [a]			Small NL Fragments (rel. int.)				Other fragments (rel. int.)		
				I	II	II+α	II	α	β	α+β	iii+α	v+α	
Peak no.	Rt (min)	Av.	$[M_{Av}-H]^-$	$[M_{PA}-H-H_2O]^-$	$[M_{AA}-H+CO-H_2]^-$	$[M_{AA}-H+CO-H_2-CO_2]^-$	$[M_{PA}-H-CO_2]^-$	$[M_{Av}-H-CO_2]^-$	$[M_{Av}-H-{}^{\bullet}CH_3]^-$	$[M_{Av}-H-CO_2-{}^{\bullet}CH_3]^-$	$[M_{AA}-H-CO_2+C_3O]^-$	$[M_{AA}-H-CO_2+C_5H_2O]^-$	Other fragments [b]
29	20.00	$2p_d$ *Z* iso.	324	171 (30)	178 (67)	134 (19)	145 (9)	280	n.a.	n.a.	160 (7)	186 (14)	174 (7), 252 (6)
30	20.26	$3p_d$	354	171 (8)	208 (31)	164 (2)	145 (4)	310	339 (11)	295 (37)	190 (2)	216 (2)	201 (4), 294 (15)
31	20.92	$3f_d$ *Z* iso.	384	201 (24)	208 (22)	164 (6)	175 (8)	340 (49)	369	325 (98)	190 (3)	216 (8)	202 (18), 189 (7), 324 (7)
32	21.11	$2f_d$ *Z* iso.	354	201 (17)	178 (26)	134 (10)	175 (6)	310	339 (3)	295 (9)	160 (4)	186 (12)	174 (8), 308 (7), 285 (6), 282 (5)
33	21.25	$2p_d$ / $4p_d$ iso.	324	171 (29)	178	134 (17)	145 (9)	280 (62)	n.a.	n.a.	160 (2)	186 (5)	174 (4), 306 (6), 309 (6), 281 (5)
34	21.36	$3f_d$	384	201 (8)	208 (20)	164 (2)	175 (5)	340	369 (12)	325 (50)	190 (1)	216 (1)	324 (13)
35	21.50	1p	282	145 (41)	162 (85)	118 (7)	119 (7)	238	n.a.	n.a.	144 (7)	n.a.	235 (22), 210 (13), 220 (12)
36	22.06	$1c_d$ [e]	324	187 (33)	162	118 (5)	161 (34)	280 (49)	309 (16)	n.d.	n.d.	n.d.	178 (46), 171 (15)
37	22.24	$2p_d$ / $4p_d$ iso.	324	171 (31)	178	134 (15)	145 (8)	280 (42)	n.a.	n.a.	160 (1)	186 (1)	
38	22.90	$2f_d$ *Z* iso.	354	201 (38)	178 (92)	134 (20)	175 (13)	310	n.d.	295 (5)	160 (4)	186 (5)	174 (4), 187 (25), 208 (12), 308 (13), 322 (13)
39	22.97	1f	312	175 (17)	162 (24)	118 (3)	149 (3)	268	297 (1)	253 (7)	144 (4)	n.a.	240 (4), 269 (6)
40	23.04	$3f_d$ *Z* iso.	384	201 (25)	208	164 (9)	175 (10)	340 (25)	369 (4)	325 (9)	n.d.	n.d.	352 (30), 149 (8), 338 (4)
41	23.22	$3f_d$ *Z* iso.	384	201 (21)	208	164 (10)	175 (9)	340 (21)	369 (6)	325 (7)	n.d.	n.d.	352 (37), 149 (8), 193 (4)
42	27.99	$1p_d$ *Z* iso.	308	171 (54)	162	118 (6)	145 (19)	264 (11)	n.a.	n.a.	144 (1)	170 (1)	240 (4)
43	28.26	6f	342	175 (13)	192 (42)	148 (6)	149 (4)	298	327 (2)	283 (10)	174 (2)	n.a.	270 (4) 160 (5)
44	28.33	$1p_d$ *Z* iso.	308	171 (49)	162	118 (5)	145 (19)	264 (11)	n.a.	n.a.	144 (1)	n.d.	240 (6)
45	29.06	$1f_d$ *Z* iso.	338	201 (75)	162	118 (10)	175 (40)	294 (25)	n.d.	279 (7)	n.d.	n.d.	292 (9), 306 (14), 271 (13), 270 (13)
46	29.68	$1p_d$	308	171 (29)	162 (43)	118 (4)	145 (14)	264	n.a.	n.a.	144 (4)	170 (10)	158 (6), 236 (6), 93 (4)
47	29.90	$1f_d$ *Z* iso.	338	n.d.	n.d.	n.d.	n.d.	n.d.	n.d.	n.d.	n.d.	n.d.	n.d.
48	30.71	$1f_d$	338	201 (29)	162 (27)	118 (3)	175 (13)	294	n.d.	279 (17)	144 (2)	170 (9)	158 (9), 266 (6), 295 (6), 269 (5), 123 (4)
49	32.86	$1p_d$ *Z* isomer	308	171 (47)	162	118 (5)	145 (18)	264 (8)	n.a.	n.a.	n.d.	170 (1)	289 (6), 239 (4), 240 (4), 261 (4)

NL, neutral loss; iso., isomer; n.d. not detected; n.a., not applicable. [a] Relative intensity threshold for diagnostic fragments, small NL fragments, and those corresponding to i+α and ii+α was ≥1, for other fragments it was ≥4. [b] Other fragments include those corresponding to fragmentation pathways iii, iv, v, and miscellaneous fragments. c Annotation confirmed with standard. [d] Annotated as 4 by comparison to the analytical standards of 2c, 2p, and 2f and a previous study,[10] which showed that 4 elutes later than 2. [e] Partial co-elution with peak 37 which has the same *m/z* might have influenced the fragments detected. The fragmentation corresponding to β was not expected for this compound.

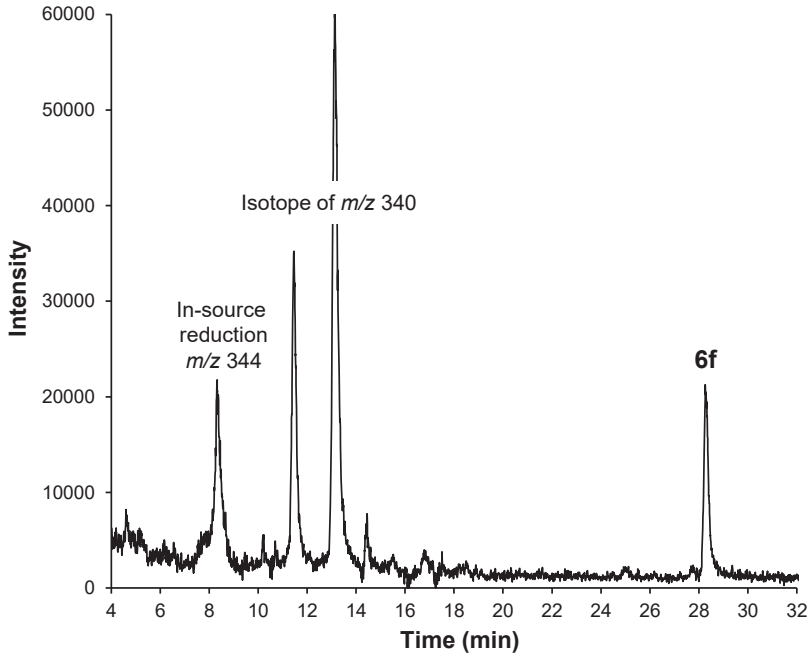

Figure S6.5. Extracted ion chromatogram of *m/z* 342 in negative ionisation mode.

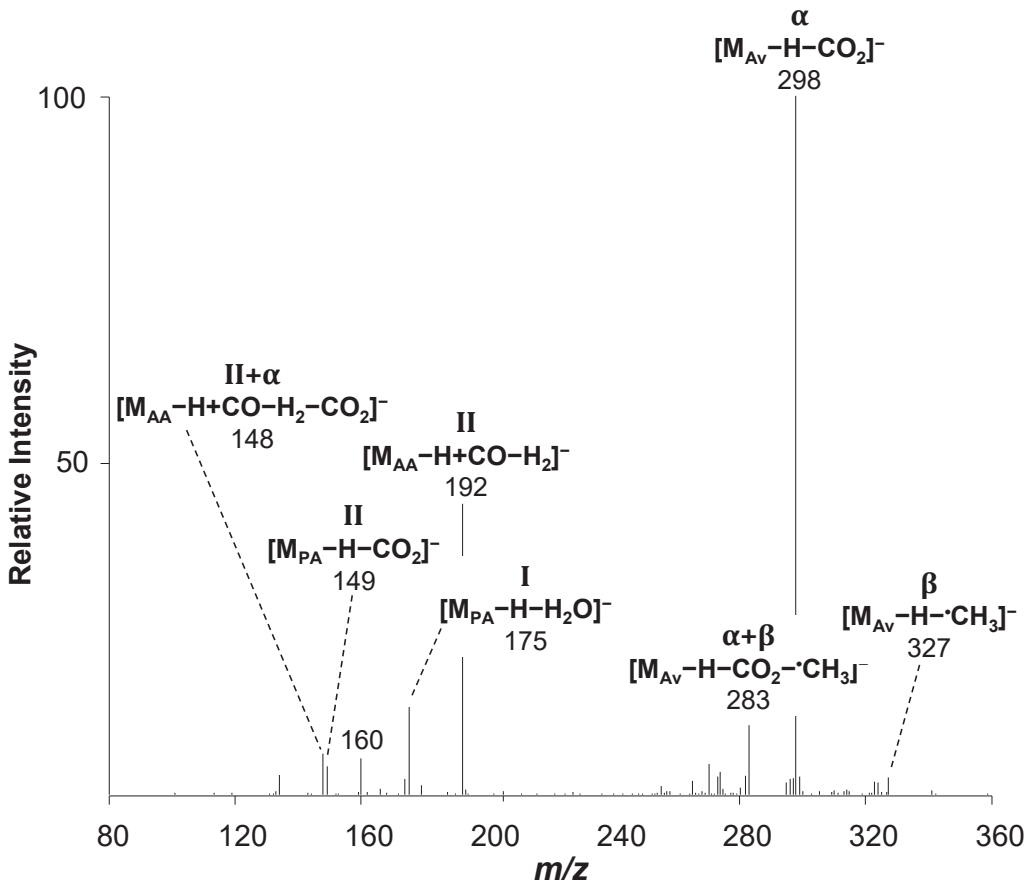

Figure S6.6. CID Fragmentation spectrum of *m/z* 342 in negative ionisation mode, which was tentatively annotated as avenanthramide 6f. Peak labels show the corresponding fragmentation pathway (**Figure 6.4A**), the fragment adduct with, and its measured *m/z*. Av, avenanthramide; AA, anthranilic acid; PA, phenylalkenoic acid.

Table S6.3. Avenanthramide content of oat seeds and seedlings in µmol avenanthramide per 100 g DM, based on area in UHPLC-PDA at 340 nm quantified using a calibration curve of 2c.

		µmol Av as 2c equivalents per 100 g DM, mean (± SD)	
Peak no.	**Av**	**Seeds [a]**	**Seedlings [b]**
G2	2c-hex	<LOQ	2 (± 0.2) [c]
2	2c	2.2 (± 0.03)	12.4 (± 0.9) [d]
3	5p	<LOQ	4 (± 0.9) [c]
G4	$5f_d$-hex	n.d.	2.3 (± 0.9)
4	5f	<LOQ	10.5 (± 2.2) [c]
5	$5c_d$	n.d.	9.2 (± 2.5)
6	2p	2.5 (± 0.04)	11.6 (± 1.5)
8	2f	2.4 (± 0.04)	22.1 (± 2.3)
9	$2c_d$	<LOQ	13.5 (± 0.8)
14	$5p_d$	<LOQ	24.9 (± 2.0)
15/16	$5f_d$/3f	<LOQ	36 (± 6.5)
18	$3c_d$	n.d.	1.6 (± 0.1) [e]
20	$2p_d$	1.1 (± 0.14)	43.5 (± 9.4)
24	$2f_d$	1.4 (± 0.03) [c]	41.7 (± 2.5)
27	$2p_d$/$4p_d$	<LOQ	1.8 (± 0.1) [f]
28	$4f_d$	<LOQ	3.2 (± 0.8)
30	$3p_d$	<LOQ	3.7 (± 0.7)
34	$3f_d$	n.d.	3.8 (± 0.3)
	Total	**9.6 (± 0.14)**	**246.7 (± 6.6)**

2c-Eq, 2c equivalents; DM, dry matter; SD, standard deviation; hex, hexose; <LOQ, below limit of quantification; n.d., not detected [a] Based on two independent replicates. [b] Based on four replicates, i.e. duplicate extractions of two independent biological replicates. [c] Co-elution with a non-avenanthramide peak. [d] Co-elution with peak G6 ($5c_d$-hex), 2c was the major ion in MS. [e] Based on duplicate extractions of one biological replicate, below LOQ in other replicate. [f] Below LOQ in one of the four replicates.

CHAPTER 7

General discussion

In this thesis, we have focused on the production, diversification, and characterisation of plant defence metabolites with antimicrobial potential. To this end, seeds were subjected to germination with simultaneous elicitation. In this chapter, the results of the foregoing chapters will be integrated and discussed alongside some unpublished results.

Prenylated stilbenoids from elicited peanuts present a class of natural compounds with promising antibacterial activity. Production and diversification of prenylated stilbenoids and (iso)flavonoids *in vitro* yielded a much wider variety of structures than what was present in nature. The potential of fungal elicitation, an established method for diversification and enhancement of secondary metabolites in legumes, was also assessed in grasses (Poaceae). In wheat and oat, benzoxazinoids and avenanthramides, respectively, were the main defence metabolites observed. The antimicrobial potential of prenylated stilbenoids and metabolites from grasses will be discussed in this chapter.

Secondary metabolites and their derivatives might be used in the food and pharmaceutical industries as antimicrobial compounds. Several challenges still need to be overcome to make application of prenylated stilbenoids in the food industry viable. Structural optimization of 1,4-benzoxazin-3-one or prenylated phenolics might make them applicable in the pharmaceutical industry. Several examples of structural optimisation by organic synthesis were presented in this thesis which resulted in lead compounds with promising antibacterial activity.

7.1. Prenylated stilbenoids from peanut

In **Chapter 1**, it was discussed that prenylated (iso)flavonoids from legumes are a promising class of natural antimicrobials. In addition, prenylated stilbenoids had previously been shown to be an interesting class of potential antimicrobials.[1,2]

7.1.1. Stability of prenylated stilbenoids

In **Chapter 2**, we aimed to isolate the individual compounds from a peanut extract to determine their antimicrobial activity. To this end, we increased the production of elicited peanut to pilot scale (~3 kg of peanut starting material). Based on previous estimates of the content of individual compounds[3] (factoring in losses during the extraction and purification processes), this should have yielded sufficient material of the main prenylated stilbenoids for extensive testing. The final amounts obtained, however, were much lower than expected. Exposure of stilbenoids to light and oxygen might have led to *E-Z* isomerisation and dimerisation,[4] both of which were observed in our analyses. Possibly, further oligomerisation led to loss of material as insoluble oligomers. The inherent instability of stilbenoids was previously described[4] and might have been exacerbated by the electron donating properties of the prenyl-group. Even though light- and oxygen-exposure were limited as much as possible during extraction and purification, we were still unable to ensure the stability of the prenylated stilbenoids. An extended investigation on the stability of prenylated stilbenoids under various conditions is therefore warranted.

7.1.2. Monomeric prenylated stilbenoids as antibacterials

Despite the aforementioned stability issues, several monomeric prenylated stilbenoids from peanut were successfully purified by preparative chromatography. Three of these compounds were found to possess moderate to good activity against the clinically relevant bacterium methicillin-resistant *Staphylococcus aureus* (MRSA). The new compound arachidin-6 (ring-prenylated piceatannol) had a MIC of 50-75 µg mL^{-1}, arahypin-5 (ring-prenylated resveratrol) had a MIC of 25-50 µg mL^{-1}, and the most potent compound, chiricanine A (chain-prenylated pinosylvin), had a MIC of 12.5 µg mL^{-1}. Non-prenylated resveratrol possessed a MIC of >200 µg mL^{-1}. The MIC values of arahypin-5 and chiricanine A are comparable to those found for several potent mono-prenylated (iso)flavonoids against gram-positive bacteria.[5] Based on the findings of **Chapter 2**, several other monomeric prenylated stilbenoids from peanut, such as arahypin-13 (ring-prenylated pinosylvin), are expected to possess comparable or even more potent antibacterial activity. We concluded that prenylated stilbenoids are promising in terms of their antibacterial activity and that they are on par with other natural antimicrobial compounds.

7.1.3. Oligomeric prenylated stilbenoids

During the purification process of monomeric prenylated stilbenoids, three pools containing mixtures of dimeric prenylated stilbenoids were also obtained (**Chapter 2**). These pools, which contained compounds such as arahypin-6 and arahypin-7, were also found to possess MIC values of 25-50 µg mL^{-1} against MRSA. Other studies have already shown that dimerisation[6-8] or oligomerisation[9] of non-prenylated resveratrol monomers can lead to enhanced antimicrobial potential. For example, the resveratrol dimers δ-viniferin and ε-viniferin possessed MIC values of 28.1 µg mL^{-1} against *S. aureus*[8] and 50-400 µg mL^{-1} against MRSA,[6,7] respectively. Several oligomers were shown to be potent, e.g. gnemonol B and gnetin E with MICs of 6.25 and 12.5-25 µg mL^{-1}, respectively, against MRSA.[9] In combination with our preliminary findings, these results indicate that dimerisation or oligomerisation of stilbenoids, potentially in combination with prenylation, presents an interesting lead for further research.

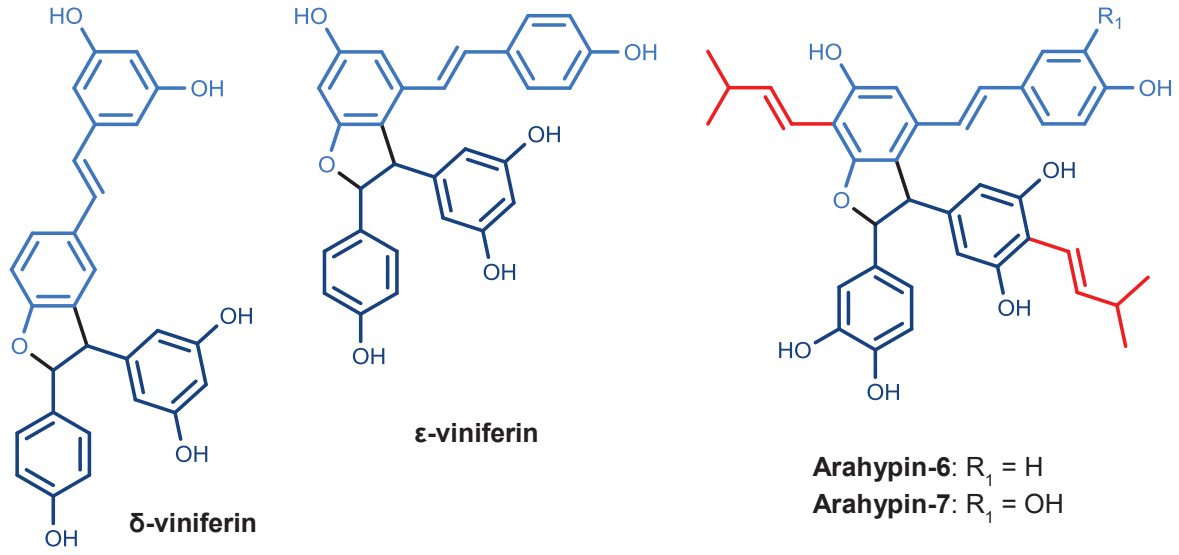

Figure 7.1. Structures of the resveratrol dimer δ-viniferin and the prenylated stilbenoid dimers arahypin-6 and arahypin-7. The bonds between the monomeric units are shown in black and prenyl-groups are shown in red.

7.2. Germination and fungal elicitation in Poaceae

Previously, germination with simultaneous elicitation by the food-grade fungus *Rhizopus* has proven to be an effective method to enhance the production of secondary defence metabolites in legumes (**Chapter 1**).[3,10] In this thesis, the same protocol was applied to species of the family of grasses (Poaceae).

7.2.1. Analysis of defence metabolites from wheat and oat

In **Chapters 3** and **6**, benzoxazinoids from wheat and avenanthramides from oat were studied. Both of these classes are known defence metabolites of their respective species. The majority of previous studies, however, had focussed on a

small subset of metabolites from these classes: the benzoxazinoids DIBOA and DIMBOA, and the avenanthramides 2p, 2c, and 2f. The metabolite profiles reported in literature were, therefore, often incomplete resulting in an underestimation of the total quantities of the metabolites. In **Chapters 3** and **6**, we developed new methods for the annotation of benzoxazinoids and avenanthramides by LC-MS. The guidelines presented in these chapters facilitate future annotation of unknown compounds from these classes. In our own work this has resulted in the annotation of a wide variety of metabolites from both classes: 23 benzoxazinoids and 28 avenanthramides, amongst which were several newly annotated compounds. Using our guidelines, future studies will be able to more easily characterise benzoxazinoids and avenanthramides, leading to a more complete coverage of the metabolites profile and more accurate quantification of total metabolite content.

7.2.2. Elicitation with *Rhizopus* in Poaceae

The improved methods for characterisation of benzoxazinoids and avenanthramides were applied to study the effect of simultaneous germination and *Rhizopus* elicitation of the species wheat, rye, and oat. In **Figure 7.2** the results of this research are summarised. For all species, an increase in the metabolite content was found upon germination. In wheat and rye there was no clear effect of elicitation on the benzoxazinoid content of the seedlings. Benzoxazinoid production in spelt (*Triticum spelta*) was also evaluated. Compared to wheat, spelt produced the same array of benzoxazinoids at lower quantities and with a similar response to germination and elicitation.

Barley was studied with regard to its production of phenol-agmatine amides. Avenanthramide content in oat (**Chapter 6**) and phenol-agmatine amide content in barley also did not seem to be affected by *Rhizopus* elicitation. In each of these experiments, visual observations confirmed that both seedlings and *Rhizopus* were able to grow successfully, indicating that there was no problem with seedling or fungal growth. Based on these results, germination with simultaneous *Rhizopus* elicitation does not achieve the desired increase in secondary metabolites in species of the family Poaceae. Moreover, the secondary metabolite profile of these species does not change to an extent comparable to that of legumes.[3,10] In comparison, in several legumes quantities of prenylated phenolics increased significantly upon *Rhizopus* elicitation during germination: stilbenoids in peanut (approx. 5-fold)[3], genistein derivatives in lupine (≥9-fold)[10], and isoflavonoids in soy (approx. 14-fold).[11] We, therefore, concluded that our elicitation protocol, which proved successful in legumes, did not translate well to grasses.

Several more generic challenges regarding germination with simultaneous fungal elicitation were encountered. Firstly, variation between batches of seedlings from the same supplier was often observed. Secondly, conditions always needed to be compromised to achieve ideal growth conditions for both the seedling and the fungus.

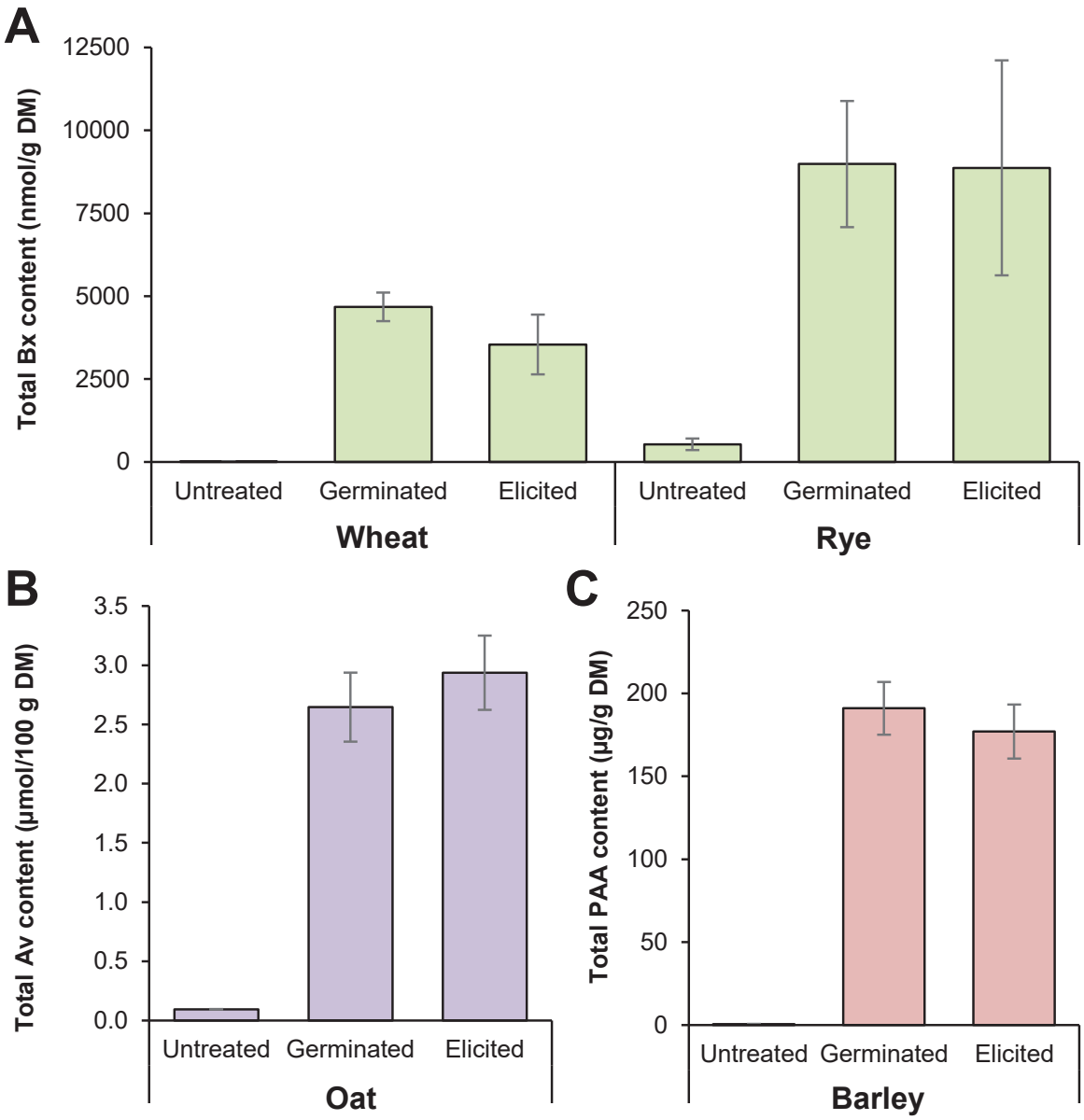

Figure 7.2. Content of specific secondary metabolites of four species of grasses which were subjected to germination and germination with simultaneous fungal (*Rhizopus*) elicitation: A, benzoxazinoids (Bx) in wheat and rye expressed in nmol Bx per g DM; B, avenanthramides (Av) in oat expressed in µmol avenanthramide 2c equivalents per 100 g DM; and C, phenol-agmatine amides (PAA) in barley expressed in µg PAA per g DM. Error bars indicate standard deviation (n = 2). DM, dry matter.

Previous studies have shown that allowing the seedlings to develop for several days before application of fungus results in more efficient production of compounds than immediate application of fungus to the ungerminated seed.[3] After application of *Rhizopus*, however, growth conditions (temperature, relative humidity) need to be adjusted to allow further development of both the seedling and the fungus. These challenges and the limited effectiveness of germination with simultaneous

fungal elicitation in grasses have inspired the exploration of alternative elicitation methods, which is further discussed in **section 7.3**.

7.2.3. Antimicrobial potential of monomeric metabolites from grasses

In **Chapter 4**, the antimicrobial activity of monomeric natural benzoxazinoids was reviewed and these compounds were found to lack antimicrobial activity. In our own experiments, oat extract (**Chapter 6**) and standards of avenanthramides 2p, 2c, and 2f were evaluated against MRSA, *E. coli* (with and without efflux pump inhibitor PaβN), *Fusarium graminearum*, and *Aspergillus niger* (unpublished data). No appreciable antimicrobial activity was detected against any of these microorganisms, the lowest MIC value was observed for avenanthramide 2c against *E. coli* + PaβN (500 µg mL^{-1}, unpublished data). Thus we concluded that monomeric avenanthramides were not considered to be potent antimicrobials. Gramine, hordenine or barley extracts enriched in phenol-agmatine amides were also found to be ineffective against MRSA, *E. coli*, or fungi (unpublished data). Overall, monomeric secondary metabolites from grasses seem to be less potent antimicrobials than monomeric prenylated (iso)flavonoids or stilbenoids. For benzoxazinoids, however, it was shown that their synthetic derivatives might be interesting lead compounds for antimicrobial compound design (**Chapters 4** and **5**), this is further discussed in **section 7.5.2**.

7.2.4. Dimerisation: the missing link in grasses?

In **Chapter 4**, the discovery of a potent antifungal benzoxazinoid dimer was discussed. The dimeric benzoxazolinone, zeaoxazolinone (**Figure 7.3**), was isolated from maize and it presents a new lead for potential antimicrobial benzoxazinoids. Similarly, in barley, hordatines (i.e. dimers of phenol-agmatine amides) are formed. These compounds were previously suggested to be potent antifungal compounds (see **Chapter 1**).[12] In analogy with barley's hordatines, bisavenanthramides (i.e. dimers of avenanthramides, phenol-anthranilic acid amides) (**Figure 7.3**)[13] might possess higher antimicrobial activity than their monomeric precursors. Antimicrobial activity of bisavenanthramides has not yet been tested experimentally. Furthermore, hordatines and bisavenanthramides can also form oligomers (e.g. trimers and tetramers) by subsequent oxidative couplings of monomers, dimers, or a combination of these.[14]

Taking into account previous observations for stilbenoids, there are several indications that dimerisation or oligomerisation might be an interesting method to enhance the antimicrobial activity of defence metabolites from grasses. These metabolites were, so far, not the main compounds detected in our germination and elicitation experiments.

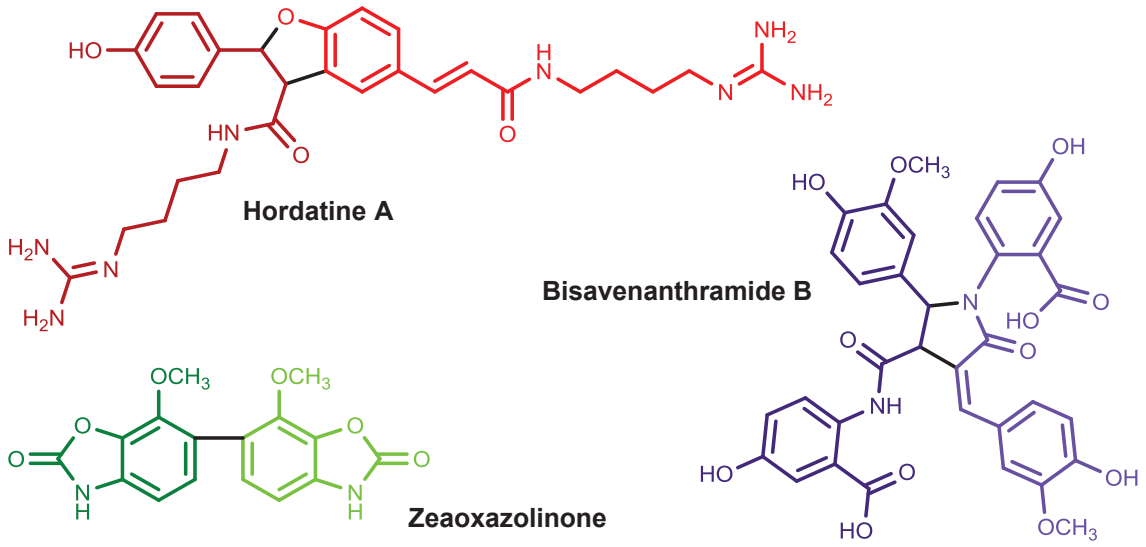

Figure 7.3. Structures the phenol-agmatine amide (red) homodimer hordatine A[12], the avenanthramide (purple) homodimer bisavenanthramide B,[13] and the benzoxazolinone (green) homodimer zeaoxazolinone. The bonds between the monomeric units are shown in black.

Preliminary results suggest that *in vitro* oxidative dimerisation, either enzymatically or chemically oxidized (unpublished data), presents a compelling alternative to achieve dimerisation or oligomerisation.

7.3. Chemical elicitation: a more universal approach?

Considering the limitations and challenges associated with germination with simultaneous fungal elicitation, as described in **section 7.2.2**, an alternative method would be of great interest. One of the suspected causes for the limited effectiveness of *Rhizopus* elicitation in grasses was that *Rhizopus* was not properly recognized by those plant species. Plants possess intricate mechanisms by which certain microbial- or pathogen-associated molecular patterns are recognized.[15] Recognition of such patterns leads to a subsequent stress response (or elicitation).[15] In agriculture, fungi of the genera *Fusarium* or *Puccinia* are commonly known to infest crops of the family Poaceae.[16] Perhaps these fungi would be recognized by the seedlings as pathogens and therefore more effectively activate defence responses. The obvious disadvantages of using more pathogenic fungi is possible toxicity to humans, for example by the ability of these fungi to produce mycotoxins (e.g. deoxynivalenol from *Fusarium graminearum*),[16] and reduced germination capacity of the seedlings. Application of these fungi, therefore, was not explored in this thesis. Rather we chose to explore an approach using chemical elicitation. Chemical elicitors, like jasmonates, are generally further downstream in the signal transduction process and play a role in the response to a wide variety of stresses, including microbial pathogens, in mono- and dicots.[17,18] They are not dependent on species-specific recognition of molecular patterns as is

the case with microbial elicitation. It was, therefore, expected that chemical elicitation would be universally applicable for grasses, legumes, and other plant families, removing the need to identify the most effective fungus for elicitation of each separate plant species.

Several commonly used chemical elicitors are of natural origin. Thus, these are technically biotic elicitors, for example the plant hormones jasmonate and salicylate. Common non-natural (abiotic) chemical elicitors are metal ions or cyclodextrin.[19-21] To investigate the feasibility of chemical elicitation, germinating seedlings of peanut were exposed to a combination of chemical elicitors. Peanut was selected for these experiments as previous studies from our laboratory provided a clear reference point for the effectiveness of germination with fungal elicitation. In **Figure 7.4**, the result of the most promising chemical treatment is shown, alongside the untreated control and elicitation with *Rhizopus*. The most effective chemical elicitor tested was a combination of β-cyclodextrin, methyl jasmonate, and methyl salicylate.

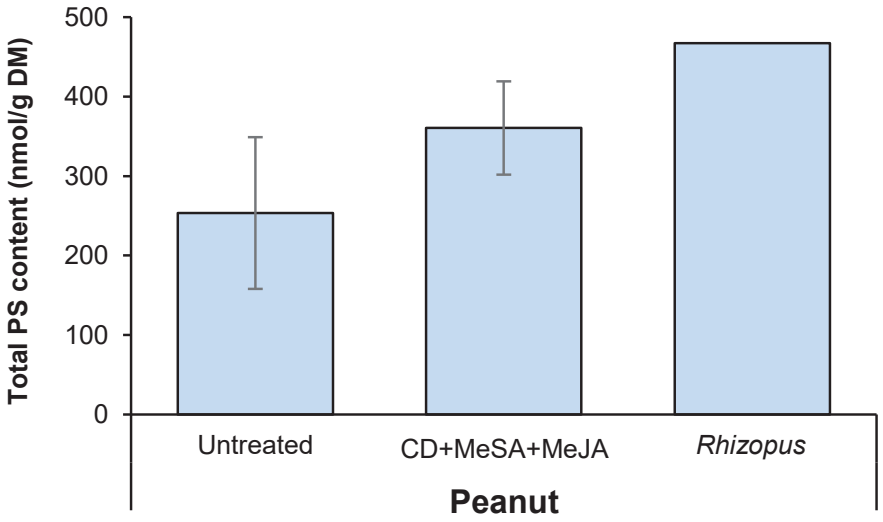

Figure 7.4. Effect of various elicitors on the prenylated stilbenoid (PS) content of peanut seedlings. Elicitation with *Rhizopus* in this setup was performed as a single control experiment. CD, β-cyclodextrin; MeSA, methyl salicylate; MeJA, methyl jasmonate.

None of the tested treatments, however, approached the effectiveness of *Rhizopus* elicitation in this set of experiments. Moreover, in previously reported experiments the increase in prenylated compounds upon elicitation with *Rhizopus* was even more extensive than what we observed here.[3,11] Overall, these results indicate that fungal elicitation more broadly activates stress response pathways, leading to the production of a higher quantity and diversity of defence metabolites.

It is likely that the most effective combination of elicitors has not yet been found. Identifying which combinations of chemical elicitors are able to replicate or improve on the effect of fungal elicitation will be a study on its own. Due to the pursuit of more promising and better developed lines of research, the experiments on

chemical elicitation were not pursued any further in this thesis. Nonetheless, it will be worthwhile to investigate this approach in a separate study considering the following benefits of a successful chemical elicitation protocol:

- Such a protocol makes use of universal stress response pathways that are conserved throughout plant families and can, therefore, be applied to different species, as demonstrated by methyl jasmonate which has been widely used.[19,20]
- Severity of the treatment can be controlled more easily by adjusting elicitor concentration,[22] rather than being dependent on variable fungal growth.
- Growth conditions can be optimized for seed germination to achieve maximum germination rate and capacity (percentage of seeds that germinates), rather than having a compromise between the ideal growth conditions for seedling and fungus.

7.4. Chemistry inspired by nature: One-pot synthetic prenylation

In the previous sections secondary metabolites from many different classes were addressed. Prenylated stilbenoids were amongst the most potent of these metabolites. One of the aims of this thesis was to explore the possibility of one-pot synthetic prenylation as a means to efficiently produce and diversify the structure of prenylated (iso)flavonoids and stilbenoids. Mainly due to instability of (prenylated) resveratrol (see also **Section 7.1.1**), which was the first backbone we selected for one-pot chemical prenylation, the progress on this aim was slower than anticipated. Despite these setbacks, some promising results were obtained which will be discussed in the following sections. Additionally, the antifungal activity of these compounds against *Saccharomyces cerevisiae* was assessed to evaluate the viability of yeast metabolic engineering for the production of prenylated compounds.

7.4.1. Synthetic prenylation of resveratrol, naringenin, and genistein

The simple one-pot synthetic prenylation method, as discussed in **Chapter 1**, was adapted for prenylation of resveratrol, naringenin, and genistein.

The starting compounds resveratrol, naringenin, and genistein were incubated in acetone with prenyl-Br (3,3-dimethylallyl bromide) in the presence of K_2CO_3 at room temperature for approximately 16 h. In **Figure 7.5**, chromatograms of the reaction mixtures are shown. The prenylation mixtures were purified on a Waters preparative RP-HPLC system, using a similar method as described in **Chapter 2**. Subsequently, the structure of the purified compounds obtained was elucidated based on MS^n, HRMS, and NMR spectroscopy. The antifungal activity against *S. cerevisiae* was evaluated by a broth microdilution assay (similar to the method used in **Chapter 2**) performed at 30 °C for 48 h (manuscript in preparation).[23]

The position of prenylation and anti-*S. cerevisiae* activity of the characterised purified compounds and the starting compounds is shown in **Table 7.1**.

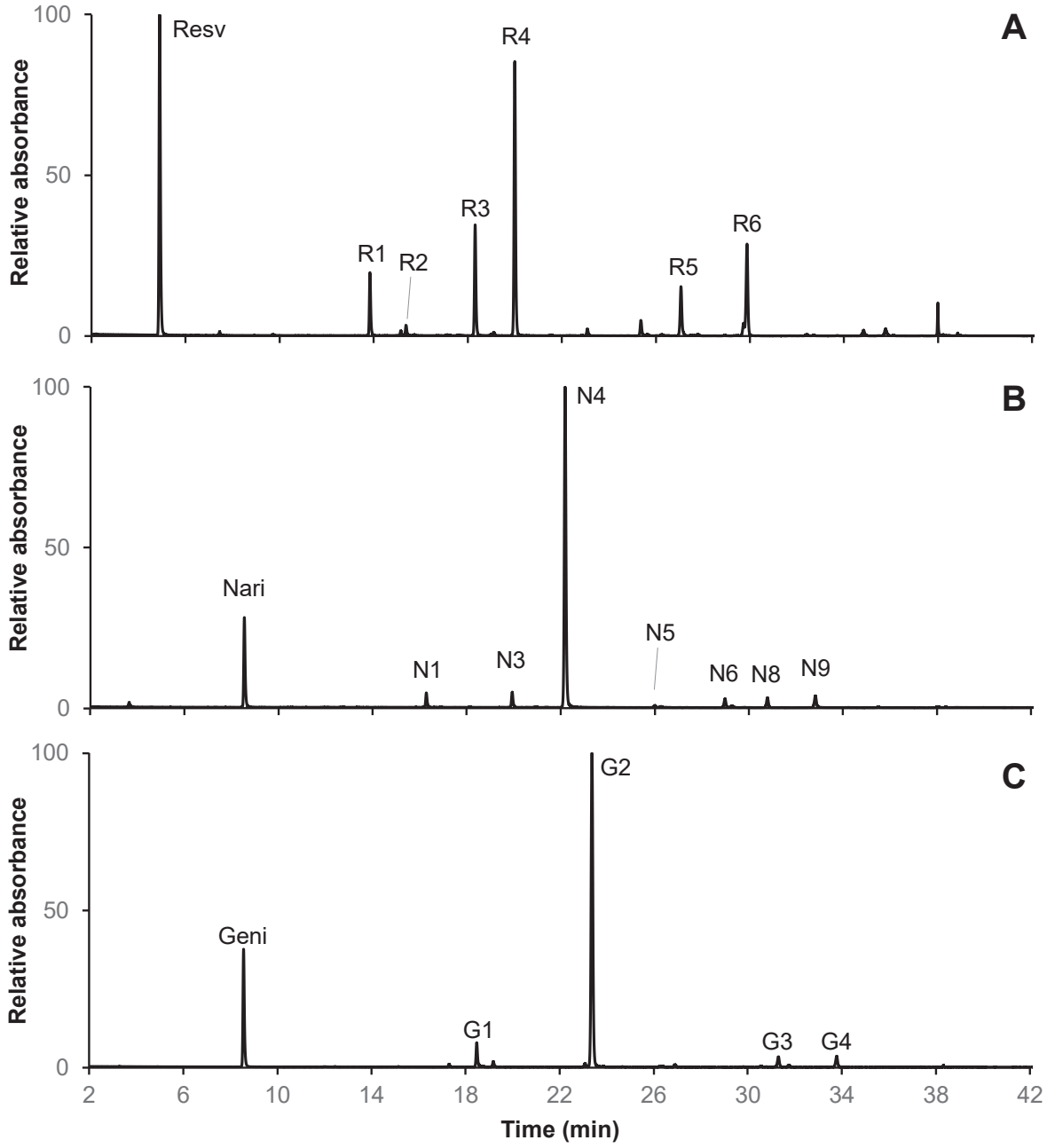

Figure 7.5. UHPLC-PDA chromatograms (260-320 nm) of resveratrol (A), genistein (B), and naringenin (C) treated with prenyl-bromide in acetone in the presence of K_2CO_3. Peak identities are shown in **Table 7.1**, peaks N2 and N7 are not visible in these chromatograms.

The conversion of resveratrol was only around 60% but the reaction yielded a wide variety of products in decent amounts (**Figure 7.5**). Addition of more prenyl-Br or using a longer reaction time did not significantly improve conversion of resveratrol and mainly tended to result in a shift toward a higher yield of tri-prenylated compounds (unpublished data). On the other hand, the conversion of genistein and

naringenin was much higher at approximately 80-90% and yielded one main product: the 7-*O*-prenyl derivative.

Table 7.1. Peak identifications of purified prenylated resveratrol, naringenin, and genistein derivatives (based on MS^n, HRMS, and NMR spectroscopy) and their anti-*S. cerevisiae* activity.

Peak	Compound	MIC (μg mL^{-1})	Backbone structures
Resv	***Resveratrol***	>200	
R1	2-*C*-prenyl-resv	>50	
R2	4-*C*-prenyl-resv [a]	>50	
R3	3-*O*-prenyl-resv	n.t.	
R4	4′-*O*-prenyl-resv	12.5	
R5	4′-*O*,2-*C*-prenyl-resv	50	
R6	4′-*O*,3-*O*-prenyl-resv	>50	
Nari	***Naringenin***	>200	
N1	8-*C*-prenyl-nari	50	
N2	3′-*C*-prenyl-nari	>50	
N3	6-*C*-prenyl-nari	>50	
N4	7-*O*-prenyl-nari	>50	
N5	6,8-*C*-diprenyl-nari	>50	
N6	7-*O*,8-*C*-diprenyl-nari	>50	
N7	7-*O*-3′-*C*-diprenyl-nari	n.t.	
N8	7-*O*,6-*C*-diprenyl-nari	>50	
N9	7,4′-*O*-diprenyl-nari	>50	
Geni	***Genistein***	>200	
G1	8-C-prenyl-geni	>25	
G2	7-*O*-prenyl-geni	>25	
G3	7-*O*,8-*C*-diprenyl-geni	>25	
G4	7,4′-*O*-diprenyl-geni	>25	
Glab	Glabridin [b]	12.5	
Amp	Amphotericin B [c]	4	

Resv, resveratrol; nari, naringenin; geni, genistein; n.t., no tested. [a] Structure identical to arachidin-2. [b] Used as a reference natural isoflavonoid with known activity against Gram-positive bacteria.[5] [c] Antifungal positive control.

The preliminary results presented in **Figure 7.5** and **Table 7.1** demonstrate that the one-pot synthetic prenylation approach was successful in producing prenylated derivatives of these three phenolic compounds and in expanding their structural diversity compared to their natural analogues.[23] Several structural features which are rare amongst natural prenylated compounds, specifically di- and *O*-prenylation, were successfully introduced. Amongst the compounds are also several synthetic analogues of natural compounds, such as 4-*C*-prenyl-resveratrol (arachidin-2), 6-*C*- and 8-*C*-prenyl-naringenin, and 8-*C*-prenyl-genistein (lupiwighteone).

7.4.2. Yeast metabolic engineering and antifungal activity of prenylated resveratrol, naringenin, and genistein

As shortly discussed in **Chapter 1**, there is an opportunity to produce prenylated compounds by expressing one of the membrane-bound plant prenyltransferases in yeast.[24] The ideal scenario would be to achieve expression of a prenyltransferase in combination with incorporation of the stilbenoid or (iso)flavonoid pathway in a metabolically engineered yeast. If successful, the yeast might be used to perform prenylation of stilbenoids or (iso)flavonoids intracellularly after which its efflux pumps might remove the prenylated compound from the cell.[25] As addressed in **Chapter 1**, the specificity of plant prenyltransferases,[26-28] however, prevents the production of prenylated compounds with a wider structural diversity than what occurs in plants. Additionally, initial attempts of producing prenylated (iso)flavonoids in yeast were unsuccessful despite successful production of naringenin (acceptor substrate).[29,30] Absence of prenylation of the available naringenin was possibly due to lack of expression of the prenyltransferase or unsuccessful incorporation of the enzyme in the membrane. Alternatively, it is possible that insufficient concentration of donor substrate was available or that the donor and acceptor substrates were not both present in the same intracellular compartment as the prenyltransferase. As discussed in **Chapter 1**, a potential hurdle is the possible antifungal activity of the resulting compounds which might inhibit yeast growth.

The antifungal MICs of the prenylated resveratrol, naringenin and genistein derivatives were higher (**Table 7.1**) than what was expected based on previous experiments against gram-positive bacteria. The only two compounds with antifungal activities in the range of previously observed antibacterial activity of prenylated (iso)flavonoids are 4'-*O*-prenyl-resveratrol and glabridin, both with MIC 12.5 μg mL^{-1}. One of the factors expected to play a major role in the low activity of prenylated compounds against *S. cerevisiae* is the presence of efflux pumps. Yeasts possess a variety of efflux pumps, such as Pdr5p and Snq2, capable of removing harmful compounds.[31] Indeed, Sasaki and co-workers (2009) suggested that 8-prenylnaringenin, which was produced upon naringenin supplementation of their yeast expressing the prenyltransferase SfN8DT-1, was mostly present in the culture medium rather than intracellularly.[25] Efflux pumps might greatly reduce the intracellular concentration of the prenylated compounds and thereby diminish their antifungal efficacy. Similar observations were made against gram-negative bacteria (e.g. *E. coli*), where the prenylated compounds alone hardly exhibited antimicrobial activity, but addition of an efflux pump inhibitor resulted in similar activity as was observed against gram-positive bacteria.[5] On the other hand, it has also been reported that prenyl-flavonoids can inhibit Pdr5p,[32] but this functionality might be limited to specific prenylated compounds.

Up to a concentration of 50 µg mL^{-1} most prenylated compounds, except one *O*-prenylated resveratrol derivative and glabridin, do not inhibit yeast growth. It has been demonstrated *S. cerevisiae* can be metabolically engineered to produce naringenin from simple precursors such as glucose or tyrosine with extracellular naringenin concentrations up to 84 µg mL^{-1}.[29,33] Unless these yields are greatly increased, there should not be any inhibition of the yeast by non-prenylated naringenin, genistein, or resveratrol (MIC >200 µg mL^{-1}). Even if naringenin would be prenylated at the *C*8 (e.g. by SfN8DT-1)[25], then at 84 µg naringenin per mL 60% conversion would be required before reaching MIC (8-*C*-prenyl-naringenin at 50 µg mL^{-1}). To conclude, our results indicate that a prenylation approach in metabolically engineered yeast is unlikely to be hindered by growth inhibition due to the prenylated products. This is assuming that MICs determined with this assay are comparable to what would be observed under normal growth conditions.
In addition to this, there are indications that yeast efflux pumps are capable of removing prenylated compounds from the yeast cell, exuding them into the culture medium. This would facilitate recovery of the prenylated compounds compared to intracellular storage.

7.5. Phytochemicals as antimicrobials: from *in vitro* to application

Most of the natural compounds presented in this thesis were not potent enough to be considered for application in the food or pharmaceutical industry. Prenylated stilbenoids, however, were found to possess sufficient activity to be applied as preservatives in food. This is shortly discussed in **section 7.5.1**. Furthermore, several synthetic compounds presented in this chapter and in **Chapter 5** present potential lead compounds for further antimicrobial drug design. This is shortly discussed in **section 7.5.2**.

7.5.1. Application in food

For application of antimicrobial phytochemicals in food, it is often preferable to use them as plant extracts rather than pure compounds. One of the main reasons is for the sake of achieving a green or clean label.[34] For example, an ingredient "peanut extract" would probably result in more positive consumer perception than "chiricanine A". One conceivable type of application for peanut stilbenoids extract might be in a peanut drink or possibly in other legume-based dairy alternatives. These types of products have recently been increasing in popularity as an alternative to dairy products. Based on the results of Aisyah and co-workers 2015)[3] elicited peanuts contain roughly 4.5 mg prenylated stilbenoids per g dry weight. Based on the results of **Chapter 2**, an average MIC of 50 µg mL^{-1} might be assumed for these compounds against *S. aureus*. If we take this as a representative MIC value for gram-positive spoilage bacteria, an equivalent of approximately 11 g of elicited peanuts would need to be added in 1 L of food

product (or 1.1 g per 100 mL). Considering that a commercial peanut drink contains 8% peanut (source: Rude Health™ Peanut Drink Organic), this could be achieved by replacing this with 1.1% elicited peanuts plus 6.9% regular peanuts. Alternatively, the required MIC value can be achieved by adding an extract with prenylated stilbenoids, the content of which should be equivalent to 1.1 g elicited peanuts. Enrichment of such an extract in prenylated stilbenoids can yield an enriched pool which contains approximately 300 mg prenylated stilbenoids per g dry pool, thus only requiring the addition of 0.17 g enriched pool per L food product. The addition of an extract or even an enriched pool of an extract might be preferable to limit the sensory impact, but financially less attractive. A possible additional advantage of adding a mixture of compounds is the possibility of synergy, especially if the compounds have various modes of action.

In addition, aspects such as interactions with food matrices, solubility, and stability should be taken into account.[35] Antimicrobial activity might be negatively affected by interaction with other food components.[34] As addressed in **section 7.1.1**, the poorly-understood stability of prenylated stilbenoids reduces the attractiveness of these compounds for such an application. Considering the current knowledge, it seems unlikely that elicited peanuts will be used as a food preservative, especially considering the stability issues.

For food, as well as for pharmaceuticals (see below), possible biological side activities such as estrogenicity[36], prooxidant effects,[37] or toxicity[38-40] of the compounds will have to be further investigated prior application. In addition, several points of attention for future research on these compounds and their synthetic derivatives are elucidation of their mode of action and the likeliness of resistance development.

7.5.2. Applications in pharmaceuticals

In the pharmaceutical industry organic synthesis is commonly used to optimize lead compounds. This offers more freedom in the type of modifications that can be implemented compared to food applications, and it usually makes production more efficient.

MIC values for antibiotics used in a medical setting are usually ≤4 μg mL^{-1} (against susceptible MOs).[41-44] Not many natural compounds possess MIC values which are this low but several promising lead compounds were presented in this thesis. For example, in **Chapter 5** novel compounds were designed *in silico* and the predicted activities of these compounds meet the requirements for MIC values of antibiotics for clinical applications. The next step will be to synthesize these compounds and assess their *in vitro* activity. For pharmaceutical applications promising MICs of antibiotics determined *in vitro* can often be related to good activity *in vivo*,[45,46] although a direct *in vitro-in vivo* correlation is not always found.[47]

Requirements for pharmaceutical lead compounds are, however, not restricted to low MIC values. Secondary requirements include: favourable absorption, distribution, metabolism, and excretion (ADME) and pharmacokinetic

characteristics of the compounds. Possibly the most well-known rules of thumb related to solubility and permeability of drugs are Lipinkski's 'rule of five'. To facilitate absorption and permeation, drug molecules should have the following properties: <5 H-bond donors, <10 H-bond acceptors, Mw <500 g mol^{-1}, and calculated logP <5.[48] Most of the compounds presented in this thesis meet at least 3 of these 4 requirements. Amongst prenylated phenolics (**Chapters 2** and **3**), the most common violation is logP exceeding 5, whereas for compounds such as stilbenoid dimers or oligomers and avenanthramides (**Chapter 6**) the maximum of 4 H-bond donors (OH and NH groups) is easily exceeded. Such characteristics might need to be further optimised for use in pharmaceutical applications.

7.6. References

[1] Araya-Cloutier, C., den Besten, H.M.W., Aisyah, S., Gruppen, H., and Vincken, J.-P. (2017) The position of prenylation of isoflavonoids and stilbenoids from legumes (Fabaceae) modulates the antimicrobial activity against Gram positive pathogens. *Food Chemistry*, 226: p. 193-201.

[2] Araya-Cloutier, C., Vincken, J.-P., van Ederen, R., den Besten, H.M.W., and Gruppen, H. (2018) Rapid membrane permeabilization of *Listeria monocytogenes* and *Escherichia coli* induced by antibacterial prenylated phenolic compounds from legumes. *Food Chemistry*, 240: p. 147-155.

[3] Aisyah, S., Gruppen, H., Slager, M., Helmink, B., and Vincken, J.-P. (2015) Modification of prenylated stilbenoids in peanut (*Arachis hypogaea*) seedlings by the same fungi that elicited them: The fungus strikes back. *Journal of Agricultural and Food Chemistry*, 63*(42)*: p. 9260-9268.

[4] Trela, B.C. and Waterhouse, A.L. (1996) Resveratrol: Isomeric molar absorptivities and stability. *Journal of Agricultural and Food Chemistry*, 44*(5)*: p. 1253-1257.

[5] Araya-Cloutier, C., Vincken, J.-P., van de Schans, M.G.M., Hageman, J., Schaftenaar, G., den Besten, H.M.W., and Gruppen, H. (2018) QSAR-based molecular signatures of prenylated (iso)flavonoids underlying antimicrobial potency against and membrane-disruption in Gram positive and Gram negative bacteria. *Scientific Reports*, 8*(1)*: p. 9267.

[6] Basri, D.F., Luoi, C.K., Azmi, A.M., and Latip, J. (2012) Evaluation of the combined effects of stilbenoid from *Shorea gibbosa* and vancomycin against methicillin-resistant *Staphylococcus aureus* (MRSA). *Pharmaceuticals*, 5*(9)*: p. 1032-1043.

[7] Basri, D.F., Xian, L.W., Shukor, N.I.A., and Latip, J. (2014) Bacteriostatic antimicrobial combination: Antagonistic interaction between epsilon-viniferin and vancomycin against methicillin-resistant *Staphylococcus aureus*. *Biomed Research International*, 2014: p. Article ID 461756.

[8] Mora-Pale, M., Bhan, N., Masuko, S., James, P., Wood, J., McCallum, S., Linhardt, R.J., Dordick, J.S., and Koffas, M.A. (2015) Antimicrobial mechanism of resveratrol-*trans*-dihydrodimer produced from peroxidase-catalyzed oxidation of resveratrol. *Biotechnology and Bioengineering*, 112*(12)*: p. 2417-2428.

[9] Sakagami, Y., Sawabe, A., Komemushi, S., Ali, Z., Tanaka, T., Iliya, I., and Iinuma, M. (2007) Antibacterial activity of stilbene oligomers against vancomycin-resistant enterococci (VRE) and methicillin-resistant *Staphylococcus aureus* (MRSA) and their synergism with antibiotics. *Biocontrol science*, 12*(1)*: p. 7-14.

[10] Aisyah, S., Vincken, J.-P., Andini, S., Mardiah, Z., and Gruppen, H. (2016) Compositional changes in (iso)flavonoids and estrogenic activity of three edible Lupinus species by germination and *Rhizopus*-elicitation. *Phytochemistry*, 122: p. 65-75.

[11] Aisyah, S., Gruppen, H., Madzora, B., and Vincken, J.P. (2013) Modulation of isoflavonoid composition of *Rhizopus oryzae* elicited soybean (*Glycine max*) seedlings by light and wounding. *Journal of Agricultural and Food Chemistry*, 61*(36)*: p. 8657-8667.

[12] Stoessl, A. (1966) The antifungal factors in barley - isolation and synthesis of hordatine A. *Tetrahedron Letters*, 7*(25)*: p. 2849-2851.

[13] Okazaki, Y., Ishihara, A., Nishioka, T., and Iwamura, H. (2004) Identification of a dehydrodimer of avenanthramide phytoalexin in oats. *Tetrahedron*, 60*(22)*: p. 4765-4771.

[14] Wilkens, A., Paulsen, J., Wray, V., and Winterhalter, P. (2010) Structures of two novel trimeric stilbenes obtained by horseradish peroxidase catalyzed

biotransformation of *trans*-resveratrol and (−)-ε-viniferin. *Journal of Agricultural and Food Chemistry*, 58*(11)*: p. 6754-6761.
[15] Jones, J.D.G. and Dangl, J.L. (2006) The plant immune system. *Nature*, 444*(7117)*: p. 323-329.
[16] Dean, R., Van Kan, J.A.L., Pretorius, Z.A., Hammond-Kosack, K.E., Di Pietro, A., Spanu, P.D., Rudd, J.J., Dickman, M., Kahmann, R., Ellis, J., and Foster, G.D. (2012) The top 10 fungal pathogens in molecular plant pathology. *Molecular Plant Pathology*, 13*(4)*: p. 414-430.
[17] Wasternack, C. and Parthier, B. (1997) Jasmonate signalled plant gene expression. *Trends in Plant Science*, 2*(8)*: p. 302-307.
[18] Lyons, R., Manners, J.M., and Kazan, K. (2013) Jasmonate biosynthesis and signaling in monocots: A comparative overview. *Plant Cell Reports*, 32*(6)*: p. 815-827.
[19] Akula, R. and Ravishankar, G.A. (2011) Influence of abiotic stress signals on secondary metabolites in plants. *Plant Signaling & Behavior*, 6*(11)*: p. 1720-1731.
[20] Namdeo, A. (2007) Plant cell elicitation for production of secondary metabolites: A review. *Pharmacognosy Reviews*, 1*(1)*: p. 69-79.
[21] Narayani, M. and Srivastava, S. (2017) Elicitation: A stimulation of stress in *in vitro* plant cell/tissue cultures for enhancement of secondary metabolite production. *Phytochemistry Reviews*, 16*(6)*: p. 1227-1252.
[22] Świeca, M. (2015) Elicitation with abiotic stresses improves pro-health constituents, antioxidant potential and nutritional quality of lentil sprouts. *Saudi Journal of Biological Sciences*, 22*(4)*: p. 409-416.
[23] de Bruijn, W.J.C., Ng, K.R., Franssen, M.C.R., de Waard, P., Chen, W.N., and Vincken, J.P., 2019. Antimicrobial activity of prenylated derivatives of resveratrol, genistein, and naringenin produced by one-pot synthesis, Manuscript in preparation.
[24] Sasaki, K., Tsurumaru, Y., Yamamoto, H., and Yazaki, K. (2011) Molecular characterization of a membrane-bound prenyltransferase specific for isoflavone from *Sophora flavescens*. *Journal of Biological Chemistry*, 286*(27)*: p. 24125-24134.
[25] Sasaki, K., Tsurumaru, Y., and Yazaki, K. (2009) Prenylation of flavonoids by biotransformation of yeast expressing plant membrane-bound prenyltransferase SfN8DT-1. *Bioscience Biotechnology and Biochemistry*, 73*(3)*: p. 759-761.
[26] Yang, T., Fang, L., Rimando, A.M., Sobolev, V., Mockaitis, K., and Medina-Bolivar, F. (2016) A stilbenoid-specific prenyltransferase utilizes dimethylallyl pyrophosphate from the plastidic terpenoid pathway. *Plant physiology*, 171*(4)*: p. 2483-2498.
[27] Chen, R.D., Liu, X., Zou, J.H., Yin, Y.Z., Ou, B., Li, J.H., Wang, R.S., Xie, D., Zhang, P.C., and Dai, J.G. (2013) Regio- and stereospecific prenylation of flavonoids by *Sophora flavescens* prenyltransferase. *Advanced Synthesis & Catalysis*, 355*(9)*: p. 1817-1828.
[28] Wang, R.S., Chen, R.D., Li, J.H., Liu, X., Xie, K.B., Chen, D.W., Yin, Y.Z., Tao, X.Y., Xie, D., Zou, J.H., Yang, L., and Dai, J.G. (2014) Molecular characterization and phylogenetic analysis of two novel regio-specific flavonoid prenyltransferases from *Morus alba* and *Cudrania tricuspidata*. *Journal of Biological Chemistry*, 289*(52)*: p. 35815-35825.
[29] Lyu, X., Ng, K.R., Lee, J.L., Mark, R., and Chen, W.N. (2017) Enhancement of naringenin biosynthesis from tyrosine by metabolic engineering of Saccharomyces cerevisiae. *Journal of Agricultural and Food Chemistry*, 65*(31)*: p. 6638-6646.
[30] Ng, K.R. and Chen, W.N., 2018. Metabolic engineering of naringenin-producing *Saccharomyces cerevisiae* to express plant prenyltransferases, School of Chemical and Biomedical Engineering, Nanyang Technological University

[31] Rogers, B., Decottignies, A., Kolaczkowski, M., Carvajal, E., Balzi, E., and Goffeau, A. (2001) The pleitropic drug ABC transporters from Saccharomyces cerevisiae. *Journal of Molecular Microbiology and Biotechnology*, 3*(2)*: p. 207-214.

[32] Conseil, G., Decottignies, A., Jault, J.M., Comte, G., Barron, D., Goffeau, A., and Di Pietro, A. (2000) Prenyl-flavonoids as potent inhibitors of the Pdr5p multidrug ABC transporter from Saccharomyces cerevisiae. *Biochemistry*, 39*(23)*: p. 6910-6917.

[33] Koopman, F., Beekwilder, J., Crimi, B., van Houwelingen, A., Hall, R.D., Bosch, D., van Maris, A.J.A., Pronk, J.T., and Daran, J.M. (2012) De novo production of the flavonoid naringenin in engineered Saccharomyces cerevisiae. *Microbial Cell Factories*, 11.

[34] Davidson, P.M., Critzer, F.J., and Taylor, T.M. (2013) Naturally occurring antimicrobials for minimally processed foods. *Annual Review of Food Science and Technology*, 4: p. 163-190.

[35] Sanchez Maldonado, A.F., Schieber, A., and Gänzle, M.G. (2015) Plant defence mechanisms and enzymatic transformation products and their potential applications in food preservation: Advantages and limitations. *Trends in Food Science & Technology*, 46*(1)*: p. 49-59.

[36] van de Schans, M.G.M., Ritschel, T., Bovee, T.F.H., Sanders, M.G., de Waard, P., Gruppen, H., and Vincken, J.-P. (2015) Involvement of a hydrophobic pocket and helix 11 in determining the modes of action of prenylated flavonoids and isoflavonoids in the human estrogen receptor. *Chembiochem*, 16*(18)*: p. 2668-2677.

[37] Rusak, G., Piantanida, I., Mašić, L., Kapuralin, K., Durgo, K., and Kopjar, N. (2010) Spectrophotometric analysis of flavonoid-DNA interactions and DNA damaging/protecting and cytotoxic potential of flavonoids in human peripheral blood lymphocytes. *Chemico-Biological Interactions*, 188*(1)*: p. 181-189.

[38] Isbrucker, R.A., Edwards, J.A., Wolz, E., Davidovich, A., and Bausch, J. (2006) Safety studies on epigallocatechin gallate (EGCG) preparations. Part 2: Dermal, acute and short-term toxicity studies. *Food and Chemical Toxicology*, 44*(5)*: p. 636-650.

[39] Buchmann, C.A., Nersesyan, A., Kopp, B., Schauberger, D., Darroudi, F., Grummt, T., Krupitza, G., Kundi, M., Schulte-Hermann, R., and Knasmueller, S. (2007) Dihydroxy-7-methoxy-1,4-benzoxazin-3-one (DIMBOA) and 2,4-dihydroxy-1,4-benzoxazin-3-one (DIBOA), two naturally occurring benzoxazinones contained in sprouts of Gramineae are potent aneugens in human-derived liver cells (HepG2). *Cancer Letters*, 246*(1-2)*: p. 290-299.

[40] Arroyo, E., Chinchilla, N., Molinillo, J.M.G., Macias, F.A., Astola, A., Ortiz, M., and Valdivia, M.M. (2010) Aneugenic effects of benzoxazinones in cultured human cells. *Mutation Research/Genetic Toxicology and Environmental Mutagenesis*, 695*(1-2)*: p. 81-86.

[41] Veloo, A.C.M., Seme, K., Raangs, E., Rurenga, P., Singadji, Z., Wekema-Mulder, G., and van Winkelhoff, A.J. (2012) Antibiotic susceptibility profiles of oral pathogens. *International Journal of Antimicrobial Agents*, 40*(5)*: p. 450-454.

[42] Steinkraus, G., White, R., and Friedrich, L. (2007) Vancomycin MIC creep in non-vancomycin-intermediate *Staphylococcus aureus* (visa), vancomycin-susceptible clinical methicillin-resistant *S. aureus* (MRSA) blood isolates from 2001-05. *Journal of Antimicrobial Chemotherapy*, 60*(4)*: p. 788-794.

[43] MacGowan, A.P. and Wise, R. (2001) Establishing MIC breakpoints and the interpretation of *in vitro* susceptibility tests. *Journal of Antimicrobial Chemotherapy*, 48: p. 17-28.

[44] Kahlmeter, G., Brown, D.F.J., Goldstein, F.W., MacGowan, A.P., Mouton, J.W., Osterlund, A., Rodloff, A., Steinbakk, M., Urbaskova, P., and Vatopoulos, A. (2003) European harmonization of MIC breakpoints for antimicrobial

susceptibility testing of bacteria. *Journal of Antimicrobial Chemotherapy*, 52*(2)*: p. 145-148.

[45] Rex, J.H., Pfaller, M.A., Galgiani, J.N., Bartlett, M.S., EspinelIngroff, A., Ghannoum, M.A., Lancaster, M., Odds, F.C., Rinaldi, M.G., Walsh, T.J., and Barry, A.L. (1997) Development of interpretive breakpoints for antifungal susceptibility testing: Conceptual framework and analysis of *in vitro–in vivo* correlation data for fluconazole, itraconazole, and *Candida* infections. *Clinical Infectious Diseases*, 24*(2)*: p. 235-247.

[46] Rodríguez, M.M., Pastor, F.J., Sutton, D.A., Calvo, E., Fothergill, A.W., Salas, V., Rinaldi, M.G., and Guarro, J. (2010) Correlation between *in vitro* activity of posaconazole and *in vivo* efficacy against *Rhizopus oryzae* infection in mice. *Antimicrobial Agents and Chemotherapy*, 54*(5)*: p. 1665-1669.

[47] Monogue, M.L., Abbo, L.M., Rosa, R., Camargo, J.F., Martinez, O., Bonomo, R.A., and Nicolau, D.P. (2017) *In vitro* discordance with *in vivo* activity: Humanized exposures of ceftazidime-avibactam, aztreonam, and tigecycline alone and in combination against New Delhi metallo-β-lactamase-producing *Klebsiella pneumoniae* in a murine lung infection model. *Antimicrobial Agents and Chemotherapy*, 61*(7)*.

[48] Lipinski, C.A., Lombardo, F., Dominy, B.W., and Feeney, P.J. (2012) Experimental and computational approaches to estimate solubility and permeability in drug discovery and development settings. *Advanced Drug Delivery Reviews*, 64: p. 4-17.

About the author

Curriculum vitae

Wouter J.C. de Bruijn was born on September 10th 1991 in Tegelen, The Netherlands. In 2009 he started his bachelor studies in Food Technology at Wageningen University. The bachelor was concluded with a thesis entitled "Changes in the carbohydrate content of mushroom compost during growth of white button mushrooms (*Agaricus bisporus*)" at the Laboratory of Food Chemistry in Wageningen. He obtained his bachelor with honours in 2012 and started his master studies in Food Technology (Wageningen University) in the same year. In the master his specialization was Ingredient Functionality, in which he focussed on the physics and chemistry of food. The master was concluded with a thesis entitled "Degradation of astaxanthin in different solvents" at the Laboratory of Food Chemistry and an industrial internship on "High protein products in fortified dairy, meal replacements and medical nutrition" at Givaudan, Naarden, The Netherlands. He obtained his master with honours in 2014 and immediately started working as a PhD candidate at the Laboratory of Food Chemistry under the supervision of Prof. Harry Gruppen and Prof. Jean-Paul Vincken. The results of his PhD research are presented in this thesis. Wouter continues to work at the Laboratory of Food Chemistry in Wageningen as a post-doctoral researcher.

List of publications

Mark Levisson, Carla Araya-Cloutier, **Wouter J.C. de Bruijn**, Menno van der Heide, José Manuel Salvador López, Jean-Marc Daran, Jean-Paul Vincken, and Jules Beekwilder (2019) Towards developing a yeast cell factory for the production of prenylated flavonoids, *Journal of Agricultural and Food Chemistry*, Accepted (In press).

Wouter J.C. de Bruijn, Sarah van Dinteren, Harry Gruppen, and Jean-Paul Vincken (2019) Mass spectrometric characterisation of avenanthramides and enhancing their production by germination of oat (*Avena sativa*), *Food Chemistry*, 277, p. 682-690.

Wouter J.C. de Bruijn, Jos A. Hageman, Carla Araya-Cloutier, Harry Gruppen, and Jean-Paul Vincken (2018) QSAR of 1,4-benzoxazin-3-one antimicrobials and their drug design perspectives, *Bioorganic & Medicinal Chemistry*, 26, p. 6105-6114.

Wouter J. C. de Bruijn, Carla Araya-Cloutier, Judith Bijlsma, Anne de Swart, Mark G. Sanders, Pieter de Waard, Harry Gruppen, Jean-Paul Vincken (2018) Antibacterial prenylated stilbenoids from peanut (*Arachis hypogaea*), *Phytochemistry Letters*, 28, p. 13-18.

Wouter J. C. de Bruijn, Harry Gruppen, and Jean-Paul Vincken (2018) Structure and biosynthesis of benzoxazinoids: Plant defence metabolites with potential as antimicrobial scaffolds, *Phytochemistry*, 155, p. 233-243.

Wouter J. C. de Bruijn, Jean-Paul Vincken, Katharina Duran, and Harry Gruppen (2016) Mass Spectrometric Characterization of Benzoxazinoid Glycosides from *Rhizopus*-Elicited Wheat (*Triticum aestivum*) Seedlings, *Journal of Agricultural and Food Chemistry,* 64(32), p. 6267-6276.

Wouter J.C. de Bruijn, Yannick Weesepoel, Jean-Paul Vincken, and Harry Gruppen (2016) Fatty acids attached to all-trans-astaxanthin alter its cis–trans equilibrium, and consequently its stability, upon light-accelerated autoxidation, *Food Chemistry*, 194, p. 1108-1115.

Yannick Weesepoel, Harry Gruppen, **Wouter de Bruijn**, and Jean-Paul Vincken (2014) Analysis of Palmitoyl Apo-astaxanthinals, Apo-astaxanthinones, and their Epoxides by UHPLC-PDA-ESI-MS, *Journal of Agricultural and Food Chemistry*, 62(42), p. 10254-10263.

Aleksandrina Patyshakuliyeva, Edita Jurak, Annegret Kohler, Adam Baker, Evy Battaglia, **Wouter de Bruijn**, *et al* (2013), Carbohydrate utilization and metabolism is highly differentiated in *Agaricus bisporus*, *BMC Genomics*, 14:663.

Overview of completed training activities

Discipline specific activities

Courses

Advanced Food Analysis	VLAG, Wageningen, 2015
Biorefinery for Biomolecules	VLAG, Wageningen, 2015
Ion Trap (Velos Pro) operations	Thermo Scientific, Wageningen, 2016
International Design and Discovery Course	CMBI, Nijmegen, 2016
Structure and Reactivity	ORC, WUR, Wageningen, 2016
Training Compound Discoverer	Thermo Scientific, Breda, 2017

Conferences

International Conference on Polyphenols	University of Technology, Vienna, Austria, 2016

General courses

VLAG PhD introduction week	VLAG, Baarlo, 2015
Project and time management	WGS, Wageningen, 2015
Techniques for writing and presenting a scientific paper	WGS, Wageningen, 2015
Research integrity	WGS, Wageningen, 2017
Career perspectives	WGS, Wageningen, 2018

Optional courses and activities

Preparation research proposal	FCH, Wageningen, 2014-2015
PhD study trip 2014 [a]	FCH, Germany – Denmark – Sweden – Finland, 2014
PhD study trip 2016 [a, b, c]	FCH, Japan, 2016
BSc and MSc thesis students supervision, presentations, and colloquia	FCH, Wageningen, 2014-2018
PhD presentations	FCH, Wageningen, 2014-2018

[a] Poster presentation. [b] Oral presentation. [c] Organising committee.

Abbreviations: VLAG, Graduate school for Advanced studies in Food Technology, Agrobiotechnology, Nutrition and Health Science; CMBI, Centre for Molecular and Biomolecular Informatics; ORC, Laboratory of Organic Chemistry (WUR); WGS, Wageningen Graduate Schools; FCH, Laboratory of Food Chemistry (WUR).

The work described in this thesis was performed at the Laboratory of Food Chemistry of Wageningen University & Research, The Netherlands.

Financial support from Wageningen University for printing this thesis is gratefully acknowledged.

Cover design by Wouter J.C. de Bruijn
Printed by Proefschrift-AIO
Edition: 250 copies